UNIVERSITY OF READING

Investigating the structure / function relationship of PLCγ2 downstream of GPVI and CLEC-2

A thesis submitted for the degree of Doctor of Philosophy

School of biological sciences

Safa Gayes

June 2024

Declaration

I confirm that this is my own work and the use of all material from other sources has been properly and fully acknowledged.

Signed: Safa Gayes

Date: 20/6/2024

Abstract

Background: Several platelet signalling pathways result in the activation of phospholipase C gamma 2 (PLCγ2), making it an important signalling hub. Both the ITAM-linked collagen receptor GPVI, and the hemITAM-containing podoplanin receptor CLEC-2, activate PLCγ2 via a similar mechanism. PLCγ2 is a large protein consisting of multiple domains. PLCγ2's molecular interaction with other proteins regulates its function, however the exact mechanism is still not fully understood. PLCγ2 also plays a similar role downstream of ITAM-linked receptors in other cells, such as B- and T-cells. In 80% of leukaemia patients who acquire resistance to ibrutinib therapy, PLCγ2 mutations have been detected. Although these mutations have been shown to lead to a gain function, it's still unknown whether these mutations might arise in platelets and what their functional effect on platelet activity might be.

Aims: Characterise the structure/function relationship of PLCγ2 downstream of (hem)ITAM receptors.

Methods: A PLC pharmacological inhibitor, U73122, was used in platelet function assays including aggregation, calcium release, and platelet adhesion and spreading to characterise the impact of PLCγ2 inhibition on platelet function mediated by GPVI and CLEC-2. To understand the structure/function relationship of PLCγ2 downstream of the (hem)ITAM receptors, construct with PLCγ2 mutations were transiently transfected in PLCγ2 knockout cells and U73122 was used to assess the calcium signalling in the cells. A CRISPR/Cas9 approach was also used to generate

PLCγ2 mutation knock-in in WT DT40 cells. Using a laser injury model, zebrafish were used as an *in vivo* model to demonstrate the effect of U73122 on PLCγ2 in thrombus formation and vascular/lymphatic development.

Results: GPVI mediated platelet aggregation and platelet spreading is more significantly affected by PLCγ2 inhibition than CLEC-2 mediated activation. U73122 inhibits calcium release in a similar manner downstream of both receptors. Using an overexpression system in PLCγ2 KO cells, PLCγ2 mutations lead to a gain of function as shown by increased signalling. However, this increased signalling was still susceptible to inhibition by U73122. Additionally, using the CRISPR/Cas9 approach, a PLCγ2 point mutation was successfully introduced in WT DT40 cells. Finally, U73122 leads to an extended time to occlusion and lack of thrombus formation in zebrafish.

Conclusion: These results confirm the essential role for PLCγ2 downstream of platelet (hem)ITAM receptor signalling. U73122 significantly decreases GPVI and CLEC-2 mediated platelet activation. Downstream of CLEC-2, U73122 decreases signalling more significantly in cells bearing mutations in the catalytic domain suggesting that the CLEC-2 signalling pathway is more reliant on the activity of the catalytic domain of PLCγ2 than GPVI. Finally, PLCγ2 has shown to play an essential role in thrombus formation in zebrafish.

Acknowledgments

First and foremost, I would like to thank my phenomenal supervisors, Craig and Alice. Before starting my PhD I was so worried about what my supervisors would be like. But I wouldn't have had a more amazing support system if I wanted to. I deeply appreciate your constant support. Thank you Craig for showing me what an amazing supervisor should be like, for always being available even when I'm interrupting your Friday evening, and for always pushing me and motivating me to work harder. I definitely appreciate you always reading my chapters so fast! Thank you Alice for always having your door open for me and answering every little silly question I have and for always asking me questions that made me think outside the box. Thank you for all the time you spent teaching me how to use the microscope! Thank you both again! Couldn't thank you enough!

Huge thank you to Johannes Eble for the rhodocytin and Mike Tomlinson for the PLCγ2 KO cells.

Big thanks to Jon Gibbins and the platelet group. Thank you Tanya for always checking my math, Kirk for helping me out with the intravital, and Yasmin for being so welcoming when I first started. Thank you Alex for helping me with the flex station and picking on "my American accent", Abdul, Fahd, Salihah and Tayseer for all the lovely chats. Also, a big shoutout to Eva for all the help and support inside and outside the lab.

Massive thanks to Kaouthar for checking on my cells when I wasn't able to and all the tissue culture shenanigans. Thank you Jomanah for buying me sweets and flowers to keep me going.

Special thanks to my buddy and my lunch partner, Carly. You are an amazing friend. Having you around definitely made things easier and more enjoyable. And thank you for the CNN, definitely made my life easier!

Most importantly, I am forever thankful and grateful to Dr. Aisha whose financial and emotional support made this PhD opportunity possible. You always supported me and made all my dream come true. I genuinely wouldn't have been here or been able to do this without you.

Mama, Munzi, from the first days of my academic journey, you were always supportive and encouraging. Your strength and resilience have inspired me every step of the way. Thank you for the sacrifices you've made to get me where I am today. Thank you for always asking how's "CRISPR" going even though you laugh at me every time I cry about my experiments failing. I think you're an expert by now! You are a mom, a dad, and a best friend. I dedicate all this to you. You are my super woman!
To my sister,Salma, thank you for being my unwavering cheerleader, my partner in laughter, and a constant source of love—I couldn't have done this without your light by my side.

Last but DEFINITLEY not least, my partner and my best friend, Fadi. I am forever grateful for all those facetime calls you spent keeping my company while writing and all the flowers and takeouts you sent me to keep me going. I'm definitely grateful to you for always putting up with my crankiness when my experiments fail and for always pretending to be interested in my zebrafish images. Thank you for believing in me since we were teenagers and for always being so proud of me and believing in me even when I doubted myself.

I also like to thank myself for all the blood (literally), tears, and sweat!

Alhamdulillah!

Presentations

Poster presentation British Society for haemostasis and thrombosis

(Aberdeen, 2022)

Oral presentation Platelet Society Meeting

(Hull, 2022)

Oral presentation Platelet Society Meeting/EuPlan meeting

(Bristol, 2023)

Abbreviations

°C-Degree Celsius

ACD -Acid citrate dextrose

ADP -Adenosine diphosphate

ANOVA -Analysis of variance

ATP -Adenosine triphosphate

BCR -B cell receptor

BLNK -B-cell linker protein

BSA -bovine serum albumin

Btk -Bruton's tyrosine kinase

Ca2+ -calcium ion

$CaCl_2$-Calcium Chloride

cAMP -cyclic adenosine monophosphate

CLEC- 2 -C-type lectin-like receptor 2

CLL -Chronic lymphocytic leukaemia

CNN-Convolutional neural network

cPLA2- cytosolic phospholipase A 2

CO_2 - Carbon dioxide

COX-1 - Cyclooxygenase enzyme 1

CRISPR - Clustered Regularly Interspaced Short Palindromic Repeats

CRP-XL -Cross linked collagen-related peptide

CVD - Cardiovascular disease

DA - Dorsal artery

DAG -1,2-diacyl-glycerol

DIC -Differential Interference Contrast

DLAV - Dorsal longitudinal anastomotic vessel

DMSO - Dimethyl sulfoxide

DPF-Days post fertilization

ECM -Extracellular matrix

EDTA -Ethylenediaminetetraacetic acid

FLS - facial lymphatic sprout

FBS - Fetal bovine serum

FcRγ - Fc receptor γ chain

Gads - Grb2 Related Adaptor Protein Downstream of Shc

GFP -Green fluorescent protein

GP - glycoprotein

GPCR - G protein coupled receptor

GPVI - Glycoprotein VI

GPO -Gly-Pro-Hyp

GPRP -Gly-Pro-Arg-Pro

hemITAM - hemi-immunoreceptor tyrosine-based activation motif

IC50 -half maximal inhibitory concentration

HPF-hours post fertilization

Ig -immunoglobulin

IP_3 - inositol-1,4,5-trisphosphate

JAK2 - Janus kinase 2

KCL-Potassium chloride

LAT - Linker of Activated T cells

LB - Luria-Bertani broth

LEC - Lymphatic endothelial cells

LTA -light transmission aggregation

Lyve^{1+}- lymphatic vessel endothelial hyaluronan receptor 1-positive

M -Molar

mg -Milligram

Mg^{2+} -Magnesium ion

$MgCl_2$ -Magnesium chloride

$MgSO_4$-Magnesium sulfate

Mins -Minutes

mL -Millilitre

mm- Millimolar

µg -Microgram

µL -Microliter

µM -Micromolar

NaCl -Sodium chloride

NFAT - Nuclear factor of activated T cells

nM -Nanomolar

NO -Nitric Oxide

PAR- Protease-activated receptors

PBA -Plate-based aggregation

PBS - Phosphate buffered saline

PCR -Polymerase Chain Reaction

PCV - Posterior cardinal vein

PGI2 - Prostacyclin

PI3K - phosphoinositide 3 -kinase

PIP2 - phosphoinositide-4,5-bisphosphate

PIP3- phosphoinositide-3,4,5-trisphosphate

PH -pleckstrin homology

PKC - Protein kinase C

PLCβ -Phospholipase β

PLCγ1- Phospholipase C gamma 1

PLCγ2 - Phospholipase C gamma 2

Prox1- prospero-related homeobox 1

PRP - Platelet rich plasma

PVDF -polyvinylidene fluoride

pY -phosphotyrosine

R - Resting

RIPA buffer - Radioimmunoprecipitation assay buffer

RPM-Revolutions per minute

RPMI -Roswell Park memorial institute

SD- Standard deviation

SDS -sodium dodecyl sulphate

SDS-PAGE -sodium dodecyl sulphate polyacrylamide gel electrophoresis

SEM- standard error of the mean

SFK -Src family kinase

SH2 - Src homology 2

SH3 - Src homology 3

SHIP - SH2-containing inositol-5 phosphatase-1

SLP-76 -SH2 domain containing leukocyte protein of 76kDa

Syk -spleen tyrosine kinase

TAE - Tris Acetate EDTA

TBST -tris buffered saline with tween

TD - thoracic duct

TXa2 -thromboxane

V -volts

VEGF - Vascular endothelial growth factor

Veh / V -vehicle

v/v -Volume/Volume

VWF -von Willebrand Factor

w/v -Weight/Volume

XLA - X-linked agammaglobulinemia

Y -tyrosine

Contents:

i.List of figures

ii.List of tables:

Chapter 1: Introduction

1.1 Platelets

Platelets are anucleate small blood cells that are generated from megakaryocytes and circulate in the human blood for 5-10 days (Thon and Italiano, 2012, Yun et al., 2016) (Morrell et al., 2014). The platelet count typically lies between the usual range of 150 - 450x10^3 platelets/μL of blood in healthy persons, making them the second most numerous blood cells (Seyoum et al., 2018). Although platelets have a major role in haemostasis and thrombosis, recent evidence suggests that platelets have several other roles in lymphatic development, enhancing immune responses, and advancement of cancer metastasis (Golebiewska and Poole, 2015, Rodvien and Mielke, 1976, Welsh et al., 2016, Josefsson et al., 2020).

Platelets remain inactive until blood vessel damage triggers their activation and consequently form a haemostatic thrombus leading to the prevention of bleeding. Due to red blood cells and shear forces, platelets flow closely to the vessel wall which enables a quick response at the injury site. Upon vessel injury, several receptors help platelets to adhere to the sub-endothelial matrix that will lead to platelet tethering and rolling. Upon platelet adhesion, a signalling cascade is initiated and facilitated by tyrosine kinases and G-coupled receptors to mediate platelet activation (Broos et al., 2011).

Upon vessel damage, the components of the extracellular matrix such as collagen, laminin, and fibronectin are exposed and lead to the initiation of hemostasis (Yurchenco, 2011). Under high shear, von Willebrand Factor (vWF), that is found in the blood or released by endothelial cells, binds to GPIbα on the platelet surface and

to collagen in the subendothelial matrix providing a link between platelet glycoprotein Ib/V/IX and collagen. This binding is crucial for initial platelet tethering and adhesion under high shear (Broos et al., 2011). In addition, α2β1 and glycoprotein VI (GPVI) also bind to exposed collagen inducing a stable adhesion and initiation of platelet signalling (Ma et al., 2007). Activated platelets then secrete the contents of alpha granules such as fibrinogen, more vWF, factor V, the contents of the dense granules including serotonin, adenosine diphosphate (ADP), and calcium (Ca^{2+}) (Blair and Flaumenhaft, 2009). Platelet activation triggers conformational change of αIIbβ3 which increases its affinity for fibrinogen and vWF leading to aggregation. Then fibrinogen and vWF function as a bridge between platelets (Lefkovits et al., 1995). As platelets begin to aggregate, more pro-haemostatic compounds are released leading to the activation of more platelets and therefore more aggregation. This eventually leads to the formation of the platelet plug (Figure 1.1) (Hawiger, 1987).

A last step is required to stabilise the platelet plug into a thrombus after it has been initiated by one of the commonly mentioned platelet activation processes. The reorganisation of the cytoskeleton occurs when fibrinogen is attached to αIIbβ3, which starts the outside-in signalling process. Due to this, clot retraction occurs which ultimately results in the haemostatic plug being more stable (Payrastre et al., 2000). The coagulation cascade is initiated as the platelets activate and the plug forms. This process activates coagulation factors, which results in stabilising the clot. The conversion of soluble fibrinogen into insoluble fibrin threads can then be facilitated by the cleavage of prothrombin to thrombin (Kim et al., 2009). Through creating a mesh-like network on aggregated platelets, the fibrin network ensures that the clot maintains its structural stability (Risman et al., 2024).

On the other hand, platelet activation and abnormal thrombus formation in the circulatory system, such as atherosclerotic plaques, contribute to the development and risk of cardiovascular disease (Willoughby et al., 2002). When arterial thrombus development occurs in pathological situations such as atherosclerosis, it has the potential to restrict the blood supply to neighbouring tissues, which can result in localised ischemia and the progression of the atherosclerotic plaques (Badimon et al., 2012). The important role of platelets in these conditions is highlighted by the fact that an expanding number of anti-platelet medications is being used in the treatment of the diseases. Therefore, it is crucial to understand the mechanisms involved in platelet activation to allow the development of novel drugs.

1.2 Platelet structure

Out of all the different cell types circulating the blood, platelets are the smallest cells with an average 2 to 5 μm diameter and 0.5 μm in thickness (White, 2013). When at rest, the disc shape of platelets is maintained by a highly specialised cytoskeleton which contains the actin cytoskeleton, the spectrin based membrane skeleton, and the marginal microtubule coil (Schwer et al., 2001). The phospholipid bilayer that makes up the plasma membrane contains embedded glycolipids, glycoproteins, and cholesterol. The plasma membrane contains several receptors such as adhesion receptors, integrins and G-protein coupled receptors that allow interactions with ligands (Rivera et al., 2009). The wide range of physiologically active molecules contained in platelet granules is one of the most interesting features of these blood cells. Platelets possess two types of granules that are located in the cytoplasm: α granules and dense granules (Flaumenhaft, 2003). The α granules contain several

molecules including fibrinogen, fibronectin, and von Willebrand factor (vWf) (Harrison and Cramer, 1993). In addition, the α granules contain multiple membrane bound receptors such as P-selectin, αIIbβ3, GPIb-IX-V complex, and GPVI (Berger et al., 1996, Thomas, 2019).

Dense granules on the other hand tend to be less abundant than alpha granules. Dense granules are responsible for the secretion of a wide range of molecules, which are released when platelets are activated. These include serotonin, Ca^{2+}, Mg^{2+}, adenosine 5' triphosphate (ATP), and adenosine 5' diphosphate (ADP) (Meyers et al., 1982).

1.3 Shape change and platelet spreading

Platelet activation and function depend on a complex mechanism that changes the morphology of platelets. As previously stated, when at rest, platelets maintain a discoid shape. However, upon platelet activation with agonists, platelets undergo a transformation from a disc shape into spherical shape. Discoid platelets undergo cytoskeletal modifications, such as the breakdown of a microtubule ring, to achieve the spherical form during platelet shape transition. Disassembly of a microtubule ring is one among the cytoskeletal alterations that discoid platelets go through during platelet shape change, leading to an intermediate spherical form. Subsequently, actin polymerization occurs, leading to the gradual elongation of filopodia allowing platelets to flatten and spread (Deranleau et al., 1982, Hantgan, 1984, Bearer, 1995). Shape change initiation and phosphorylation of the regulating myosin light chain are strongly correlated, according to earlier studies (Daniel et al., 1984). Actin filament interaction and polymerization of platelet myosin are correlated with agonist-

dependent phosphorylation of the protein (Cox et al., 1984, Lebowitz and Cooke, 1978, Scholey et al., 1980).

Another key mediator involved in platelet shape change is ADP. The initiation of platelet shape change by ADP is the result of a complex interplay between molecular events and signalling pathways. Platelets change their shape, secrete the contents of their granules, and generate thromboxane A2 in response to ADP stimulation (Jin and Kunapuli, 1998). One of the primary receptors mediating ADP-induced platelet aggregation is the purinoceptor P2Y1, which is also essential for platelet shape change in response to ADP (Fabre et al., 1999). P2Y1 and P2Y12 are G-protein coupled receptors (GPCRs) that, when bound by ADP, initiate signalling pathways that lead to calcium mobilisation and aggregation. While P2Y12 receptors bind to Gi proteins, amplifying and stabilising the aggregation response, P2Y1 begins ADP-mediated shape change and platelet aggregation via Gq proteins causing a transitory increase in cytoplasmic Ca^{2+}(Jin and Kunapuli, 1998).

1.4 Calcium Release

The activation of platelets is induced by several agonists such as ADP, collagen, and thromboxane (TxA2) that eventually lead to an increase in the concentration of intracellular calcium. In platelets, calcium plays a part in platelet aggregation by degranulation or inside-out activation of integrin αIIbβ3 , and shape change (Varga-Szabo et al., 2009). Calcium release from intracellular stores requires the activation of phospholipase C (PLC) and in platelets there are two PLC isoforms: PLCγ and PLCβ. When activated, PLCγ2 hydrolyses phosphoinositide-4,5- bisphosphate (PIP2), producing inositol-1,4,5-trisphosphate (IP_3) and 1,2-diacyl-glycerol (DAG) (Bird et al., 2004). IP_3 causes calcium to be released form intracellular stores,

whereas DAG is responsible for the entry of calcium from the extracellular compartment. Protein kinase C (PKC) is also activated by DAG, which, in conjunction with a rise in calcium, results in degranulation and a change in the conformation of αIIbβ3 (Berridge et al., 2003, Bird et al., 2004).

Calcium and PKC play a crucial role in platelet activation, especially in αIIbβ3 activation. This is essential for both, platelet aggregation and thrombus formation. When platelets are stimulated and activated by agonists, this initiates a signalling cascade that result in the increase of the intracellular calcium (Stefanini et al., 2009, Liu et al., 2023). A highly controlled mechanism involving inside-out signalling is involved in the activation of integrin αIIbβ3. When platelets are at rest, integrin αIIbβ3 has a low affinity, but when activated, it conforms to a high affinity state. The binding of talin to the cytoplasmic tails of αIIb subunits and kindlin to the β3 subunits correspondingly facilitates this transition. This mechanism is enhanced by raised intracellular Ca^{2+} levels and PKC activity (Kasirer-Friede et al., 2014).

A number of cytoskeletal and signalling proteins are phosphorylated when calmodulin-dependent kinases are activated by direct Ca^{2+} binding to calmodulin (Beck et al., 2014). Integrin activation is affected by many proteins that are phosphorylated by PKC. As an example, the talin-integrin connection is stabilised when the cytoskeletal protein vinculin is phosphorylated by PKC, which increases its binding affinity for talin(Perez-Moreno et al., 1998).

Furthermore, phosphorylation of the cytoplasmic tail of β3 integrin by PKC enhances its ability to interact with other adaptor proteins, which in turn promotes integrin clustering and high-affinity ligand binding. This integrin activation allows fibrinogen

and other ligands to bind, hence mediating platelet-platelet interactions and forming a stable thrombus (Shattil and Newman, 2004).

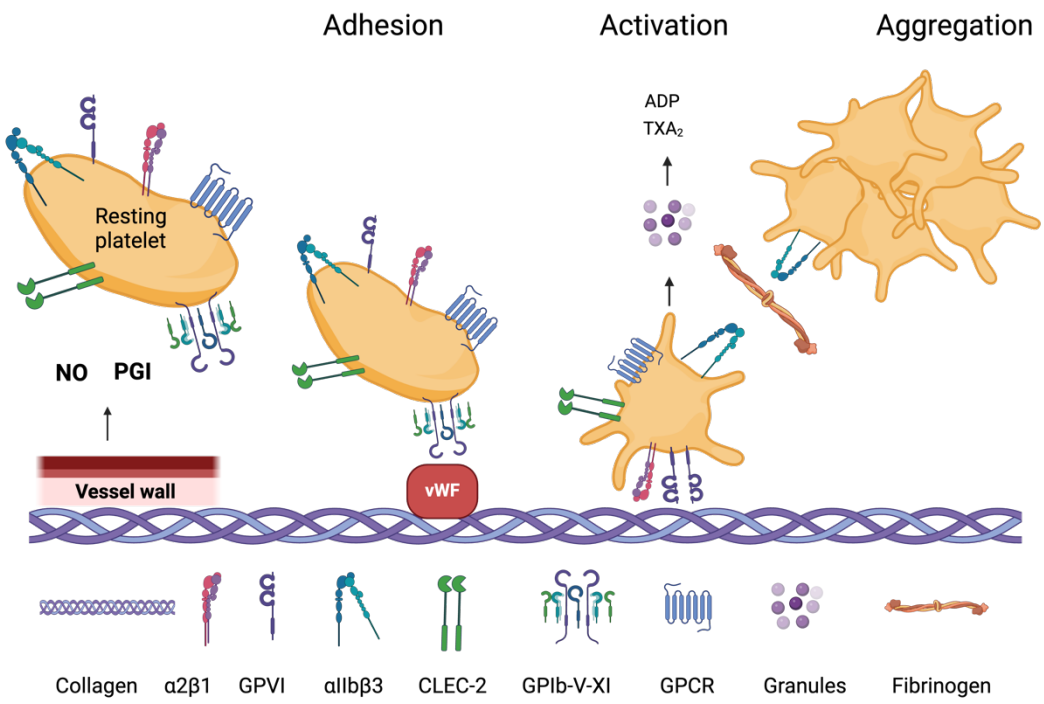

Figure 1.1: Schematic diagram of platelet adhesion, activation and aggregation.

Platelets are maintained at rest by nitric oxide (NO) and prostacyclin (PGI) released from endothelial wall. Upon injury, Von Willebrand factor (vWF) and collagen are exposed. High shear causes interaction between vWF and GPIb-V-XI complex allowing platelet tethering. This slows down platelets and enable α2β1 and GPVI interaction with collagen. This firm adhesion results in a and dense granule secretion and release of TxA2 and ATP. This in turn lead to activation of GPCRs and integrin αIIbβ3. αIIbβ3 binds to fibrinogen which results in forming a thrombus.

1.5 GPVI

1.5.1 Structure

Immunoreceptor-tyrosine-based activation motif (ITAM) containing proteins are an important group of platelet receptors. The ITAM, which consists of two Yxx(L/I) sequences spaced 6-12 amino acid residues apart, is found in the intracellular domain (Gibbins et al., 1997). There are three ITAM-linked receptors in human platelets: the Fc receptor γ chain which is associated with GPVI (GPVI/FcRγ), FcγRIIA, and C-type lectin-like receptor-2 (CLEC-2) which has a hemITAM; a single YxxL motif (Hughes et al., 2013).

Examining the signalling events that trigger platelet activation through collagen led to the identification of GPVI as the main signalling receptor (Clemetson et al., 1982). GPVI is a 62 kDa collagen-based receptor (Jung and Moroi, 2008) with 3000-4000 copies expressed on the human platelet surface (Mangin et al., 2012). Human GPVI consists of 319 amino acids with a signal sequence that has 20 amino acids (Clemetson et al., 1999, Miura et al., 2000, Jandrot-Perrus et al., 2000).
With only 51 amino acids, human GPVI's intracellular domain (C-terminus) is on the short side, but this is even shorter in mice where the GPVI intracellular domain is just 27 amino acids (Best et al., 2003) (Nieswandt and Watson, 2003, Moroi and Jung, 2004). In addition, the intracellular domain of GPVI has a region that is rich in proline, which allows the SH3 domains of the Src family kinases Fyn and Lyn to attach themselves via their SH3 domain (Ezumi et al., 1998, Suzuki-Inoue et al., 2002). A salt bridge between an Aspartic acid and an Arginine in the transmembrane domains of FcRγ and GPVI, respectively, allows GPVI to form a receptor complex with the Fc receptor FcRγ chain (Berlanga et al., 2002). The GPVI-FcRγ receptor

complex contains an immunoreceptor tyrosine-based activation motif (ITAM) and is a feature which FcRγ-chain shares with B cells and T cell receptors (Clemetson et al., 1999).

GPVI belongs to the immunoglobulin superfamily (Tsuji et al., 1997) and has two Ig domains, D1 and D2 within the extracellular region. These two domains are connected by a linker region and are connected to the cytoplasmic tail via glycosylated stalk region (Bori-Sanz et al., 2003). Both monomers and dimers of GPVI can be found on the surface of platelets (Miura et al., 2002). On resting platelets, the monomeric form predominates and has a reduced functional affinity for binding collagen (Jung et al., 2012). In contrast, the dimeric form is more frequent on activated platelets. Additionally, it has been discovered that GPVI may assemble into oligomers on the surface of platelets, and that the different degree of GPVI clustering is determined by different GPVI agonists (Poulter et al., 2017). Therefore, the recruitment of signalling molecules necessary for GPVI signal transduction may be aided by this development of oligomers.

1.5.2 GPVI ligands

As previously stated, collagen is the key endogenous ligand for GPVI, which is crucial for platelet function and haemostasis. Although the vasculature contains nine different forms of collagen, only types I and III form big fibrils and bind GPVI with higher affinity. Through the GPIb-IX-V complex and immobilised von Willebrand factor, platelets are able to bind themselves to exposed collagen fibres when they are subjected to significant shear stress. As a result of this tethering, collagen is able to establish a connection with the low-affinity GPVI receptor complex. This

connection, in turn, provides intracellular signals that activate integrins, such as α2β1 and αIIbβ3, from the inside out, and further clusters GPVI. By attaching α2β1 to collagen and αIIbβ3 to VWF, these interactions increase the activation of GPVI and promote secure attachment and spread (Watson et al., 2000, Nieswandt et al., 2001a).

While collagen is an endogenous ligand for GPVI, the exogenous ligand collagen-related peptide (CRP) was found to mimic collagen and has 10 repetitions of the Gly-Pro-Hyp (GPO) sequence which might cause platelet aggregation, regardless of α2β1(Morton et al., 1995). CRP was shown to react selectively with GPVI and to activate tyrosine-phosphorylation in platelets in a way comparable to collagen (Asselin et al., 1997).

Similar to collagen, fibrin is another endogenous ligand that triggers the GPVI signalling cascade through tyrosine phosphorylation (Alshehri et al., 2015a). Fibrin, unlike collagen, can recognise both monomers and dimers of GPVI (Mammadova-Bach et al., 2015). In addition, previous research has recognised that recombinant dimeric GPVI had the ability to attach to fibrin. This finding was subsequently validated by using platelets that lacked GPVI, which also demonstrated a decrease in procoagulant activity (specifically, the polymerization of fibrinogen) (Mammadova-Bach et al., 2015).

On another note, fibrinogen has been suggested as a potential endogenous ligand for GPVI. This was established by observing that platelets lacking GPVI were unable to spread on fibrinogen. Additionally, unlike wild-type (WT) mouse platelets, human-

GPVI-transgenic mouse platelets spread on fibrinogen (Mangin et al., 2018) potentially highlighting the difference between mouse and human platelet biology.

1.5.3 GPVI signalling

GPVI signalling is initiated upon its binging to collagen, CRP, or other ligands leading to receptor clustering. Following GPVI clustering, the Src Family kinases (SFK) Lyn and Fyn phosphorylate the FcRγ -chain ITAM (Ezumi et al., 1998, Quek et al., 2000). This leads to recruiting and activating the cytosolic tyrosine kinase Syk through its tandem SH2 domains to the ITAM (Chen et al., 1996) and is phosphorylated by SFKs (Kurosaki et al., 1994) which in turn promotes the phosphorylation of the adaptor protein Linker of Activated T cells (LAT), and the recruitment of adaptor proteins such as SH2 domain containing leukocyte protein of 76kDa (SLP-76) that form a LAT signalosome. The LAT signalosome plays a crucial role in phospholipase C γ2 (PLCγ2) recruitment, and the SH2 domain of LAT provides docking sites for PLCγ2 through its phosphotyrosine residues (Watanabe et al., 2001). After Syk phosphorylates LAT, the adaptor proteins SLP-76, Gads, and Grb2 are recruited (Asazuma et al., 2000, Gross et al., 1999, Hughes et al., 2008). Upon activation, PI3K is recruited to the signalosome and catalyses PIP2 into PIP3 which leads to the recruitment of Btk and PLCγ2. Either SFK or Syk lead to the phosphorylation of Btk. Phosphorylated Btk and Syk will initiate the activation of PLCγ2 (Mazharian et al., 2010). Although both SFKs and Syk may phosphorylate PLCγ2 (Liao et al., 1993, Rodriguez et al., 2001), Btk is believed to be the primary kinase that regulates PLCγ2 phosphorylation (Quek et al., 1998). Following its activation, PLCγ2 hydrolyses PIP2 to IP_3 and DAG. The IP_3 then binds the IP_3 receptors found in the

endoplasmic reticulum and leads to the release of calcium (Figure 1.2) (Kaibuchi et al., 1983, Werner et al., 1992).

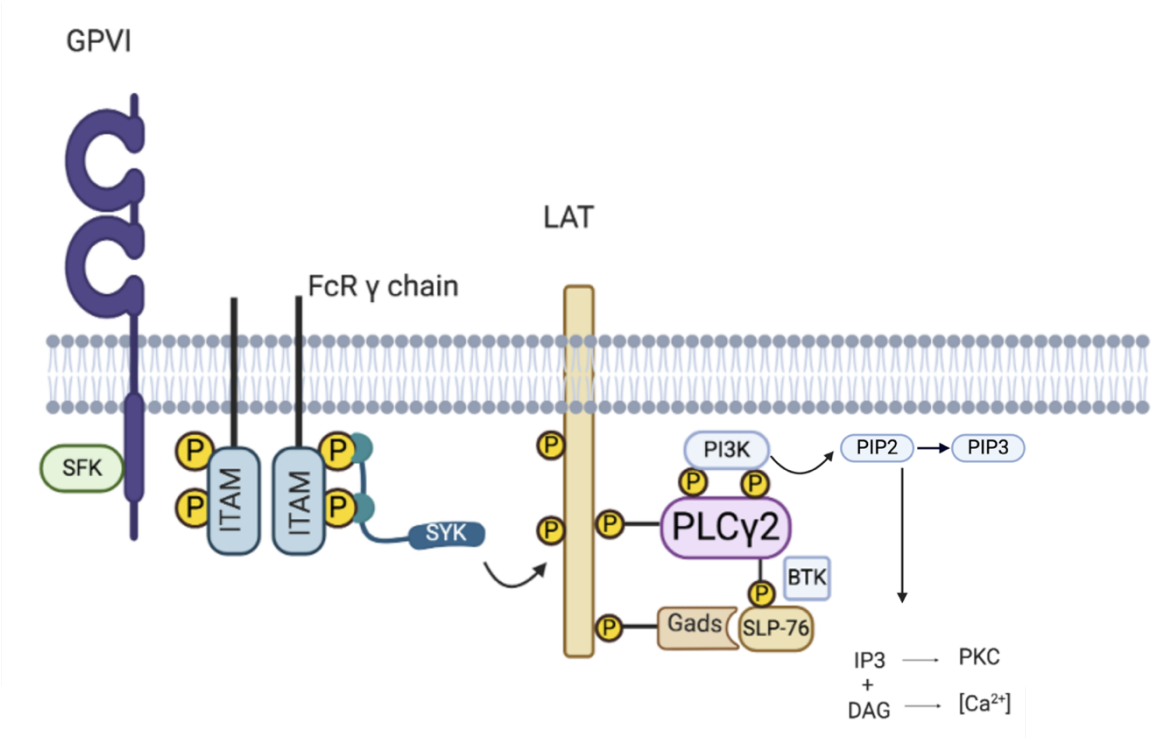

Figure 1.2: GPVI signalling pathway.

Agonist binding leads to GPVI clustering. This results in phosphorylating SFK that in turns phosphorylate the ITAM in the FcR γ -chain leading to Syk activation. Syk promotes LAT phosphorylation which recruits Gads and SLP-76 forming a LAT signalosome. PI3K is also phosphorylated and catalyses PIP2 to PIP3 that in turn recruits Btk and PLCγ2. Phosphorylated Btk and Syk mediate PLCγ2 activation. PLCγ2 hydrolyses PIP2 to IP_3 and DAG.

1.5.4 GPVI function

GPVI has always been perceived to play a main role in preventing blood loss after an injury. Although in literature, GPVI has been portrayed as a key player in platelet activation and primary haemostasis (Arthur et al., 2007), this illustration of GPVI and its main role in haemostasis is not supported in human and mouse phenotypes that lack GPVI (Michelson et al., 2019).

Although GPVI deficient patients have slightly prolonged bleeding time and lack of response to collagen, they usually have normal platelet number and size (Sugiyama et al., 1987). It was observed that patients that do not express GPVI due to mutations in the GP6 gene, have only minor bleeding diathesis (i.e. tendency to bruise or bleed) which indicates a change in haemostasis (Arthur et al., 2007).
To determine whether GPVI is essential for hemostasis, previous studies have examined the bleeding time in mice. There has been conflicting evidence on the bleeding time in GPVI deficient mice. Mice treated with an anti-GPVI antibody displayed a slightly prolonged bleeding time (Nieswandt et al., 2001b). Whereas null mice, according to another group, have a normal bleeding time (Kato et al., 2003). This could imply that whereas GPVI may be essential for hemostasis in some, it may not be in others.

GPVI is a substantial factor to the development of arterial thrombosis (Massberg et al., 2003). Under flow conditions *in vitro*, platelets isolated from GPVI deficient individuals failed to adhere to collagen (Moroi et al., 1996). Similar results were also seen in mice. Normal and large thrombi were observed in blood isolated from WT GPVI mice whereas mice lacking either GPVI or FcRγ had significantly smaller thrombi on collagen (Kato et al., 2003). The role GPVI plays in thrombus formation *in vivo* was further investigated by Alshehri et al. Using an $FeCl_3$ injury model in GPVI deficient mice, the authors showed that the lack of GPVI led to a significant delay or lack of occlusion and constant thrombus embolisation in contrast to WT mice where after 20 minutes full occlusion was observed (Alshehri et al., 2015a) .

On another note, GPVI has been linked to cancer metastatic progression suggesting its role in non-haemostatic functions. This was highlighted by the ability of GPVI to bind to galectin 3, a protein expressed in colon cancer cells (HT29) containing a collagen matrix (Dovizio et al., 2013). A number of processes that are associated with the development of cancer can be affected by prostanoids that are generated by cyclooxygenase (COX)-2. This study shows that abnormal COX-2 expression was prevented by GPVI receptor inhibitors, and galectin-3 function inhibitors (Dovizio et al., 2013). These findings provide more evidence that GPVI-mediated inhibition of collagen binding sites could play a significant role in controlling colon cancer spread.

It has been previously established that platelets have also an additional role in preserving the structural integrity of blood vessels (Watson et al., 2010). This was established by Kitchens and Weiss where endothelial thinning was demonstrated in rabbits rendered thrombocytopenic by an antiplatelet antiserum (Kitchens and Weiss, 1975). It was also observed that thrombocytopenia is often accompanied by petechiae, which form when red blood cells leak out of the endothelium layer through the open channels (Aursnes and Pedersen, 1979). This process is mediated by and maintained by platelets and GPVI respectively (Watson et al., 2010). It was speculated that the GPVI can bind to its agonists within the endothelial, collagen and laminin, when the layer is ruptured leading to its activation. The release of the α granules as a result stimulates proliferation of lymphatic endothelial cells facilitating the repair of the damaged endothelial layer (Boulaftali et al., 2013, Kisucka et al., 2006).

Thromboinflammation is a medical condition defined by abnormal thrombotic and inflammatory responses which lead to organ damage. Furthermore, it implies that platelets have a role in vascular-related inflammation, which is commonly found in the microcirculation (Jackson et al., 2019). The activation of coagulation is believed to be the driving force behind the thromboinflammatory process and anticoagulant medications have been found to be useful, but with potential bleeding effects (Fan et al., 2016).

In thromboinflammation, GPVI is involved in two processes. It has a major effect on inflammation and is essential for the thrombotic response. For example, GPVI-mediated platelet activation may aggravate atherosclerosis, through stimulating the development of thrombus on ruptured plaques and the release of pro-inflammatory cytokines, which intensify the inflammatory process (Jamasbi et al., 2015). The therapeutic potential of targeting GPVI stems from its ability to reduce both clot formation and inflammation without totally eliminating the platelet's critical function in normal haemostasis. Also, these drugs may reduce the inflammatory aspect of thromboinflammation by lowering platelet production of pro-inflammatory cytokines.

1.6 CLEC-2

In 2000, C-type lectin 2 was identified in a bioinformatics screen for natural killer receptors (Colonna et al., 2000). CLEC-2 was subsequently identified in platelets using the snake venom rhodocytin (Suzuki-Inoue et al., 2006). Then, the identification of its endogenous ligand, podoplanin, in 2007 made CLEC-2 of huge interest (Suzuki-Inoue et al., 2007). CLEC-2 plays several roles in the regulation of inflammatory responses, thrombosis, haemostasis, liver regeneration, and reducing

cholestatic liver damage (Mourão-Sá et al., 2011, Kono et al., 2017, Maruyama et al., 2020).

1.6.1 Structure

CLEC-2 is a 32 kDa type II transmembrane protein that was initially recognised in immune cells (Colonna et al., 2000, Sobanov et al., 2001). There are between 2000-4000 copies of CLEC-2 expressed in human platelets (Gitz et al., 2014) whereas CLEC-2 is expressed 10 times more (around 40,000) in mouse platelets (Zeiler et al., 2014). CLEC-2 consists of 229 amino acids and contains 3 domains: N-terminal intracellular domain, transmembrane domain, and C-terminal extracellular domain (Gitz et al., 2014). Unlike GPVI, CLEC-2 contains a hemITAM - a single YxxL motif within its intracellular domain (Hughes et al., 2013), but the signalling pathway is similar to GPVI. The extracellular domain is made up of a stalk region and a carbohydrate-like recognition domain (CTLD) which is so called such due to the fact it lacks the conserved amino acids needed to attach to carbohydrates (Colonna et al., 2000) .

On resting platelets, CLEC-2 is found as a dimer (Hughes et al., 2010b) and upon ligand binding with either its endogenous ligand (podoplanin) or exogenous ligand (rhodocytin), CLEC-2 dimers cross-link leading to the clustering of the receptor (Suzuki-Inoue et al., 2011, Suzuki-Inoue et al., 2018).

1.6.2 CLEC-2 ligands

CLEC-2 has several ligands that have been previously identified in the literature. This includes podoplanin, rhodocytin, hemin, and fucoidan. Rhodocytin, also referred

to as aggretin, was the first exogenous CLEC-2 ligand that was identified. It was isolated in the late 1990s from the venom of the Malayan pit viper *Calloselasma rhodostoma* (Huang et al., 1995, Shin and Morita, 1998). After it was discovered that the snake toxin could cause strong platelet aggregation through a pathway that was dependent on the Src family kinase, researchers started looking for a receptor for rhodocytin. Initially, it was believed that rhodocytin would operate as a mediator for platelet activation through the collagen receptor $\alpha 2\beta 1$. This assumption was made on the basis of the ability of large doses of antibodies against the integrin to inhibit activation (Suzuki-Inoue et al., 2001). However, this hypothesis was questionable due to fact that other evidence did not find any binding between recombinant or wild type $\alpha 2\beta 1$ that has been isolated from platelets and immobilised rhodocytin (Eble et al., 2001). According to Shin and Morita, rhodocytin is shown to form a tetramer, which is comprised of two α chains and two β chains (Shin and Morita, 1998). Along with the tyrosine phosphorylation of CLEC-2, many of the signalling molecules shared with the GPVI signal transduction pathway are triggered by rhodocytin (Parguiña et al., 2012). Furthermore, it is worth noting that rhodocytin has the ability to cause platelet aggregation, marked by a distinct lag phase. This aggregation is reliant on the presence of SFKs, Syk, and PLCγ2 (Suzuki-Inoue et al., 2007). There is a possibility that the distinctive lag phase corresponds to the amount of time necessary for the clustering of CLEC-2.

The fact that podoplanin-expressing tumour cells cause platelet aggregation in a way that is remarkably similar to that of rhodocytin played a significant role in the identification of podoplanin as an endogenous ligand for CLEC-2 (Suzuki-Inoue et al., 2007). The expression of podoplanin can be seen on cells that are not part of the

blood vasculature, such as kidney podocytes, lymphatic endothelial cells, choroid plexus cells, and lung epithelial cells (Breiteneder-Geleff et al., 1999). Although the Podoplanin-CLEC-2 connection is likely unimportant in traditional primary haemostasis and arterial thrombosis, it may have a significant impact in several other diseases (Suzuki-Inoue et al., 2010). Similarly to rhodocytin, podoplanin-mediated platelet aggregation depends on Src family kinases and PLCγ2, and it is also preceded by a lag phase (Chang et al., 2015, Christou et al., 2008).

Additionally, fucoidan has been identified as a potential exogenous ligand for CLEC-2. Fucoidan is a type of sulphated polysaccharide that is mainly found in several species of seaweed, such as *Fucus vesiculosus*. According to Manne et al., fucoidan does indeed cause platelets to aggregate and secrete granules. It is suggested that this agonist acts similarly to a (hem)ITAM agonist since phosphorylation of Syk, LAT, SFK, and PLCγ2 is also seen, and it is eliminated when treated with an inhibitor of SFK and Syk (Manne et al., 2013). It was observed that at low doses of fucoidan, the aggregation was lost in the CLEC-2 knockout mouse platelets, but not in the GPVI knockouts. Nevertheless, CLEC-2 knockout mice still show some aggregation when exposed to higher fucoidan concentration, which indicates that additional receptors play a role in the activation of platelets stimulated by fucoidan (Manne et al., 2013). Furthermore, even at high doses of fucoidan, platelet aggregation was eliminated in a double knockout model of CLEC-2 and GPVI (Alshehri et al., 2015b). These findings indicate the possibility that fucoidan can activate platelets through CLEC-2 and, to a lesser extent, GPVI. On the other hand, according to recent studies, fucoidan does not have the same phosphorylation pattern as rhodocytin i.e. there

was a lack of phosphorylation of important tyrosine residues in Syk and PLCγ2 (Kardeby et al., 2019).

Hemin, or the ferric Fe^{3+} form of heme, is a by-product of intravascular homolysis and has recently been found to be an agonist of CLEC-2. The process of aggregation, granule release, and activation of αIIbβ3 were all induced by hemin. Additionally, when human recombinant dimeric forms of GPVI (hFc-GPVI) were preincubated with hemin, platelets could still aggregate, but not with hFc-CLEC-2, identifying CLEC-2 as the hemin receptor (Bourne et al., 2021).

1.6.3 CLEC-2 signalling

HemITAMs and ITAMs signal in a similar manner sharing several kinases in common. As previously described, CLEC-2 is found as a dimer and upon ligand binding with either its endogenous ligand (podoplanin) or exogenous ligand (rhodocytin) (Shin and Morita, 1998), leads to the clustering of the receptor (Hughes et al., 2010b). This leads to the tyrosine phosphorylation of the hemITAM by Src family kinases resulting in the activation of Syk (Suzuki-Inoue et al., 2018). However, other studies have shown that SFKs regulate Syk and Syk is responsible for CLEC-2 phosphorylation and signal transduction (Séverin et al., 2011, Spalton et al., 2009, Hughes et al., 2015). Similarly to GPVI, the activation of Syk leads to a signalling cascade that results in the phosphorylation and activation of LAT, SLP-76, and eventually PLCγ2. The phosphorylation of the LAT adaptor protein by Syk is responsible for its interaction with PI3K and PLCγ2 through their SH2 domains (Moroi and Watson, 2015). Btk and Tec are recruited following the conversion of PIP2 into PIP3 by active PI3K (Hyvönen and Saraste, 1997). Platelet activation

mediated by CLEC-2 requires Btk as opposed to GPVI mediated signalling. This was demonstrated by Nicolson et al., when their results displayed that the Btk kinase activity is essential downstream of CLEC-2 but not GPVI. GPVI mediated platelet function was blocked by 20 times higher concentration of Btk inhibitors that those inhibiting CLEC-2 mediate platelet activation. The reason for this selectivity is that GPVI does not require Btk kinase activity, while human platelet CLEC-2 does.(Nicolson et al., 2021). PLCγ2 hydrolyses PIP2 to IP_3 and DAG leading to calcium release and PKC activation (figure 1.3) (Berridge et al., 2003). As a result, the contents of dense granules and α-granules are secreted and the activation of integrin αIIbβ3 through inside-outside signalling causes platelet aggregation (Ma et al., 2007).

In addition, a difference between CLEC-2 and GPVI in regard to signalling events downstream of Syk is that GPVI absolutely requires SLP-76 whereas in its absence high concentrations of rhodocytin can still facilitate weak activation (Suzuki-Inoue et al., 2011, Fuller et al., 2007). Also, unlike GPVI, it has been previously established that CLEC-2 is reliant on the secondary mediators (TxA2 and ADP), where the inhibition of ADP and TxA2 production led to the reduction of CLEC-2 phosphorylation (Pollitt et al., 2010).

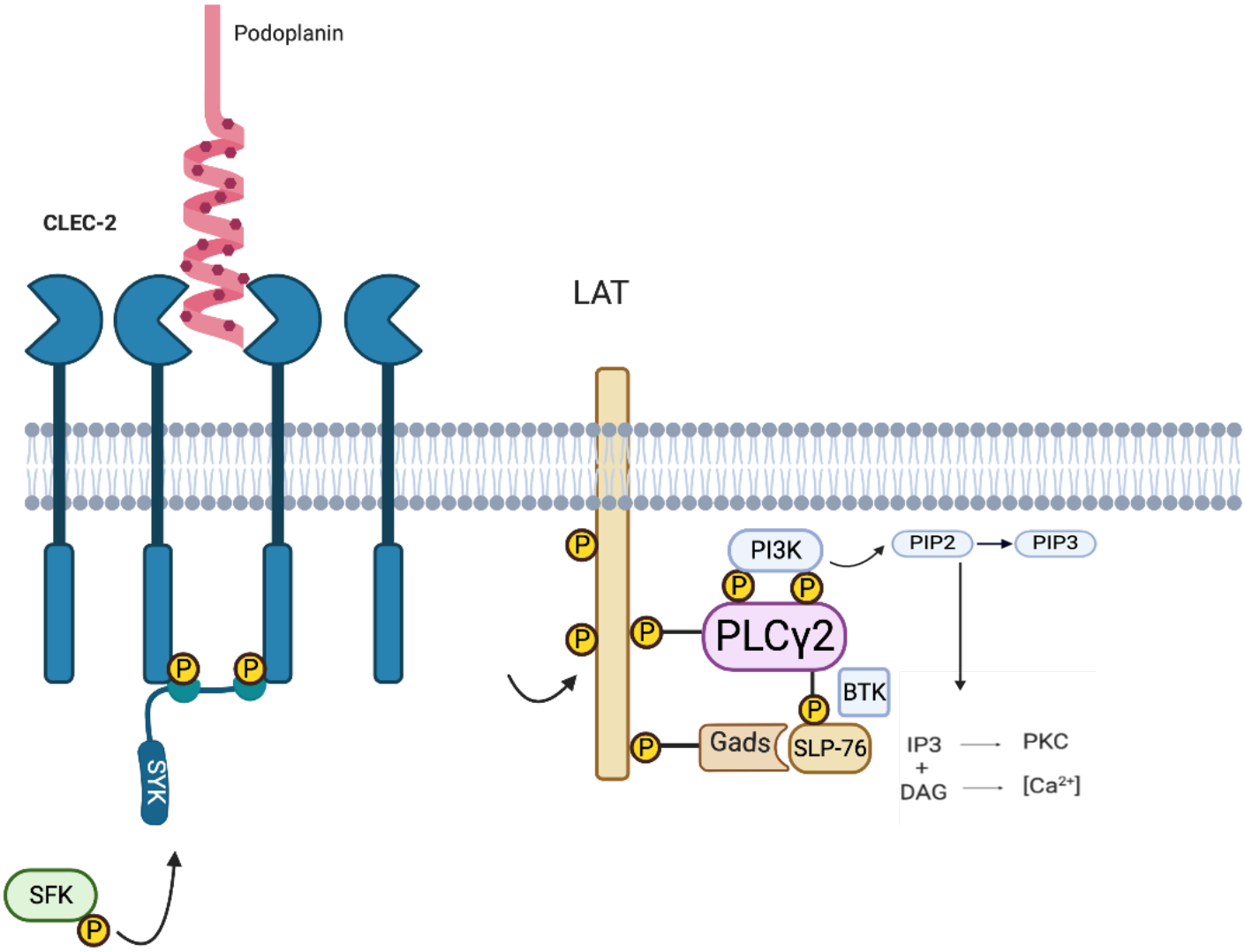

Figure 1.3: CLEC-2 signalling pathway

Agonists bind to CLEC-2 leading to clustering allowing Syk to bind to the phosphorylated hemITAM. SFK phosphorylate Syk which leads to LAT phosphorylation that results in the activation of SLP-76 and Gads. PI3K is also phosphorylated and catalyses PIP2 to PIP3 that in turn recruits Btk and PLCγ2. SFK and Syk phosphorylate Btk. Phosphorylated Btk and Syk mediate PLCγ2 activation. PLCγ2 hydrolyses PIP2 to IP_3 and DAG leading to calcium release and PKC activation.

The role CLEC-2 plays in haemostasis and thrombosis is questionable. May et al., examined the role of CLEC-2 by producing platelets lacking CLEC-2. This was carried out *in vivo* by administering an anti-CLEC-2 antibody. By measuring platelet aggregation, their results have demonstrated that the CLEC-2 deficiency completely abolished platelet aggregation induced by rhodocytin. However, platelet aggregation

in response to other agonists such as collagen and thrombin was not affected in the absence of CLEC-2 (May et al., 2009). Nonetheless, different results were observed when examining the effect of CLEC-2 depletion on thrombus formation under flow. Thrombus formation was examined using a $FeCl_3$ injury model. Their results have shown that under flow, CLEC-2 deficient platelets were able to adhere, yet aggregate formation and stability was reduced. This suggests that CLEC-2 plays a role in mediating stable thrombus formation. This study has also examined whether CLEC-2 has an effect on bleeding time in mice. Indeed, mice lacking CLEC-2 had an extended bleeding time in comparison to control mice (May et al., 2009).

Furthermore, the role of CLEC-2 in thrombus formation was examined by Suzuki et al using laser injury models in genetically modified CLEC-2 deficient mice. Upon laser injury of the mesenteric capillaries, CLEC-2 deficient mice failed to form a stable thrombus in comparison to WT mice where blood flow washed away the platelets as they were only loosely adhered to the vessel wall (Suzuki-Inoue et al., 2010). In contrast, CLEC-2 deficient mice showed no significant increase in tail bleeding time in comparison the WT control mice. It is worth noting however that in this study, mice were genetically deficient in CLEC-2 whereas the study by Nieswandt et al., used a monoclonal antibody to induce CLEC-2 depletion (Suzuki-Inoue et al., 2010).

Similarly, Hughes et al., have also reported the effect of CLEC-2 deficiency on platelet activation using CLEC-2-deficient mouse platelets generated through radiation chimeras. Their results demonstrate that although CLEC-2 deficient platelets exhibit normal tail bleeding time in mice and they have normal aggregation on collagen under flow, they do not respond to CLEC-2 agonists (Hughes et al.,

2010a). This is key as it suggests no role for CLEC-2 in thrombus formation, while other studies do.

Similarly to GPVI, evidence in the literature suggests that CLEC-2 plays a role in thromboinflammation as well. The interaction of CLEC-2 with its endogenous ligand podoplanin in thromboinflammation results in platelet activation, resulting in the prothrombotic process coupled with the modulating inflammatory response. In events associated with ischaemic stroke where damage to the blood-brain barrier and neurons has occurred, CLEC-2 plays this dual role in cancer, facilitating metastasis of tumour cells and formation of blood clots (Meng et al., 2021). CLEC-2 also controls the inflammatory response and organ injury in infectious conditions like sepsis (Xie et al., 2020). Consequently, due to its important function in mediating the relationship between inflammation and thrombosis, CLEC-2 is a potential therapeutic target for the management of thromboinflammatory disorders.

Deep vein thrombosis (DVT) is a condition characterised by the formation of blood clots due to the slow or blocked flow of blood, leading to a lack of oxygen supply (hypoxia). DVT is a thromboinflammatory condition because this triggers the production of inflammatory mediators. Payne et al. have shown that platelet inducible CLEC-2 knockout mice do not produce thrombi in a stenosis model, exacerbating deep vein thrombosis (DVT) compared to wild-type (WT) controls (Payne et al., 2017).

Previous studies have examined the vital role CLEC-2 plays in lymphatic and vascular development. In a study conducted by Suzuki et al., CLEC-2 deficiency in mice led to high neonatal lethality (Suzuki-Inoue et al., 2010). Also, out of 326 CLEC-

2 deficient mice, only 2 mice survived until the age of 8 weeks which raises the question if these 2 mice are truly representative model of a CLEC-2 knockout. When examining the reason behind this, they observed that CLEC-2 deficiency led to cutaneous haemorrhage, oedema, lymphatic drainage failure, and blood-filled lymphatic vessels in mice (Carramolino et al., 2010). Similarly, in studies examining the CLEC-2 signalling molecules such as PLCγ2 (Ichise et al., 2009b), Syk, and SLP-76 (Sebzda et al., 2006) in CLEC-2 deficient mice, blood filled lymphatic were also observed. This is a result of the lack of separation of the lymphatic-vascular vasculature (Abtahian et al., 2003). Altogether, these results highlight the important role CLEC-2 and its downstream signalling molecule play in the in lymphatic-vascular development.

The potential role of CLEC-2 in mediating cancer metastasis has been also examined. This is due do the fact that the CLEC-2 ligand, podoplanin, has been found to be expressed on some types of cancer cells such as brain tumour cells, squamous cell carcinoma, seminoma, and melanoma. Therefore, it was hypothesised that the interaction between CLEC-2 in platelets and the podoplanin expressed in tumour cells could promote tumour metastasis (Raica et al., 2008, Kan et al., 2014). Shirai et al., have observed that cancer metastasis was reduced by blocking the interaction between CLEC-2 and podoplanin. As a result, this sheds a light on the potential role of CLEC-2 in mediating tumour metastasis (Shirai et al., 2017).

1.7 Phospholipase C enzymes

1.7.1 PLCβ

Phospholipase C enzymes are important for hydrolysing inositol phospholipids to produce IP_3 and DAG. In mammals, PLCs are found in four different families (β, γ, δ, ε) (Haas and Stanley, 2007). Activation of circulating platelets occurs upon agonist binding to cell-surface receptors, which in turn activates protein kinases and guanine nucleotide binding regulatory proteins (G proteins), and the production of lipid second messengers. Two separate groups of enzymes, the β and γ isoforms of phospholipase C are responsible for producing lipid second messengers when G protein-coupled receptors are stimulated. Receptors coupled to G proteins that include a $G\alpha_q$ subunit activate the four isoforms of PLCβ found in human platelets. The $G_{\beta\gamma}$ mediated activation of PI3Kγ occurs when receptors coupled to G proteins with a Ga_i subunit are stimulated (Lian et al., 2005, Rittenhouse, 1996). The PLCβ isoforms are responsible for the hydrolysis of PIP2, which results in the production of IP_3 and DAG (Rhee and Bae, 1997) . This then leads to intracellular calcium release and PKC activation (Lapetina et al., 1985, Brass and Joseph, 1985).
It has been documented that a bleeding diathesis and impaired platelet aggregation and secretion *in vitro* can be caused by a hereditary PLCβ2 impairment suggesting the crucial role PLCβ in plays in platelet signalling (Lee et al., 1996b, Sun et al., 2004).

A study by Lian et al., have examined the potential role of PLCβ2 in platelet activation. Using a model of chemical-induced injury and PLCβ2 deficient mice, they examined the platelets' clotting abilities. Occlusion was observed over 30 minutes and there was no arterial occlusion in PLCβ2 deficient mice. Whereas WT mice

formed a stable thrombus over 30 minutes. Next, the role of PLCβ2 in platelet spreading was further investigated by spreading washed WT and PLCβ2 deficient mouse platelets on fibrinogen for 45 minutes. WT platelets were able to spread extensively at 15- and 30-minutes post spreading, however PLCβ2 knockouts had impaired platelet spreading. Nonetheless, when platelet spreading was examined at 45 minutes, WT and PLCβ2 deficient platelets had a similar spreading pattern. Similar results were seen in PI3Kγ deficient platelets. The *in vivo* impairment could be caused by the crucial functions of both PLCβ and PI3Kγ in arranging the platelet cytoskeleton, as the results of reduced platelet spreading implies. Given the shear forces experienced by blood vessels, cytoskeletal dynamics play a pivotal role in platelet adhesion to the vessel wall (Lian et al., 2005). It is possible that they have a malfunction in the process of ADP-mediated actin dynamics. This could explain the failure of PI3K deficient platelets to spread on fibrinogen coated surfaces. In conclusion, based on the reduced cytoskeleton reorganisation capability, decreased fibrinogen spreading, and inability to generate persistent thrombi *in vivo*, this study implies that PLCβ2 and PI3Kγ are crucial in the dynamics of platelet cytoskeletons.

1.7.2 PLCγ2

1.7.2.1 Structure

PLCγ can be found in two isoforms, PLCγ1 and PLCγ2. While PLCγ1 is expressed in several cell types, PLCγ2 is mainly expressed in hematopoietic cells. And as previously described, PLCγ2 is a key signalling hub downstream of (hem)ITAM receptors.

PLCγ2 is 147kDa protein that has 1265 amino acids consisting of 8 domains: An N-terminal PH domain, an X and Y catalytic domains with a multidomain insert in between consisting of split PH domain, N-terminal SH2 domain (nSH2), C-terminal SH domain (cSH2), and SH3 domain (Figure 1.4) (Gresset et al., 2010, Nakamura and Fukami, 2017). The Pleckstrin homology (PH) domain consists of approximately 100 amino acids (Wang et al., 1994). Through its ability to bind to phosphatidylinositol such as PIP3, the PH domain plays a main role in the protein translocation to the cell membrane and binding (Lemmon et al., 1995, Falasca et al., 1998). Adjacent to the PH domain is the EF-hand domain. There is a lack of evidence on the exact function of the EF domain in PLCγ2. However, there are some studies that examined the function of the EF domain in different PLC isoforms where the EF domain has been found to be mainly responsible for calcium binding (Grobler and Hurley, 1998). All PLC isoforms contain and a catalytic X and Y domain forming the split TIM barrel which is the most conserved region across PLC isoforms (Rhee and Choi, 1992). These domains are responsible for the catalytic activity of PLC enabling the hydrolysis of PIP2 into IP_3 and DAG (Wang et al., 2014). PLCγ also consists of C-terminal copy of a tandem pair of PLCγ2 SH2 domains (cSH2), as well as the nSH2 domain, SH3 domain, and split PH domain. The Src homology 2 (SH2) domain plays a crucial role in regulating the activity of PLCγ2. Due to fact that it includes the primary autoinhibitory areas, such as the C-terminal SH2 domain which plays a crucial role in the suppression of PLCγ2 activity, the SH2 domain is necessary for the activation of PLCγ2 (Zhou et al., 2012a). Typically, changes or mutations in the SH2 domain in many signalling proteins influence the stability of the domain, the residues that interact with the catalytic domain, or the involvement of the domain in ligand binding (Zhou et al., 2012a). Additionally, SH2 domains are known

for their capacity to recognise tyrosine-phosphorylated regions, making them important mediators in transducing and modulating physiological signals from protein-tyrosine kinases (Huang et al., 2008).

Another essential part of PLCγ2 ‘s activity is the SH3 domain, which mediates interactions with other proteins. The SH3 domain has a role in binding substrates to protein tyrosine kinases such as Src, Fyn, and Lyn (Weng et al., 1994). In addition, it is thought that the SH3 domain is responsible for regulating enzymatic activity via protein-protein interaction (Anderson et al., 1998). Previous studies have also demonstrated that SH3 domains interact with some ligands by binding to proline-rich sequences that include a conserved core motif of PXXP (Alexandropoulos et al., 1995). Moreover, the SH3 domain may play a role in guiding PLCγ2 to a subcellular region where it may regulate actin polymerization, via modulating the interaction of PLCγ2 with the actin cytoskeleton (Bar-Sagi et al., 1993).

In PLCγ2, the C2 domain is an essential component for its function, since it is involved in a number of activities that are essential to its operation. This includes its role in activation, membrane binding, and translocation PLCγ2 to particular cellular sites (Nishida et al., 2003). In this study, it was demonstrated that the C2 domain plays a crucial role in the activation of PLCγ2, which is dependent on Ca^{2+} influx. Additionally, their results have demonstrated the failure of PLCγ2 to translocate to the membrane upon the deletion of the C2 domain. Altogether, this emphasises the role of the C2 domain in mediating the PLCγ2 translocation which is dependent on the calcium influx (Nishida et al., 2003).

Based on the findings of mutational research conducted on PLCγ2 in DT40 cells, it was proposed that the activation of PLCγ2 in the SH2-SH3 domains downstream of the BCR is partially dependent on tyrosine phosphorylation and Btk is primarily responsible for phosphorylating these sites. Although the phosphorylation on Y1197 and Y1217 that are located in the C terminal are facilitated by Btk, it is suggested that this can also be mediated by Syk (Rowley et al., 1995, Rodriguez et al., 2001, Hashimoto et al., 1999).

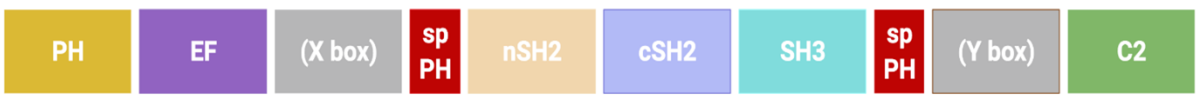

Figure 1.4: PLCγ2 domains

The PLCγ2 protein is made of a PH domain at the N-terminus, and catalytic X and Y domains in between EF-hand motifs and C2 domain. PLCγ2 also has an extra PH domain divided by one SH3 and two SH2 domains.

1.7.2.2 PLCγ2 in platelets

The role PLCγ2 plays in mediating platelet function has been previously investigated using genetically mutated mice (table 1.1). In a study conducted by Wang et al., the PLCγ2 deficient mice were noticeably smaller in size than the wild types. They also observed spontaneous bleeding in PLCγ2 deficient mice (Wang et al., 2000). This was further investigated by Mangin et al., where the bleeding time was assessed in order to assess a potential primary haemostasis deficiency. When compared to heterozygotes or wild-type mice, the bleeding period was drastically extended in

animals with the PLCγ2 $^{-/-}$ mutation. Additionally, there was no evidence that this deficiency was caused by a lower platelet count or an altered platelet shape. Furthermore, platelet aggregation was measured in order to determine whether or not platelets require PLCγ2 in various signalling pathways by stimulating platelets with several agonists such as collagen, thrombin, and ADP. When induced by 50 μg/mL^{-1} bovine collagen, platelet aggregation in PLCγ2 $^{-/-}$ mouse platelets were significantly decreased but not completely abolished in comparison to WT platelets. Although Wang et al., have previously reported a complect lack of platelet aggregation, Mangin et al., have shown a slight aggregation response (6.1%) around 3 minutes when stimulated by collagen. This was followed by a decreased level of platelet aggregation which is explained by a delay in the shape change in platelets (Mangin et al., 2003). In contrast, PLCγ2 deficiency had no effect on platelet aggregation induced by ADP and thrombin. Due to this low increase in aggregation induced by collagen in PLCγ2 deficient mice, the platelets' morphological changes were analysed using scanning electron microscopy. At rest, PLCγ2 $^{+/+}$ platelets exhibited a regular discoid shape. PLCγ2 $^{+/+}$ platelets formed large aggregates after 3 minutes and underwent shape change with extended filopodia quickly after 30 seconds of collagen stimulation. PLCγ2 deficient platelets on the other hand, did not exhibit major shape change as they were mostly discoid and only formed small aggregates after 4 minutes of collagen stimulation. The platelets then formed extended filopodia at 5 minutes. They also evaluated the role PLCγ2 plays in mediating platelet secretion. PLCγ2 $^{+/+}$ and PLCγ2 $^{-/-}$ washed platelets were loaded with [^{3}H] serotonin and stimulated with either thrombin or collagen. When stimulated with thrombin, there was no significant difference in [^{3}H] serotonin released in both PLCγ2 $^{+/+}$ (84 ± 2%) and PLCγ2 $^{-/-}$ (83 ± 11%). In contrast, when stimulated with

collagen, PLCγ2 $^{-/-}$ platelets had a significant decrease in secretion on comparison to PLCγ2 $^{+/+}$ platelets where granule secretion in PLCγ2 $^{+/+}$ was 49 ± 0,65% and 1.25 ± 0.75% in PLCγ2 $^{-/-}$ platelets (Mangin et al., 2003).

As previously mentioned, collagen can also stimulate α2β1. Therefore, it is possible that another collagen receptor, possibly integrin α2β1, is involved because PLCγ2 $^{-/-}$ platelets could not aggregate in response to GPVI ligands. By blocking α2β1, using a mAb (Hmα2), platelet aggregation and shape change were completely abolished in response to collagen in PLCγ2 deficient platelets. Furthermore, aggregation was assessed in PLCγ2 deficient platelets and FcRγ deficient platelets in the presence of JAQ-1 which blocks the CRP-GPVI binding site in order to assess the potential GPVI/FcRγ and PLCγ2 independent activation pathways. This led to a complete inhibition of aggregation stimulated by collagen.

Finally, by inhibiting the P2Y1 and P2Y12 receptors, the roles of ADP and TXA2 in the PLCγ2 independent platelet response was examined. The results have demonstrated that collagen-induced aggregation was unaffected, however around 4-5 minutes, shape change was detected. This suggests that ADP and TxA2 are necessary for shape change but do not play a role in αIIbβ3 mediated activation pathway (Mangin et al., 2003).

1.7.2.3 The role of PLCγ2 in adaptive immunity

The B-cell receptor (BCR) complex is made of membrane bound immunoglobulin and Igα/Igβ heterodimer (Schamel and Reth, 2000) .Similarly, to GPVI and CLEC-2, Igα/Igβ have cytoplasmic domains that contain an ITAM (Kurosaki, 2011). B-cell receptor signalling is similar to that of GPVI i.e., through an ITAM signalling pathway,

particularly through PI3K and PLCγ2 (Woyach et al., 2012). Antigen binding leads to BCR stimulation which initiates ITAM phosphorylation by SFK (Lyn) that leads to recruiting Syk to the phosphorylated ITAM (Kurosaki, 2011, Yamamoto et al., 1993). This leads to the formation of the signalosome containing several proteins such as the kinases Syk and Btk, and the B- cell linker (BLNK) (Woyach et al., 2012). Playing an analogous role to LAT and SLP-76 in platelets, BLNK phosphorylation allows it to bind to Btk and PLCγ2 (Kurosaki, 2011).

The specific kinase (or kinases) causing PLCγ2 phosphorylation in B cell is unknown, though. PLCγ2 phosphorylation induced by BCR was inhibited by gene disruption of Lyn or Syk (Takata et al., 1994). Nevertheless, it is difficult to confirm whether PLCγ2 is a direct substrate of Lyn or Syk in B cells considering that tyrosine phosphorylation of BLNK, creation of PIP3, and activation of Btk all takes place following Lyn/Syk activation. Given that the level of BCR-induced tyrosine phosphorylation of PLCγ2 was higher in a B-cell line from mice that overexpresses Btk (Fluckiger et al., 1998, Scharenberg et al., 1998) and significantly lower in a B-cell line from chickens that are deficient in Btk (DT40), it has been suggested that PLCγ2 may serve as a substrate for Btk (Takata and Kurosaki, 1996). Additionally, IP_3 production, and an increase in the cytosolic free Ca^{2+} concentration was not induced by BCR activation in the DT40 cells that lack Btk. The results showed that this kinase did not play a significant impact in the phosphorylation of PLCγ2, when tested with human B cells that express mutant versions of Btk. Human X-linked agammaglobulinemia (XLA) is caused by Btk gene mutations. Similar to the Btk-deficient DT40 cells, B cells isolated from XLA patients have significantly reduced IP_3 and Ca^{2+} responses. On the other hand, the XLA cells showed a standard rise in

PLCγ2 tyrosine phosphorylation in response to BCR stimulation, unlike the chicken cells (Fluckiger et al., 1998). Despite evidence of Btk's function in platelets, XLA patients do not experience bleeding as a side effect (Quek et al., 1998). This suggest that the high doses and off target effect of ibrutinib is what causes bleeding in patients.

Moreover, Kim et al., have demonstrated that PLCγ2 is phosphorylated on Y753, Y759, Y1197, and Y1217 in response to B-cell receptor stimulation in Ramos cells (B lymphocyte cell line) and murine splenic B cells using antibodies specific to each of the phosphorylation sites. Phosphorylation of Y1217 was three times higher in cells that were highly stimulated via this receptor compared to Y753 or Y759. In contrast, only Y753 or Y759 were phosphorylated whereas there was no phosphorylation observed of Y1217 in convulxin stimulated platelets (Kim et al., 2004). Phosphorylation of the Y391 residue on CD19, the BCR coreceptor, is also an essential part of the BCR / PLCγ2 signalling complex that is triggered when the BCR is engaged with an antigen. In a signalling complex involving Lyn, Vav, Grb2, and p85 of PI3K, PLCγ2 immunoprecipitates with CD19, possibly via their SH2 domains, indicating a tight multimeric interaction with the cell membrane (Brooks et al., 2000). Using genetically PLCγ2 deficient mice was the first step to investigate the functional need of PLCγ2 -mediated signalling in B cells. This was achieved by inserting a neomycin cassette into the second exon, which encodes the enzymatic function. These PLCγ2 -deficient mice were able to survive into adulthood, but they exhibited severe abnormalities in B cell growth and function. Also, these animals had impaired pro-B cell development and a decrease in mature B cells. Antibody production was decreased due to the lack of PLCγ2 activity, and as predicted, BCR activation did not

cause calcium flux or mitogenic promotion of B cell proliferation. Serum immunoglobulin (Ig) M, G2a, and G3 and T cell-independent antibody production were also decreased (Wang et al., 2000).

Studies by Hashimoto et al., and Su et al., had demonstrated the significance of BLNK in PLCγ2 function during the development of B cells. This was achieved via generating BLNK$^{-/-}$/PLCγ2 $^{-/-}$ mice by deleting the enzymatic PIP2 domains of PLCγ2 (Hashimoto et al., 2000, Xu et al., 2006). When compared to animals lacking either BLNK or PLCγ2, mice lacking both genes exhibited a more noticeable abnormality in early B cell progenitors around the Pro-B cell stage. Also, PLCγ2 heterozygous animals on a BLNK-deficient background had lower PLCγ2 biochemical function and B cell development compared to BLNK$^{-/-}$/PLCγ2 $^{+/+}$ mice, which indicates that the PLCγ2 expression level was relevant where PLCγ2 heterozygous mice has less PLCγ2 expression (Xu et al., 2006). However, it should be noted that immature B cells express three times more PLCγ2, BLNK, and Btk than mature B cells, which results in higher phosphorylation of PLCγ2 driven by BCR. This highlights that PLCγ2 levels do not remain constant during B cell development (Benschop et al., 2001).

Table 1.1: Different PLCγ2 models and phenotypes

Mouse model	Phenotype
PLCγ2 knockout (PLCγ2 $^{-/-)}$	Decreased platelet aggregation (Mangin et al., 2003). Severe immune deficits, hindered B-cell growth(Wang et al., 2000).
PLCγ2 $^{flox/flox}$ (deletion of PIP2 binding site)	Defects in B cell development at the pre-B cell stage (Hashimoto et al., 2000).
PLCγ2^{Ali5} (D993G)	Gain-of-function effect (Gossmann et al., 2016). Mice develop spontaneous inflammation (Bernal-Quirós et al., 2013).
PLCγ2^{Ali14} (Y495C)	Increased basal and stimulated activity of PLCγ2. Heightened immune responses and increased susceptibility to autoimmune and inflammatory diseases (Magno et al., 2019).
PLCγ2 ^{P522R}	A protective PLCγ2 mutation with properties reduces the development of Alzheimer's disease (Tsai et al., 2023).
BLNK$^{-/-}$/PLCγ2 $^{-/-}$	Abnormality in early B cell progenitors around the Pro-B cell stage(Xu et al., 2006)

1.7.2.4 Role of PLCγ2 in immune deficiency

PLCγ2 has been linked to immunodeficiency symptoms. This includes common variable immunodeficiency (CVID), PLCγ2 -associated antibody deficiency and immunological dysregulation (PLAID), and immunodeficiency syndrome. While CVID is far more genetically varied and mutations in the *PLCG2* gene are thought to be

responsible for 2% of documented instances of CVID (Bogaert et al., 2016), a gain-of-function amino acid mutation in the PLCγ2 gene is the main cause of PLAID (Ombrello et al., 2012, Zhou et al., 2012b).

Along with many of the common clinical symptoms of CVID, such as granulomatous disease, allergies, autoimmune disease, and an abnormally low concentration of IgG with recurrent infections, patients with PLAID often experience a type of cold temperature-induced hives known as cold urticaria (Ombrello et al., 2012, Giannelou et al., 2014). Examining the involvement of PLCγ2 's cSH2 domain, which is impacted in PLAID patients, may help explain the underlying mechanism involved in the PLAID phenotype. Research conducted *in vitro* showed that following BCR signalling, the early signalling complex was stabilised by the cSH2 domain of PLCγ2, in conjunction with low phosphorylation of Syk, Btk, and BLNK. This hindered downstream signalling due to a decreased clustering of BCR specific antigen engagement by T and B cells, which is necessary to activate and differentiate B cells, and allows antibody secretion and formation of B cell memory. This suggests that impaired cellular movement of the antigen-engaged BCR may be partially responsible, for the PLAID syndrome (Wang et al., 2014).

1.7.2.5 PLCγ2 in cancer

Chronic lymphatic leukaemia (CLL) is a B-cell malignancy and the most common leukaemia in adults (Gaidano et al., 2012). The B-cell receptor signalling pathway plays a major role in the pathogenicity of CLL. When expressed on malignant B-cells, BCR promotes the survival, maturation and, proliferation of the malignant cells (Ghia et al., 2008, Herishanu et al., 2011, Stevenson et al., 2011). Therefore, CLL

treatments are based on targeting and inhibiting the BCR signalling pathway such as kinase inhibitors idelaslisib (PI3Kδ inhibitor), fostamatinib (Syk inhibitor), and ibrutinib (Btk inhibitor) (Wiestner, 2015). Ibrutinib, an irreversible inhibitor of Btk, is a first-in-class medication that has been primarily employed for the treatment of chronic lymphocytic leukemia (CLL) (Pan et al., 2007). While ibrutinib is generally well tolerated, various clinical studies have linked ibrutinib to an increased risk of serious bleeding (Lipsky et al., 2015).

Ibrutinib raises the risk of bleeding events due to its off target effects and its effect on platelet aggregation and function, according to studies (Ninomoto et al., 2020). Another factor contributing to the bleeding propensity associated with ibrutinib is the impairment of GPVI-mediated platelet function (Rigg et al., 2016).
Platelets isolated from patients treated with ibrutinib demonstrate impaired reactivity when stimulated by collagen or CRP (Bye et al., 2015). Additionally, aggregation of human platelets mediated by CLEC-2 is impeded by the presence of low doses of ibrutinib (Nicolson et al., 2021). In this study, ibrutinib was used as control since the inhibition of Btk activity by ibrutinib would therefore inhibit PLCγ2 activity.
The mechanism of how Btk and PLCγ2 induce CLL is very essential to understand, as mutations in PLCγ2 and/or Btk have been discovered in 11 to 90% of ibrutinib-refractory CLL patients (Ahn et al., 2017, Gángó et al., 2020, Lampson and Brown, 2018). Very intriguingly, two distinct studies have identified that individuals with CLL did not have any PLCγ2 or Btk mutations prior to Ibrutinib therapy (Kanagal-Shamanna et al., 2019, Maddocks et al., 2015). It was also demonstrated that uncommon subclones with PLCγ2 mutations are more likely to be favored during CLL progression following Ibrutinib therapy (Landau et al., 2017, Burger et al., 2016). Several PLCγ2 mutations have been detected in patients that have acquired

ibrutinib resistance. Ibrutinib resistance in CLL was found to be associated with PLCγ2 hypermorphic gain-of-function genetic mutations such as in R665W (SH2 domain), S707Y (SH2 domain), L845F (spPH domain), and D993G (TIM,Y box)), (Koss et al., 2014, Woyach et al., 2014b). In the literature, the effect of these mutations has been examined using a protein overexpression system in multiple cell lines. The R665W and L845F mutations have been shown to increase the enzymatic activity of PLCγ2, which results in increased B-cell receptor activity. In addition, the R665W and L845F mutations cause PLCγ2 to function without requiring Btk and enables it to develop resistance to ibrutinib in CLL patients (Liu et al., 2015)

When examined in BCR signalling, D993G also shows an increase in IP_3 and Ca^{2+} when cells are stimulated (Magno et al., 2019). Although these mutations have been widely researched in relation to CLL and ibrutinib resistance, it is uncertain if these or other mutations may occur in platelets, and what influence they may have on platelet (hem)ITAM receptor signalling. In addition to the previously mentioned ibrutinib resistant mutations, there are several other *PLCG2* mutations summarised in table 1.2. Frequency in human population was obtained from www.gnomad.broadinstitute.org/.

As previously mentioned, the effect of the PLCγ2 gain - of function mutation PLCγ2 ’s function has been investigated using a protein overexpression system. Although using an overexpression system can be rapid and simple, the high level of protein expression tends to be not physiologically representative to the normal level of the protein. Therefore, the CRISPR/Cas9 gene editing technique will be used in this study to generate PLCγ2 mutation knock-ins in order to study their effect on PLCγ2 function.

PLCγ2 has been also found to mediate a role in diffuse large B cell lymphoma (DLBCL). In a study where 86 patients were examined, PLCγ2 was highly expressed in 54 patients, which was around 63%. *In vitro*, cells derived from these patients were shown to undergo proliferation suppression, apoptosis induction, and cell cycle arrest after being treated with the PLC inhibitor (U73122). Interestingly, the authors hypothesised that higher levels of PLCγ2 signalling may have improved overall survival, which might be due to the enhanced cellular proliferation and subsequent susceptibility to cytotoxic medicines caused by greater PLCγ2 signalling (Huynh et al., 2015)

Table 1.2: Describes the expected functional problems and frequency of multiple PLCG2 mutations

Mutation	Position in Protein	Expected Functional Problem	Frequency in human population (%)
A708P	SH2 domain	Structural alteration, impacts signalling (Walliser et al., 2018)	< 0.0005%
D993N	SH2 domain	Alters interaction with other proteins(Rogers et al., 2021, Diop et al., 2022)	< 0.001%
L848P	SH2 domain	Structural disruption, affects binding(Neves et al., 2018)	< 0.001%
M1141L	PH domain	Affects binding affinity (Jackson et al., 2021)	0.0005%
P552R	SH2 domain	Affects enzyme regulation/ increasing intracellular calcium release(Magno et al., 2019)	< 0.001%
Y495C	PH domain	Can alter the enzyme's active site, potentially reducing its catalytic efficiency (Magno et al., 2019)	< 0.0005%

1.7.2.6 Role of PLCγ2 in lymphatic and vascular development

During the process of development, the lymphatic vasculature is believed to have originated from the blood vasculature. The expression of the transcription factor prospero-related homeobox 1 (Prox1) in a subset of venous endothelial cells has been shown to be the initiating factor in the differentiation of lymphatic endothelial cells (LECs), according to previous research (Wigle and Oliver, 1999).

While the ligand for vascular endothelial growth factor receptor (VEGFR) 2 and 3, vascular endothelial growth factor (VEGF) C (Joukov et al., 1996), is essential for lymphatic vessel creation, it is not necessary for Prox1-induced LEC specification (Karkkainen et al., 2004). The lymphatic vasculature develops specialised components and differentiates from the blood vasculature throughout later stages of development. There have been previous studies that demonstrated blood-lymph shunts and the presence of lymphatic vessel endothelial hyaluronan receptor 1-positive (Lyve1^{+}), lymphatic endothelial cells (LECs), and blood endothelial cells (BECs) in mice that lacked either SLP-76 or Syk (Prevo et al., 2001, Abtahian et al., 2003).

Ichise et al., have investigated role that PLCγ2 plays in the development of lymphatic and blood vasculature using a genetic approach. A spontaneous mutant mouse line that exhibited blood-filled lymphatic capillaries was found to carry a null mutation of the PLCγ2 gene, which encodes PLCγ2. This was discovered by the process of positional candidate cloning (Ichise et al., 2009a). Their results have demonstrated that in the course of development, the lymphatic tubes that were developing in embryos that lack PLCγ2 were filled with blood which might indicate the failure of separation of the lymphatic vessels from the blood vessels. Also, the lymph sacs that were filled with blood included Lyve1^{+} LECs as well as CD31^{+}, and Lyve1^{-} BECs.

However, this phenotype was not observed in the WT mice (Ichise et al., 2009a). Based on these observations, it may be concluded that PLCγ2 plays a crucial part in the process of sustaining the separation of blood and lymphatic vasculature. Therefore, this will be further examined in this study by using another approach. The role PLCγ2 plays in the lymphatic/vascular development will be investigated using the PLCγ2 inhibitor, U73122, in zebrafish embryos (section 5.3.3).

1.7.2.7 PLCγ2 pharmacological inhibitors

The role of PLCγ2 in several platelet functions has previously been studied using a pharmacological inhibitor, U73122. U73122,(1-6-((17β-3-methoxyestra-1,3,5(10)-trien-17-yl)amino)hexyl-1 H -pyrrole-2,5-dione), is a potent inhibitor of PLC activity and was initially identified in 1989 (Bleasdale et al., 1989). The original purpose of U73122 was to study the function of PLC isoforms in receptor-mediated cell activation and it has been found to specifically inhibit PLC-dependent activities in human platelets and neutrophils (Smith et al., 1990, Bleasdale et al., 1990). The inhibitory mechanism includes the alkylation of a cysteine residue in the catalytic domain of PLC (Klein et al., 2011). U73122's mechanism of action involves the inhibition of the hydrolysis process of PIP into IP_3, resulting in a reduction of free cytosolic calcium ions (Ca^{2+}) (Yule and Williams, 1992). The activation of membrane-bound PLC has been suggested to be the mediating factor for any reaction sensitive to the inhibitor when U73122 is employed in conjunction with its structural analogue (U73343) (figure 1.5), which is normally utilised as an inactive control molecule (Burgdorf et al., 2010).

The inhibitory effect of U73122 on platelet activation induced by several agonists has been previously established in the literature. U73122 has been shown to significantly

decrease the increase in calcium levels in platelet stimulated by collagen and thrombin (Heemskerk et al., 1997b). A very recent study has studied the effect of U73122 on platelet spreading and adhesion on fibrinogen (Nigam et al., 2024). On the other hand, there is no evidence on the effect of U73122 on CLEC-2 mediated platelet activation. This will be investigated in this thesis.

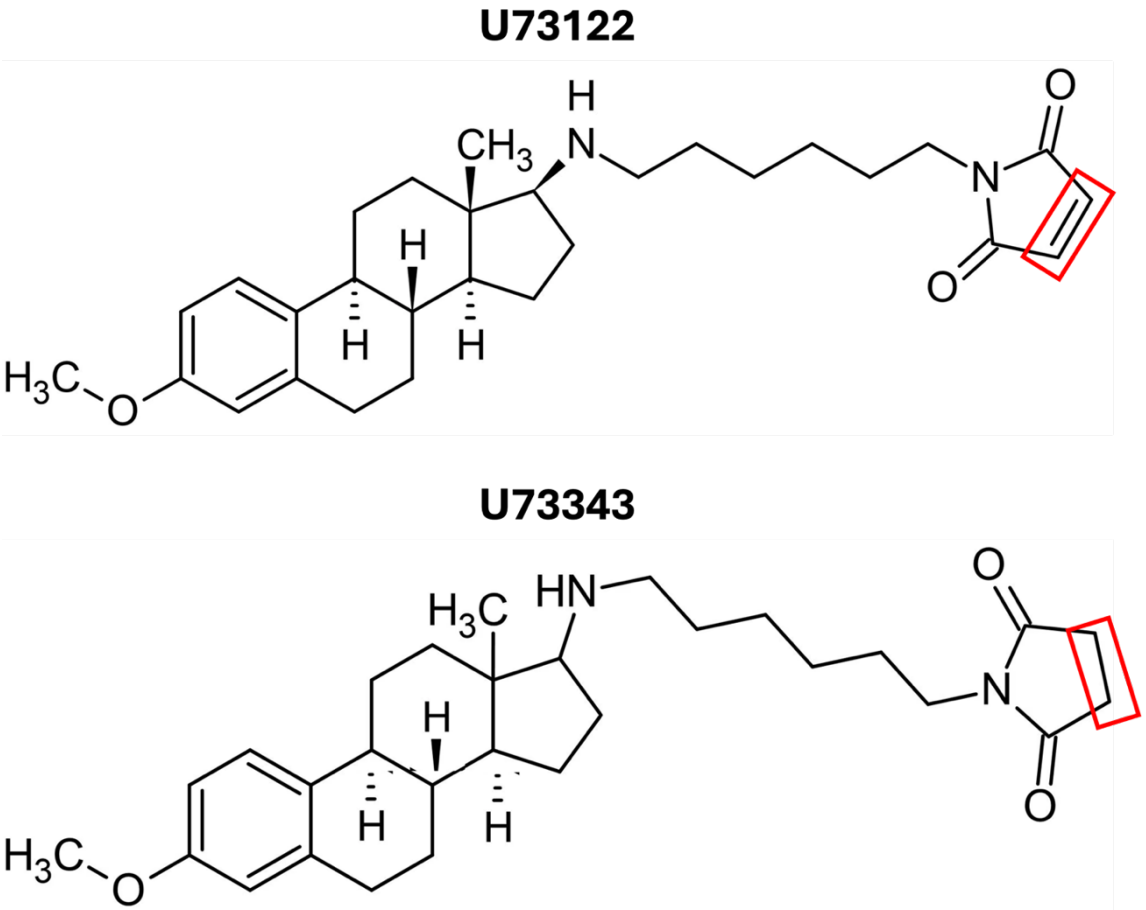

Figure 1.5: Molecular structure of U73122 and U73343.

Highlighted in the red box is the only structural difference between U73122 and U73343. U73122 has a maleimide whereas U73343 has a succinimide. Adapted from (Klein et al., 2011)

1.8 Using NFAT assay to study signalling downstream hemITAM receptors.

When investigating cell signalling in DT40 cells, the nuclear factor of activated T cells (NFAT)-luciferase reporter assay can be used. This is a sensitive assay that can detect low calcium production in a cell and enables the quantification of NFAT transcriptional activity in response to different stimuli, offering valuable information on the signalling pathways and molecular processes that govern NFAT activity in these cells (Tomlinson et al., 2007).

For the NFAT luciferase assay, cells are transfected with the NFAT reporter construct, 3 copies of the AP-1(NFAT-activator-protein) which is derived from interleukin-2 (IL-2) gene, and luciferase enzyme (Clipstone and Crabtree, 1992) (Shapiro et al., 1996). Intracellular signalling is induced upon the binding of agonist to its corresponding receptor leading to an increase in the calcium within the cell. In a resting state, NFAT proteins are usually inactive and phosphorylated. However, in response to the rise in calcium levels, serine-threonine phosphatase calcineurin is activated and therefore can lead to NFAT dephosphorylation and nuclear translocation. Concurrently, NFAT and AP-1 can also be activated and phosphorylated by RAS/mitogen-activated protein kinase (MAPK) (Macian, 2005). Luciferase may then be translated and transcribed once the NFAT and AP-1 proteins have been translocated to the nucleus. Finally, when ATP is added, luciferin is then catalysed by the luciferase enzyme leading to the production of light (figure 1.6). Maintaining NFAT dephosphorylation and nuclear localization requires sustained calcineurin activation, which is effectively accomplished even at extremely modest continuous Ca^{2+} increases that are only marginally over baseline values (Dolmetsch et al., 1997). Therefore, the NFAT assay is highly sensitive and a preferred assay when measuring calcium signalling within cell.

The NFAT luciferase reporter assay usually includes a positive control. It is well known that PMA (Phorbol 12-Myristate 13-Acetate) and ionomycin are used as positive controls in NFAT tests (Yaseen et al., 1994). It is well-established that these chemicals initiate downstream gene expression by promoting NFAT activation and nuclear translocation. The protein kinase C (PKC) activator PMA is responsible for inducing the activation of the (NFAT) pathway through the PKC-mediated signalling pathway (Seo et al., 2016). Contrarily, the intracellular calcium levels are increased by the calcium ionophore ionomycin, which is necessary for the nuclear translocation of NFAT. Therefore, by passing the need of agonist binding, PMA and ionomycin will result in an NFAT signal through the PKC signalling pathway allowing them to be used as a positive control.

(A)

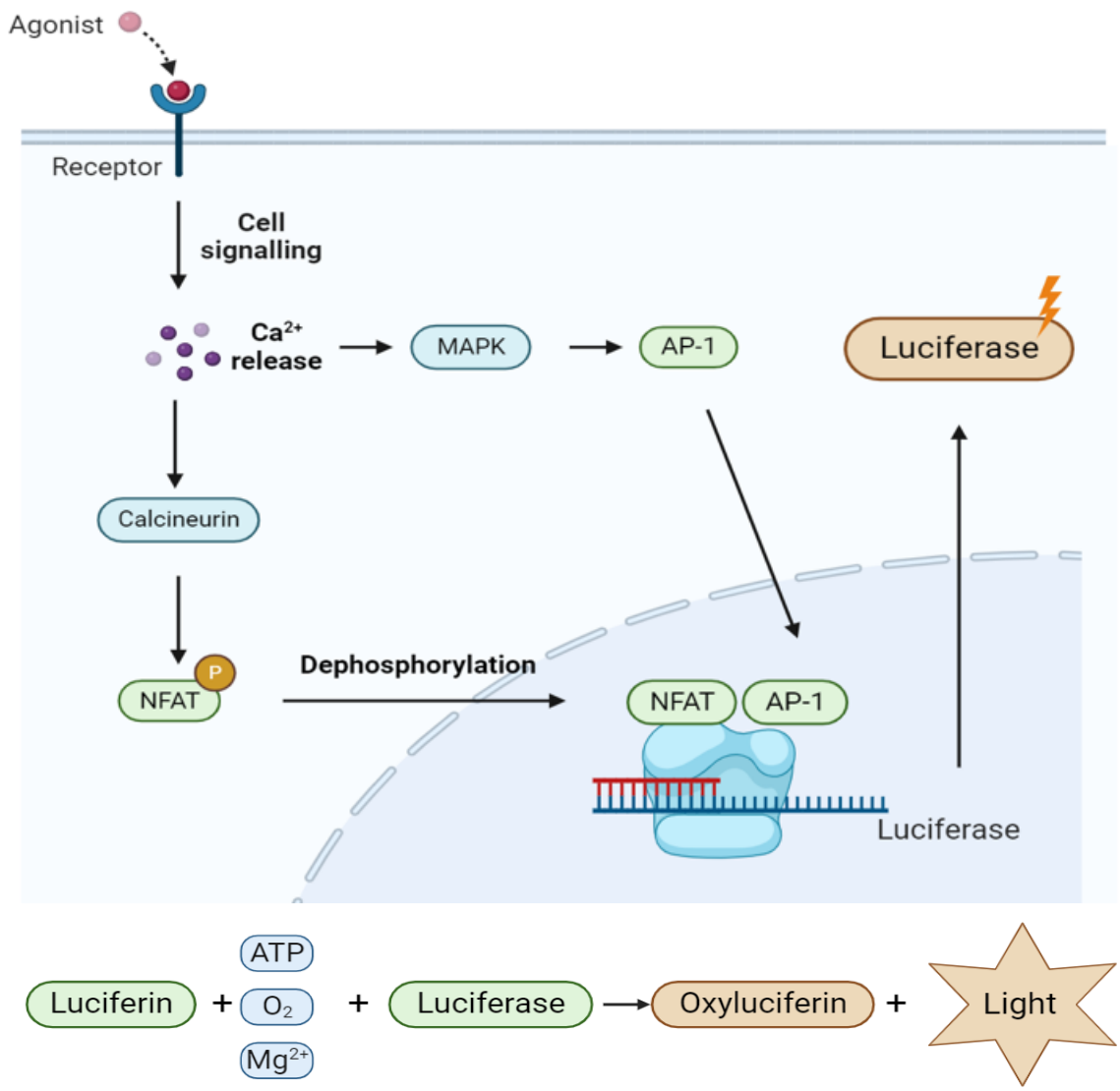

(B)

Figure 1.6: The mechanism of the NFAT-luciferase assay.

(A) Tyrosine kinases are activated upon the agonist binding to the receptor. This leads to the release of calcium which in turn activate calcineurin. Calcineurin dephosphorylates NFAT leading to its nuclear translocation. Simultaneously calcium leads to MAPK release and AP-1. Transcription of the luciferase enzyme is then initiated upon the binding of the NFAT and AP-1 to the promoter. (B) luciferin is catalysed to oxyluciferin and light by a combination of luciferin, ATP, O_2, $Mg^{2+}$and luciferase.

1.9 Using Zebrafish as an *in vivo* model

Zebrafish (*Danio rerio*) has emerged as an effective model organism for investigating thrombosis and lymphatic/vascular development given their unique genetic, morphological, and physiological properties (Jung et al., 2017, Zhu et al., 2016). Zebrafish have genetic and functional similarity to humans, which makes them a suitable model for studying human disorders. Due to their clear embryos, fast development, and the use of advanced genetic tools, *in vivo* experiments that are difficult to conduct in other model species may be carried out with great detail(Choi et al., 2021, Angom and Nakka, 2024). The zebrafish's capacity to endure substantial blood loss and rebuild tissues has made them invaluable in thrombosis studies. Fluorescence microscopy allows for real-time study of the development and dissolution of thrombus in zebrafish embryos due to their transparent nature(Schurgers et al., 2016, Jagadeeswaran et al., 2005). Moreover, zebrafish has emerged as and *in vivo* model to investigate vascular and lymphatic development. This is due to various advantages including preserved developmental pathways and the capacity to view vessel development in live embryos. With arteries, veins, and a lymphatic network, the zebrafish vascular system resembles those of humans functionally (Jung et al., 2017, Yaniv et al., 2006). Transgenic zebrafish lines that produce fluorescent proteins in endothelial cells can be used to examine the dynamic processes of angiogenesis and lymphangiogenesis (Yaniv et al., 2006). Using zebrafish as a model has also allowed the further investigation of the lymphatic system development which is less understood in comparison to the vascular system. The identification of crucial lymphatic indicators, such as Prox1 and VEGFC, in zebrafish has improved the understanding of lymphatic development and associated diseases (Yaniv et al., 2006, Del Giacco et al., 2010). Consequently,

zebrafish will be used and an *in vivo* model in this thesis to further understand the role of PLCγ2 in thrombus formation and vascular/lymphatic development.

1.10 Aims and hypothesis.

PLCγ2 is a key signalling hub, playing a role in a number of platelet signalling pathways. These include the collagen receptor GPVI which activates via an ITAM, and the podoplanin receptor CLEC-2, which activates through a similar mechanism known as a hemITAM. PLCγ2 is a large, multi-domain protein. The regulation of its function is through molecular interactions with a number of signalling proteins, although this is not fully understood. PLCγ2 plays a similar role downstream of ITAM-linked receptors in other cells, namely B-cells. PLCγ2 mutations have been identified in 80% of patients who develop resistance to ibrutinib therapy. However, it is unknown what the functional effect of these mutations on signalling by platelet (hem)ITAM receptors might be. Therefore, using a PLCγ2 pharmacological inhibitor, U73122, and genetic manipulation will enable the understanding of the structure/function relationship of PLCγ2 downstream of (hem)ITAM receptors.

1.10.1 Aims of this thesis:

- To characterise the effect of the PLCγ2 inhibitor, U73122, downstream of GPVI and CLEC-2 using platelet function assays.
- To characterise the PLCγ2 mutations R665W, L845F, S707Y, and D993G and to use them as a tool in order to understand their effect on PLCγ2 function using an overexpression system and CRISPR/Cas9 as a novel approach.
- To investigate the role of PLCγ2 in lymphatic and blood vasculature development, and thrombus formation *in vivo* using U73122 and zebrafish as a model.

1.10.2 Hypotheses:

- Pharmacological inhibition of PLCγ2 will lead to a significant decrease in platelet activation
- Ibrutinib-resistant PLCγ2 mutation will lead to gain of function in DT40 cells.
- The PLCγ2 inhibitor U73122, will severely decrease the ability of zebrafish embryos to form a stable thrombus

Chapter 2: Materials and methods

2.1 Materials

Rhodocytin was a gift from Dr. Johannes Eble (University of Münster, Münster, Germany).

PLCγ2 knockout and wild type DT40 cells were a gift from Dr. Mike Tomlinson (University of Birmingham, Birmingham, UK).

Donor templates and guide RNA plasmids were generated by Selorm Segbefia.

Unless mentioned, all other reagents were from Sigma Aldrich (Poole, UK).

Table 2.1.1 Primary antibodies

Antibody	Application	Species	Dilution	Source
PLCγ2 (Q-20)	Western Blotting	Rabbit	1:200	Santa Cruz (Dallas, Texas)
pY1217 PLCγ2	Western Blotting	Rabbit	1:500	Cell Signalling Technology (London, United Kingdom)
pY525/6Syk	Western Blotting	Rabbit	1:500	Cell Signalling Technology (London, United Kingdom)
pY416 SFK	Western Blotting	Rabbit	1:500	Cell Signalling Technology (London, United Kingdom)
pY223 BTK	Western Blotting	Rabbit	1:500	Cell Signalling Technology (London, United Kingdom)

Phosphotyrosine (4G10)	Western Blotting	Mouse	1:1000	Millipore (Massachusetts, USA)
beta Tubulin loading control monoclonal antibody (BT7R)	Western Blotting	Mouse	1:2000	Thermofisher

Table 2.1.2 Secondary antibodies

Antibody	Application	Species	Dilution	Source
Alexa Fluor 647 conjugated donkey anti-rabbit	Western Blotting	Donkey	1:4000	Invitrogen
Alexa Fluor 488 conjugated goat anti-mouse	Western Blotting	Goat	1:4000	Invitrogen
Donkey anti-Rabbit IgG (H+L) Highly Cross-Adsorbed Secondary Antibody, Alexa Fluor 647	Western Blotting	Donkey	1:4000	Invitrogen

2.2 Methods

2.2.1 Platelet function assays

2.2.1.1 Preparation of washed human platelets

This method was approved by the University of Reading Research Ethics Committee (Ref: UREC 20/20). 50 mL of blood was drawn from consenting healthy drug free donors into vacutainers with 3.2% sodium citrate. Whole blood was centrifuged at 102 x g for 20 minutes at 20°C. The platelet-rich plasma (PRP) was then decanted into a 50 mL falcon tube and 150 µL/mL of acid citrate dextrose (ACD) (71mM citric acid, 85 mM sodium citrate, and 110mM glucose) and 10µL prostacyclin (PGI_2 125µg/mL) were added. PRP was centrifuged at 1413 x g for 10 minutes. Platelet poor plasma was discarded, and the pellet was resuspended in 25mL Tyrode's buffer (2.9mM KCl ,134mM NaCl, 0.34mM, 12mM $NaHCO_3$, Na_2HP0_4,20mM HEPES, 1mM $MgCl_2$ and 5mM glucose pH 7.3) and 3mL ACD. Platelet number was counted using a Sysmex counter (Sysmex, UK). 10µL prostacyclin was added and platelets were centrifuged again at 1413 x g for 10 minutes. The pellet was then resuspended in the appropriate volume of Tyrode's buffer. Platelets were then rested for 30 minutes to allow the effects of prostacyclin to wear off.

2.2.1.2 Preparation of ADP sensitive platelets.

This method was approved by the University of Reading Research Ethics Committee (Ref: UREC 20/20). 50 mL of blood was drawn from consenting healthy drug free donors into vacutainers with 3.2% sodium citrate. 150 µL/mL of ACD was added and whole blood was centrifuged at 102 x g for 20 minutes at 20°C. Platelet rich plasma was aspirated and dispensed into 15mL falcon tubes and platelet number was

counted using a Sysmex counter (Sysmex, UK). PRP was then centrifuged at 350 x g for 20 minutes. Platelet poor plasma was aspirated, and the platelet pellet was resuspended in the appropriate volume of Tyrode's buffer.

2.2.1.3 Plate-based aggregometry (PBA)

40µL of washed platelets ($4x10^8$ cells/mL) were added to black clear bottom 96-well plates (Greiner Bio One). Platelets were incubated with 5µL of U73122 (PLCγ2 inhibitor) (Stratech, Cambridge, UK), U73343 (U73122's analogue) (Stratech, Cambridge, UK), ibrutinib (Stratech, Cambridge, UK), or vehicle (0.1% (v/v) DMSO) for 5 minutes prior to addition of indicated concentrations of CRP, rhodocytin, or ADP. The plate was shaken using BioShake iQ (Q Instruments) at 1200 rpm and 37˚C for 5 minutes for CRP and ADP, and 10 minutes of rhodocytin. The absorbance was measured at 405 nm using a FlexStation.

2.2.1.4 Light transmission aggregometry (LTA)

222.5µL of washed platelets ($4x10^8$ cells/mL) were added to glass aggregometer cuvettes. 2.5µL of U73122, U73343, ibrutinib, or vehicle (0.1% (v/v) DMSO) were added to washed platelets and incubated for 5 minutes at room temperature. Platelets were stirred using magnetic fleas for 30 seconds before adding 25µL of the final indicated concentration of CRP (Cambcol, Cambridge) or rhodocytin. Aggregation was monitored for 5 minutes at 37°C with constant stirring (1200rpm) using a light transmission aggregometer (Helena biosciences, Gateshead UK).

2.2.1.5 Calcium Flux

Whole blood was centrifuged at 102 x g for 20 minutes to obtain PRP. After counting platelets, PRP was incubated with 2 μM of FURA 2-AM (Thermofisher, Massachusetts, USA) at 37 °C for 1 hour. Platelets were then pelleted at 1413 x g for 20 minutes and resuspended in Tyrode's solution to $4x10^8$ cells/mL. Platelets were incubated with U73122, U73343, ibrutinib, or vehicle control for 5 minutes at room temperature before the addition of 40μL of agonists. Calcium fluorescence measurements were recorded using a FlexStation with excitation at 340 and 380 nm and emission at 510 nm over 5 minutes.

2.2.1.6 Platelet spreading assay

Glass coverslips were coated with 300μL of 10μg/mL CRP, 300nM rhodocytin, or 100μg/mL fibrinogen at 4°C overnight. Coverslips were then washed 3 times with PBS and blocked with 5 mg/mL heat denatured BSA in PBS for 45 minutes at room temperature. Coverslips were washed 3 times with PBS. Washed platelets (1×10^7/mL) were pre-treated with U73122, U73343, ibrutinib or vehicle control (0.01 % DMSO (v/v)) for 5 minutes. Pre-treated platelets (300μL) were incubated on coverslips for 45 mins at 37°C. Coverslips were washed 3 times with PBS before fixing adherent platelets with 10% formalin for 10 mins. Slides were mounted using hydromount and imaged using differential interference contrast (DIC) microscopy on a Nikon eclipse Ti2 using a 100x objective. Platelet spread area was analysed using convolutional neural network (CNN) (Kempster et al., 2022b).

2.2.1.7 Convolutional neural network (CNN)

The original 16-bit DIC images were obtained with 2424 × 2424 dimensions of using a Nikon eclipse Ti2 inverted microscope. These images were then rescaled and transformed to 8-bit images with dimensions of 970 x 970. Rescaled images were then run through the CNN for automated measurements of number of platelets and platelet area (Kempster et al., 2022a).

2.2.1.8 Platelet sample preparation for SDS-PAGE and immunoblotting.

222.5µL of washed platelets ($4x10^8$ cells/mL) were incubated with integrilin (9µM), indomethacin (10µM), and apyrase (2U/mL) for GPVI induced signalling, and integrelin (9µM) for CLEC-2 mediated signalling. 2.5µL of indicated concentrations of U73122, U73343, ibrutinib, or vehicle (0.1% (v/v) DMSO) were added to washed platelets and incubated for 5 minutes at room temperature. 25µL of the final indicated concentration of CRP or rhodocytin were added under stirring conditions. GPVI stimulated platelets were stirred for 3 minutes and CLEC-2 stimulated platelets were stirred for 5 minutes at 37°C prior to lysis with 6X sample buffer (12% (w/v) Sodium Dodecyl Sulphate (SDS), 30% (v/v) glycerol, 0.15M Tris-HCl (pH 6.8), 0.001% (w/v) Brilliant Blue R, 30% (v/v) β-mercaptoethanol). Samples were boiled for 5 minutes at 95°C and frozen for SDS-PAGE.

Platelet lysates were separated using 10% SDS-PAGE gels. The gels were immersed in a solution containing 1X Tris/Glycine/SDS (25mM Tris, 192mM glycine, 0.1% (w/v) SDS, pH 8.3) within a Mini-PROTEAN tetra vertical electrophoresis cell (Bio-Rad, CA, USA). Gels were run at 120V for 60 to 90 minutes. Precision plus protein TM Dual colour standards (BioRad) was used as a molecular weight marker. Two pieces of filter paper were then soaked in Towbin buffer (192 mM glycine, 25 mM Tris, 20% (v/v) methanol, pH 8.3). Polyvinylidene difluoride (PVDF) membrane

was activated by soaking in methanol for 30 seconds and then in Towbin buffer. Using BioRad semi-dry Trans-Blot Turbo Transfer System, proteins were transferred onto PVDF (Immobilon-BioRad) membrane at 15V for 40 minutes.

To block non-specific binding, membranes were incubated in 5% (w/v) Bovine serum albumin (BSA) in Tris-buffer saline with 0.1% Tween (TBST) (20mM Tris, 140mM NaCl, 0.1% (v/v) Tween, pH 7.6) at room temperature with agitation for 1 hour. The membrane was then incubated in stated antibodies (Table 2.1.1) diluted in 5% (w/v) BSA at 4°C overnight. The blots were then washed with 1X TBST 3 times for 10 minutes each with agitation to wash away non-specifically bound antibodies. The membranes were then incubated in secondary antibodies (Table 2.1.2) diluted in 2.5% (w/v) BSA for 1 hour at room temperature with agitation. Finally, the membranes were washed with 1X TBST in the same way three times for 10 minutes each and imaged using a Typhoon FLA 9500 from GE Healthcare Life Sciences. B-Tubulin was used as a loading control with Alexa Fluor 488 conjugated goat anti-mouse. The amount of the target protein in the blots was quantified by measuring the signal intensity using Image J. Bands were quantified by measuring the pixels of each and normalized against tubulin.

2.2.2 Generating PLCγ2 knock ins using CRISPR/Cas9 approach

2.2.2.1 Cell culture

The wild type (WT) DT40 chicken B-cell line and PLCγ2 knockouts (KO) were cultured in RPMI 1640 media with 10% (v/v) Foetal bovine serum (FBS), 1%(v/v) chicken serum, 100 U/mL penicillin, 100 µg/mL streptomycin, 20 mM glutamine, and 50 µM 2-mercaptoethanol and kept at 37°C in 5% CO_2. Cells were cultured and maintained at $2x10^5$ cells/mL.

2.2.2.2 Plasmid preparation and salt ethanol precipitation

Previously prepared glycerol stocks (prepared by Selorm Segbefia) were plated on to agar plates with 100µg/mL ampicillin and incubated at 37°C overnight. Colonies were then selected and inoculated in 200mL Luria-Bertani (LB) broth with 100µg/mL ampicillin and incubated with shaking at 255 rpm at 37°C overnight. Using a GenElute maxiprep kit, plasmid DNA was extracted and isolated from bacterial colonies according to manufacturer instructions and concentrated to 1mg/mL using salt ethanol precipitation.

To precipitate plasmid DNA, salt ethanol precipitation was used. A 1/10 volume of sodium acetate (3M $C_2H_3NaO_2$ pH 5.2) followed by 2 volumes of 100% ethanol were added to the sample. After 15 minutes of incubation at room temperature, DNA was pelleted for 30 minutes at 16,000 x g at 4°C. The supernatant was discarded, and the resulting pellet was rinsed with 70% ethanol and centrifuged again. Excess ethanol was removed, and the pellet was air-dried for 5 minutes. The DNA was then dissolved in sterile double distilled water (ddH_20) to yield a concentration of 1µg/mL. DNA concentration is measured using the Nanodrop.

2.2.2.3 Donor repair template plasmid linearization and purification

To increase the efficiency of homology directed repair, the donor DNA plasmid was incubated overnight with the restriction enzyme BamHI-HF (New England Biolabs, Massachusetts, USA) (20 units of enzyme per 1µg of DNA in a 50µL reaction) at 37°C. The sample was analysed on a 1% (w/v) agarose gel to confirm linearisation. For linearised donor DNA purification, the restriction digest was mixed with one volume of Phenol: Chloroform: Isoamyl Alcohol (24:24:1) (Thermofisher, Massachusetts, USA) and shaken by hand for 20 seconds, centrifuged at 6,000 x g

for 5 minutes, and the top aqueous layer removed. The DNA was then precipitated using salt ethanol precipitation as described in section 2.2.2.2.

2.2.2.4 Transfection of WT DT40 cells

$2x10^7$ cells/mL of WT DT40 cells were transfected in 400µL of serum-free RPMI media. To generate knock-ins, cells were incubated with 10µg of guide RNA (gRNA) plasmid and 10µg of donor or linearized donor DNA plasmid for 10 minutes. Cells were then transfected using BioRad Gene Pulser II Electroporation System set at 350V and 500 µF and allowed to recover for 10 minutes. Transfected cells were then incubated in 10mL of complete DT40 media for 20 hours at 37°C in 5% CO_2.
To generate clonal colonies a serial dilution was performed using RPMI media with 2µg/mL puromycin and plated into 96-well plates. After 7-14 days, single-cell colonies were picked into 24-well plates then expanded into T-25 flasks for further characterisation.

2.2.2.5 Cell lysis for SDS-PAGE and immunoblotting

To confirm that transfection did not result in a protein knockout, WT DT40 cells and potential PLCγ2 mutation knock ins were analysed using SDS- page and western blotting. Cells ($2x10^6$ cells/mL) were pelleted and washed with 1X PBS. Cells were centrifuged and resuspend to $1x10^7$ using 1X RIPA buffer (150mM NaCl, 25mM Tris-HCl pH 7.6, 0.1% (w/v) SDS, 1% (w/v) Sodium deoxycholate, and 1% (v/v) Triton) and protease inhibitor cocktail (aprotinin (10µg/mL), leupeptin (10µg/mL), pepstatin (1µg/mL), AEBSF (200µg/mL), and phosphatase inhibitor sodium orthovanadate (5µM). Cells were lysed on iced for 30 minutes prior to centrifugation at 16,000 x g for 10 minutes to remove insoluble debris. Supernatant was removed and sample

buffer (6X) was added, and the lysates were boiled at 95°C and frozen prior to SDS-PAGE and western blotting (as previously described in section 2.2.1.7).

2.2.2.6 Genomic DNA extraction

1mL of WT DT40 and potential knock-in cells were collected, centrifuged at 200 x g for 5 minutes and washed with 1X PBS. Cells were pelleted again and lysed in 100µL of DT40 lysis solution (20 mM EDTA, 40 mM Tris–HCl, 200 mM NaCl, pH 8.0, 0.5% (w/v) SDS, 0.5% 2-mercaptoethanol). After adding 4µL of Proteinase K (20 mg/mL), samples were incubated overnight at 55°C. 70 µL of 5M NaCl was added, and the samples were vortexed for 15 seconds and incubated on ice for 15 minutes. Samples were centrifuged at 12,000x g for 30 minutes at 4°C, and the cleared DNA solution was transferred to a clean tube and precipitated with 250µL of 100% ethanol. Samples were centrifuged at 12,000 x g for 2 minutes and the DNA precipitate was washed with 500µL of 70% ethanol. Samples were centrifuged again at 12,000 x g for 1 minute at 4 °C and air-dried for 5 minutes to remove any residual ethanol and resuspended in 15 µL ddH_2O.

2.2.2.7 Touchdown PCR

Following genomic DNA extraction, DNA amplification was performed using REDtaq. DNA (10ng) was mixed with 5µL 10X REDtaq Reaction buffer, 2.5µL of each forward and reverse primers (10µM final), 1µL dNTPs (200µM), 2.5µL REDtaq DNA polymerase, and ddH_2O up to 50µL. The thermal cycling conditions were 95°C for 3 minutes, followed by 10 cycles of: 95°C for 30 seconds, 67°C for 45 seconds, and reduced by 1°C each cycle until reaching 55°C, and 72°C for 45 seconds. Then 20 cycles of 95 °C for 30 seconds, 55°C for 45 seconds, 72°C for 45 seconds. Following

that, 72°C for 5 minutes for a final extension. PCR products were then visualised following electrophoresis using a 1% (w/v) agarose gel.

PCR product was then cleaned using Monarch® PCR & DNA Cleanup Kit (5µg) and sent for sequencing to Eurofins Genomics confirm the presence of the desired mutation.

2.2.2.8 NFAT assay

WT DT40 cells were transfected with 10µg of NFAT-luciferase plasmid (Tomlinson et al., 2007) and 2µg of each GPVI and FcRγ or 10µg of CLEC-2 containing plasmids. Control cells were transfected with pEF6, pcDNA3, and the NFAT vector. For NFAT assay for site directed mutagenesis, PLCγ2 knockout cells were transfected with 10µg WT PLCγ2, pcDNA3, or plasmid containing the desired mutation. Cells were incubated at 37°C for 16-20 hours. Cells were then counted and resuspended in media at 2×10^6 cells/mL. Cells (50µL) were aliquoted in duplicate and stimulated with 50µL of Horm collagen (10µg/mL), rhodocytin (50nM), or with phorbol 12-myristate 13-acetate (PMA – 50ng/mL) and ionomycin (1 µM) as a positive control. For testing the effect of the PLCγ2 inhibition, 1µM, 3µM, and 10µM of U73122 (Stratech, Cambridge, UK) or vehicle (0.1% (v/v) DMSO) were added to cells for 5 minutes prior to addition of the agonists. Following agonist addition, cells were incubated for 6 hours at 37°C in 5% CO_2 and then stored at -80°C overnight.

Cells were lysed with 11µL of luciferase harvest buffer (200mM $NaPO_4$, 10% (v/v) Triton X-100, and 4mM dithiothreitol) and incubated for 5 minutes at room temperature. 100µL of luciferase assay buffer (20mM $MgCl_2$, 200mM $NaPO_4$, and 10mM ATP) was added to an equal volume of lysed cells. After adding 50µL of 1mM

D-luciferin, the luminescence was measured using NOVOstar MicroPlate luminometer (BMG Labtech) with 10 seconds intervals.

2.2.2.9 Site directed mutagenesis

PCR was used to create PLCγ2 mutations in the whole WT human (h)PLCγ2 plasmid. 5ng of hPLCγ2 plasmid was mixed with 2X Phusion master mix (ThermoFisher), 100μM of deoxynucleotide triphosphates (dNTPs), 2.5 μL of each forward and reverse primers containing mutation sites (10μM final), and ddH_2O up to 50μL. This method was adapted from (Scott et al., 2002)The thermal cycling conditions were 98°C for 30 seconds, followed by 25 cycles of 98 °C for 30 seconds, 57°C for 2 minutes, and 72°C for 1 minute. Following by 72°C for 5 minutes for a final extension. PCR products were then visualised following electrophoresis using a 1% (w/v) agarose gel.

Mutated plasmid was incubated with 4μL DpnI (New England Biolabs, Massachusetts, USA) to digest the parental DNA and, 5μL of 1X rCutSmart buffer and ddH_2O up to 50μL. The mixture was incubated at 37°C for 3 hours prior to salt ethanol precipitation.

2.2.2.10 Transformation

Mutated plasmids were transformed using DH5α Escherichia coli. 4 μL of constructs was incubated with competent cells for 30 minutes on ice. Cells were heat-shocked at 42°C for 30 seconds and transferred back to ice for 2 minutes. 250 μL of Super Optimal broth with Catabolite repression (S.O.C) was added to the cells and vigorously shaken at 250 rpm for 1 hour at 37°C. Cells were spread on the LB-Agar plates containing 100 μg/mL ampicillin and incubated at 37°C overnight.

2.2.3 Zebrafish

2.2.3.1 Zebrafish maintenance

All zebrafish experiment were conducted under zebrafish project licence (P69D89ECA) and personal license (I96393111). The zebrafish reporter line *Tg(lyve1: DsRed; Kdrl:GFP)* was obtained from the UCL zebrafish facility. The lyve1 promoter induces the production of red fluorescent protein (DsRed) specifically in lymphatic cells, while the Kdrl promoter induces the expression of green fluorescent protein (GFP) specifically in blood vessel cells. Animals were maintained at 28°C in a 12/12 light/dark cycle in an automatic aquatics system (Tecniplast). For breeding, 2 females and 1 male were randomly selected and separated using a tank divider in spawning tanks (Tecniplast) overnight. Spawning was initiated the next morning by the initiation of light and the removal of the tank divider. Embryos were collected after 30 minutes. Embryos were maintained in 1X E3 media (5 mM NaCl, 0.17 mM KCl, 0.33 mM $CaCl_2$, 0.33 mM $MgSO_4$) in petri dishes at 28°C.

2.2.3.2 Toxicology screening in zebrafish

6 hours post fertilization, 20 embryos were randomly selected for each condition and grouped into 6-well plates. Embryos were treated with concentrations of U73122, U73343, Ibrutinib or vehicle control (0.1% (v/v) DMSO) for 72 hours at 28°C. Drug solutions were changed, and survival was observed every 24 hours and until 72 hours post fertilisation(hpf). The criteria for evaluating survival were spontaneous movement, a reaction to mild tapping on the plate, and observing visible heartbeat using GX stereo microscope model XTL3.

2.2.3.3 Lymphatic and Vasculature observation in zebrafish

6 hours post fertilization, 20 embryos were randomly selected for each condition and grouped into 6-well plates. Embryos were treated with concentrations of U73122, U73343, Ibrutinib or vehicle control (0.1% (v/v) DMSO) for 72 hours at 28°C. Drug solutions were changed every 24 hours until 72 hpf. Treated embryos were anesthetised in tricaine solution (75mg MS-222,150mg Sodium bicarbonate, pH 6-7), fixed in 4% (w/v) paraformaldehyde (PFA), and immobilised in 1% (w/v) low melting UltraPure Agarose in 1X E3 media in a 35mm glass bottom Ibidi µ-Dish. Mounted embryos were imaged on a Nikon A1R fluorescence confocal microscope using 4X and 10X objectives. Still images were taken using z stacks 10µm apart. Images presented in this study are maximum projections of z series stacks. Prior to analysis, images were blinded. The number of intersegmental vessels was counted manually. The length of intersegmental vessels was measured using Image J.

2.2.3.4 Laser-induced thrombosis in zebrafish larvae

4 days post fertilisation, 20 larvae were randomly selected for each condition and grouped into 6-well plates. Embryos were treated with concentrations of U73122, U73343, Ibrutinib or vehicle control (0.1% DMSO (v/v)) in E3 media for 2 hours at 28°C. Treated larvae were anesthetised in tricaine solution (75mg MS-222,150mg Sodium bicarbonate, pH 6-7) for 5 minutes, and immobilised in 1% (w/v) low melting UltraPure Agarose in 1X E3 media in a 35 mm glass bottom Ibidi µ-Dish. Embryos were visualised using a yokogawa csu-x1 microscope using 40X water immersion objective lens. Laser injury of the caudal artery directly above the cloaca was performed blindly using a 3i Ablate laser with laser power 13 and 4 pulses. Time to occlusion was observed for 5 minutes with 5 seconds intervals. Thrombus size was

also measured blindly measured using Image J. The Freehand Tool in ImageJ was selected to trace thfiue boundaries of the thrombus manually, outlining the perimeter of each thrombus on the image. The area enclosed by the freehand selection was then calculated using the 'Measure' function in ImageJ

2.2.4 Data and statistical analysis

All generated graphs and statistical tests were performed using GraphPad Prism 7. Statistical significance was determined using one-way ANOVA with Dunnett's post-test and the data is presented as mean ± standard deviation (SD), two-way ANOVA with Tukey post-test and the data is presented as mean ± SD. Statistical significance in time to occlusion and thrombus formation was determined using Mann-Whitney U test.

Chapter 3: Using platelet function assays to investigate the role of PLCγ2 downstream of GPVI and CLEC-2.

3.1 Introduction

3.1.1 PLCγ2 deficiency downstream GPVI and CLEC-2

As previously described, GPVI and CLEC-2 share similar tyrosine-kinase linked signalling pathways. PLCγ2 is a common signalling hub downstream of both receptors and several studies have examined its role in platelet function. In a number of studies, PLCγ2 has been shown to play an important role in platelet activation downstream of GPVI (Zheng et al., 2015, Suzuki-Inoue et al., 2003b). In order to explore the contribution of PLCγ2 in the activation of platelets stimulated by collagen, platelets were isolated from mice deficient in PLCγ2 and platelet aggregation triggered by collagen was assessed. In PLCγ2 deficient mouse, platelet aggregation was greatly reduced when induced by either high or low collagen concentrations. Despite the fact that collagen induced aggregation was greatly hindered in PLCγ2 deficient platelets, residual aggregation occurred (Mangin et al., 2003). It was shown that both GPVI and integrin α2β1 were necessary for this residual activation, which in turn led to an ADP/TxA2-dependent response via the activation of phosphoinositide 3-kinase (PI3K) and integrin αIIbβ3. Moreover, In the absence of PLCγ2, PLCγ1 can facilitate partial platelet activation by collagen and CRP (Suzuki-Inoue et al., 2003a). However, platelet aggregation was not induced in PLCγ2 deficient mice by direct activation of GPVI with CRP (Mangin et al., 2003). This suggests that PLCγ2 plays a significant role downstream of GPVI.

PLCγ2 also plays a role in mediating platelet spreading. Although there is a lack of evidence in the literature on the role of PLCγ2 in mediating platelet spreading when induced by CRP, previous studies have examined the role of PLCγ2 in mediating

platelet spreading on collagen and fibrinogen. Inoue et al,. have shown that PLCγ2 deficient mouse platelets display limited spreading but normal adhesion on collagen in comparison to WT platelets (Inoue et al., 2003), whereas Wonerow et al,. have demonstrated that PLCγ2 deficient platelets fail to spread on fibrinogen coated surfaces (Wonerow et al., 2003). This indicates that PLCγ2 has an important role in mediating platelet spreading.

The critical role PLCγ2 plays downstream of CLEC-2, when induced by rhodocytin, was also determined using PLCγ2 deficient mice. It was found that the absence of PLCγ2 resulted in no platelet response to low concentrations of rhodocytin (3-10nM), however intermediate concentrations (20-30nM) resulted in platelet shape change. This was argued by the authors that this may be due to the action of low levels of PLCγ1 as seen downstream of GPVI (Suzuki-Inoue et al., 2006) (Suzuki-Inoue et al., 2003a).

The role for PLCγ2 in CLEC-2 signalling can also be seen during development. CLEC-2 deficiency in mouse models results in the presence of blood-filled lymphatic vessels during the middle stage of gestation due to a failure in the separation of the blood vasculature and lymphatic vasculature (Bertozzi et al., 2010). This phenotype results in perinatal mortality for the majority of offspring. Additionally, the same phenotype is found in mouse models deficient in the hematopoietic proteins Syk, SLP-76, and PLCγ2, all of which are key proteins in the CLEC-2 signalling pathway (Abtahian et al., 2003, Sebzda et al., 2006, Ichise et al., 2016). This sheds light on a potential mechanism and role by which blood cells play in regulating growth and development in mice.

Although PLCγ2 plays a role downstream of CLEC-2 in platelet aggregation, there is a lack of evidence in the literature on the role PLCγ2 plays in mediating platelet

spreading and calcium release downstream of CLEC-2. Therefore, this role was further investigated in this study.

3.1.2 PLCγ2 pharmacological inhibitors

The activity of U73122 on phospholipase C (PLC) isoforms in platelets has been previously established in the literature. In a study conducted by Heemskerk et al., the authors proposed that U73122 effectively inhibits the activity of PLC isoforms. The effect of U73122 on PLCβ was examined by measuring elevations in cytosolic calcium triggered by thrombin. Collagen stimulated platelets were used to investigate the calcium signal induced by PLCγ2. The TxA2-dependent elevation in calcium was examined in thapsigargin stimulated platelets (Heemskerk et al., 1997). Additionally, U73122 demonstrated a dose-dependent inhibition of platelet functions, including inhibition of platelet aggregation and levels of intracellular calcium release (Pulcinelli et al., 1998).

It was established that when induced by collagen, U73122 inhibited platelet aggregation with IC50 values ranging from 1-3μM (Heemskerk et al., 1997a). Whereas its analogue, U73343, was shown to have no effect on aggregation stimulated by collagen (Bleasdale et al., 1990). Additionally, U73122 and its analogue U73343 effectively decreased the rise in calcium levels triggered by collagen. 5μM of U73122 inhibited the increase in Ca^{2+} peak to 0.4% of control and 20μM of U73343 resulted in a reduction in calcium to 7% in comparison to untreated control platelets. One possible explanation for this effect is that collagen evoked TxA2 production is inhibited when cytosolic phospholipase A2 (cPLA2) activation is inhibited (Heemskerk et al., 1997a).

3.2 Aims and hypothesis

3.2.1 Aims:

- To characterise the effect of the PLCγ2 inhibitor, U73122, downstream of GPVI and CLEC-2 using platelet aggregation, platelet spreading, calcium release and tyrosine phosphorylation.
- To investigate the role PLCγ2 plays in mediating platelet activation downstream of GPVI and CLEC-2.

3.2.2 Hypothesis

Pharmacological inhibition of PLCγ2 will inhibit platelet responses downstream of GPVI and CLEC-2.

3.3 Results

3.3.1 Pharmacological inhibition of PLCγ2 impairs GPVI and CLEC-2 mediated aggregation

Aggregometry tests for platelets are commonly used to study their function. This can be by light transmission aggregometry (LTA) or plate-based aggregometry (PBA). While LTA is more widely used and shows aggregation in real time (Born, 1962), PBA allows for higher throughput. PBA tends to be more time efficient as it allows the testing of multiple concentrations of multiples agonists more rapidly than LTA due to the 96-well plate, high-throughput format. Additionally, PBA requires less platelet volume (Chan et al., 2018). Therefore, PBA was firstly used to characterise the effect of U73122 on platelet aggregation when induced by CRP, rhodocytin, or thrombin. However, PBA provides only an endpoint result and small delays in the onset of platelet aggregation are less likely to manifest. This can be important when using rhodocytin as an agonist because rhodocytin induces platelet aggregation with a lag phase before the onset of aggregation which can be missed when using PBA (Bergmeier et al., 2001). Therefore, PBA was used for an initial screen of the effect of U73122 on a range of agonists and concentrations, followed by the use of LTA to obtain higher-resolution, time-resolved aggregation data.

Washed platelets were prepared as described in (section 2.2.1.1) and incubated with 1μM, 3μM, or 10μM of U73122 or vehicle control for 5 minutes at 37°C. Platelets were then stimulated with CRP or thrombin and shaken at 37°C for 5 minutes or stimulated with rhodocytin and shaken at 37°C for 10 minutes. This longer time for rhodocytin ensured that aggregation had occurred, as the lag phase resulted in

varied results at a 5-minute timepoint. End-point aggregation was read using a Flexstation.

The inclusion of thrombin as an agonist was used to assess the effect of U73122 on other PLC isoforms. Thrombin induces platelet activation by interacting with protease-activated receptors (PAR) located on the surface of platelets through G protein-coupled receptors (GPCRs). In response, the Gq, G12, and possibly Gi family members are activated by these receptors, which then activates PLCβ.
Figure 3.1 shows that when stimulated by 0.5-3μg/mL CRP, 1μM of U73122 significantly reduced platelet aggregation to approximately 50% of the vehicle, whereas aggregation was nearly abolished at 3μM and 10μM of U73122.
In platelets stimulated by 100nM rhodocytin, 1μM and 3μM of U73122 had no significant effect on aggregation. Large error bars, however, highlight the fact that one donor was less responsive to the drug compared to the others. Nevertheless, 10μM of U73122 abolished aggregation significantly.
When stimulated with 300nM rhodocytin on the other hand,1μM, 3μM, and 10μM of U73122 significantly inhibited platelet aggregation. This further highlights the inconsistent donor that had a relatively higher response to 100nM rhodocytin in comparison to others.

U73122 demonstrated a significant inhibitory effect on thrombin induced aggregation at 3μM and 10μM. These results show evidence that U73122 inhibits PLCβ but perhaps to a lesser extent as 1μM of U73122 had no effect on reducing aggregation in thrombin stimulated platelets but had a significant effect on CRP and rhodocytin stimulated platelets.

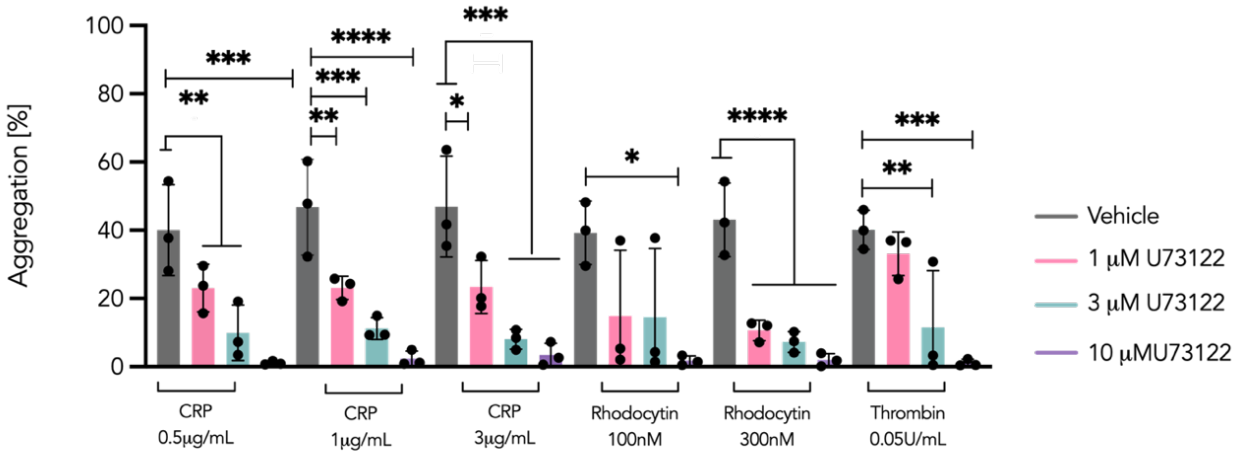

Figure 3.1: U73122 inhibits plate-based aggregation stimulated by CRP, rhodocytin, and thrombin compared to vehicle control.

Washed platelets ($4x10^8$/mL) were treated with U73122 or vehicle control (DMSO 0.1% (v/v)) for 5 minutes at 37°C before the addition of the indicated final concentrations of CRP, rhodocytin, or thrombin. Plate-based aggregation was measured after 5 minutes using a FlexStation (n=3). Statistical significance was determined using one-way ANOVA with Dunnett's post-test. Graph shows mean ± SD. *p ≤ 0.05, **p ≤ 0.01, ***p ≤ 0.001, **** p ≤ 0.0001.

In order to further examine the effect of the PLCγ2 inhibitor on other isoforms of PLC, PBA was used to test the effect of U73122 on platelet aggregation stimulated by multiple concentrations of ADP. ADP acts via two G-protein-coupled receptors, P2Y1 and P2Y12, to stimulate platelet aggregation (Gachet, 2008). An increase in cytosolic calcium is caused by the coupling of P2Y1 to Gαq, which stimulates phospholipase Cβ (PLCβ) (Van Kolen and Slegers, 2006).

For this experiment, we introduced U73343 which is a close analogue of U73122. U73343, is reported to have no effect on PLC's and therefore was used a negative control. However, U73343 inhibits cPLA2 activation, which in turn lowers arachidonic acid release and TxA2 synthesis (Heemskerk et al., 1997a).

ADP sensitive platelets were prepared as the ADP receptors are desensitised during the washing phases by fast centrifugation of the platelets and as a result, washed

platelets are less receptive to ADP. ADP sensitive platelets were incubated with 1μM, 3μM or 10μM of U73122, U73343, or vehicle control for 5 minutes at 37°C. Platelets were then stimulated with the stated concentrations of ADP and shaken for 5 minutes. End-point aggregation was read using a Flexstation.

Figure 3.2 A shows that platelet aggregation levels stimulated with 0.1μM, 1μM, and 3μM ADP are somewhat similar to unstimulated platelets. Also, when platelets were stimulated with 0.1μM 10μM 30μM, and 100μM ADP, only the highest concentration of U73122 (10μM) has a significant effect on platelet aggregation in comparison to the vehicle control. In contrast, when stimulated by 1μM and 3μM of ADP, 3μM and 10μM of U73122 significantly reduced platelet aggregation. On the other hand, U73343 had no significant effect on platelet aggregation stimulated by ADP (figure 3.2 B). These results demonstrate that U73122 is not PLCγ2 specific but can also affect other PLC isoforms such as PLCβ.

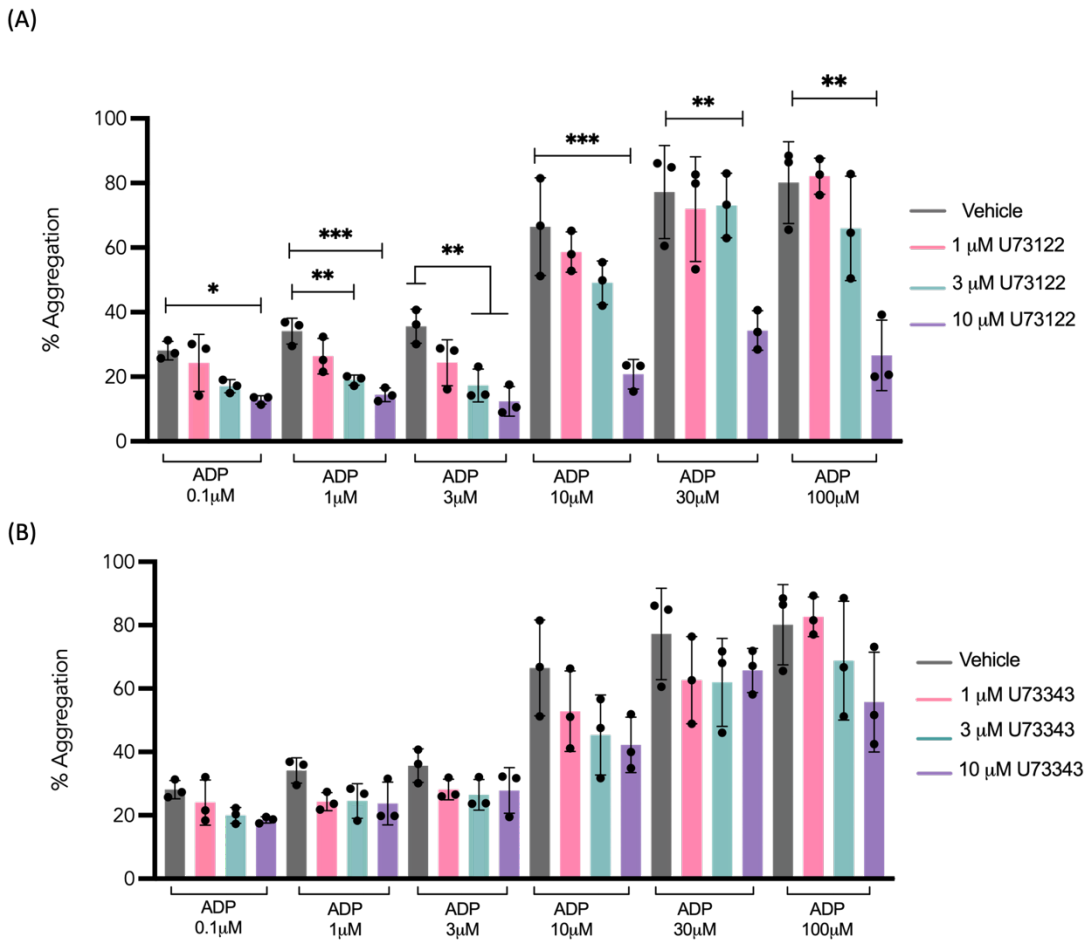

Figure 3.2: U73122 inhibits plate-based aggregation when stimulated with ADP, but U73343 has no effect compared to vehicle control.

ADP sensitive platelets were treated with (A) U73122, (B) U73343, or vehicle control (DMSO 0.1% (v/v)) for 5 minutes at 37°C before the addition of ADP. Plate-based aggregation was measured after 5 minutes using a FlexStation (n=3). Statistical significance was determined using one-way ANOVA with Dunnett's post-test. Graph shows mean ± SD. *$p \leq 0.05$. **$p \leq 0.01$, ***$p \leq 0.001$

3.3.2 Inhibition of PLCγ2 by U73122 significantly inhibits (hem)ITAM mediated platelet aggregation in light transmission aggregometry.

Using PBA can be time efficient when screening multiple concentrations of multiple agonists. The screen using PBA allowed a selection of agonists and inhibitor concentrations to be taken forward for testing using light transmission aggregometry (LTA). Additionally, although PBA can provide high throughput results, it's an end

point method. Therefore, it was important to observe the effect of U73122 on platelet aggregation induced by CRP and rhodocytin in real time using LTA. LTA shows platelet aggregation in real time, therefore small changes or delays can be observed. This is specifically important when studying platelet aggregation induced by rhodocytin due to the observed lag phase (Suzuki-Inoue et al., 2007).
As PBA was an initial screening for the PLCγ2 inhibitor U73122 and multiple concentrations of multiple agonists, no control drugs were used. However, as previously described, U73122's analogue was used as a negative control to rule out the possible off target effects on PLA2. Additionally, ibrutinib was used as a positive control. Btk leads to the activation of PLCγ2 and therefore inhibition of Btk using ibrutinib should also inhibit PLCγ2.

Washed platelets were prepared and incubated with a range of concentrations of U73122, U73343, ibrutinib, or vehicle control for 5 minutes. Platelets were stirred for 30 seconds before stimulation with CRP or rhodocytin. Platelet aggregation was measured for 5 minutes. As shown in figure 3.3A, and 3.3B, a low concentration of U73122 (1μM) had no significant effect on GPVI mediated aggregation. At 3μM, U73122 had a significant effect on decreasing platelet aggregation. At the highest concentration (10μM), U73122 also had a significant effect on decreasing platelet aggregation in comparison to the untreated control in CRP stimulated platelets. U73343 on the other hand, has no significant effect on platelet aggregation when stimulated with CRP. Consistent with previous studies, ibrutinib significantly inhibited GPVI mediated aggregation at all concentrations. It is worth noting that surprisingly, washed platelets seemed to be less sensitive to U73122 in PBA than LTA.

When stimulated by 100nM rhodocytin, Figure 3.4 A, B shows that U73122 had a small but significant effect on reducing platelet aggregation only at 10μM. Surprisingly, U73343 also slightly but significantly reduced platelet aggregation downstream of CLEC-2 at the highest concentration (10μM). Ibrutinib caused a large and significant reduction in platelet aggregation, to less than 20%, at 1μM, 3μM, and 10μM. Similar to results obtained from the PBA assay, U73122 had a small effect on decreasing rhodocytin stimulated platelet aggregation but only at its highest concentration. However, the percentage of aggregation in LTA (around 95%) seems much higher than that the percentage of aggregation PBA (around 40%).

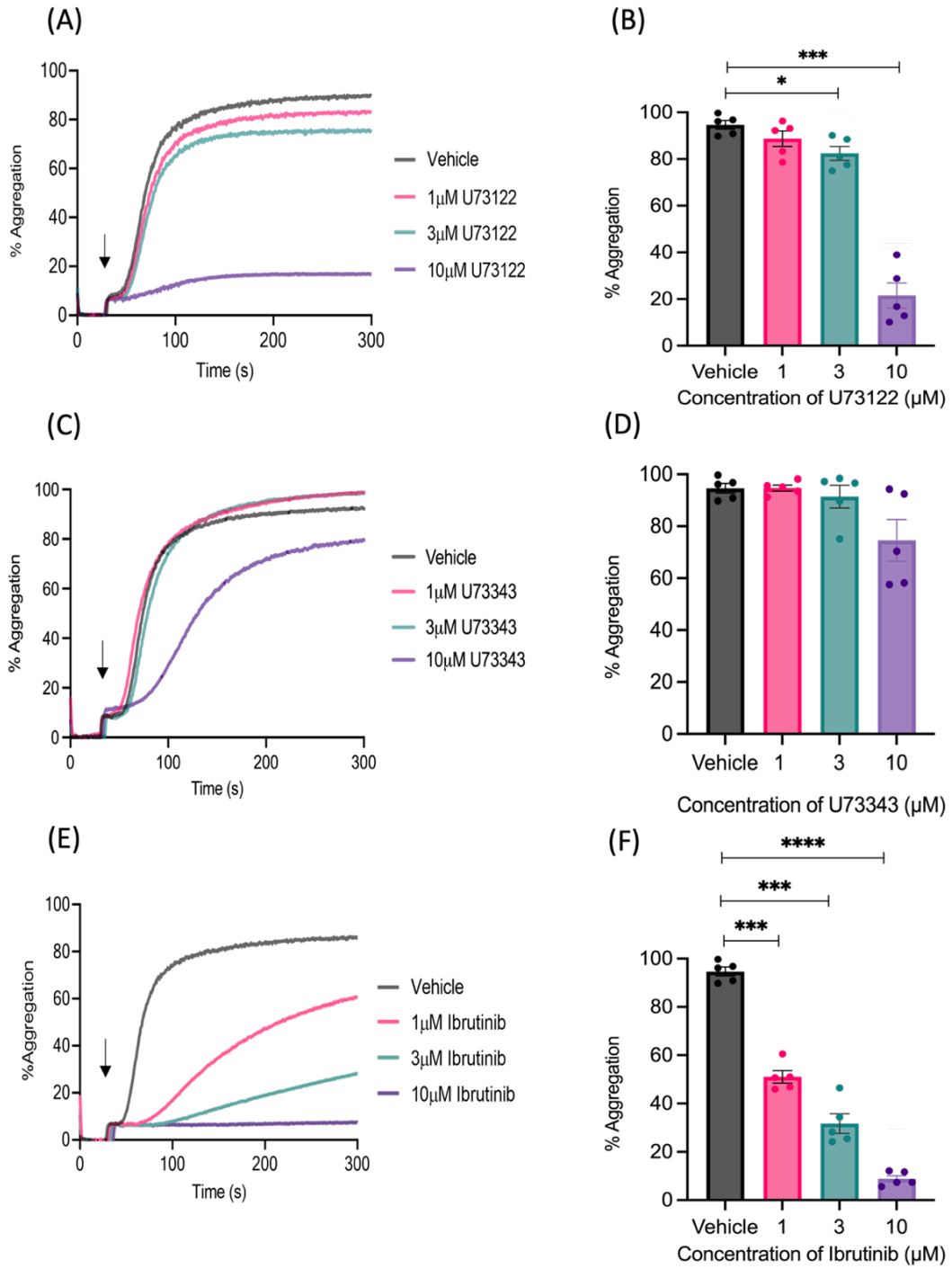

Figure 3.3: High concentrations of U73122 inhibits GPVI mediated platelet aggregation.

Washed platelet ($4x10^8$/mL) were incubated with the indicated final concentrations of U73122, U73343, Ibrutinib, or vehicle control (DMSO 0.1% (v/v)) for 5 minutes. The addition of 3μg/mL CRP, was added as indicated by the arrow, and light transmission aggregation was measured for 5 minutes. (A, C, E) show representative aggregation traces and (B, D, F) show quantified values of maximum aggregation of (n=5). Statistical significance was determined against the vehicle control using one-way ANOVA with Dunnett's post-test. Graph shows mean ± SD. *$p \leq 0.05$, ***$p \leq 0.001$, **** $p \leq 0.0001$.

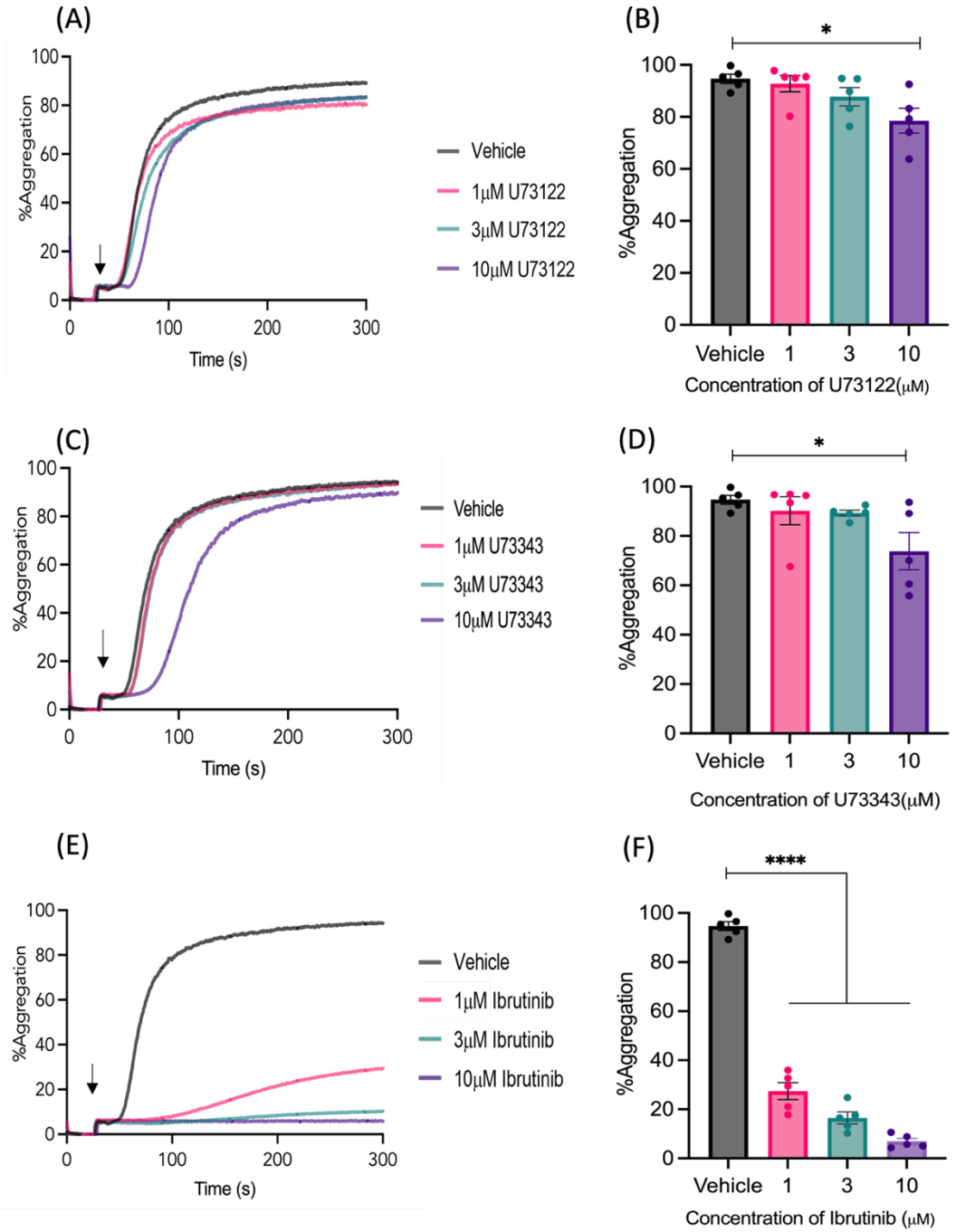

Figure 3.4*: High concentrations of U73122 and U73343 inhibit CLEC-2 mediated platelet aggregation.*

Washed platelet ($4x10^8$/mL) were incubated with the indicated final concentrations of U73122, U73343, Ibrutinib, or vehicle control (DMSO 0.1% (v/v)) for 5 minutes. The addition of 100nM rhodocytin, was added as indicated by the arrow, and light transmission aggregation was measured for 5 minutes. (A, C, E) show representative aggregation traces and (B, D, F) show quantified values of maximum aggregation of (n=5). Statistical significance was against the vehicle control and determined using one-way ANOVA with Dunnett's post-test. Graph shows mean ± SD. *$p \leq 0.05$, **** $p \leq 0.0001$.

3.3.3 Inhibition of PLCγ2 by U73122 significantly inhibits (hem)ITAM mediated increase of calcium flux

The activation of PLCγ2 in platelets leads to the initiation of a signalling cascade that results in the release of calcium (Bird et al., 2004). Therefore, examining the calcium signal can provide a direct readout of PLCγ2 activity. Given the complex nature of aggregation and the conflicting results above, this offers a simpler way to focus on PLCγ2 activity. U73122 has been previously used to study calcium flux induced by thrombin, thromboxane A2, collagen, and thapsigargin (Heemskerk et al., 1997a). However, this inhibitor has not been used to study GPVI specific calcium flux (as collagen will also activate integrin α2β1), or CLEC-2 mediated calcium flux. Therefore, U73122 was used to investigate its effect on calcium signalling downstream GPVI and CLEC-2 evoked by CRP and rhodocytin, respectively.

PRP was incubated with a Ca^{2+} sensitive dye, Fura-2 AM, for 1 hour before being pelleted and resuspended in Tyrode's buffer at $4x10^8$ platelets/mL. The platelets were then incubated with 1μM, 3μM, and 10μM of U73122, U73343, ibrutinib, or vehicle control for 5 minutes at room temperature before stimulation with 1μg/mL CRP or 100nM rhodocytin. Calcium fluorescence measurements were recorded for five minutes using a FlexStation.

When stimulated with CRP, calcium traces show that the vehicle control has a high increase in calcium flux compared to resting platelets (Figure 3.5). In the presence of U73122 however, there is a decrease in the calcium flux in a concentration dependent manner. Figure 3.5B shows that when quantifying the change in peak (height of the peak – resting sample), platelets treated with 1μM,3μM and 10μM of U73122 show a significant decrease in calcium signalling. U73343 showed no significant effect on calcium signalling (Figure 3.5 C, D) suggesting that the decrease in the calcium signal, when treated with U73122, may be due to the specific inhibition

of PLC isoforms rather than inhibition of PLA2. Consistent with previous studies, 1μM, 3μM and 10μM of ibrutinib significantly inhibited calcium release (Figure 3.5 E, F).

Similarly, to GPVI, U73122 had a similar effect on calcium signalling downstream CLEC-2 (Figure 3.6 A, B). All concentrations of U73122 have a statistically significant inhibitory effect on the calcium flux induced by 100nM rhodocytin when compared to the vehicle control. Figure 3.6 C, D show that U73343 had no statistically significant inhibitory effect on rhodocytin induced calcium flux.

Ibrutinib, displayed a similar effect downstream CLEC-2 to that seen downstream of GPVI (Figure 3.6 E, D). All concentrations of Ibrutinib tested (1μM,3μM, and 10μM) significantly abrogated calcium signalling by CRP and rhodocytin. All together, these results demonstrate the important role PLCγ2 plays in calcium signalling downstream of GPVI and CLEC-2.

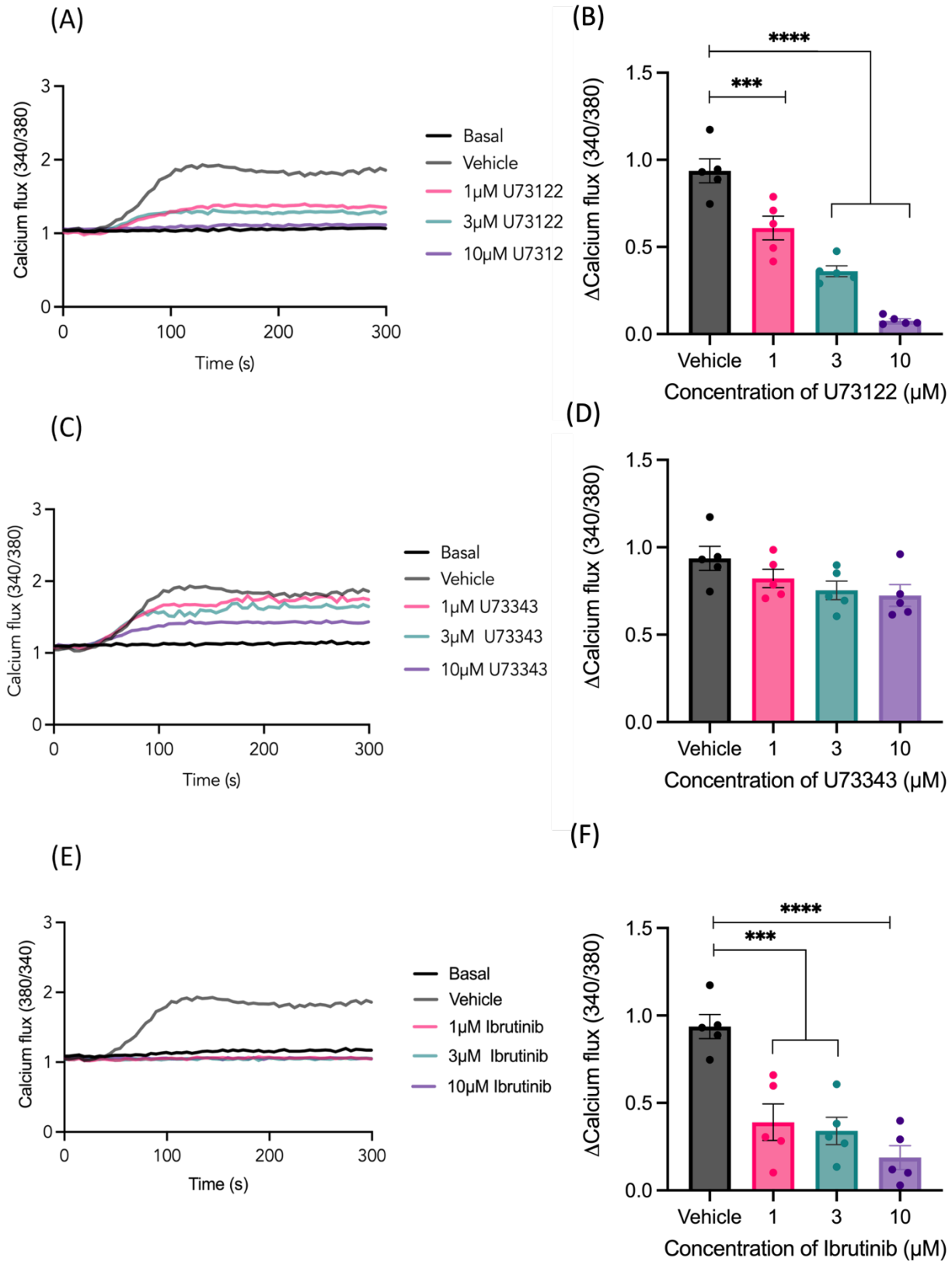

Figure 3.5: U73122 inhibits calcium flux downstream of GPVI.

Fura-2 loaded platelet were prepared and treated with U73122, U73343, Ibrutinib or vehicle control (DMSO 0.1% (v/v)) for 5 minutes. After the addition of 1μg/mL CRP, calcium flux was measured for 5 minutes. (A, C, E) representative calcium flux traces (B, D, F) quantified peak heights were plotted (n=5). Statistical significance was calculated against vehicle control using one-way ANOVA against vehicle with Dunnett's multiple comparison. Graph shows mean ± SD. *p ≤ 0.05. **p ≤ 0.01 ***p ≤ 0.001, **** p ≤ 0.0001.

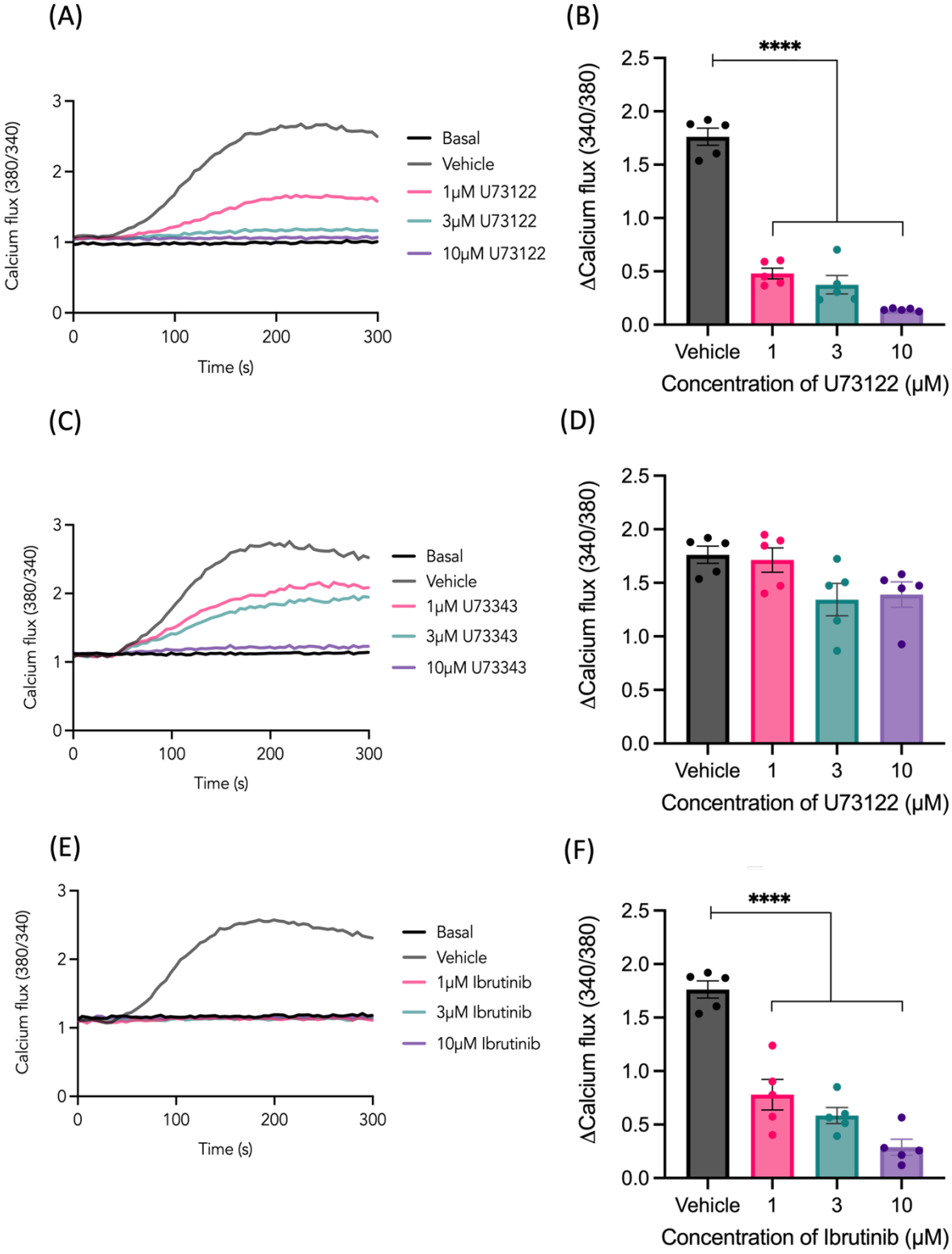

Figure 3.6: U73122 inhibits calcium flux downstream of CLEC-2.

Fura-2 loaded platelet were prepared and treated with U73122, U73343, Ibrutinib or vehicle control (DMSO 0.1% (v/v)) for 5 minutes. After the addition of 100nM rhodocytin, calcium flux was measured for 5 minutes. (A, C, E) representative calcium flux traces (B, D, F) quantified peak heights were plotted (n=5). Statistical significance was calculated against vehicle control using one-way ANOVA against vehicle with Dunnett's multiple comparison. Graph shows mean ± SD. *p ≤ 0.05. **p ≤ 0.01 ***p ≤ 0.001, **** p ≤ 0.0001.

3.3.4 Platelet adhesion on CRP and rhodocytin is inhibited by U73122

Although the role of PLCγ2 in mediating platelet spreading and adhesion has been previously studied using mouse models, the impact of U73122 on human platelet adhesion and spreading has not previously been investigated. Therefore, to further characterise U73122 and to further understand the role of PLCγ2 in platelet activation, platelet adhesion and spreading, platelets were allowed to interact with a range of immobilised agonists in the presence and absence of U73122, U73343, and ibrutinib.

Washed platelets ($1x10^7$/mL) were incubated with multiple concentrations of U73122, U73343, ibrutinib, or a vehicle control prior to spreading on agonist coated coverslips (3µg/mL CRP, 100nM rhodocytin, or 100µg/mL fibrinogen). Coverslips were then mounted and imaged using Nikon TiE2 microscope using differential phase contrast (DIC) with a 100X objective lens. Images were then analysed using a convolutional neural network (CNN) to measure the number of adhered platelets and the spread platelet area (Kempster et al., 2022b).

Representative DIC images (figure 3.7A) and figure 3.7B shows the striking effect of U73122 on platelet adhesion. Concentrations above and including 1µM U73122 completely abolished platelet adhesion (number of platelets per field of view) on CRP. At the highest concentration (10µM), U73343 resulted in a small but significant decrease in platelet adhesion to CRP coated surfaces suggesting that other lipases may play a role in facilitating platelet adhesion on CRP. However, U73343 had no significant effect on platelet spreading. In the presence of CRP, ibrutinib had a

significant effect on platelet adhesion at 3μM and 10μM. Whereas platelet spreading on CRP was only significantly decreased at 10μM of ibrutinib.

These results indicate that the inhibition of PLCγ2 by U73122 has a potent effect on platelet adhesion.

(A)

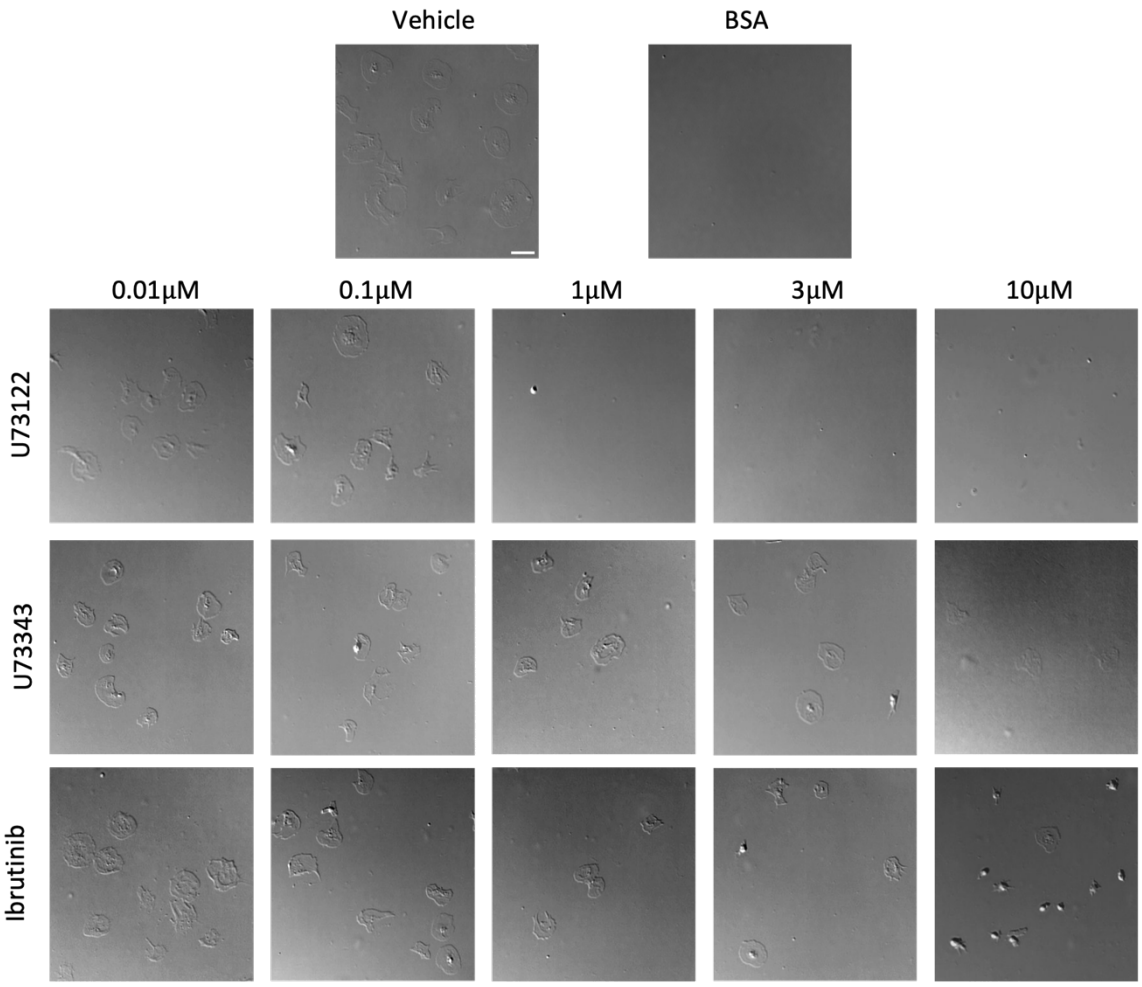
Vehicle
BSA
0.01µM
0.1µM
1µM
3µM
10µM
U73122
U73343
Ibrutinib

(B)

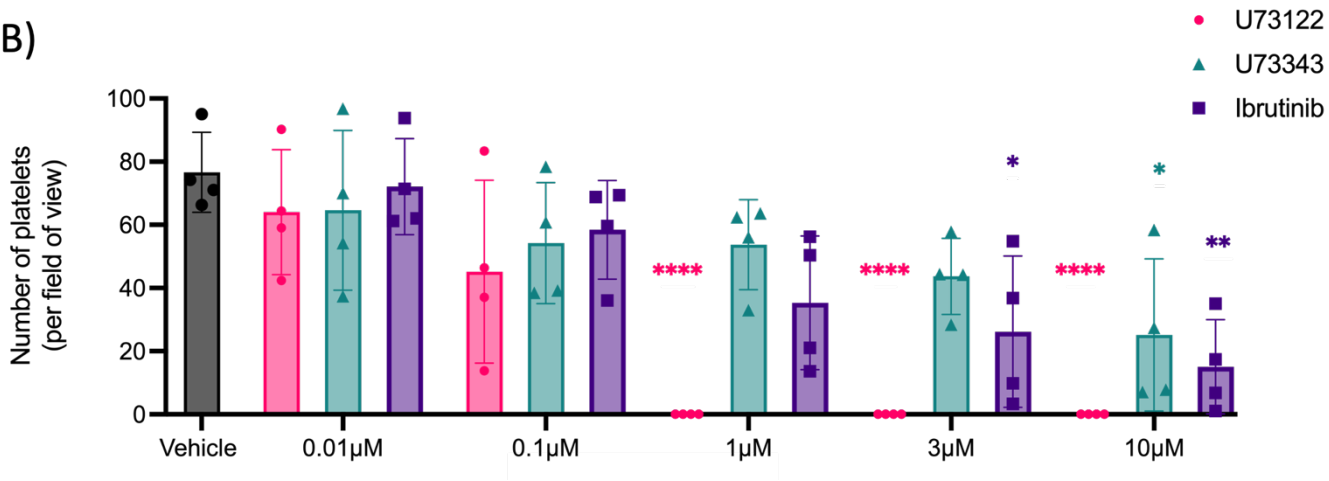
U73122
U73343
Ibrutinib
Number of platelets
(per field of view)
100
80
60
40
20
0
Vehicle
0.01µM
0.1µM
1µM
3µM
10µM
****
****
****
*
*
**

(C)

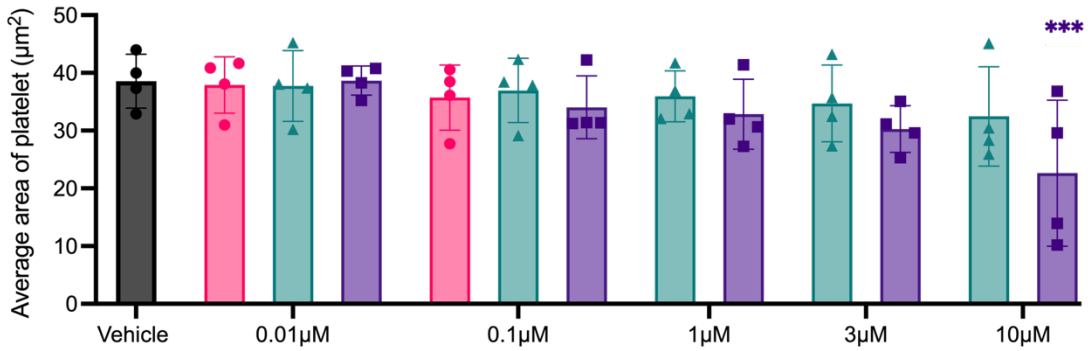

Figure 3.7: Platelet adhesion on CRP is inhibited by U73122 and Ibrutinib but not U73343.

Washed platelets ($1x10^7$/mL) were treated with U73122, U73343, ibrutinib, or vehicle control (DMSO 0.1% (v/v)) for 5 minutes. Platelets were spread on 10 µg/mL CRP or 5 mg/mL BSA control for 45 minutes. Coverslips were fixed, mounted, and imaged on a Nikon TiE2 microscope with a 100x objective (n=4). (A) Representative DIC images, scale bar = 20µm. A convolutional neuron network (CNN) was used to analyse (B) platelet number and (C) platelet spread area. Statistical significance was calculated against vehicle using two-way ANOVA with Tukey post-test. Graph shows mean ± SD. *p ≤ 0.05, **p ≤ 0.01***p ≤ 0.001, **** p ≤ 0.0001.

Until this study, platelet spreading on rhodocytin coated surfaces had not previously been established in the literature. Therefore, to investigate the effect of PLCγ2 in CLEC-2 mediated spreading, washed platelets were treated with U73122, U73343, ibrutinib, or vehicle control for 5 minutes prior to spreading on 100nM rhodocytin. Coverslips were mounted and imaged as previously described. Figure 3.8 demonstrates that platelets are able to adhere and spread on rhodocytin surfaces. When examining the number of vehicle treated platelets adhering to coated surfaces, rhodocytin seems to have fewer adherent platelets in comparison to CRP. U73122 significantly reduced platelet adhesion at 1μM, 3μM, and 10μM (figure 3.8B). U73122 also had a significant effect on platelet spreading. Where all concentrations significantly decreased the average area of platelets spread on rhodocytin (figure 3.8C).

Although U73343 had no significant effect on the number of platelets adhering to rhodocytin, 10μM of U73343 had a small but significant effect on decreasing the average area of adhering platelets.

(A)

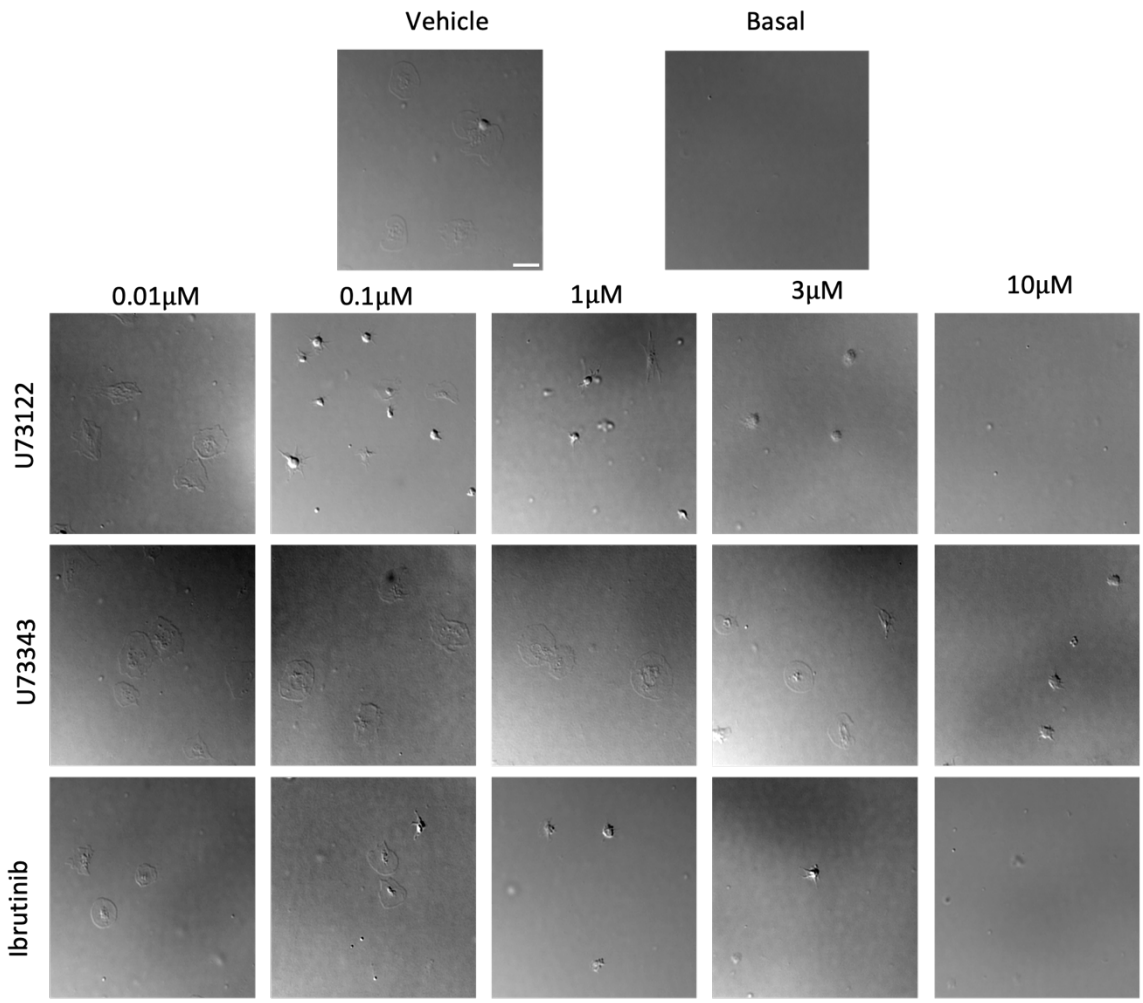
Vehicle
Basal
0.01µM
0.1µM
1µM
3µM
10µM
U73122
U73343
Ibrutinib

(B)

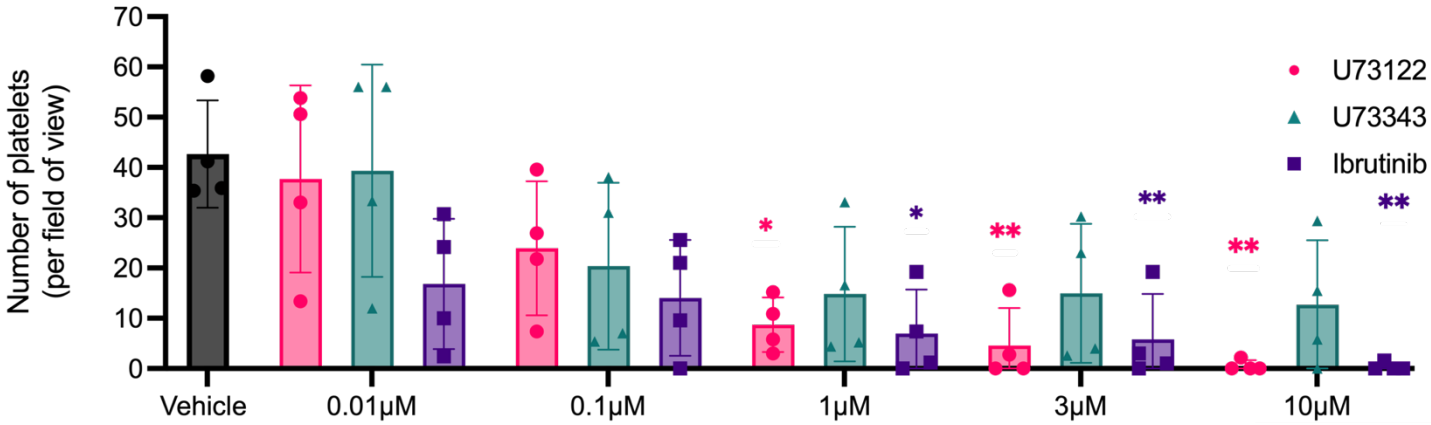
Number of platelets
(per field of view)
70
60
50
40
30
20
10
0
Vehicle
0.01µM
0.1µM
1µM
3µM
10µM
U73122
U73343
Ibrutinib
*
*
**
**
**
**

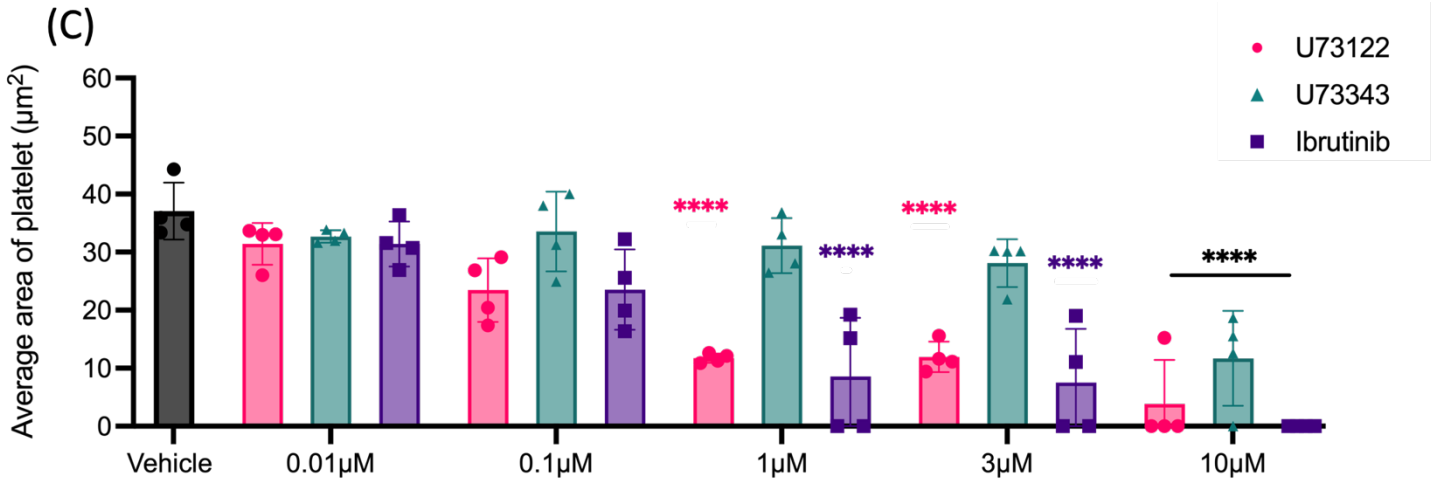

Figure 3.8: Platelet spreading on rhodocytin is inhibited by U73122, Ibrutinib, and U73343 at highest concentration.

Washed platelets ($1x10^7$/mL) were treated with U73122, U73343, ibrutinib, or vehicle control (DMSO 0.1% (v/v)) for 5 minutes. Platelets were spread on 100nM rhodocytin or 5 mg/mL BSA control for 45 minutes. Coverslips were fixed, mounted, and imaged on a Nikon TiE2 microscope with a 100x objective (n=4). (A) Representative DIC images, scale bar = 20μm. A convolutional neuron network (CNN) was used to analyse (B) platelet number and (C) platelet spread area. Statistical significance was calculated against vehicle using two-way ANOVA with Tukey post-test. Graph shows mean ± SD. *p ≤ 0.05, **p ≤ 0.01***p ≤ 0.001, **** p ≤ 0.0001.

To further investigate the role of PLCγ2 downstream αIIbβ3, washed platelets were treated with U73122, U73343 and ibrutinib prior to spreading on 100μg/mL fibrinogen. As previous studies showed that PLCγ2 deficiency in mice decreases platelet spread area, similar results were expected (Zheng et al., 2015). Figure 3.9 demonstrates that U73122 had a significant effect on inhibiting platelet adhesion to fibrinogen starting from 1μM and complete inhibition at 3μM and 10μM. Also, U73122 showed a significant decrease in platelet spreading at 1μM. U73343 on the other hand had no significant effect on platelet adhesion nor spreading. Although in previous studies it has been established that ibrutinib inhibits platelet adhesion on fibrinogen, we were unable to replicate this result as ibrutinib showed no significant

effect on platelet adhesion or spreading (Bye et al., 2015). However, as seen in figure 3.9B and figure 3.9C, the large error bars indicate some variability in the response to ibrutinib. Where in some donors ibrutinib seems to affect platelet adhesion and spreading but not in others.

There is a striking difference in the effect of inhibiting PLCγ2 using U73122 in platelet aggregation and platelet adhesion and spreading. U73122 slightly decreased platelet aggregation at 3μM and had a huge effect on inhibiting platelet aggregation at 10μM. In platelet adhesion and spreading however, U73122 had a potent effect on platelet adhesion. Where 1μM completely abolished platelet adhesion on several agonist-coated surfaces. This highlights the activity U73122 has on other PLC isoforms such PLCγ1 and possibly PLCβ2 which is required for platelet adhesion and show a new perspective to PLCγ2 which was not covered in previous working using KO models.

(A)

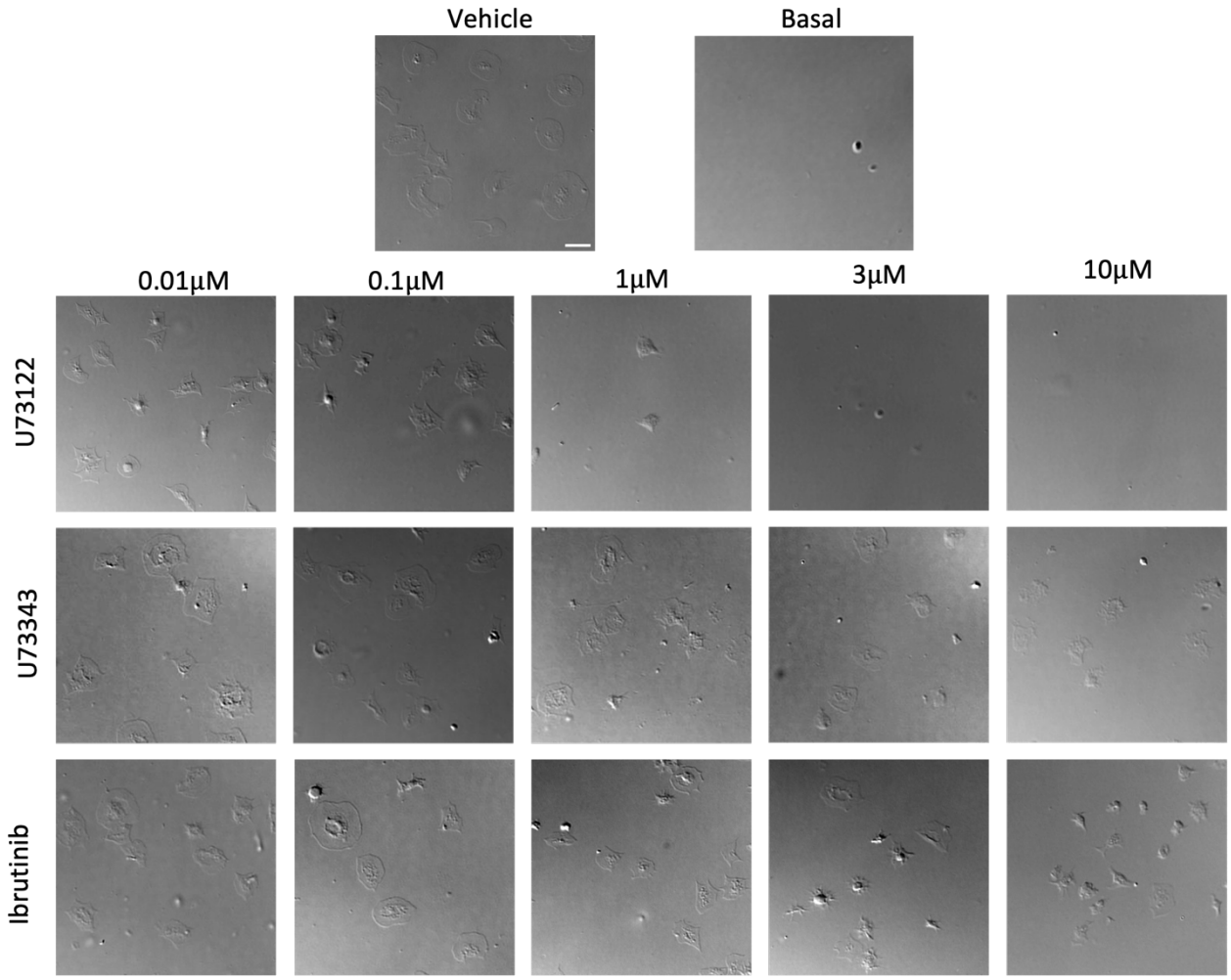
Vehicle
Basal
0.01µM
0.1µM
1µM
3µM
10µM
U73122
U73343
Ibrutinib

(B)

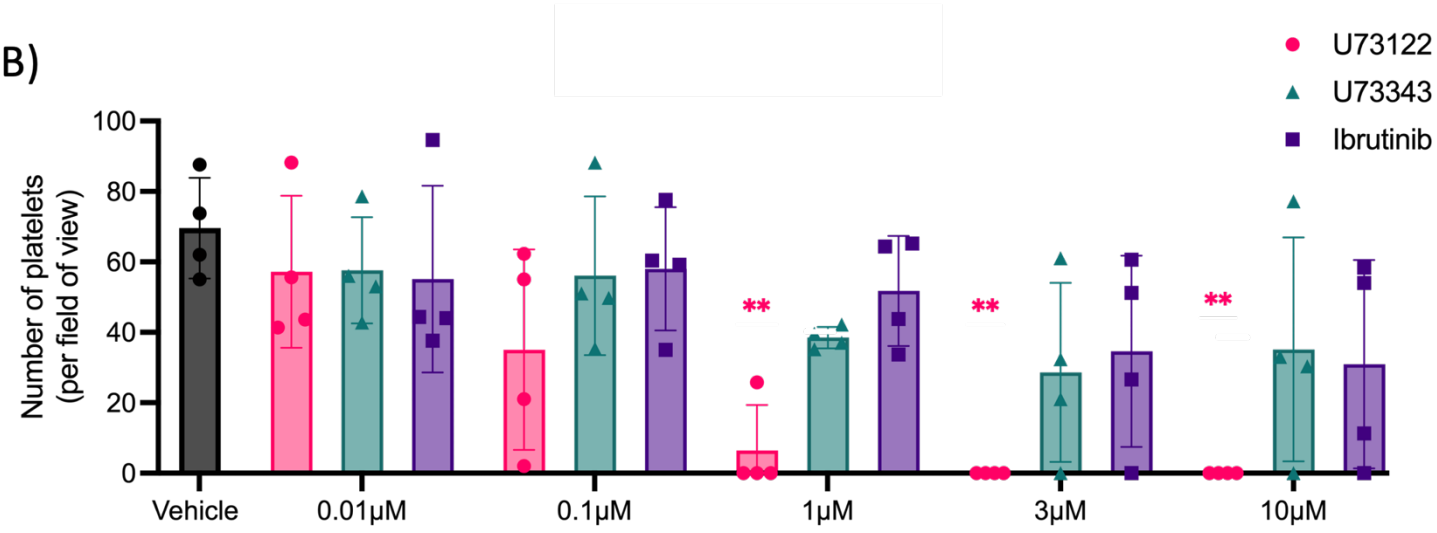
U73122
U73343
Ibrutinib
Number of platelets
(per field of view)
100
80
60
40
20
0
**
**
**
Vehicle
0.01µM
0.1µM
1µM
3µM
10µM

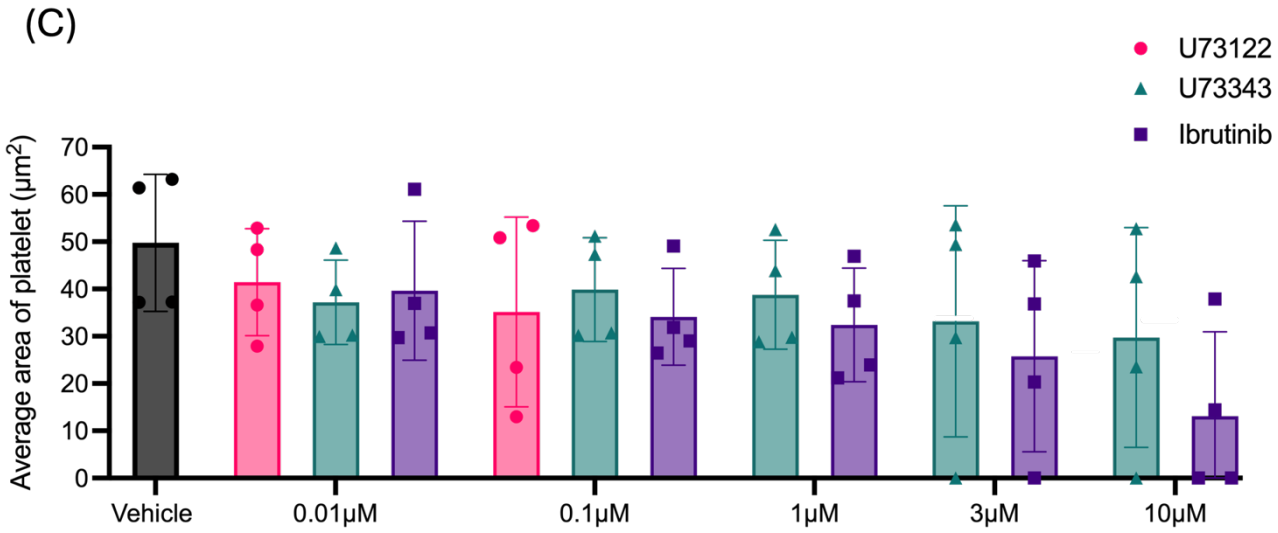

Figure 3.9: Platelet adhesion on fibrinogen is inhibited by U73122 and not U73343.

Washed platelets($1x10^7$/mL) were treated with U73122, U73343, ibrutinib, or vehicle control (DMSO 0.1% (v/v)) for 5 minutes. Platelets were spread on 100μg/mL fibrinogen or 5 mg/mL BSA control for 45 minutes. Coverslips were fixed, mounted, and imaged on a Nikon TiE2 microscope with a 100x objective (n=4). (A) Representative DIC images, scale bar = 20μm. A convolutional neuron network (CNN) was used to analyse (B) platelet number and (C) platelet spread area. Statistical significance was calculated against vehicle using two-way ANOVA with Tukey post-test. Graph shows mean ± SD. *p ≤ 0.05, **p ≤ 0.01***p ≤ 0.001, **** p ≤ 0.0001.

3.3.5 The PLCγ2 inhibitor, U73122, has no significant effect on tyrosine phosphorylation downstream of (hem)ITAM receptors.

To confirm that the effects of U73122 were not via off-target inhibition of the upstream signalling pathway, which involves a number of tyrosine kinases, western blotting was performed for a number of key signalling proteins (PLCγ2, Btk, Syk, and SFKs). Total tyrosine phosphorylation, along with protein specific tyrosine phosphorylation sites, was measured in CRP and rhodocytin stimulated platelets. When examining tyrosine phosphorylation downstream GPVI, washed platelets were incubated with integrilin (to prevent aggregation), and apyrase and indomethacin (to prevent the secondary mediators ADP and thromboxane respectively) prior to treatment with U73122, U73343, or ibrutinib for 5 minutes. Platelets were then stimulated with 1μg/mL CRP for 3 minutes and lysed with 6X sample buffer. On the other hand, when investigating CLEC-2 induced signalling, platelets were only incubated with integrilin as secondary mediators are essential for CLEC-2 signalling (Badolia et al., 2017, Pollitt et al., 2010). Washed platelets were incubated with the indicated concentration of U73122, U73343, ibrutinib of vehicle control for 5 minutes and stimulated with 300nM rhodocytin for 5 minutes prior to lysis with 6X sample buffer. Membranes were cut using a razor blade prior to blotting. Protein tyrosine phosphorylation was examined using SDS-PAGE and western blotting with phospho-specific antibodies.

Figure 3.10 shows that U73122 and U73343 had no effect on total tyrosine phosphorylation following CRP stimulation when compared to the vehicle control. In contrast, figure 3.10B and E demonstrates that the phosphorylation of PLCγ2 Y1217 and Src Y418 was reduced to close to basal level when treated with 1μM ibrutinib, respectively. Moreover, 0.1μM and 1μM of ibrutinib significantly inhibits the phosphorylation of Btk pY223 downstream of GPVI (figure 3.10C).

Similarly, U73122 and U73343 had no effect on total tyrosine phosphorylation of proteins downstream of CLEC-2. In contrast, figure 3.11 A, the upper panel shows that for 300nM rhodocytin stimulated platelet only 1μM of ibrutinib resulted in a decrease in total tyrosine phosphorylation when compared to the vehicle control. Similarly, there was a significant decrease in the phosphorylation of Syk Y525/6 in platelets treated with 1μM of ibrutinib (figure 3.11 D). Moreover 0.1μM and 1μM ibrutinib inhibited Btk pY223 phosphorylation to basal levels (figure 3.11 C) and significantly reduced PLCγ2 Y1217 phosphorylation (figure 3.11 B). On the other hand, ibrutinib had no effect on Src Y418 phosphorylation downstream of CLEC-2 (figure 3.11 D).

Altogether, these results demonstrate that unlike ibrutinib, U73122 has no significant effect on tyrosine phosphorylation downstream both of GPVI and CLEC-2.

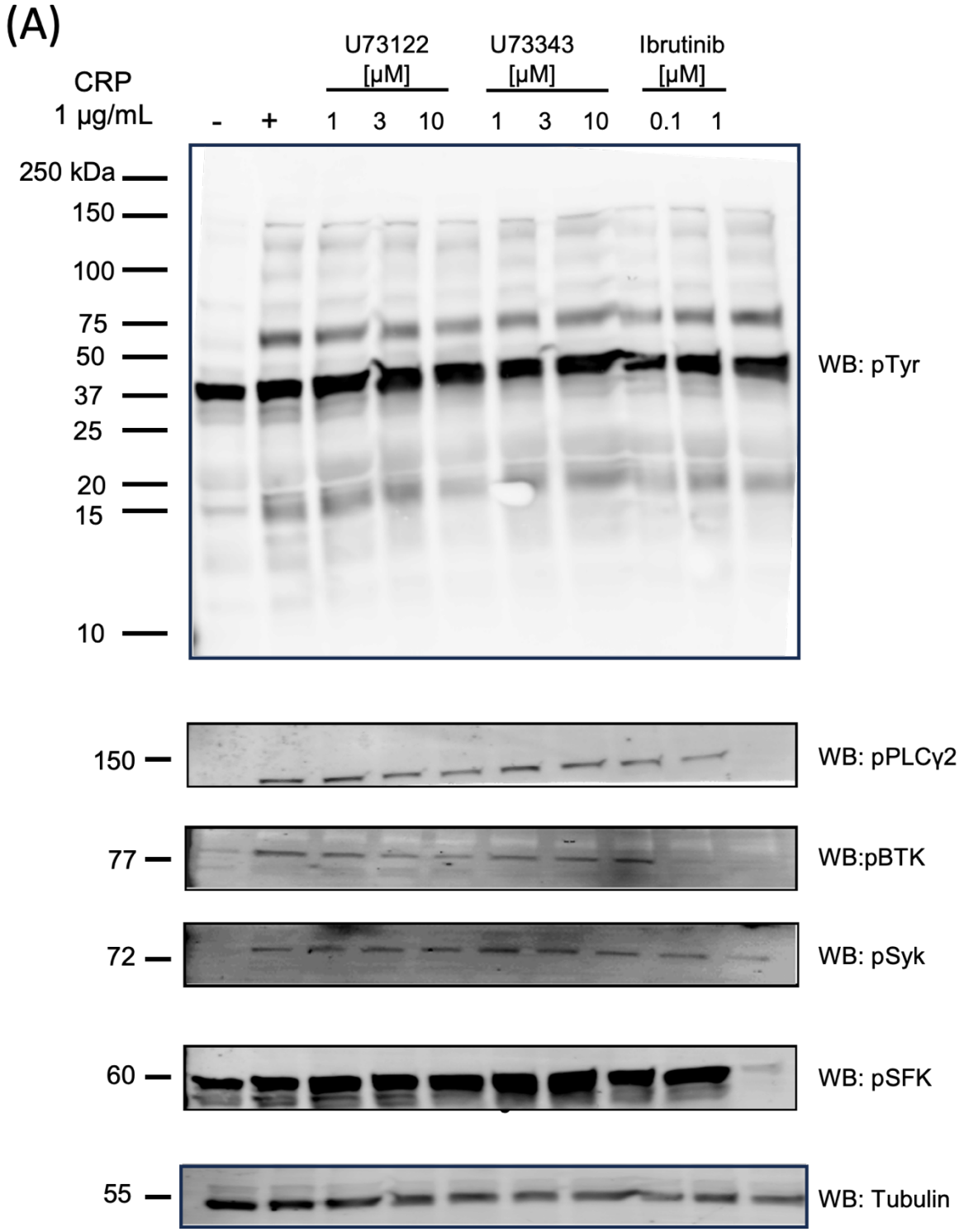
(A)
CRP
1 μg/mL
U73122
[μM]
U73343
[μM]
Ibrutinib
[μM]
- + 1 3 10 1 3 10 0.1 1
250 kDa
150
100
75
50
37
25
20
15
10
WB: pTyr
150
WB: pPLCγ2
77
WB:pBTK
72
WB: pSyk
60
WB: pSFK
55
WB: Tubulin

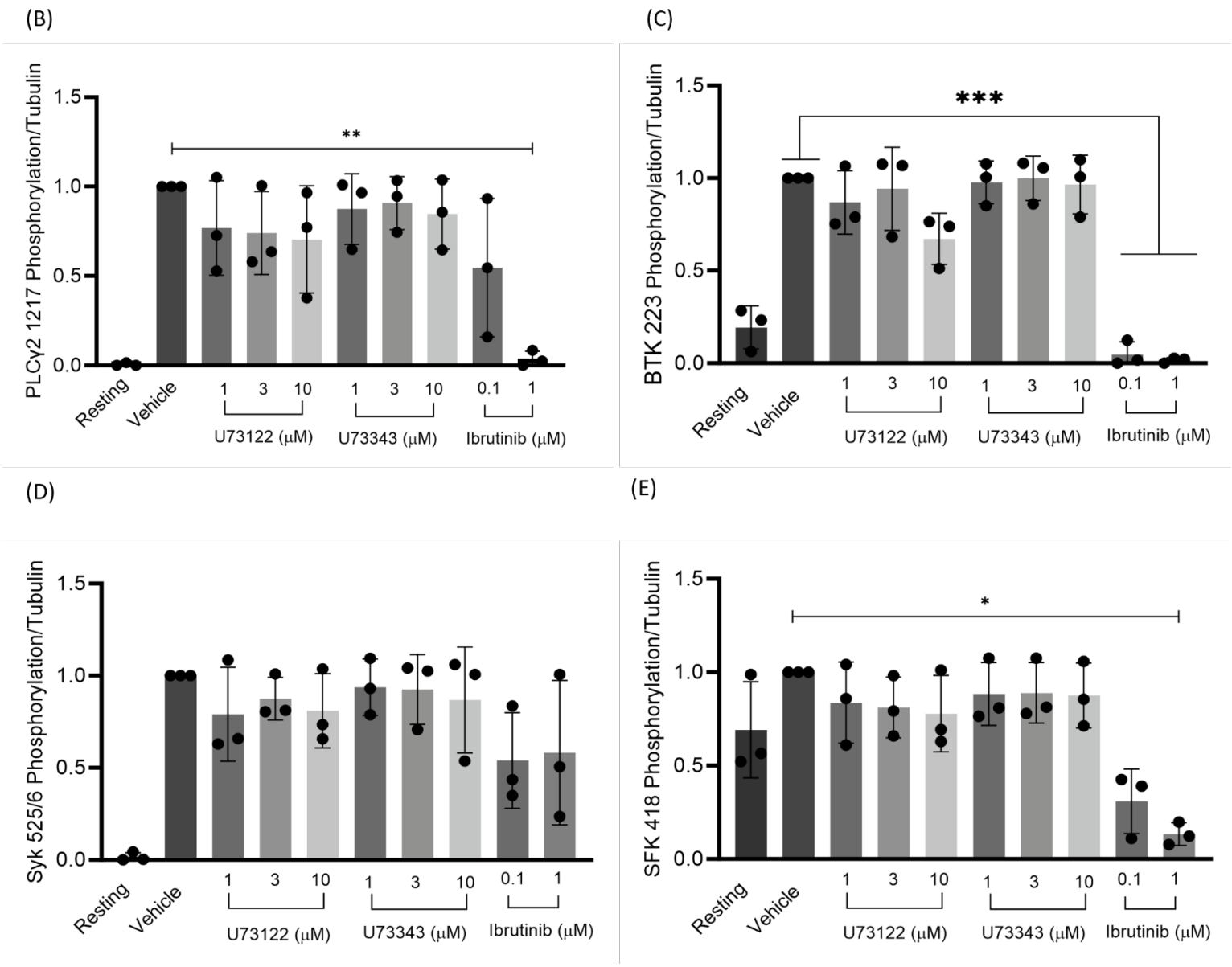

Figure 3.10: U73122 has no effect on protein phosphorylation downstream of GPVI.

Washed platelets ($4x10^8$/mL) were incubated with indomethacin (10μM), integrilin (9μM), and apyrase (2U/mL) prior to treatment with indicated concentrations of U73122, U73343, Ibrutinib, or (DMSO 0.1% (v/v)) for 5 minutes. Platelets were then stimulated with 1μg/mL CRP for 3 minutes and lysed using 6X reducing sample buffer. Lysates were resolved using SDS-PAGE and western blotting for whole cell tyrosine phosphorylation or kinase specific tyrosine phosphorylation. Phosphorylation levels were quantified using Image J (n=3). (A) Representative blot. (B) Quantified phosphorylation levels of PLCγ2, (C) Btk, (D) Syk, and (E) SFK. Statistical significance was calculated against the vehicle control using one-way ANOVA with Dunnett's post-test. Graph shows mean ± SD. *$p \leq 0.05$, **$p \leq 0.01$, ***$p \leq 0.001$.

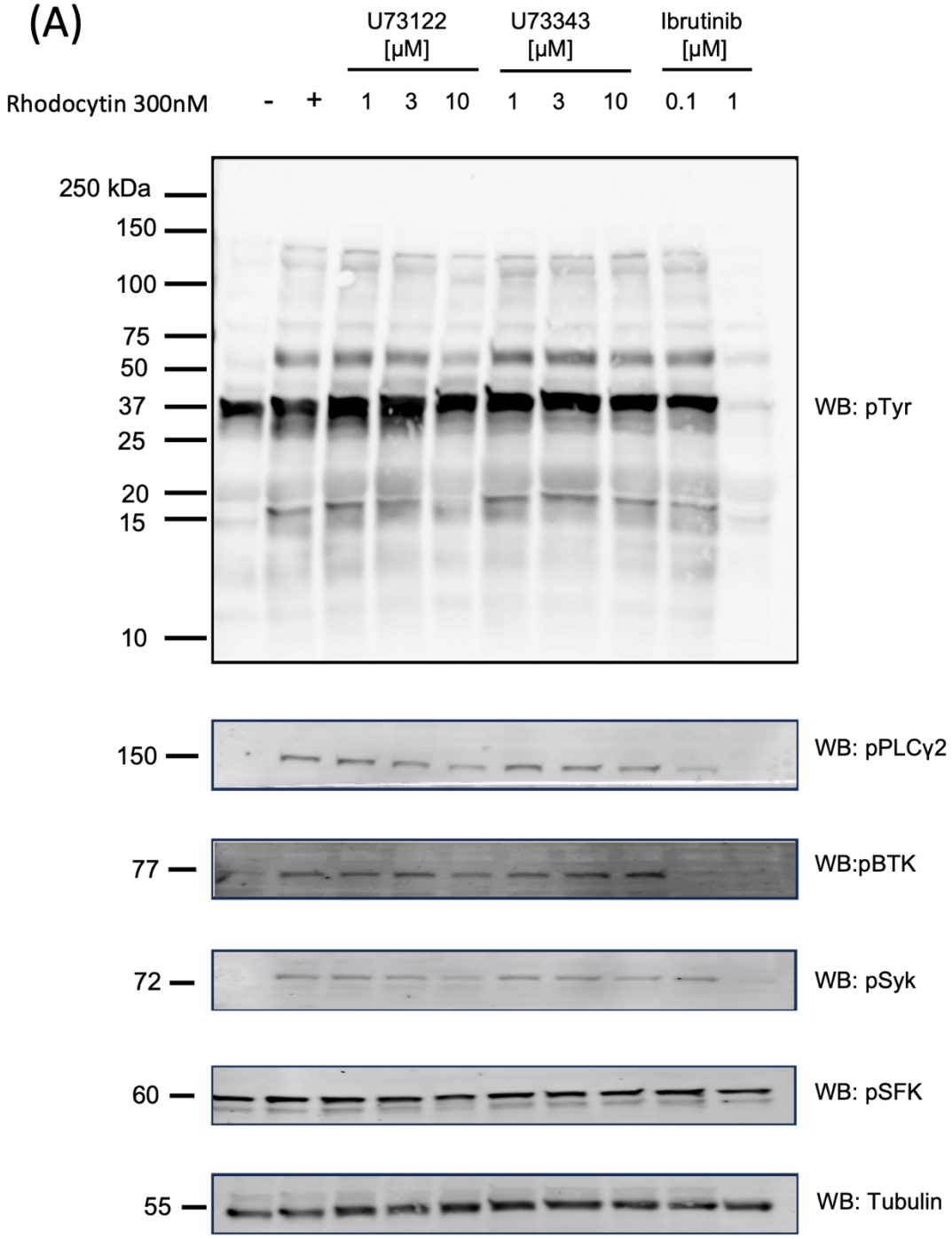
(A)
U73122 [μM]
U73343 [μM]
Ibrutinib [μM]
Rhodocytin 300nM
- + 1 3 10 1 3 10 0.1 1
250 kDa
150
100
75
50
37
25
20
15
10
WB: pTyr
150
WB: pPLCγ2
77
WB:pBTK
72
WB: pSyk
60
WB: pSFK
55
WB: Tubulin

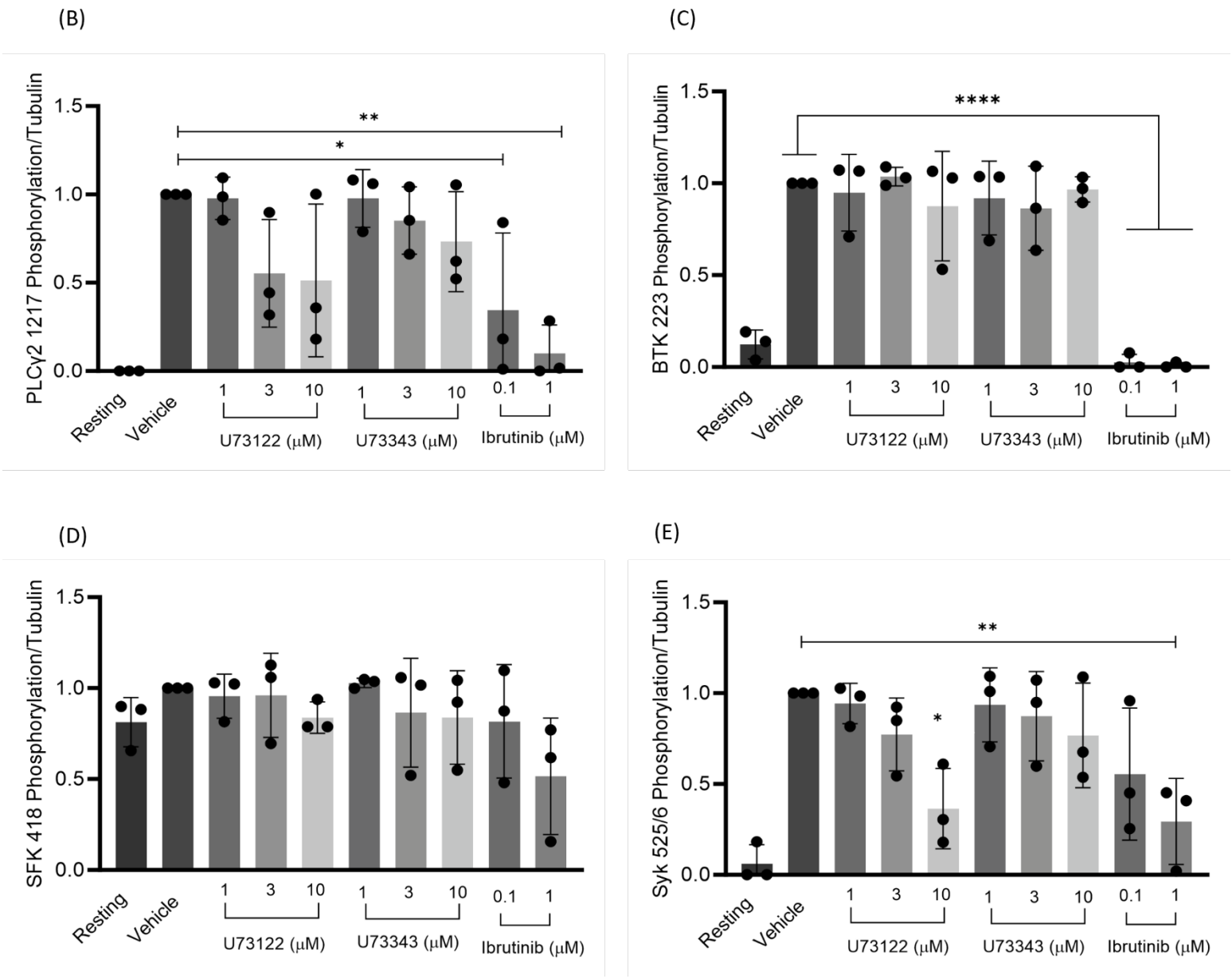

Figure 3.11: U73122 has no effect on protein phosphorylation downstream of CLEC-2.

Washed platelets ($4x10^8$/mL) were incubated with indomethacin (10μM), integrilin (9μM), and apyrase (2U/mL) prior to treatment with indicated concentrations of U73122, U73343, Ibrutinib, or (DMSO 0.1% (v/v)) for 5 minutes. Platelets were then stimulated with 300nM of Rhodocytin for 5 minutes and lysed using 6X reducing sample buffer. Lysates were resolved using SDS-PAGE and western blotting for whole cell tyrosine phosphorylation or kinase specific tyrosine phosphorylation. Phosphorylation levels were quantified using Image J (n=3). (A) Representative blot. (B) Quantified phosphorylation levels of PLCγ2, (C) Btk, (D) Syk, and (E) SFK. Statistical significance was calculated against the vehicle control using one-way ANOVA with Dunnett's post-test. Graph shows mean ± SD. *p ≤ 0.05, **p ≤ 0.01, ***p ≤ 0.001.

3.4 Discussion

The overall aim of this chapter was to characterise the effect of the PLCγ2 inhibitor, U73122, downstream of GPVI and CLEC-2 using platelet aggregation, platelet spreading, calcium release and tyrosine phosphorylation. It was especially important to characterise the effects of U73122 more specifically downstream of CLEC-2 as this has not been previously established in the literature.

When examining platelet aggregation mediated by CLEC-2, 100nM, and 300nM of rhodocytin were used as lower rhodocytin concentrations such as 10nM and 30nM were found to have little to no effect on platelet aggregation. This could be explained by the lag phase in CLEC-2 mediated aggregation. When using light transmission aggregometry, U73122 seems to have a bigger effect on GPVI-induced aggregation in comparison to CLEC-2 induced aggregation. This could be explained by the fact that secondary feedback mechanisms play a role in CLEC-2 mediated aggregation. This could also imply that the PLCγ2 catalytic activity may be more important downstream of GPVI than CLEC-2.

The effect of inhibiting PLCγ2 by U73122 on platelet aggregation stimulated by CRP is consistent with a previous study. Mangin et al,. showed that platelet aggregation was not induced in PLCγ2 deficient mice by direct activation of GPVI with CRP (Mangin et al., 2003). On the other hand, when induced by 100nM rhodocytin, only 10μM of U73122 had a significant effect on reducing platelet aggregation. Also, 10μM of U73122 reduces CRP-induced platelet aggregation to almost 20% whereas only to 80% in rhodocytin-induced platelet aggregation.

In previous studies where PLCγ2 deficient mice were used, the lack of PLCγ2 was found to completely abolish the platelet reactivity to low amounts of rhodocytin (3-10nM). Nevertheless, the shape change observed in response to intermediate concentrations (20-30nM) was maintained. This might indicate that there is a low amount of PLCγ1 (Suzuki-Inoue et al., 2006). Through a mechanism that is dependent on Src kinase, CRP is able to promote the tyrosine phosphorylation of PLCγ1 at its regulatory site, which is located at Tyr 783, in mouse platelets, but not in human platelets. Also, unlike mice, human platelets contain over 100 times more PLCγ2 than PLCγ1 (Lee et al., 1996a), and this disparity may mask PLCγ1's function.

When testing U73122's structural analogue, U73343, it showed no significant effects on platelet aggregation induced by CRP, suggesting that the decrease in platelet aggregation is due to the direct inhibition of PLC isoforms by U73122. Surprisingly, 10μM of U73343 had a small but significant effect on reducing platelet aggregation when stimulated by 100nM rhodocytin. This could be explained by the fact that CLEC-2 is highly dependent on positive feedback signalling via and thromboxane A2 (TxA2). In support of this, Heemskerk et al., have previously shown that U73343 suppresses cPLA2 activation, which in turn decreases arachidonic acid release and TxA2 synthesis (Heemskerk et al., 1997a).

The effect of ibrutinib on GPVI-mediated aggregation has been previously established. As previously mentioned, ibrutinib has been found to impair platelet function starting from low concentrations (1μM) (Levade et al., 2014). Consequently, ibrutinib has been used as a positive control as the inhibition of Btk will in turn inhibit

the activity of PLCγ2 and its effect on platelet aggregation is well established. Consistent with the literature, 1μM, 3μM, and 10μM have a significant effect on reducing platelet aggregation evoked by GPVI. Although a similar effect was seen on CLEC-2 evoked platelet aggregation which is also consistent with the literature (Nicolson et al., 2021), 1μM ibrutinib decreased platelet aggregation to almost 40% downstream of GPVI and to 20% downstream of CLEC-2. This is consistent with previous studies that have shown that Btk inhibitors that impair GPVI signalling are used at concentrations more than 20 times higher than at those concentrations needed to inhibit CLEC-2-mediated platelet function in humans (Nicolson et al., 2018, Nicolson et al., 2021). The reason behind this selectivity is that GPVI does not require Btk kinase activity, whereas human platelet CLEC-2 function does. This highlights that there is a significant distinction in the function of Btk downstream GPVI and CLEC-2 as the kinase dead Btk fails to signal for the latter. In relation to PLCγ2, a study by Nicolson et al., has shown that platelets stimulated with high concentrations of CRP (10μg/mL) were able to aggregate normally despite the lack of Btk induced PLCγ2 phosphorylation. Additionally, transfection of a kinase-dead Btk in Btk KO DT40 cells restore GPVI signalling. This provides support for the idea that Btk facilitates the activation of PLCγ2 as an adaptor protein (Nicolson et al., 2018) .

As previously mentioned, the examination of the calcium signal can offer a direct readout of the activity of PLCγ2. Therefore, the inhibition of PLCγ2 is believed to have a significant effect on decreasing calcium release. A previous study examining the role of PLCγ2 downstream of the integrin αIIbβ3 have shown that PLCγ2 deficient mouse platelets and platelets treated with U73122 showed a negligible

amount of calcium flux (Goncalves et al., 2003). Additionally, Heemskerk et al., have previously shown the effect of inhibiting PLCγ2 by U73122 on calcium release stimulated by thrombin and collagen. U73122 significantly decreases calcium release in thrombin and collagen stimulated platelets (Heemskerk et al., 1997a). However, the effect of U73122 on calcium release induced by CRP or rhodocytin is not directly addressed in the literature. Therefore, this was tested in this study. And the results have demonstrated that U73122 decreases calcium release significantly downstream of both GPVI and CLEC-2.

The effect of U73122 was then investigated on platelet adhesion and spreading. The literature lacks evidence on whether platelets are able to spread or adhere to rhodocytin coated surfaces. Although the ability of platelets to adhere and spread through the CLEC-2 receptor has been previously studied using podoplanin (Navarro-Núñez et al., 2015). This study, figure 3.7A, demonstrates that platelets can adhere and spread on 100nM rhodocytin. It is worth noting however, that the average number of platelets adhering to rhodocytin are 40 platelets per field of view whereas the average number of platelets adhering to CRP is around 70 per field of view. Although more platelets seem to adhere to CRP-coated surfaces, the average area of platelets (spreading) on CRP and rhodocytin seems similar (40μm^2).
On another note, it has been previously established, using PLCγ2 KO models, that the absence of PLCγ2 reduces the ability of platelets to spread and adhere in mouse platelets. In this study, the role PLCγ2 plays in platelet spreading and adhesion was examined using a different approach and in human platelets. Using the PLC inhibitor, U73122, completely abolished platelet adhesion on CRP coated surfaces and

significantly decreases platelet adhesion and spreading on rhodocytin coated surfaces.

Nevertheless, it is important to note that there are notable differences in platelet proteomes between mice and humans. In general, mouse platelets tend to contain more copies of certain proteins than human platelets. For instance, in human platelets, there are around 4000 copies of CLEC-2 whereas mice contain 40,000 copies. Human and mouse platelet express between 4000 to 6000 and 23,300 copies of Syk, respectively. Moreover, mice contain 11,300 copies of PLCγ2 in contrast to 2000 copies in humans. There is no evidence regarding the number of copies of PLCγ1 in human platelets, however mice contain around 61 copies (Dunster et al., 2015, Zeiler et al., 2014, Burkhart et al., 2012). This could further highlight some of the differences seen in the results when using PLCγ2 knockout mice in contrast to the pharmacological inhibition of PLCγ2 in human platelets. U73122 has shown a significant effect on decreasing platelet spreading and adhesion downstream of the hemITAM receptors. This confirms the role PLCγ2 plays in mediating platelet adhesion and spreading downstream of GPVI and CLEC-2. Additionally, U73122 seems to have a more significant effect on platelet adhesion evoked by GPVI suggesting that PLCγ2 catalytic activity might me more significant downstream of GPVI.

Interestingly, U73343 (U73122's analogue) had a significant effect on platelet adhesion on CRP at its highest concentration (10μM). However, this can be explained by the large error bars and the variability of response from one donor to the other.

In conclusion, this chapter characterised the PLC inhibitor U73122 downstream of GPVI and for the first time downstream of CLEC-2. It investigates the effect of inhibiting PLCγ2 downstream of hemITAM receptors using a pharmacological inhibitor and emphasises the significant role PLCγ2 plays in platelet aggregation, calcium release, adhesion, and spreading.

Chapter 4: Characterising the effect of point mutations on PLCγ2 function using CRISPR gene editing and overexpression approaches.

4.1 Introduction

4.1.1 DT40 cells

PLCγ2 is a critical signalling molecule expressed not only in platelets but also in B-cells. The B cell receptor (BCR), CLEC-2, and GPVI share similarities in their signalling pathway. The BCR compromises Igα and Igβ which are transmembrane proteins that possess an extracellular domain resembling immunoglobulin (Ig), a transmembrane domain, and similarly to GPVI and CLEC-2 a cytoplasmic region containing an ITAM (Lockey et al., 2022). As platelets lack a nucleus, genetic modification is not possible, but due to similarities in the signalling between GPVI and BCR, B-cells can serve as a useful model to investigate PLCγ2 downstream of ITAM receptors (Rodriguez et al., 2001).

DT40 cells are an adaptable model system used in studying several cellular functions. They were first obtained from a female domestic chicken's bursal lymphoma induced by avian leucosis virus infection (Baba et al., 1985). DT40 cells have been widely utilised to investigate DNA repair and cell signalling (Ji et al., 2009). DT40 cells grow rapidly and are easy to handle. They are also easy to transfect compared to other cell lines and are easily genetically manipulated due to their high targeted-to-random DNA integration ratio. It is also easy to achieve homologous recombination within DT40 cells. Meiosis relies on this process to guarantee genetic variety and precise repair of DNA double-strand breaks which makes them the preferred model when studying gene knockouts (Buerstedde and Takeda, 1991). These qualities have established them as a significant resource for

studying various biological processes. Additionally, DT40 cells have played a crucial role in understanding the functions of several platelet receptors, such as GPVI and CLEC-2 due to their ease of transfection and expression of key ITAM signalling proteins (Suzuki-Inoue et al., 2006). Furthermore, DT40 cells have the essential signalling components necessary for platelet (hem)ITAM receptor signalling, including Syk, Lyn, and PLCγ2. Altogether, this makes DT40 cells a useful cell line model to study PLCγ2 and PLCγ2 mutations.

4.1.2 *PLCG2* mutations

Chronic lymphatic leukaemia (CLL) is a B-cell malignancy and the most common leukaemia in adults (Gaidano et al., 2012). The B-cell receptor signalling pathway plays a major role in the pathogenicity of CLL. When expressed on malignant B-cells, the BCR promotes the survival, maturation, and proliferation of the malignant cells (Ghia et al., 2008, Herishanu et al., 2011, Stevenson et al., 2011). Therefore, several CLL treatments are based on targeting and inhibiting the BCR signalling pathway, such as kinase inhibitors idelaslisib (PI3Kδ inhibitor), fostamatinib (Syk inhibitor), and ibrutinib (Btk inhibitor) (Wiestner, 2015). Although ibrutinib has shown high efficacy in some patients, others have acquired resistance to the drug. It is believed that 80% of patients that developed resistance to ibrutinib have PLCγ2 mutations. This is associated with *PLCG2* mutations: R665W (p.Arg665Trp) on the SH2 domain, S707Y (p.Ser.707.Tyr) also on the SH2 domain, L845F (p.Leu845Phe) on the spPH domain, and D993G (p.Asp993Gly) on the Y box (Koss et al., 2014, Woyach et al., 2014a) (figure 4.1).

D993G is located in the catalytic domain of PLCγ2 and leads to an increase of PLCγ2 activity (Everett et al., 2009). The D993G mutation is recognised for causing

immunological dysfunction (Yu et al., 2005) . This can be by impacting enzyme activity, possibly by disrupting the autoinhibitory interface, destabilising the regulatory domain, or changing interaction with the membrane (Magno et al., 2019). D993G has been linked to the development of intense autoinflammatory responses and deficits in antibody production. The D993G mutation is also linked to a rare primary immunodeficiency syndrome and associated with an increased ability to stimulate improved downstream signalling and calcium flux when the BCR is activated. When examined in BCR signalling, this mutated form of PLCγ2 results in increased IP_3 and Ca^{2+} when cells are stimulated (Magno et al., 2019). Furthermore, Everett *et al.,* investigated the role of the D993G mutation beyond B-cells. Their data showed that in epdiermal growth factor (EFG) stimulated COS cells (a fibroblast-like cell line), D993G also showed enhanced PLCγ2 activation which was determined by measuring the inositol phosphate production (Everett et al., 2009).

The R665W and L845F mutations have also been classified as a gain-of-function mutations, which results in increased B-cell receptor activity. In addition, the R665W and L845F mutations cause PLCγ2 to function without requiring Btk and enables B cells to develop resistance to ibrutinib in CLL patients (Liu et al., 2015). In a study by Wallister et al., the effect of R665W and L845F on PLCγ2 activity was examined by measuring [^{3}H] inositol phosphate formation in COS-7 cells. In comparison to cells transfected with WT PLCγ2, cells transfected with R665W and L845F mutant versions of PLCγ2 significantly increased basal inositol phosphate formation by 18-fold. In addition, in PLCγ2-deficient DT40 cells with overexpression of R665W and L845F mutant forms of PLCγ2 and endogenous wild-type Btk, BCR-mediated PLCγ2 activation was susceptible to pharmacologic inhibitors of Syk and Lyn but resistant to ibrutinib. These findings point to the presence of BCR-originating protein-tyrosine

kinase pathways that activate R665W without relying on Btk and induce ibrutinib resistance even in tumour cells that lack Btk mutations. This suggests the possibility of employing tailored therapy approaches (Walliser et al., 2016).

A study conducted by Woyach *et al.,* examined the functional effect of R665W and L845F in HEK 239T and DT40 cells. When looking at calcium flux in DT40 cells following stimulation of the BCR with IgM antibody, cells with R665W and L845F mutations treated with ibrutinib had 4 times higher calcium flux (Woyach et al., 2014b). It has been suggested in the literature that R665W is expected to enhance the stability of an active form of PLCγ2 by influencing allosteric networks, therefore promoting the binding of the phosphorylated peptide to the cSH2 domain (Liu et al., 2020). In addition, these mutations can destabilise the SH2 domain itself, change residues that interact with the catalytic domain, or directly disrupt ligand binding (Zhou et al., 2012a). Another factor that could affect the structure of the protein is the nature of the amino acid change. At position 665, a positive charge is lost when arginine (R) is replaced with tryptophan (W). This has the potential to destabilise hydrogen bonding networks and ionic interactions, which are essential for the structure and function of domains (Shonnard et al., 1996).

Although the L845F mutation leads to a gain of function in PLCγ2, it is believed that this mutation has no impact on the overall structure of the spPH domain (Walliser et al., 2016). However, adding phenylalanine (F) instead of leucine (L) results in a bigger and more inflexible side chain. This has the ability to cause steric conflicts with nearby residues, which may cause changes in local conformation or even structural changes in the protein as a whole (Mishra et al., 2008, Fersht et al., 1992).

The final mutation investigated in this study is S707Y. Similarly to R665W and L845F, S707Y has been linked to prolonged BCR signalling that does not require Btk

function, hence causing resistance to ibrutinib therapy (Woyach et al., 2014b). The substitution in PLCγ2 is in the C-terminal SH2 (cSH2) domain. However, it is believed that the increase of intracellular signalling and gain of function caused by S707Y is due to its disruption to the auto inhibitory SH2 domain. This mutation is located near three established phosphorylation sites, indicating that it might potentially provide a novel phosphorylation site in PLCγ2. It is expected that the mutation will impact the function of the protein. Computational projections indicate that it may change the residues that interact with the catalytic domain or destabilise the SH2 domain (Zhou et al., 2012a). Due to the fact that the R665W is located on the same domain S707Y, it is hypothesised that they are likely to have similar effects.

Furthermore, the S707Y mutation has been associated with a dominantly inherited autoinflammatory disease characterised by immunodeficiency, referred to as PLCγ2-associated antibody deficiency and immune dysregulation (APLAID). Additional research has also linked patients with cold-induced urticaria and immune dysregulation to the S707Y mutation (Neves et al., 2018). Although these mutations have been extensively studied in relation to CLL and ibrutinib resistance, it is unknown whether these, or other mutations may arise in platelets, and what the functional effect on signalling by platelet (hem)ITAM receptors might be. Therefore, in this study we use these mutations as a tool to understand their effect on PLCγ2 domains and consequently their effect on the protein function and structure downstream of the platelet receptors GPVI and CLEC-2.

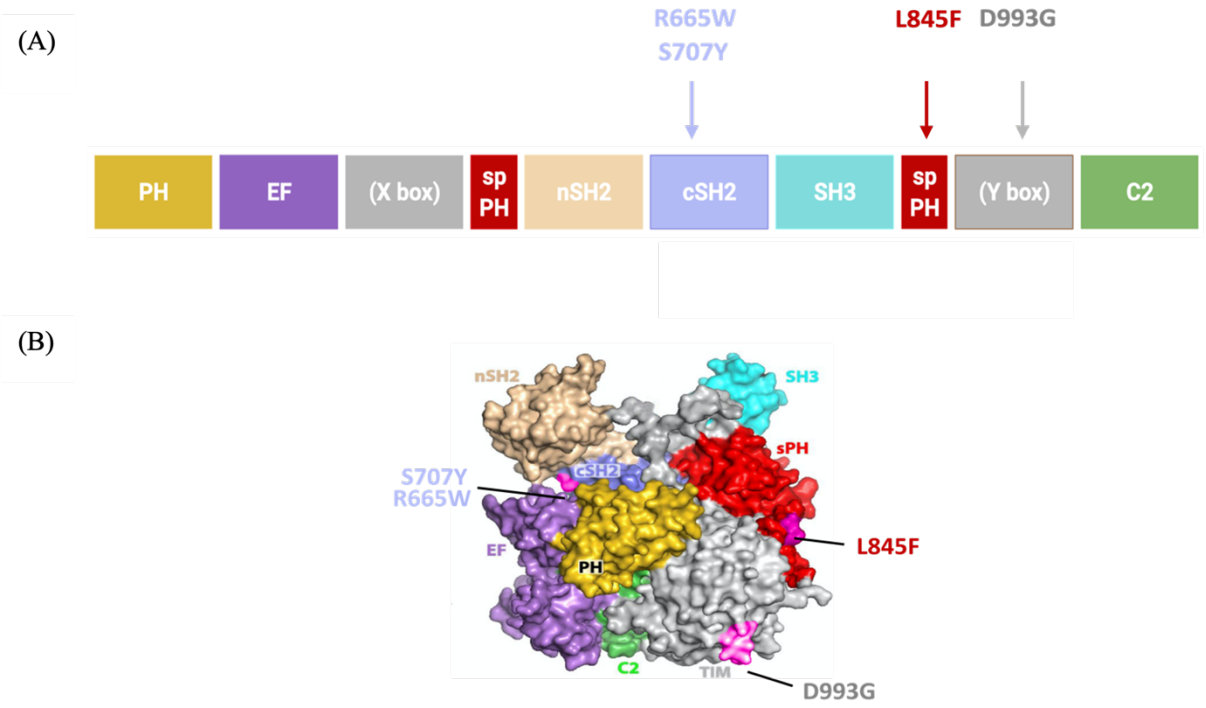

Figure 4.1: PLCγ2 domains and mutations.

The PLCγ2 protein is made of a PH domain at the N-terminus, and catalytic X and Y domains in between EF-hand motifs and C2 domain. PLCγ2 also has an extra PH domain split by one SH3 and two SH2 domains. (A) Linear presentation of PLCγ2 domains. Arrows indicate location of drug-resistant mutations. (B) 3-dimentional structural model of PLCγ2 domains. Indicated in pink is the location of mutations linked to drug resistance. Adapted from (Tsai et al., 2023).

4.1.3 Protein overexpression and CRISPR/Cas9

Protein overexpression systems are crucial in the field of molecular biology. These systems use the modification of cellular machinery to amplify the production of proteins, that can be used in order to identify and study new proteins and their functions (Rine, 1991). In an overexpression system, the cDNA of a gene of interest is inserted into a plasmid and induced by a plasmid promoter located upstream of the cloned DNA. Typically, the promoter is chosen because it is constitutively active therefore and the gene will be continuously transcribed (Prelich, 2012). All of the previously mentioned *PLCG2* mutations have been studied using a protein

overexpression system. Plasmids containing PLCγ2 with the desired mutations were transfected in a range of cells and their effect on the protein and/or cell function was then studied. This approach was used in this study in order to understand the function of PLCγ2 downstream of GPVI and CLEC-2 and to provide comparison to using alternative approaches such as CRISPR/Cas9 gene editing. However, overexpression systems have their limitations. It is considered to be a qualitative experiment because the expression level of the protein of interest may not be similar to the endogenous level of protein expression (Prelich, 2012).

4.1.3.1 CRISPR/Cas9

The Clustered regularly interspaced short palindromic repeats (CRISPR) – Cas9 (CRISPR/Cas9) technology has completely transformed the field of gene editing technologies, providing accuracy and flexibility in modifying genetic material. CRISPR/Cas is an immune defence mechanism naturally found in bacteria and uses a nuclease guided by ribonucleic acid (RNA) to cleave genetic material of pathogens invading the bacteria (Rodríguez-Rodríguez, 2019). There are 3 types of CRISPR systems: type I, II, and III. Type II CRISPR/Cas9 is developed from *Streptococcus pyogenes* and contains the Cas9 nuclease, a specific CRISPR RNA (crRNA), and a trans-activating CRISPR RNA (tracRNA) with a scaffolding ability. The crRNA and the tracRNA are combined together creating a single-guided RNA (sgRNA). In this system, the DNA will be targeted by the Cas9 nuclease guided by 20 nucleotide sgRNA. A 5'-NGG protospacer adjacent motif (PAM) site proceeds the DNA of interest where a double-stranded break (DSB) will be made (Ran et al., 2013). When cleaved by the Cas9 nuclease, the cleaved locus will go through DNA damage repair. The repair can be through two different pathways, homology-directed repair

(HDR) or non-homologous end joining (NHEJ). NHEJ is considered to be error-prone where the generated DSB re-ligates without a repair template. This may result in either insertion or deletion (indel) mutations (Figure 4.2). Hence, gene knockouts can be readily generated via NHEJ.

On the other hand, HDR occurs less frequently than NHEJ however it tends to be a more accurate repair mechanism than NHEJ. It requires a repair template that can either be a single-stranded DNA oligonucleotide (ssODNs) or a double-stranded DNA (dsDNA) template with homology arms. The template is used to fix the double strand break through homology guided repair. The template, which has the desired changes, is then added to the DNA. Moreover, HDR usually occurs only in dividing cells (Saleh-Gohari and Helleday, 2004). The CRISPR/Cas9 system had been previously well established in the literature as it was utilised to generate knockouts and introduce point mutation knock-ins. Therefore, in this study, CRISPR/Cas9 approach will be used to generate the PLCγ2 mutation knock in in DT40 cells. Using CRISPR to generate knock-ins is advantageous. Where unlike using the overexpression approach, the level of protein expression in the cells is physiologically representative to normal level of protein.

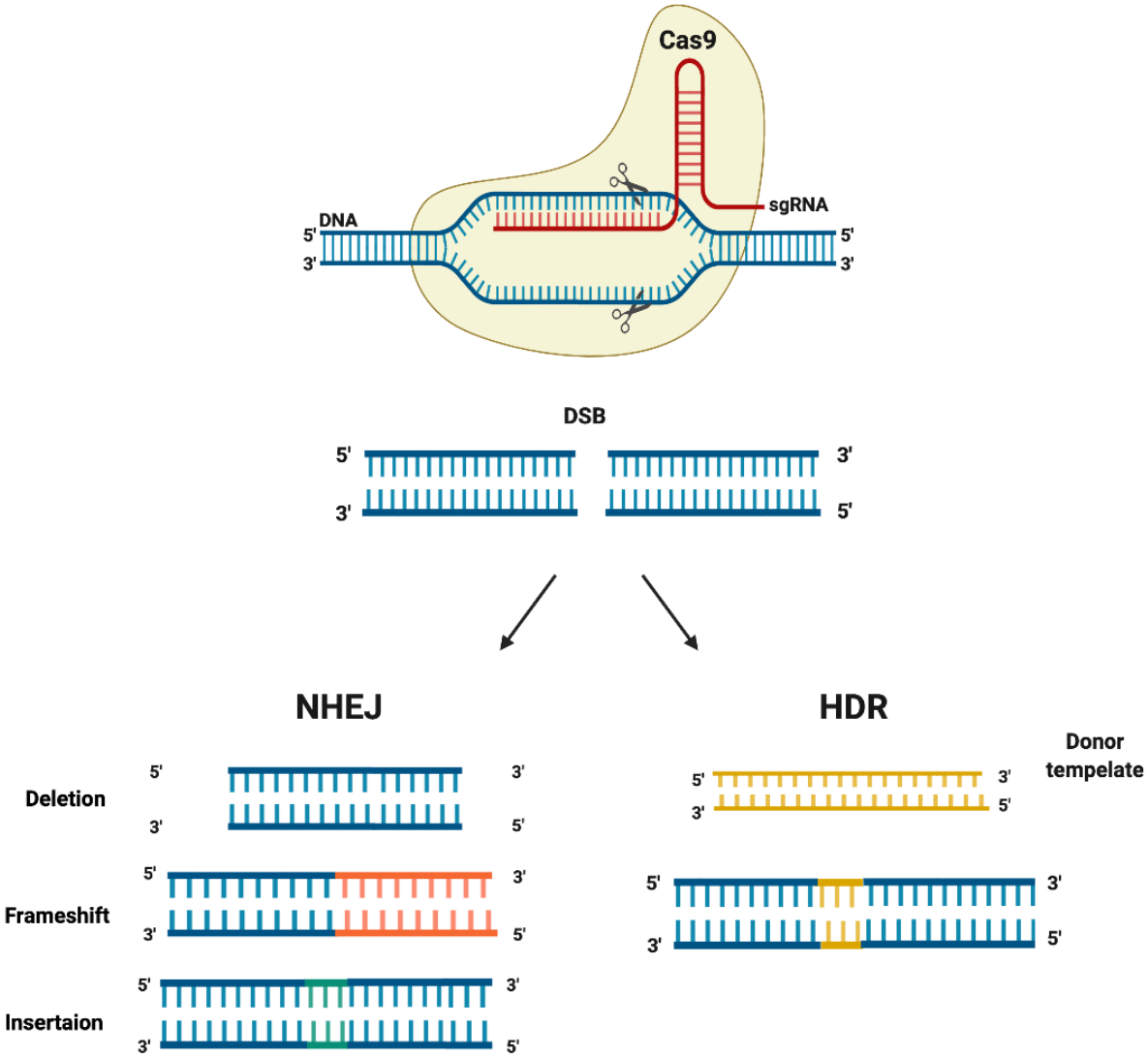

Figure 4.2: CRISPR/Cas9 mechanism.

With the guidance of the sgRNA, Cas9 enzyme will cleave the DNA resulting in a DSB. The DSB can be repaired in two pathways. NHEJ where the DSB can be repaired by the DNA repair machinery and without repair template results in deletion that can result in frameshift, or insertion. HDR pathway, however, utilizes a repair temperate allowing specific editing.

4.2 Aims and hypothesis

4.2.1 Aims:

- To elucidate the effect of ibrutinib-resistance linked *PLCG2* mutations downstream of GPVI and CLEC-2 using an overexpression system, CRISPR/Cas9 gene editing, and the NFAT luciferase reporter assay.
- To examine the effect of the PLCγ2 inhibitor, U73122, on PLCγ2 mediated function in the presence of gain of function mutations.

4.2.1.1 Hypothesis:

PLCG2 mutations will lead to a gain of function phenotype downstream of CLEC-2 and GPVI which will be resistant to the PLCγ2 inhibitor U73122.

4.3 Results

4.3.1 U73122 affects the PLCγ2 mediated calcium release in WT DT40 downstream hem (ITAM) receptors.

The effect of the PLCγ2 inhibitor, U73122, on platelet activation mediated by GPVI and CLEC-2 was previously established in chapter 3. In this chapter, we wanted to further examine its effect on PLCγ2 function in WT DT40 cells and in PLCγ2 KO cells expressing gain of function mutations. This was established by measuring calcium release in DT40 cells using the NFAT luciferase reporter assay (described in section 1.8).

WT DT40 cells were transfected with an NFAT-luciferase plasmid along with GPVI and FcRγ or CLEC-2 plasmids. Cells were also transfected with empty vectors as control. Cells were stimulated with either 10μg/mL collagen or 100nM rhodocytin for 6 hours, and luciferase activity was measured.

Figure 4.3 shows that in comparison to stimulated cells transfected with empty vectors, stimulated cells transfected with the GPVI/FcRγ or the CLEC-2 plasmid display a significant increase in signalling. In collagen stimulated cells (figure 4.3A), U73122 decreased the NFAT- luciferase activation in a concentration-dependent manner. At 1μM, U73122 has a small but significant effect on decreasing GPVI-mediated signalling but a slightly bigger effect at 3μM. At 10μM, U73122 had a much bigger effect on the NFAT-luciferase activation where it was decreased to a basal level. Similar results were seen in the rhodocytin stimulated cells (figure 4.3 B).

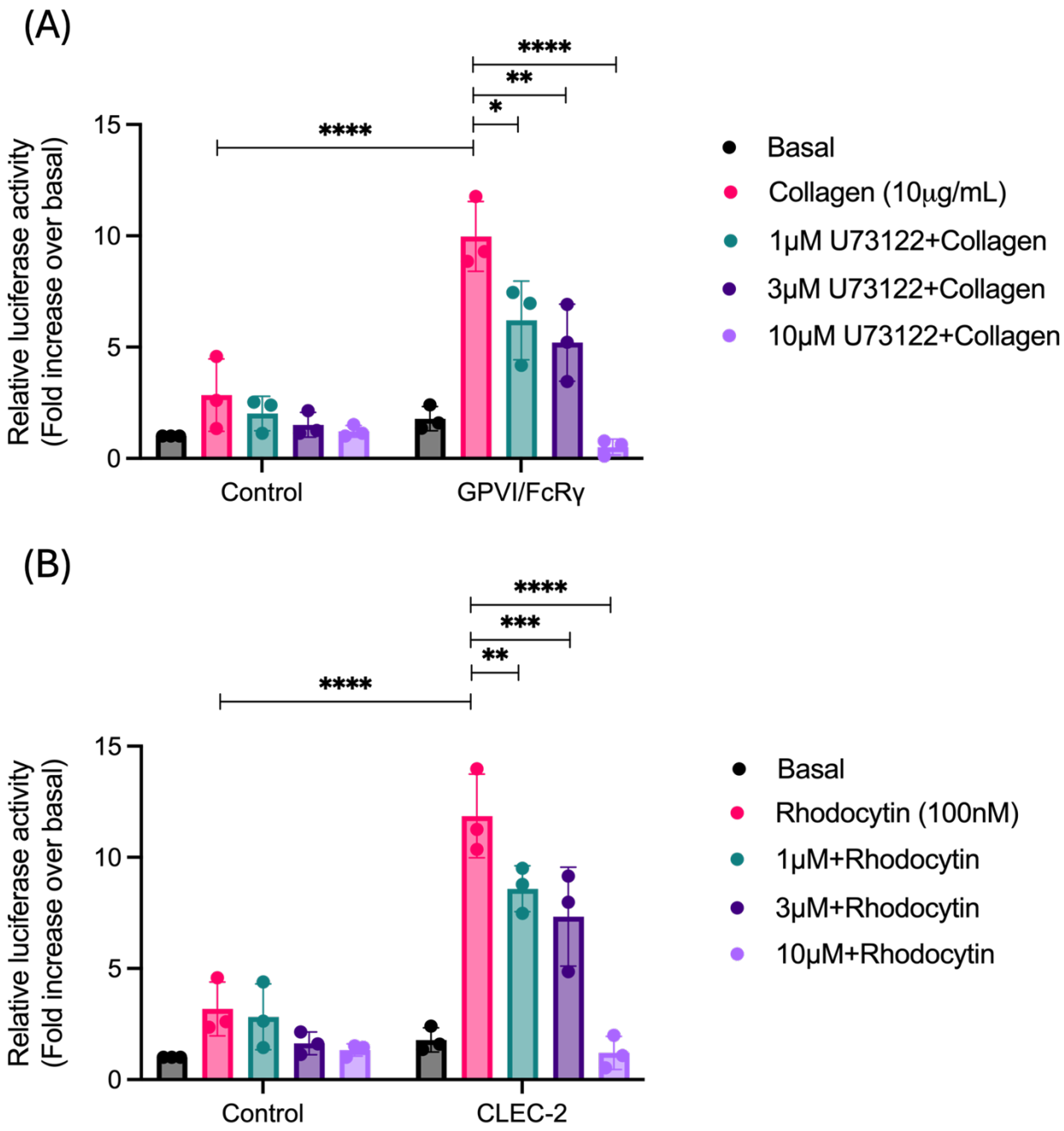

Figure 4.3: U73122 significantly inhibits GPVI and CLEC-2 mediated signalling in WT DT40 cells. WT DT40 cells were transfected with 2μg of both GPVI and FcRɣ plasmids or 10μg of CLEC-2 plasmids. Cells were also transfected with 7.5μg of NFAT-luciferase plasmids. Transiently transfected cells were stimulated with either (A) 10μg/mL collagen or (B) 100nM rhodocytin for 6 hours prior to measuring the luciferase activity (n=3). Statistical significance was determined using Two-way ANOVA with Tukey's post-test. Graph shows mean ± SD. *$p \leq 0.05$. **$p \leq 0.01$, **** $p \leq 0.0001$.

4.3.2 U73122 affects the PLCγ2 mediated calcium release in cells bearing gain-of – function mutations downstream of hem (ITAM) receptors.

As previously described, the effect of *PLCG2* mutations, thought to be responsible for the resistance to ibrutinib treatment in CLL patients, has been established in the literature and investigated downstream of BCR using a protein overexpression system. A similar approach was used in this study to further investigate the effect of the *PLCG2* mutations in platelet hem(ITAM) receptors. Using CRISPR to generate knock-ins is advantageous. Where unlike using the overexpression approach, the level of protein expression in the cells is not physiologically representative to normal level of protein.

In order to generate the mutated plasmids, forward and reverse primers with the desired mutations were generated using Benchling. Site directed mutagenesis was used to create *PLCG2* mutations in WT human (h)PLCγ2 using the primers in table 4.1. The parental DNA was digested using the restriction enzyme DpnI for 3 hours, and the mutated plasmids were then precipitated using salt ethanol precipitation (figure 4.4). Sanger sequencing was used to confirm the presence of the desired mutations.

Table 4.1: Primers designed to create PLCγ2 point mutations.

Mutation	Primers
R665W	Forward: 5' GAGGATTCCCtGGGACGGGGC 3' Reverse: 5' GCCCCGTCCCaGGGAATCCTC 3'
S707Y	Forward: 5' CTGGGGACCTaCGCCTATTTTG 3' Reverse: 5CAAAATAGGCGtAGGTCCCCAG3
L845F	Forward: 5' ACAATCCCTTcGGGTCTCTTTG 3' Reverse: 5' CAAAGAGACCCgAAGGGATTGT 3'
D993G	Forward: 5' CAAAGAGTTGgCTCTTCAAACTACGAC 3' Reverse: 5' GTCGTAGTTTGAAGAGcCAACTCTTTG 3

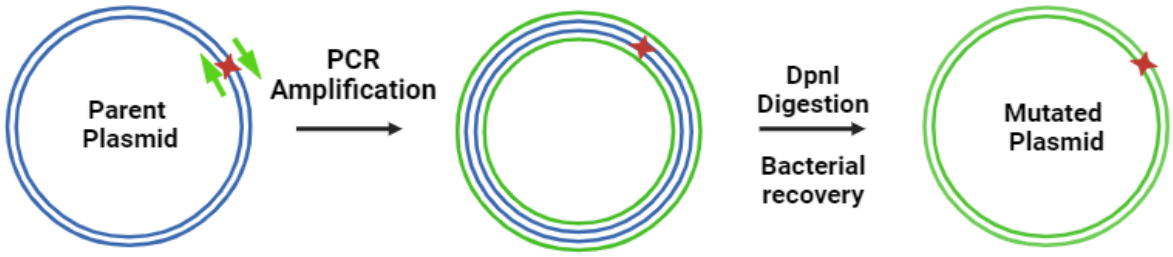

Figure 4.4: Site directed mutagenesis.

By PCR amplification, the designed primers with the desired mutation (green arrows) are used to amplify the plasmid generating the mutation. The non-mutated parental plasmid is then digested using the restriction enzyme DpnI. The digested product was salt ethanol precipitated and transformed into competent *E. coli*.

Previous studies have established that *PLCG2* mutations R665W, L845F, S707Y, and D993G are hyper-functional downstream of the B-cell receptor using an overexpression system. This approach was used in this study and the effect of the mutations was investigated downstream of GPVI and CLEC-2. Furthermore, the effect of the PLCγ2 inhibitor, U73122, on the calcium release in cells containing the mutation was also tested. PLCγ2 knockout cells were transfected with an empty vector (pcDNA) as control, WT hPLCγ2 plasmid, or plasmids containing the desired mutation. Cells were also transfected with NFAT-luciferase plasmid along with GPVI and FcRγ or CLEC-2 plasmids. Cells were stimulated with either collagen or rhodocytin, and luciferase activity was measured.

When stimulated with 10μg/mL collagen, all *PLCG2* mutations led to a gain of function (figure 4.5). Stimulated cells had a significant increase in the NFAT-luciferase activation when compared to the WT hPLCγ2. Although U73122 significantly decreased the signalling in collagen stimulated WT DT40 cells (figure 4.3 A), it seems to have no significant effect on PLCγ2 KO transfected with WT hPLCγ2 cells (figure 4.5). However, it is worth noting that the level of the NFAT-luciferase activation in untreated and stimulated WT DT40 (figure 4.3) is two times higher than in the PLCγ2 knockout cells transfected with WT hPLCγ2 (figure 4.5). In cells with SH2 domain mutations such as R665W and S707Y (figure 4.5, A, B), U73122 reduced the NFAT-luciferase activation significantly at 3μM and 10μM. Whereas in cells containing mutations affecting the catalytic domain, L845F and D993G (figure 4.5, C, D) U73122 had a significant effect only at its highest concentration (10μM). This suggests that the mutations on the catalytic domain may be less susceptible to the inhibitory action of U73122.

Alterations in interactions with regulatory proteins and substrates can also be achieved through mutation of the SH2 domain, such as R665W. This may also mean, that the enzyme depends on these linkages more with its hyperactivity. It is thus possible that the impairment of U73122 inhibition would be less noticeable when these interactions are abrogated.

Similar results were observed when cells were stimulated with rhodocytin (figure 4.6). All mutations had a significant increase in NFAT-luciferase activation in comparison to WT PLCγ2 cells. In cells transfected with R665W and L845F (figure 4.6 A, C), U73122 caused a significant decrease of the NFAT-luciferase activation only at 10μM. On the other hand, 3μM and 10μM of U73122 significantly reduced signalling in cells with the S707Y and D993G mutations (figure 4.6 B, D).

To ensure that the level of PLCγ2 in PLCγ2 KO cells transfected with WT hPLCγ2 or the mutated forms of PLCγ2 were expressed at similar levels, SDS PAGE and western blotting were used. PLCγ2 KO cells and cells transfected with mutated plasmids were prepared as previously described. Figure 4.7 shows that the level of PLCγ2 expressed in and PLCγ2 KO bearing the gain of function mutations and WT hPLCγ2 is the same.

Altogether, these results demonstrate that the *PLCG2* mutations associated with ibrutinib resistance are hyperreactive in response to GPVI and CLEC-2 mediated signalling. This agrees with previous studies. However, the mutated forms of PLCγ2 can be inhibited by U73122 suggesting that the mutations do not affect the lipase or catalytic activity of PLCγ2.

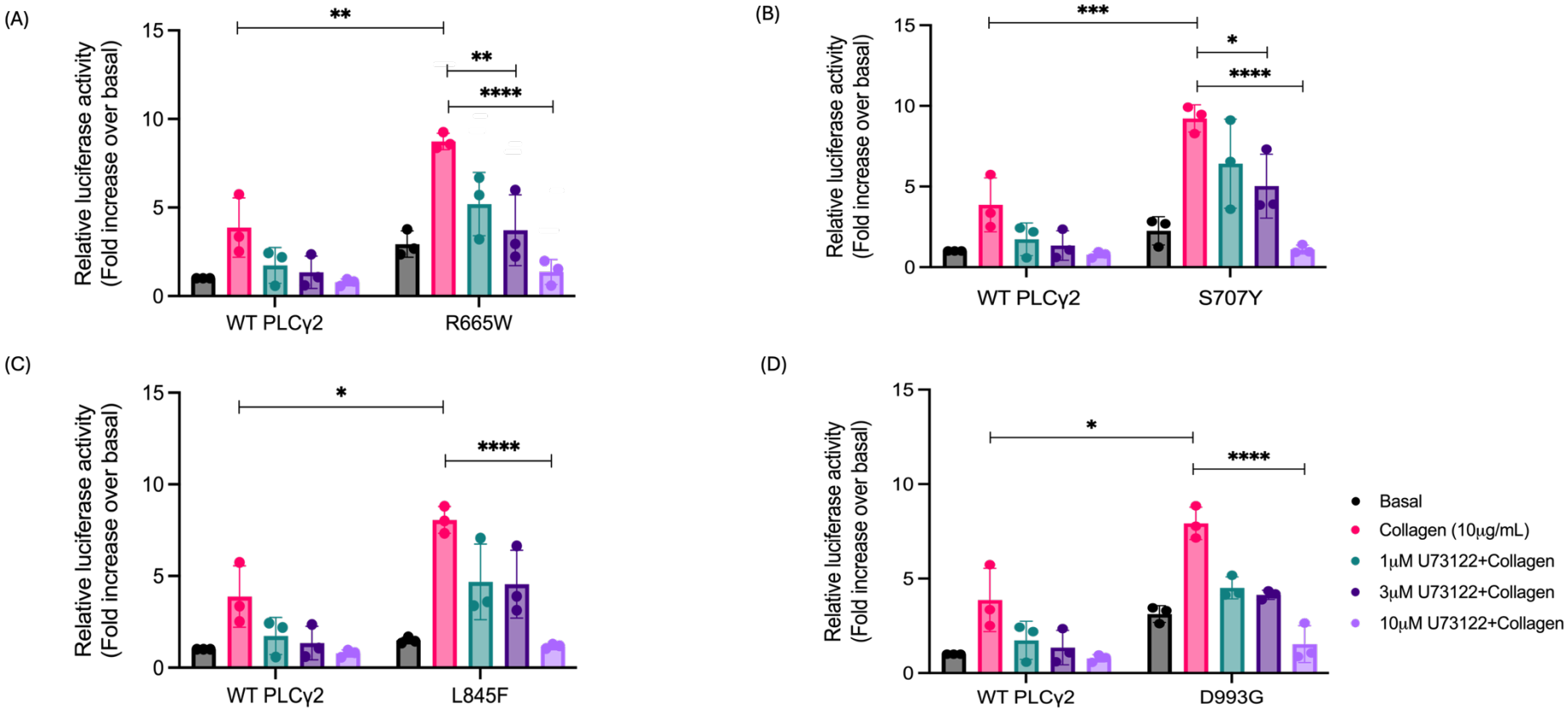

Figure 4.5: PLCγ2 mutations lead to a gain of function downstream of GPVI which can be significantly decreased by U73122.

PLCγ2 KO cells were transfected with 10 μg of either WT PLCγ2, (A) R665W PLCγ2, (B) S707Y PLCγ2, (C) L845F PLCγ2, or (D) D993G PLCγ2 along with 2μg GPVI/FcRɣ and 7.5μg NFAT-luciferase plasmids. Transiently transfected cells were stimulated with 10μg/mL collagen for 6 hours prior to measuring the luciferase activity (n=3). Statistical significance was determined using Two-way ANOVA with Tukey's post-test. Graph shows mean ± SD. *$p \leq 0.05$. **$p \leq 0.01$, ***$p \leq 0.001$, **** $p \leq 0.0001$.

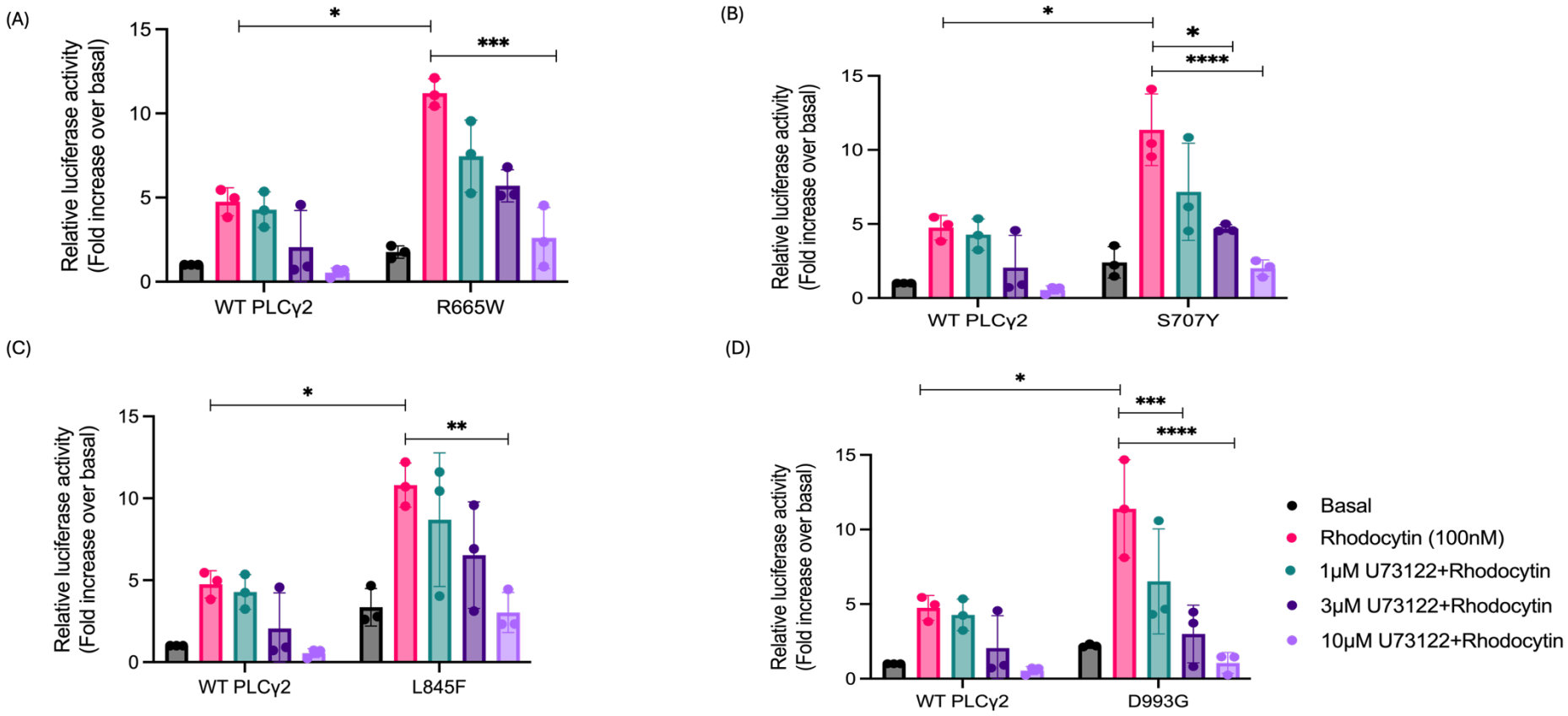

Figure 4.6: PLCγ2 mutations lead to a gain of function downstream of CLEC-2 which can be significantly decreased by U73122.

PLCγ2 KO cells were transfected with 10 μg WT PLCγ2, or plasmids containing (A) R665W, (B) S707Y, (C) L845F, or (D) D993G mutation along with 10μg CLEC-2 and 7.5μg NFAT containing plasmids. Transiently transfected cells were stimulated with 100nM rhodocytin for 6 hours prior to measuring the luciferase activity (n=3). Statistical significance was determined using Two-way ANOVA with Tukey's post-test. Graph shows mean ± SD. *$p \leq 0.05$. **$p \leq 0.01$, ***$p \leq 0.001$, **** $p \leq 0.0001$.

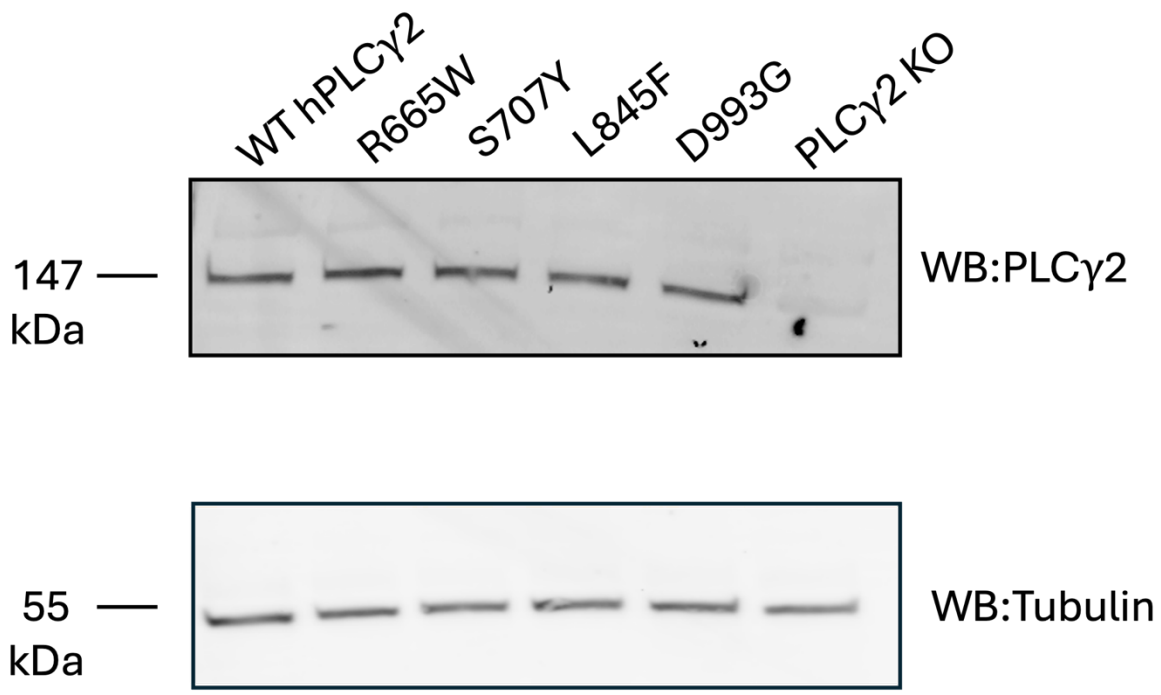

Figure 4.7: PLCγ2 is expressed at similar levels in PLCγ2 knockout cells bearing WT hPLCγ2 and PLCγ2 mutations.

$1x10^6$ of transfected cells were lysed using 1x RIPA buffer. Lysates were boiled for 5 minutes, centrifuged, and resolved using SDS-PAGE and western blotting for PLCγ2 with anti-tubulin as loading control.

4.3.2.1 PLCγ2 is highly conserved in human and chicken.

Previous studies investigating the effect of *PLCG2* mutations used an overexpression system to do so. Although this can be time efficient, overexpression systems do not always replicate the expression of endogenous protein levels as the most commonly used expression plasmids use constitutively active promoters. Therefore, the relative level of protein compared to other signalling elements, or positive and negative regulators, is unlikely to be present in these experiments. This has the potential to mask or exaggerate effects compared to what would happen in the cells of interest. Hence, in this study, the CRISPR/Cas9 gene editing approach was used to introduce PLCγ2 mutation knock-ins in chicken B-cells (DT40s) in order to investigate the effect of *PLCG2* mutations on PLCγ2 function. The reasoning behind choosing a cell line is due to the fact that platelets lack a nucleus which makes genetic manipulation impossible. Therefore, it was important to confirm that PLCγ2 is conserved between humans and chicken. It was also vital to confirm that the amino acids in the function altering mutations were also conserved.

The PLCγ2 protein sequence from different species was aligned. PLCγ2 protein sequences from (Homo sapiens, AAH18646.1) and chicken (Gallus gallus, XP_040537268.1) were aligned using multialin (http://multalin.toulouse.inra.fr/multalin/) and presented with ESPrit 3. The location of the PLCγ2 domains were determined using Simple Module Architecture Research Tool (SMART). Figure 4.5 shows that PLCγ2 is 82.48% conserved between chicken and humans. There are some sequence differences in the SH2 domain and some in the PH domain. However, this does not affect the mutations (highlighted in black boxes and arrows) as their location is conserved between the species and therefore can be targeted using the CRISPR/Cas9 gene editing approach.

PH domain

```
                 1        10        20        30        40        50
Human            .MSTTVNVDSLAEYEKSQIKRALELGTVMTVFSFRKSTPERRTVQVIMETRQVAWSKTAD
Chicken          MPRKSVDYGELPEYEKSQIKRTLELGTVMTVFSIKKSSLERRTIQVIMETRQVAWSKTAD
consensus>50     mmrksV#vdeLaEYEKSQIKRaLELGTVMTVFSikKSslERRT!QVIMETRQVAWSKTAD

                60        70        80        90       100       110
Human            KIEGFLDIMEIKEIRPGKNSKDFERAKAVRQKEDCCFTILYGTQFVLSTLSLAADSKEDA
Chicken          KIEGFLDLMEIKEIRPGKNSKDFERCKA.KHREEHCFTIFYGTQFVLNTLSLAADSKGDA
consensus>50     KIEGFLDiMEIKEIRPGKNSKDFERaKAvkqkE#cCFTIlYGTQFVLnTLSLAADSKeDA

               120       130       140       150       160       170
Human            VNWLSGLKILHQEAMNASTPTIIESWLRKQIYSVDQTRRNSISLRELKTILPLINFKVSS
Chicken          DKWLCGLNILYQEVMRAPTPAITESWLRKQIYSVDQTRRNSISLRELKAVLPQVNFKVSS
consensus>50     vnWLcGLnILyQEvMnApTPaIiESWLRKQIYSVDQTRRNSISLRELKa!LPl!NFKVSS

               180       190       200       210       220       230
Human            AKFLKDKFVEIGAHKDELSFEQFHLFYKKLMFEQQKSILDEFKKDSSVFILGNTDRPDAS
Chicken          MKFLKDKFAEIGAHKEELSFEQFHLFYKKIMFEQQKSILDEFKKDSSVFILGNTDRPDAS
consensus>50     mKFLKDKFvEIGAHK#ELSFEQFHLFYKKiMFEQQKSILDEFKKDSSVFILGNTDRPDAS

               240       250       260       270       280       290
Human            AVYLRDFQRFLIHEQQEHWAQDLNKVRERMTKFIDDTMRETAEPFLFVDEFLTYLFSREN
Chicken          AVHLHDFQRFLLHEQQESWAQDLSKVRERMTEFVDDTMRETAEPFLFVDEFLTYLFAKEN
consensus>50     AVyLhDFQRFLiHEQQEhWAQDLnKVRERMTeF!DDTMRETAEPFLFVDEFLTYLFakEN
```

TIM (x box) domain

```
               300       310       320       330       340       350
Human            SIWDEKYDAVDMQDMNNPLSHYWISSSHNTYLTGDQLRSESSPEAYIRCLRMGCRCIELD
Chicken          SIWDEKYDTIDVQDMNNPLSHYWISSSHNTYLTGDQLRSESSTEAYIRCLRMGCRCIELD
consensus>50     SIWDEKYDa!DvQDMNNPLSHYWISSSHNTYLTGDQLRSESSpEAYIRCLRMGCRCIELD

               360       370       380       390       400       410
Human            CWDGPDGKPVIYHGWTRTTKIKFDDVVQAIKDHAFVTSSFPVILSIEEHCSVEQQRHMAK
Chicken          CWDGPDGKPIIYHGWTRTTKIKFDDVVQAIKDHAFVTSEYPVILSIEEHCSVEQQRHMAK
consensus>50     CWDGPDGKP!IYHGWTRTTKIKFDDVVQAIKDHAFVTSe%PVILSIEEHCSVEQQRHMAK

               420       430       440       450       460       470
Human            AFKEVFGDLLLTKPTEASADQLPSPSQLREKIIIKHKKLGPRGDVDVNMEDKKDEHKQQG
Chicken          VFKEVFGDQLLMKPVEASADQLPSPTQLKEKIIIKHKKLGPKGDIDVNLEDKKEEKKQQG
consensus>50     vFKEVFGDlLLmKPvEASADQLPSPsQLkEKIIIKHKKLGPkGD!DVN$EDKK#EhKQQG
```

nSH2 domain

```
               480       490       500       510       520       530
Human            ELYMWDSIDQKWTRHYCAIADAKLSFSDDIEQTMEEEVPQDIPPTELHFGEKWFHKKV.E
Chicken          ELYMWDAIEQQWTRHYCAIADGKLSFSDVIEQNADEDSSKEVKRTELHLKEKWFHGKMKE
consensus>50     ELYMWDaI#QqWTRHYCAIADaKLSFSDvIEQnm#E#vpq#!kpTELHlgEKWFHgKvkE

               540       550       560       570       580       590
Human            KRTSAEKLLQEYCMETGGKDGTFLVRESETFPNDYTLSFWRSGRVQHCRIRSTMEGGTLK
Chicken          GRTTAEKLLQEYCAEMGGKDGTFLVRESEAFPNDCTLSFWRSGRVQHCRIRSSSDGDTVK
consensus>50     gRTsAEKLLQEYCmEmGGKDGTFLVRESEaFPNDyTLSFWRSGRVQHCRIRSsm#GdTvK
```

cSH2 domain

```
               600       610       620       630       640       650
Human            YYLTDNLTFSSIYALIQHYRETHLRCAEFELRLTDPVPNPNPHESKPWYYDSLSRGEAED
Chicken          YYLTDNVTFDSIYDLIQHYKEVHLRCAEFDLRLTDAVPNPSPHENKDWYYSNLSRGEAED
consensus>50     YYLTDNvTFdSIYdLIQHYkEvHLRCAEF#LRLTDaVPNPnPHEnKdWYYdnLSRGEAED
```

R665W S707Y

```
               660       670       680       690       700       710
Human            MLMRIPRQGAFLIRKREGSDSYAITFRARGKVKHCRINRDGRHFVLGTSAYFESLVELVS
Chicken          MLMRIPRQGAFLIRKRDEPDSFAMTFRAEGKVKHFRIQQEGRHFVLGTSAYFESLVELVT
consensus>50     MLMRIPRQGAFLIRKR#epDS%AiTFRAeGKVKHfRI#q#GRHFVLGTSAYFESLVELVs
```

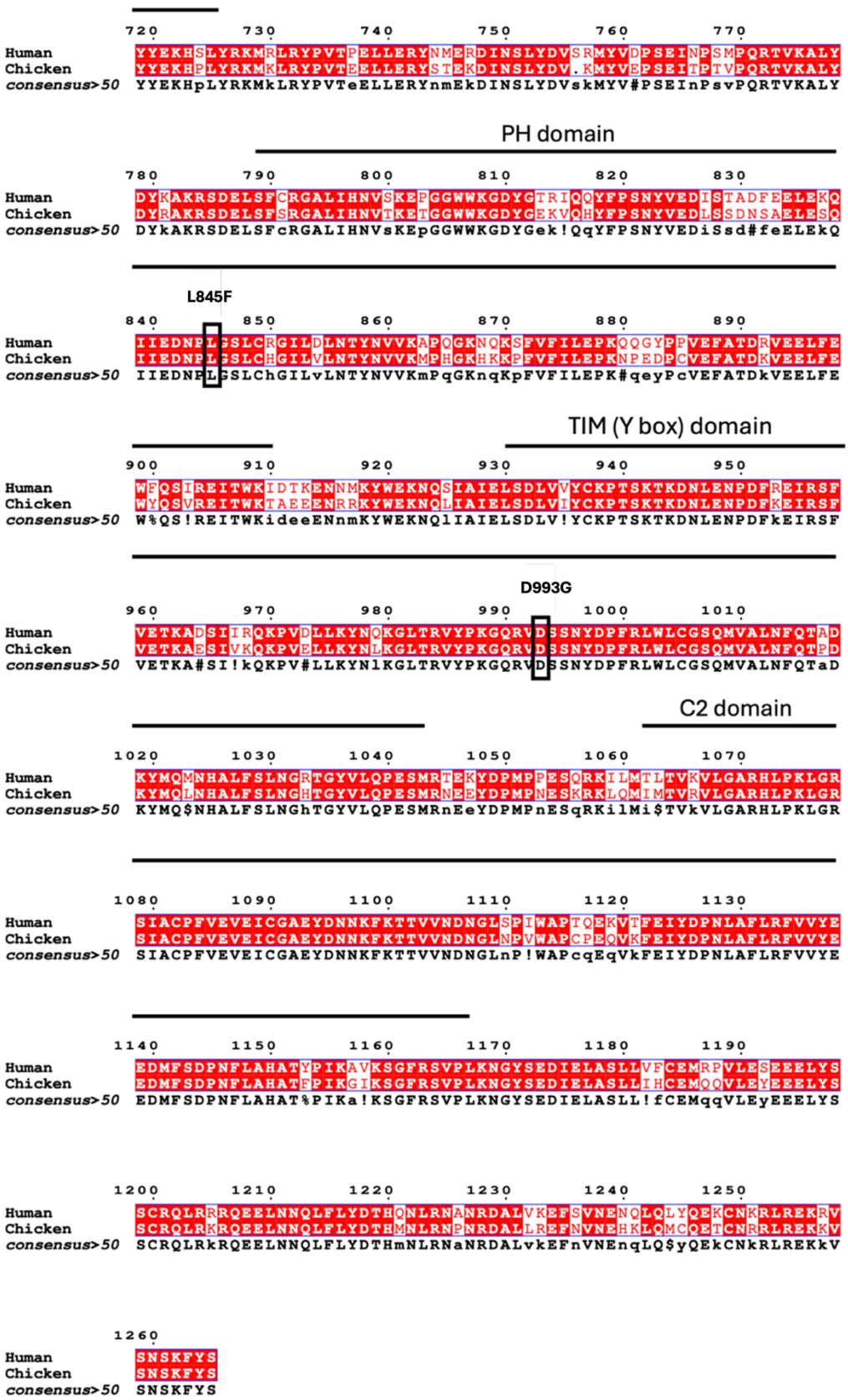

Figure 4.8: PLCγ2 protein mutations are conserved across several species.

PLCγ2 sequences from (Homo sapiens, AAH18646.1) and chicken (Gallus gallus, XP_040537268.1) were aligned using multialin and displayed using ESPrit3. Highlighted in red are conserved amino acids across species. Black boxes and arrows highlight PLCγ2 mutation sites (R665W, S707Y, L845F, and D993G).

4.3.3 Designing strategy of HDR, guide RNA, and primers.

Donor repair template plasmids, which include homology arms flanking the alteration site, are required for making targeted DNA alterations. Donor templates were designed using Benchling software by changing the DNA codon in order to insert the desired point mutation. 300 base pairs (bp) were selected around the mutation with 150 bp flanking each side. A silent mutation was added to change the protospacer adjacent motif (PAM) site (figure 4.10). This step is necessary to prevent the guide from re-cutting the repaired genomic DNA avoiding the generation of a knockout (Ran et al., 2013).

Guide RNAs (gRNAs) were also designed using Benchling (figure 4.9). The guides were selected based on their proximity to the mutation, where a larger distance between the DNA cut and the mutation site can lead to a decrease in efficiency. It was also essential to select guides with the lowest off-target effects which was determined using Hsu calculations (Hsu et al., 2013). Guides where also selected based on their highest activity, which is determined by the likelihood of the Cas9 nuclease to cause double strand breaks when combined with the guide (Doench, 2016). Oligonucleotides and plasmid donor templates were purchased from Eurofins genomics. To confirm the PLCγ2 knock-ins in WT DT40 cells, primers which flanked the mutation site were designed to screen for the point mutations (Table 4.3). Forward and reverse primers were designed using Benching. Primers were purchased from Eurofins Genomics.

Table 4.2 Guide RNA sequence and donor templates designed for PLCγ2 knock-ins in DT40 cells.

Mutation	Guide RNA, notes	Donor template	Mutated Donor template
R665W CGA→TGG	TAGCAACTTGAGTCGAGGAG Yellow: guide RNA Red:mutated PAM site Green: mutation site (small letters are the changed bases to create the mutation	TCTGTTGTTAGTAACGCTACCTGTTAGTGT TACTGAATTACATTAGACAAGCTTTGTAAT CCTTTGTCCATTTTGATTTTTGACTGTTGT AGTTGGTACTATAGCAACTTGAGTCGAGG AGAGGCAGAAGACATGCTGATGAGAATTC CTtGgGATGGAGCCTTTCTAATTAGAAAGA GAGATGAGCCTGATTCATTTGCCATGACT TTCAGGTATGAATATATTATCTAGTAGCCA ACAGTGTTCTGGGTTTTCTTTTGTTTGTTT GTTTTTCTCTCATTTAAAAATGGGCTTTTT TGAG	TCTGTTGTTAGTAACGCTACCTGTTAGT GTTACTGAATTACATTAGACAAGCTTTG TAATCCTTTGTCCATTTTGATTTTTGACT GTTGTAGTTGGTACTATAGCAACTTGAG TCGAGGAGAAGCAGAAGACATGCTGAT GAGAATTCCTtGgGATGGAGCCTTTCTA ATTAGAAAGAGAGATGAGCCTGATTCAT TTGCCATGACTTTCAGGTATGAATATATT ATCTAGTAGCCAACAGTGTTCTGGGTTT TCTTTTGTTTGTTTGTTTTTCTCTCATTTA AAAATGGGCTTTTTTGAGTC
S707Y TCA→TAT	CTTTGAGAGTTTAGTGGAGC Yellow: guide RNA Red: mutated PAM site Green: mutation site (small letters are the changed bases to create the mutation	AGTTTGCAGCACTGATGCTTTCACTATGC CAAGTACCAATACCTTTAACAGCACTTGT ACTTGTTTCACAGAGCTGAGGGGAAGGT GAAGCACTTCCGAATTCAGCAAGAAGGTC GCCATTTTGTGCTTGGAACGTatGCCTACT TTGAGAGTTTAGTGGAGCTGGTAACATAC TATGAGAAGCACCCTCTGTACAGGAAAAT GAAATTACGTTACCCTGTGACTGAGGAGC TGCTGGAGCGCTACAGCACAGTAAGTGA TGTCCTTTGTATGAGTGCCACGTGCTTTA GCAGATGGAGTCCC	AGTTTGCAGCACTGATGCTTTCACTATG CCAAGTACCAATACCTTTAACAGCACTT GTACTTGTTTCACAGAGCTGAGGGGAA GGTGAAGCACTTCCGAATTCAGCAAGA AGGTCGCCATTTTGTGCTTGGAACGTat GCCTACTTTGAGAGTTTAGTGGAGCTCG TAACATACTATGAGAAGCACCCTCTGTA CAGGAAAATGAAATTACGTTACCCTGTG ACTGAGGAGCTGCTGGAGCGCTACAGC ACAGTAAGTGATGTCCTTTGTATGAGTG CCACGTGCTTTAGCAGATGGAGTCCC
L845F TTA→TTT	GTACTAAATACCTACAATGT Yellow: guide RNA Red: PAM site Unable to mutate PAM site so 2 silent mutations introduced in the guide sequence instead Green: mutation site (small letters are the changed bases to create the mutation	GAATTAGTTTGCCTTTTAAATATTACAGTG GACCTGCTTTCAATGAAAGTGTAATTAGA GTTAGTGGTGTGTATTTATTTGTTAATATT CTGTGCAGAAGGCTGTGTCAGCTGTATCT CGTGTTTTTCACAGATTTtTTGAGGACAATC CATTtGGATCTCTGTGTCATGGCATATTGG TACTAAATACCTACAATGTTGGTATGTACT TTCTGATTTGTATATGTTGACTCCTGAACT TTCTGTGCTGAAGAGGATCCCTTGTGTTT AGCATAAAATACTTGGCTTTGAAAACTATT TATATT	GAATTAGTTTGCCTTTTAAATATTACAGT GGACCTGCTTTCAATGAAAGTGTAATTA GAGTTAGTGGTGTGTATTTATTTGTTAAT ATTCTGTGCAGAAGGCTGTGTCAGCTGT ATCTCGTGTTTTTCACAGATTTtTTGAGGA CAATCCATTtGGATCTCTGTGTCATGGCA TATTGGTACTAAATACCTAcAAcGTTGGT ATGTACTTTCTGATTTGTATATGTTGACT CCTGAACTTTCTGTGCTGAAGAGGATCC CTTGTGTTTAGCATAAAATACTTGGCTTT GAAAACTATTTATATT
D933G GAC→GGT	ACTATGACCCATTTCGCCTC Yellow: guide RNA Red: mutated PAM site Green: mutation site (small letters are the changed bases to create the mutation	CTCTCCCTTGTGTAGAAAATCCTGATTTCA AAGAAATACGTTCCTTTGTGGAAACCAAG GCAGAAAGTATTGTTAAGCAAAAGCCGGT TGAGTTGCTGAAATACAACTTGAAGGGAC TGACACGTGTCTATCCTAAAGGACAGAGG GTTGgtTCATCAAACTATGACCCATTTCGC CTCTGGCTTTGTGGCTCTCAGATGGTGGC TCTTAACTTTCAGACTCCAGGTAATGTTCC ATTTAAAAAGGATTCTGTCCACGTTCTATT TGTGCATCTGTGAATCCTCTGTTAAAAGC AGGTCCAC	CTCTCCCTTGTGTAGAAAATCCTGATTT CAAAGAAATACGTTCCTTTGTGGAAACC AAGGCAGAAAGTATTGTTAAGCAAAAGC CGGTTGAGTTGCTGAAATACAACTTGAA GGGACTGACACGTGTCTATCCTAAAGG ACAGAGGGTTGgtTCATCAAACTATGAC CCATTTaGaCTaTGGCTTTGTGGCTCTCA GATGGTGGCTCTTAACTTTCAGACTCCA GGTAATGTTCCATTTAAAAAGGATTCTG TCCACGTTCTATTTGTGCATCTGTGAAT CCTCTGTTAAAAGCAGGTCCAC

Table 4.3: Primers designed for sequencing PLCγ2 point mutations.

Mutation	Primers
R665W	Forward: 5'ACGCTACCTGTTAGTGTTACTGA 3' Reverse: 5' ACCCAGAACACTGTTGGCTACT 3'
S707Y	Forward: 5' GCTGAGGGGAAGGTGAAGCACT 3' Reverse: 5' CCATCTGCTAAAGCACGTGGCA 3'
L845F	Forward: 5' ACAGTGGACCTGCTTTCAATGA 3' Reverse: 5' ACACAAGAGACCCTCTTCAGCACA 3'
D993G	Forward: 5' TCTTTCTTCCTGTATAACAGCCCT 3' Reverse: 5' GAGCCACCATCTGAGAGCCACA 3'

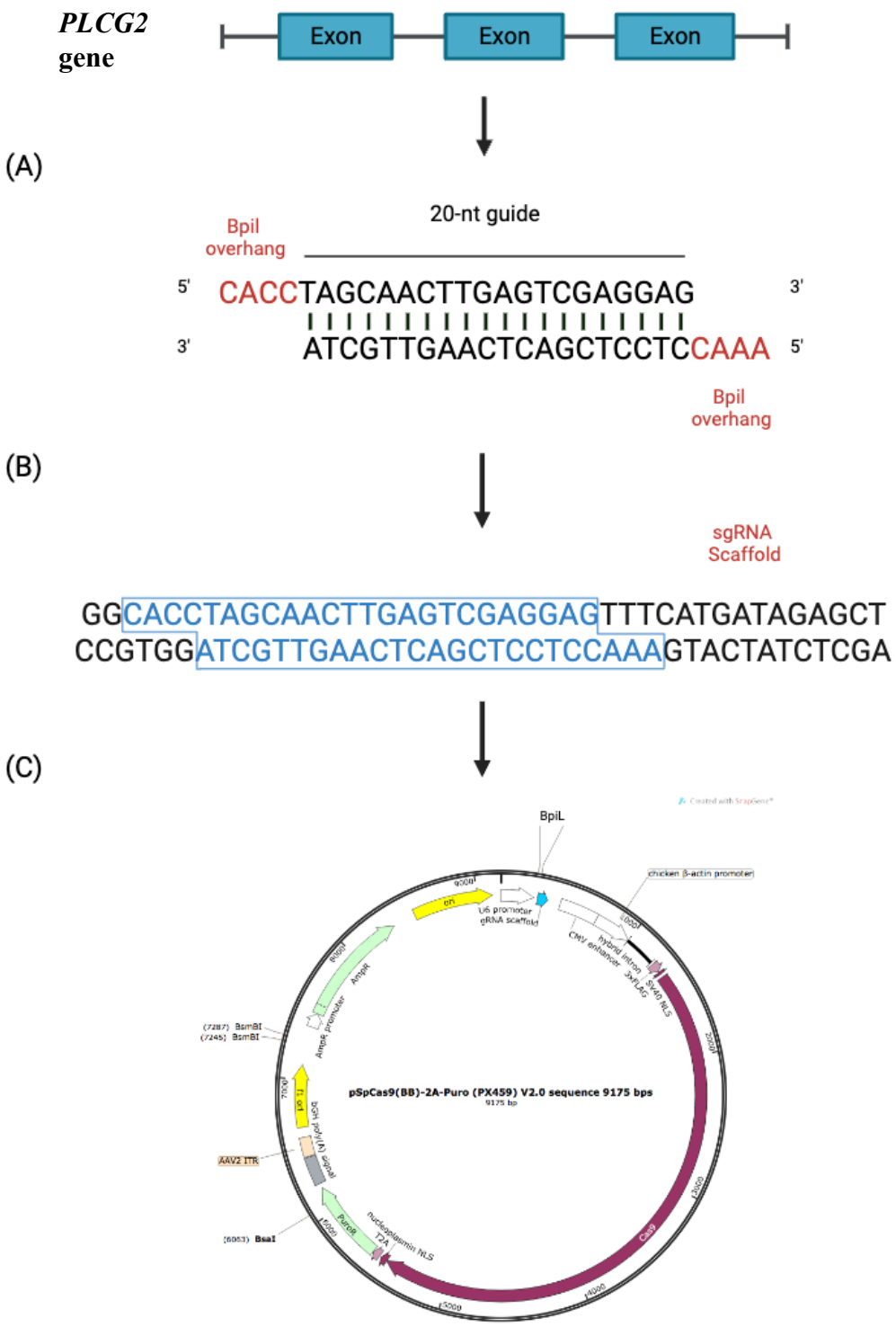

Figure 4.9: Guide RNA selection and preparation.

Guides to generate mutation knock-in were selected based on their best off-target and on-target score. (A) BpiI overhangs were added to allow ligation into pSpCas9 (BB) 2A-Puro vector. (B) Guides are then annealed and phosphorylated prior to (C) ligation into pSpCas9 (BB) 2A-Puro vector (Vector adapted from Addgene).

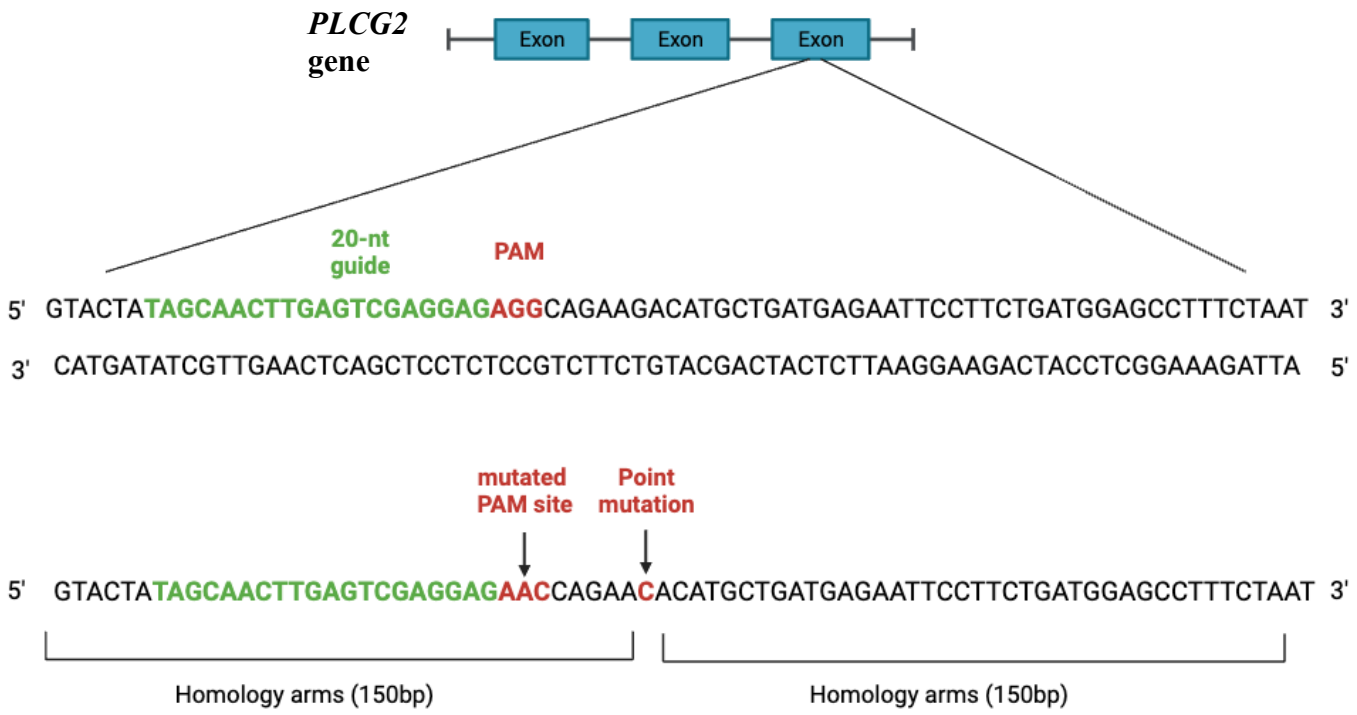

Figure 4.10: Donor template design strategy.

HDR template with 150 bp homology arms flaking mutation site is designed. Following the 20 nt gRNA is the PAM site where a silent mutation is introduced to prevent Cas9 from recutting. And desired point mutation is introduced.

linearised plasmids were used, the plasmid was incubated with EcoRI-HF at 37°C overnight. The digest was run on a 1% agarose gel to confirm plasmid linearisation and subsequently purified using GenElute gel extraction kit.

Following transfection, cells were plated out into 96-well plated and stable clones were selected using puromycin. The host plasmid contains a puromycin resistance gene allowing cells containing the plasmid to grow. After 2-3 weeks of puromycin selection, stable colonies were then selected and expanded into 24-well, and then 6-well plates. Cells were then lysed and analysed using western blot to confirm the presence of PLCγ2. A platelet lysate and a WT DT40 lysate were both used as

positive control, whereas a PLCγ2 knockout DT40 lysate was used as negative control.

As shown in Table 4.4, for all the mutations, cells transfected with the linearised plasmid resulted in the growth of less colonies in comparison to cells transfected with non-linearised plasmid. Although S707Y, L845F, and D993G knock-in transfections led to the growth of stable clones, when screened using western blotting some of the colonies lacked the expression of PLCγ2 suggesting that the gene has been disrupted resulting in protein knockout instead while others still expressed PLCγ2 but lacked the mutation.

In contrast, when transfected with non-linearised plasmid, one of the R665W knock-in transfections contained the *PLCG2* mutation. Figure 4.11A shows that colonies 1, 2 and 5 express PLCγ2 and were therefore taken forward for sequencing to confirm the presence of the mutation R665W. Genomic DNA extracts were prepared and the region around the mutation was amplified using touchdown PCR (Table 4.3 R665W forward and reverse primers).

To confirm the success of touchdown PCR, the PCR product was run on 1% agarose gel and an expected band (238bp) was observed and extracted using a GenElute gel extraction kit. The purified PCR product was sequenced using R665W forward primers (Table 4.3) by Eurofins genomics. Sequencing results confirmed the successful knock-in of the R665W mutation where the amino acid Arginine(R) was substituted with the amino acid tryptophan (W) (figure 4.10 (B)).

However, transfecting the cells using the CRISPR/Cas9 approach led to the introduction of an additional unintended mutation upstream of R665W as shown in figure 4.11. Therefore, it was not possible to take this mutated cell line further and

test the effect of the mutation, R665W, on PLCγ2 activity. Where the effects observed could be driven by the random mutation upstream.

Table 4.4: Number of colonies grown following stable selection

Mutation	Number of colonies with linearised plasmid	Number of colonies with non-linearised plasmid	Number of colonies with mutation
R665W	5	1	1
S707Y	2	10	0
L845F	1	3	0
D993G	6	20	0

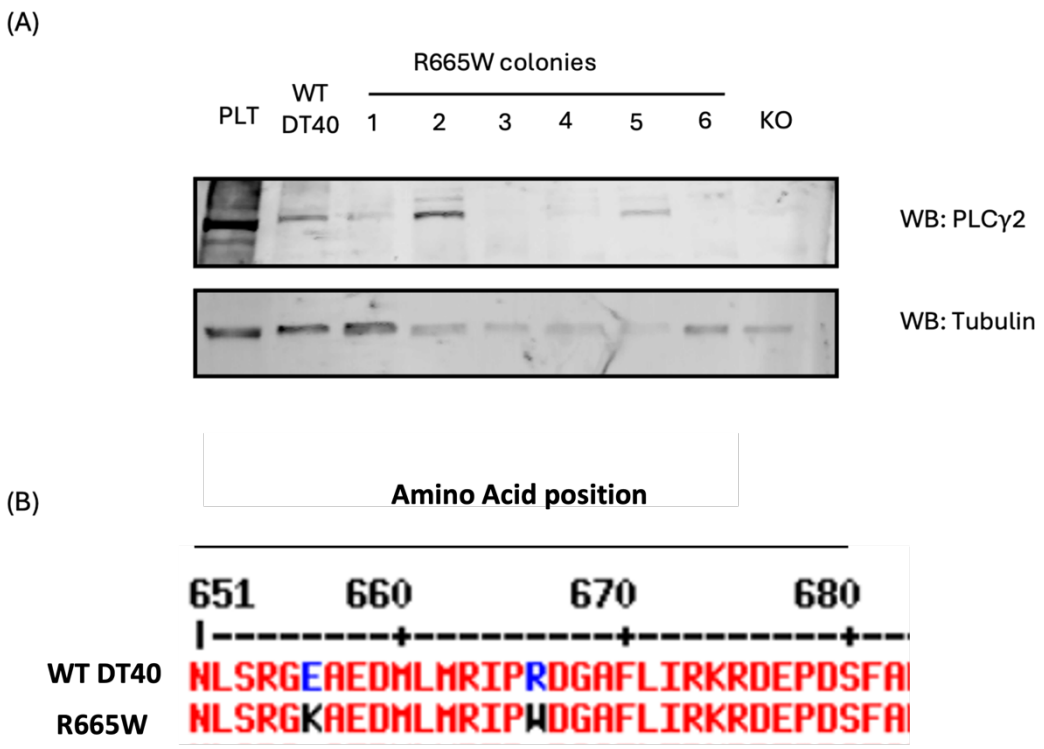

Figure 4.11: CRISPR/Cas9 introduced PLCγ2 mutation, R665W, in DT40 cells.

(A) $1x10^7$ of WT DT40 cells and stable cell mutant clones were lysed using 1x RIPA buffer. Cells were lysed for 30 minutes prior to adding 6X SB and boiled for 5 minutes. Cells were centrifuged and resolved using SDS-PAGE and western blotting for PLCγ2 with anti-tubulin as loading control. (B) DNA sequencing results of R665W knock-in shows the substitution of arginine to tryptophan at amino acid position 665.

4.4 Discussion

In this chapter, plasmids containing PLCγ2 mutations were transiently transfected in PLCγ2 knockout cells and their effect on PLCγ2 function was determined by examining the luciferase activity using an NFAT-luciferase assay and compared to WT PLCγ2. Additionally, following the previous characterization of the PLCγ2 inhibitor, U73122, in human platelets its effect on cells bearing the mutations has also been tested.

In the previous chapter, the effect of U73122 was tested on several platelets functions and was found to have a significant effect especially at a high concentration (10μM). So, it was hypothesised that it would have a similar effect on DT40 cells.

When measuring signalling in DT40 cells after PLCγ2 activation, the NFAT-luciferase-reporter assay may be utilised as it is an extremely sensitive and high throughput assay Tomlinson et al., 2007, Takata and Kurosaki, 1996, Tomlinson et al., 2001).

The effect of U73122 on the NFAT-luciferase activation was first assessed in collagen or rhodocytin stimulated WT DT40 cells. U73122 has a similar effect on both GPVI and CLEC-2 mediated signalling where it significantly decreased the NFAT-luciferase activation in a concentration dependent manner. These results are similar to the results seen in (section 3.3.3) when the calcium flux was measured downstream of GPVI and CLEC-2 in platelets. These results also align with previous studies showing that U73122 successfully reduces PLC mediated signalling pathways by blocking the hydrolysis of PIP2 to IP3 and DAG (Bleasdale et al., 1990).

It is worth noting that downstream of GPVI, U73122 decreased the calcium flux in platelets in a concentration dependent manner whereas all concentration of U73122 had a big effect on decreasing the calcium flux downstream of CLEC-2.

When looking at unstimulated cells, cells bearing the PLCγ2 mutations showed a small but non-significant increase in the NFAT-luciferase activation in comparison to the expression of WT PLCγ2. This is not surprising as previous studies have shown that these mutations are hyperactive (Zhou et al., 2012a). Surprisingly, in both collagen and rhodocytin stimulated PLCγ2 KO cells that were transfected with WT hPLCγ2, U73122 had no effect on decreasing the NFAT-luciferase activation.

When stimulated with either collagen or rhodocytin, all the mutations led to a significant increase in the NFAT-luciferase activation in comparison to cells with WT PLCγ2. Due to the fact that these mutations led to gain-of function and are resistance to ibrutinib, it was hypothesised that the U73122 might not have a significant effect. Surprisingly, U73122 had a significant effect on decreasing NFAT-luciferase activation. In cells with the SH2 domain mutations, R665W and S707Y, U73122 had a significant effect on decreasing the NFAT-luciferase activation at 3μM and 10μM when stimulated by collagen. Whereas cells transfected with the PH domain mutation L845F, and the catalytic domain mutation D993G, U73122 had a significant effect on decreasing the NFAT-luciferase activation only at its highest concentration (10μM).

PLCγ2's SH2 domain, as previously described, is required for binding to phosphorylated tyrosine residues of signalling proteins, such as receptor tyrosine

kinases. This contact is necessary for PLCγ2's activation and localization within the cell. The role of the SH2 domain is to activate PLCγ2, which then hydrolyzes PIP2 into IP_3 and DAG that are essential for calcium signalling. Consequently, a mutation on the SH2 domain such as R665W and S707Y, might lead to a change in the binding affinity. Hence, SH2 domain mutations may potentially affect signalling by changing the structure of the protein and therefore its binding affinity to phosphorylated tyrosine residues. This is likely to influence on how well the protein interacts with others. Although R665W has been shown to lead to a gain of function, it is probable that the inhibition of the PLCy2 catalytic activity by U73122 will counteract the hyperreactivity caused by the mutation.

PLCγ2's stability and activity independent of upstream signals may be improved by structural alterations brought about by the L845F mutation, which may affect its regulatory activity or increase the enzyme's essential activity. D993G on the other hand is located on the catalytic domain of PLCγ2. Consequently, PLCγ2's catalytic activity or stability may be improved, and its dependence on upstream signals including interactions that U73122 would potentially inhibit may be reduced as a result of a conformational change. This could explain why cells bearing the mutations R665W and S707Y were more susceptible to U73122.

The effect of U73122 on the activity of PLCγ2 mutations downstream CLEC-2 was slightly different. In rhodocytin stimulated cells, U73122 had significant effect on decreasing the NFAT-luciferase activation in cells bearing the D933G mutation at 3μM and 10μM. This could suggest that the CLEC-2 signalling pathway is more

reliant on the activity of the catalytic domain of PLCγ2 than GPVI. Whereas GPVI mediated signalling could be more reliant on the SH2 domain.

Although using an overexpression system to transiently express PLCγ2 mutations in PLCγ2 KO DT40s can be time efficient, it does not physiologically mimic the amount of endogenous protein expressed. Therefore, in this project the CRISPR/Cas9 gene editing approach was used to genetically induce PLCγ2 specific knock-in point mutants. Using both approaches will allow a comparison between the two, and up until the time of this study there was no evidence in the literature on the use of CRISPR/Cas9 to investigate the functional effects of PLCγ2 mutations.

The CRISPR/Cas9 gene editing approach required transfecting the DT40 cells with a gRNA Cas9 containing plasmid and a donor template plasmid. Some transfections resulted in growth of colonies lacking the expression of PLCγ2. This might be due to a number of reasons. This might be due to the fact that HDR failed to happen and NHEJ occurred leading to complete protein knockout. Another possibility might be that the Cas9 enzyme failed to create a DSB in the first place which will prevent the cells form repairing it. This can happen if the Cas9 remains bound and does not release (Knight et al., 2015). Other transfection attempts resulted in the complete knockout of PLCγ2 instead of the knock-in of the mutations. This is can also be due to NHEJ taking place instead of HDR. Another explanation to this might be the fact that DT40 have low HDR efficiency (around 20%) and hence a knockout will more likely be generated that a knock-in (Abu-Bonsrah et al., 2016).

Regardless, there are strategies that can be implemented to increase the chances of success. Studies have suggested using a linearised plasmid when transfecting the cells instead. To further optimize the chance of HDR, we linearised the donor

template plasmid with restriction enzymes. This has been suggested by Ran et al., to result in a more efficient repair. However, a linearised plasmid might be better integrated as circular plasmids can undergo random fragmentation at various locations throughout the plasmid to facilitate integration (Song and Stieger, 2017). In this study, although testing this approach resulted in the growth of colonies, when sequenced the cells did not contain the desired mutation.

Lastly, when compared to double-stranded DNA (dsDNA), the utilisation of single-stranded DNA (ssDNA) in CRISPR systems provides an advantage. In terms of efficiency and cytotoxicity, research has shown that utilising ssDNA is more effective and less harmful than utilising double-stranded DNA dsDNA (Eroglu et al., 2023).

Additional PLCγ2 mutations, such as A708P and M1141L, are rare mutations that are primarily associated with autoinflammatory diseases and certain immunodeficiencies. Specifically, they have been linked to PLAID (PLCγ2-associated antibody deficiency and immune dysregulation) and APLAID (autoinflammation and PLCγ2-associated antibody deficiency) (Walliser et al., 2018, Novice et al., 2020). A708P and M1141L can have significant implications for platelet reactivity and cardiovascular risk. These mutations may lead to a gain-of-function alteration in PLCγ2 (Martín-Nalda et al., 2020, Novice et al., 2020), resulting in increased platelet activation through enhanced signal transduction pathways. Consequently, this heightened platelet reactivity can increase the risk of thrombotic events, such as myocardial infarction or ischemic stroke, indicating a hypercoagulable state that necessitates careful monitoring and potential antiplatelet therapy. Carriers of the A708P and M114L mutations may therefore face an elevated risk of cardiovascular events due to this increased platelet reactivity.

The effect of A708P and M114L on platelet reactivity and PLCγ2 activity can also be investigated using the either the CRISPR/Cas9 or the overexpression approach.

To study the effect of A708P and M114L on platelet reactivity, the CRISPR/Cas9 or the overexpression approach could be used. This mutation could be introduced into a cell line, such as DT40 cells, in order to study intracellular signalling and protein interaction.

Furthermore, in order to examine the effect of these mutations on platelet activity and thrombus formation, zebrafish could be used an *in vivo* model. Where CIRSPR/Cas9 is used to knock-in these mutations and thrombus formation is examined using laser injury.

Chapter 5: U73122 prevents thrombosis and increases occlusion time in zebrafish embryos.

5.1 Introduction

5.1.1 Zebrafish as a biological model for thrombosis.

The zebrafish model (*Danio rerio)* possesses several benefits making it an ideal model for researching thrombosis. They have rapid generation times of approximately 2-4 months, and they are suitable for large scale screening due to their high reproductive capacity, and ease of fertilisation (Weyand and Shavit, 2014, Lang et al., 2010). Moreover, the transparent nature of zebrafish embryos and larvae permits high-resolution, non-invasive visualisation of organs and biological processes *in vivo* (Gregory et al., 2002).

Zebrafish have a significant level of genetic similarity to humans where 70% of human genes are orthologous to zebrafish genes (Howe et al., 2013). There is a great number of parallels between the zebrafish and the human haemostatic system that have led to zebrafish being an extremely useful model for studying thrombosis and haemostasis. Although zebrafish do not possess platelets, zebrafish thrombocytes serve a similar purpose as human platelets. The initial identification of zebrafish thrombocytes was made by the morphological investigation of peripheral blood smears. Zebrafish blood comprises adult erythrocytes, leukocytes, and thrombocytes, both of which are nucleated, in contrast to the anucleate nature of human platelets and erythrocytes (Jagadeeswaran et al., 1999). Zebrafish also have common genes encoding elements of platelet adhesion, activation, and aggregation,

that are also present in humans. This includes vwF, GPIb, GPIIb, fibrinogen, αIIbβ3 and P-selectin (Jagadeeswaran et al., 1999, Lang et al., 2010). Although zebrafish lack GPVI, Hughes et al., have found that similarly to the GPVI collagen receptor in mammals, G6f-like (G6fL) is a functional receptor for collagen in zebrafish thrombocytes (Hughes et al., 2012). In addition, it has been determined that CLEC-2 and podoplanin have orthologues in zebrafish (Alice Pollitt, personal communication). Moreover, zebrafish have coagulation factors and thrombocyte receptors (Jagadeeswaran et al., 2005), and they exhibit a response to anticoagulant and antiplatelet medications such as warfarin (Jagadeeswaran and Sheehan, 1999), aspirin, clopidogrel, and diltiazem (Zhang et al., 2017) that are often employed in clinical therapy. Moreover, previous research has demonstrated that agonists such as ADP, ristocetin, and arachidonic acid are capable of stimulating zebrafish thrombocytes, which is in line with the agonists used to aggregate human platelets. These results confirmed the conservation of ADP, thrombin, ristocetin, and vWF receptors (Jagadeeswaran et al., 1999).

5.1.2 Laser induced injury in zebrafish.

Due to the presence of all the components seen in the mammalian coagulation cascade, zebrafish have been used as a model for investigating thrombosis. The study of thrombosis in zebrafish has been facilitated by several methods

. This was either by using chemicals such as phenylhydrazine or ferric chloride which are known to cause vascular injury in mammals, or alternatively by laser induced injury (Jagadeeswaran et al., 2004). Using laser induced injury, studies investigated fibrinogen's function in early haemostasis (Freire et al., 2020) and the evaluation of antithrombotic medications (Zhu et al., 2016). Using this assay, vascular injury can

be induced by a pulsed nitrogen laser targeting either the dorsal artery or the caudal vein resulting in occlusion. Therefore, using the laser injury model tends to be more specific and precise than using chemical-induced injuries due to the fact that it can target specific areas without affecting surrounding areas. This qualifies laser induced injury as the preferred model when studying thrombosis in zebrafish (Jagadeeswaran et al., 2004, Jagadeeswaran et al., 2011).

5.1.3 Vascular system development in zebrafish.

As previously described, platelets play a role in blood and lymphatic vasculature development. More specifically, the role PLCγ2 plays in this development was also examined in mouse models. To further examine the role PLCγ2 plays in mediating the development of blood and lymphatic vasculature in this study, zebrafish was used as an *in vivo* model. Within the past several years, zebrafish have become a significant vertebrate model system for researching the development of the vascular system. Zebrafish have several vascular properties that are quite similar to those in humans and to other animals. This includes possessing a closed circulatory system, and the anatomical structure and molecular mechanism of vascular development (Isogai et al., 2001). In addition, recent research has demonstrated that zebrafish contain a lymphatic vascular system, which makes it an excellent model for examining the development of this distinct and independent vascular network (McKinney and Weinstein, 2008).

When it comes to the development of the vertebrate embryo, the establishment of the cardiovascular system is an extremely important factor. The two distinct cell populations, primitive hematopoietic cells, and vascular endothelial precursor cells

(also known as angioblasts) are both produced by hemangioblasts throughout embryogenesis (Eilken et al., 2009, Lancrin et al., 2009). Endothelial and hematopoietic cells in zebrafish embryos develop in close proximity to one other, similar to other vertebrates, and are believed to originate from a shared progenitor know as haemangioblast(Kobayashi, 2018, Vogeli et al., 2006). Although zebrafish embryos exhibit unique spatial development of two cell lineages compared to other vertebrates, it is believed that they are dependent on the same genetic programmes to develop (Detrich et al., 1995). Vascular system development in zebrafish includes two processes: vasculogenesis and angiogenesis. Vasculogenesis is the process by which angioblasts generate new blood vessels whereas angiogenesis refers to the process by which new blood vessels develop from existing vessels (Risau et al., 1988). Vascular development is known to depend on a number of important elements. Previous literature has established that vasculogenesis and angiogenesis both depend on the vascular endothelial growth factor (VEGF) family and its receptors (VEGFR) (Carmeliet et al., 1996, Ferrara et al., 2003). When angioblasts begin to migrate from the lateral plate mesoderm to the midline, which occurs at around 12 hours post fertilisation (hpf) in zebrafish, vasculogenesis begins. Then at approximately 20 hpf, the dorsal aorta (DA) (figure 5.2 A) is formed when angioblasts develop into arterial precursor cells and the posterior cardinal vein (PCV) (figure 5.2 A) is formed when they differentiate into venous precursor cells. Then at approximately 22 hpf, sprouting angiogenesis takes place from the DA. This occurs after main axial arteries have been formed. At 28-30 hpf, the sprouting vessels that would become the future intersegmental vessels (ISV) as shown in figure 5.2 A, expand dorsally until they eventually converge at the level of the dorsal neural tube.

They then fuse with nearby vessels to create the dorsal longitudinal anastomotic vessel (DLAV) (figure 5.2 A) (Childs et al., 2002, Hogan and Schulte-Merker, 2017). In a study by Wang et al., the role of Btk in vascular development of zebrafish larvae was investigated via the inhibition of Btk by ibrutinib. Firstly, they observed that treating zebrafish with ibrutinib resulted in pericardial edema, lower heart rate, and a shorter body length of the zebrafish. Moreover, treating embryos with 1μM ibrutinib had no significant effect at 6 days post fertilisation in contrast to treating the fish with 20μM which led to 100% lethality at 12 hpf. Furthermore, 60% of the zebrafish embryos survived when treated with 5μM ibrutinib whereas all embryos died when treated with 10μM at 6 days post fertilisation. This study has also shown that that 5μM and 10μM of ibrutinib decreased the percentage of the normally developed ISVs significantly in comparison to control embryos. Since there is no evidence of a direct connection between Btk and angiogenesis, the target protein that ibrutinib suppresses in angiogenesis is not believed to be Btk. This was confirmed in zebrafish embryos by Btk knockdown by Btk morpholinos and by treatment with spebrutinib, another well-known Btk inhibitor where the impact on angiogenesis was negligible (Wang et al., 2020).

5.1.4 Lymphatic system development in zebrafish.

The lymphatic system is necessary for the maintenance of fluid homeostasis and also plays a major role in in immunity (Baluk et al., 2007). Although significant, when compared to blood vessels, lymphatic vessels are less well understood in terms of their formation and function, despite their significance. This is mostly due to challenges with *in vivo* lymphatic channel imaging. Additionally, in comparison to the

vascular system, the lymphatic system develops at a later stage (starting from 48 hpf) (Jung et al., 2017, Feng et al., 2021).

With the emergence of zebrafish as a popular model for *in vivo* research, several studies have demonstrated that there are numerous physical, genetic, and functional traits of lymphatic vessels in other vertebrates are also shared by the lymphatic system of zebrafish (Küchler et al., 2006). Most of the research has made use of body transparency and different transgenic and tracing methods to study zebrafish lymphatic development throughout the embryonic stage. Numerous studies conducted in the past have characterised the process of lymphangiogenesis in zebrafish embryos. This process involves the formation of the trunk lymphatic network, the face lymphatic network, and the intestinal lymphatic network (Feng et al., 2021). Additionally at 36 hpf, the facial lymphatic sprout (FLS) is formed when lymphangioblasts sprouting from the common cardinal vein begin to generate face lymphatic vessels. Beginning their migration from the posterior cardinal vein 48 hpf, the lymphangioblasts lining the trunk lymphatic veins will eventually migrate to the dorsal myoseptum and undergo a metamorphosis into parachordal lymphangioblasts. By 120 hpf (5 days post-fertilization (dpf)), the fish's lymphatic vasculature progresses to form artery alongside the dorsal longitudinal anastomotic vessel the thoracic duct (TD) under the dorsal aorta (DA) and the dorsal longitudinal lymphatic ash shown in figure 5.2 B(Jung et al., 2017, Okuda et al., 2012).

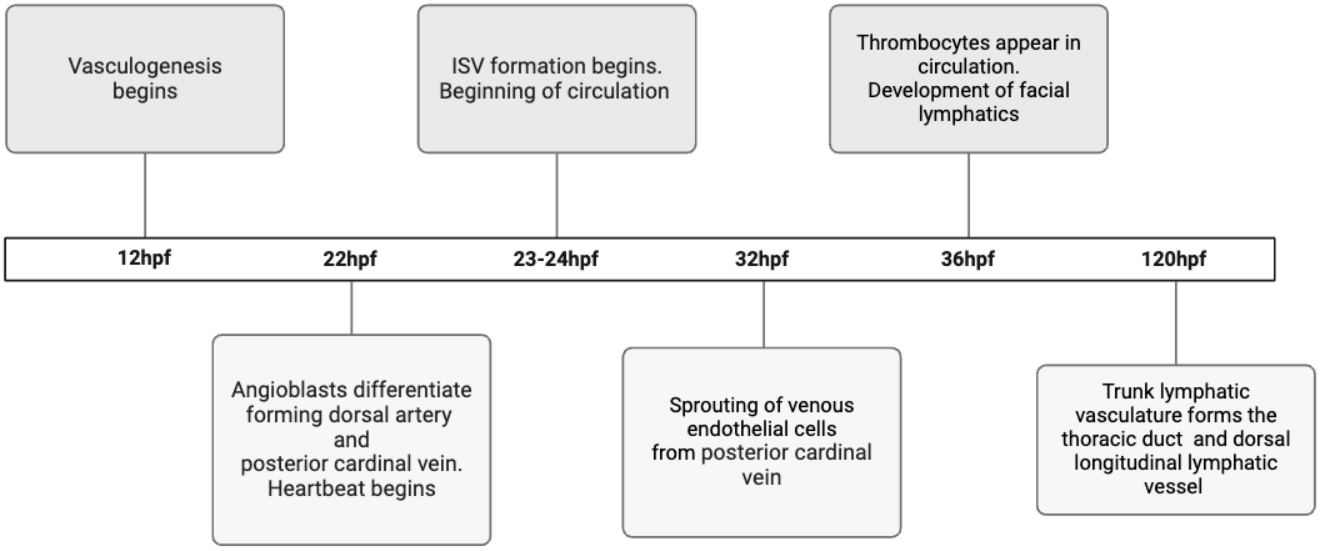

Figure 5.1: Timeline of key vascular and lymphatic developmental stages

Timeline shows key developmental stages of vascular and lymphatic system of zebrafish over 120 hours post fertilisation (hpf).

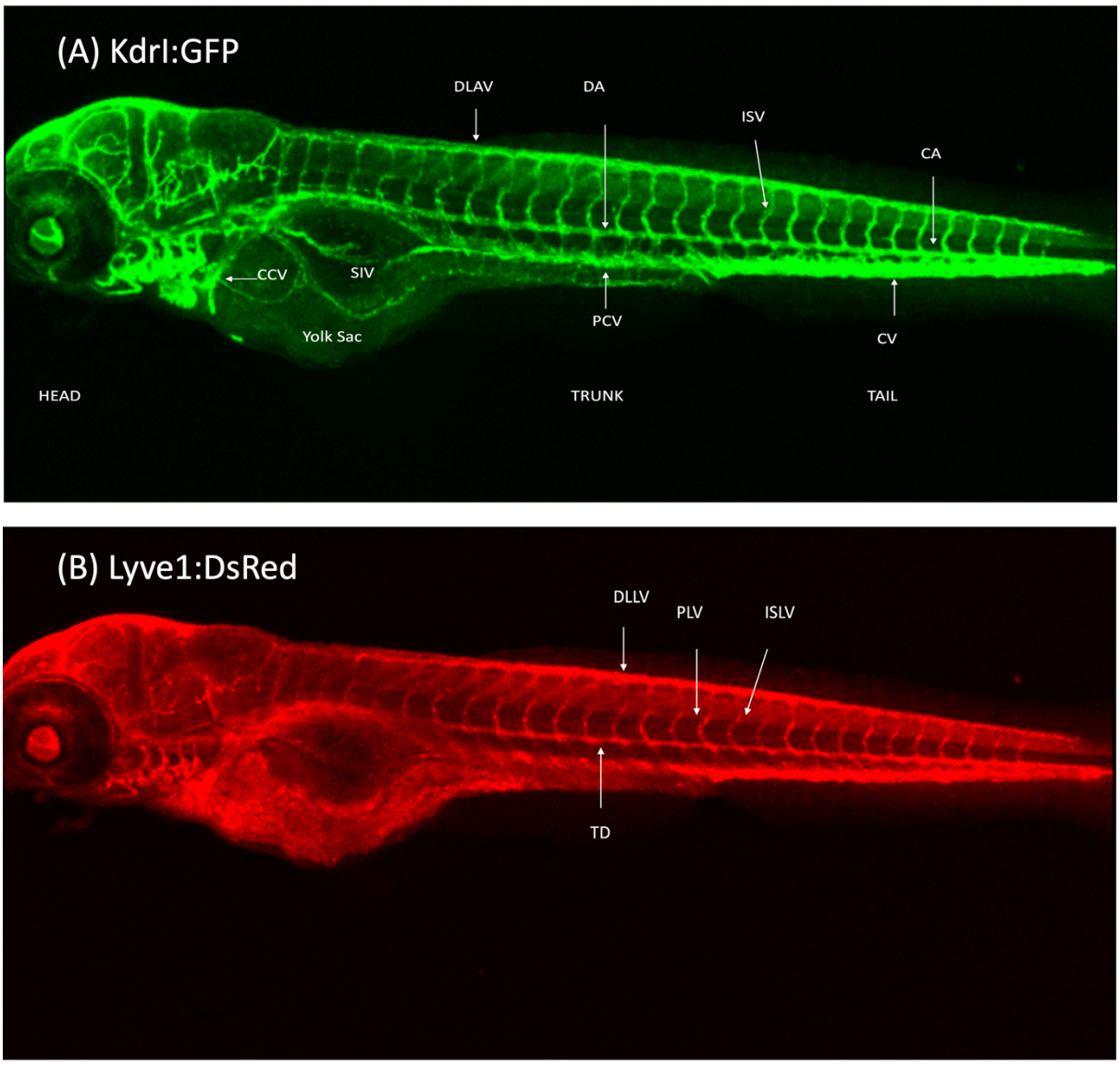

Figure 5.2: The anatomy of the vascular and lymphatic system in zebrafish at 96 hpf

Tg (lyve1: DsRed; kdrl: GFP) embryos were fixed, mounted and imaged using confocal microscopy at 96 hpf. Highlighted in the vascular system (A) are the common cardinal vein (CCV), supraintestinal artery (SIV), dorsal longitudinal anastomotic vessel (DLAV), dorsal artery (DA), posterior cardinal vein (PCV), caudal artery (CA), and caudal vein (CV). The lymphatic system (B) shows dorsal longitudinal lymphatic vessel (DLLV), parachordal lymphatic vessel (PLV), thoracic duct (TD), and the intersegmental lymphatic vessels (ISLV).

5.2 Aims and hypothesis

5.2.1 Aims:

- To characterise the effect of PLCγ2 inhibition by U73122 on the vascular and lymphatic vasculature development in zebrafish embryos.
- To investigate the role PLCγ2 plays in thrombus formation in zebrafish embryos.

5.2.2 Hypothesis:

Pharmacological inhibition of PLCγ2 will inhibit thrombus formation and lead to defects in the development of the lymphatic vasculature in zebrafish embryos.

5.3 Results

5.3.1 PLCγ2 is conserved in human and zebrafish.

In this thesis, the role of PLCγ2 has been investigated using human platelets and a DT40 cell model. Zebrafish has been used in this an *in vivo* model in order to characterise the effect of U73122 on PLCγ2. Therefore, it was first important to confirm that PLCγ2 is conserved across humans and zebrafish.

PLCγ2 protein sequences from (*Homo sapiens*, AAH18646.1) and Zebrafish (*Danio rerio* AAI64582.1) were aligned using Multialin (http://multalin.toulouse.inra.fr/multalin/) and presented with ESPrit 3 (https://espript.ibcp.fr/ESPript/ESPript/). The location of the PLCγ2 domains were determined using Simple Module Architecture Research Tool (SMART).

Using ESPrit 3, it was determined that the mean percentage of identity between the human and zebrafish PLCγ2 is around 57%. Also, while the human PLCγ2 consists of 1265 amino acids, PLCγ2 in zebrafish constitutes of 1240 amino acids.

PH domain

```
                1         10        20        30        40        50        60
human           MSTTVNVDSLAEYEKSQIKRALELGTVMTVFSFRKSTPERRTVQVIMETRQVAWSKTADK
zebrafish       MAGRAHQGDLTEYKKSLIKRDLEMGIVMTVYRQRI...ERLTVQVIMETRQVAWSRTANK
consensus>50    MagrvnvddLaEYeKSlIKRdLE$GiVMTV%rfRistpERlTVQVIMETRQVAWSkTA#K

                          70        80        90       100       110
human           IEGFLDIMEIKEIRPGKNSKDFERAKAVRQKE...DCCFTILYGTQFVLSTLSLAADSKE
zebrafish       TEGVLDIFEIREVRPGKNSKEFDRFKDHKDRNTDPNTCFTIFYGSQFVLNTLSLGADSVE
consensus>50    iEGvLDImEIkE!RPGKNSK#F#RfKdvk#k#tdp#cCFTIlYGsQFVLnTLSLaADSvE

                120       130       140       150       160       170
human           DAVNWLSGLKILHQEAMNASTPTIIESWLRKQIYSVDQTRRNSISLRELKTILPLINFKV
zebrafish       DAEKWLTGLELLRDETLAAHTPEIIESWLRKQMYSVDQTKKNSITMKELKSLLPQMNFKV
consensus>50    DAvnWLsGLeiLh#Ea$nAhTPeIIESWLRKQiYSVDQTkkNSIs$kELKsiLPliNFKV

                180       190       200       210       220       230
human           SSAKFLKDKFVEIGAHKDELSFEQFHLFYKKLMFEQQKSILDEFKKDSSVFILGNTDRPD
zebrafish       PCGRFLKDKFAALGAKKEVLDFEQFHKFYNSLIFDNQKSILDEFKKETCAFILGNGDQP.
consensus>50    pcakFLKDKFveiGAhK#vLdFEQFHlFYnkLiF##QKSILDEFKK#scvFILGNgDqPd

                240       250       260       270       280       290
human           ASAVYLRDFQRFLIHEQQEHWAQDLNKVRERMTKFIDDTMRETAEPFLFVDEFLTYLFSR
zebrafish       ...IQLSDFQRFLLYQQRETWANNLNQVRELMTIFIDDTMRETNDPAFILEEFLSFLFSK
consensus>50    asa!yLrDFQRFLiy#QqEhWA##LNqVRElMTiFIDDTMREtn#Pfliv#EFLs%LFSk
```

TIM (x box) domain

```
                300       310       320       330       340       350
human           ENSIWDEKYDAVDMQDMNNPLSHYWISSSHNTYLTGDQLRSESSPEAYIRCLRMGCRCIE
zebrafish       ENQIWDDKFSEICPLDMNNPLSHYWINSSHNTYLTGDQLRSEPSTEAYVRCLRLGCRCVE
consensus>50    ENqIWD#K%de!dmlDMNNPLSHYWInSSHNTYLTGDQLRSEpSpEAY!RCLR$GCRC!E

                360       370       380       390       400       410
human           LDCWDGPDGKPVIYHGWTRTTKIKFDDVVQAIKDHAFVTSSFPVILSIEEHCSVEQQRHM
zebrafish       LDCWNGPE.EPIIYHGWTRTSKIKFKDVVKAINDHAFATSEYPVVLSIEEHCDVKQQKMM
consensus>50    LDCW#GP#geP!IYHGWTRTsKIKFdDVVqAInDHAFvTSe%PV!LSIEEHCdVeQQkmM

                420       430       440       450       460       470
human           AKAFKEVFGDLLLTKPTEASADQLPSPSQLREKIIIKHKKLGPRGDVDVNMEDKKDEHKQ
zebrafish       AQVFKDVFQDKILMEPLEPEAEQLPSPTQLKGKIIIKHKKLNI..DQTFGRKDLRKGDKQ
consensus>50    AqvFK#VFqDliLmePlEaeA#QLPSPsQLkeKIIIKHKKLnirgDvdvnmeDlkdedKQ
```

nSH2 domain

```
                480       490       500       510       520       530
human           QGELYMWDSIDQKWTRHYCAIADAKLSFSDDIEQTMEEEVPQDIPPTELHFGEKWFHKKV
zebrafish       .GELFIWDPIDERWYRHYCVIENKTLYYAEENDEEEEKSVQSC...TELHQSEPWFHGRM
consensus>50    qGEL%iWDpID#kWyRHYCvIe#akLy%a##i##emEeeVqqdippTELHfgEkWFHgkv

                540       550       560       570       580       590
human           .EKRTSAEKLLQEYCMETGGKDGTFLVRESETFPNDYTLSFWRSGRVQHCRIRSTMEGGT
zebrafish       SEGRMTAERLLQEYCAESGGVDGTFLVRESDTFVNDCTLSFWRSGRVQHCRIRSCLEGGH
consensus>50    sEgRmsAEkLLQEYCmEsGGvDGTFLVRES#TFvNDyTLSFWRSGRVQHCRIRSc$EGGh
```

cSH2 domain

```
                600       610       620       630       640       650
human           LKYYLTDNLTFSSIYALIQHYRETHLRCAEFELRLTDPVPNPNPHESKPWYYDSLSRGEA
zebrafish       TVYFLTENLHFPSVYALIYYYRDNLLRCQDFNLRLTEYVPKPDTHQLEGWFYSNLSRGEA
consensus>50    lvY%LT#NLhFpS!YALIyyYR#nlLRCq#F#LRLT#yVPnP#pH#legW%YdnLSRGEA

                R665W                                                S707Y
                660       670       680       690       700       710
human           EDMLMRIPRDGAFLIRKREGSDSYAITFRARGKVKHCRINRDGRHFVLGTSAYFESLVEL
zebrafish       EDYLMRIPRDGAFLIRQREDSDSYAITFRGEGLVKHCRIHKDGSMYILGTSSEFDSLVEL
consensus>50    EDmLMRIPRDGAFLIRqREdSDSYAITFRaeGlVKHCRInkDGrm%!LGTSayF#SLVEL
```

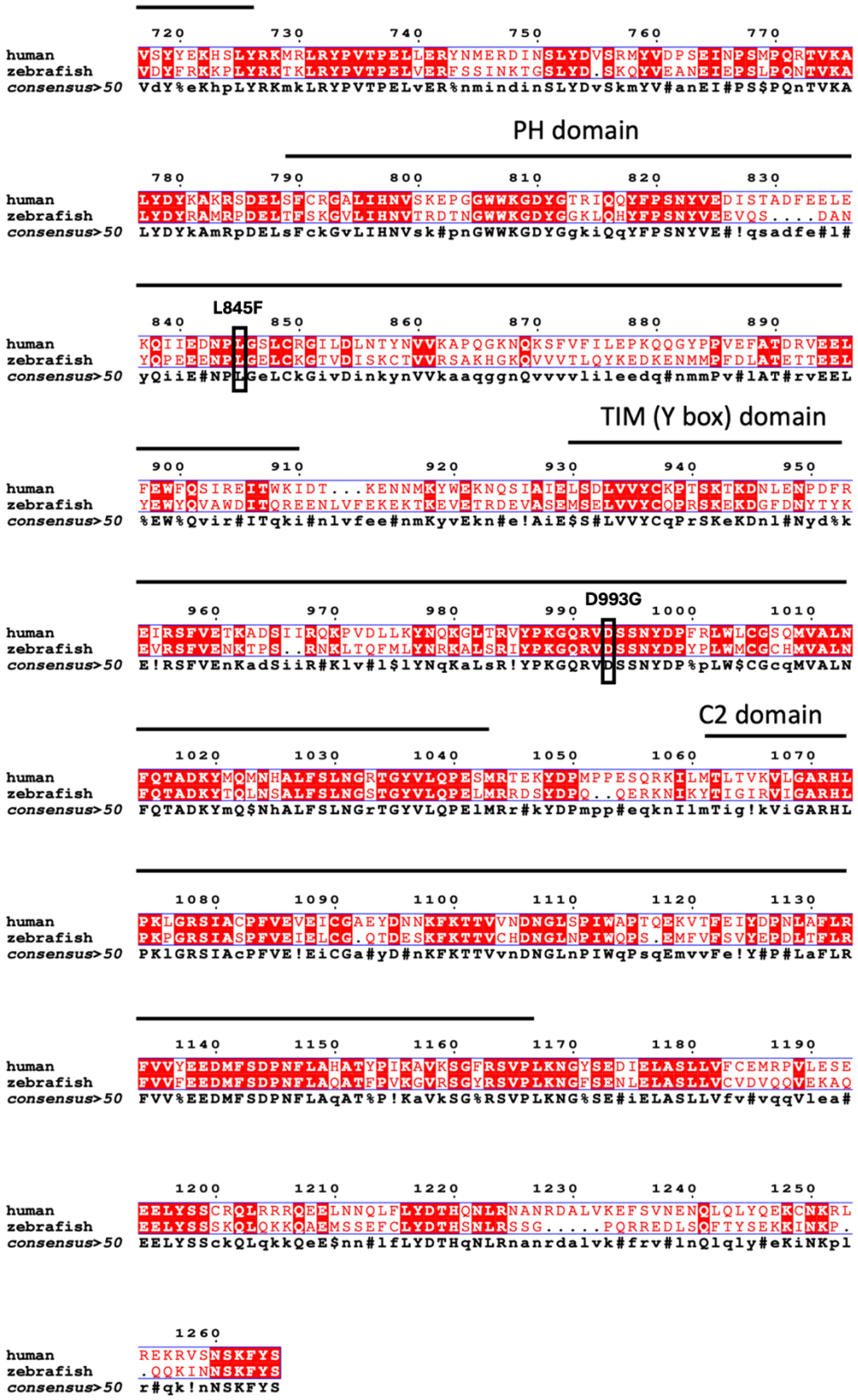

Figure 5.3: PLCγ2 protein is conserved between humans and zebrafish.

PLCγ2 sequences from humans (Homo sapiens, AAH18646.1) and zebrafish (Danio rerio AAI64582.1) were aligned using multialin and displayed using ESPrit3. Highlighted in red are conserved amino acids across species. Black lines highlight PLCγ2 domains.

5.3.2 The PLCγ2 inhibitor, U73122, is lethal to zebrafish embryos.

Zebrafish has also gained popularity as a valuable model for toxicity screening due to its transparent nature, ease of maintenance, fecundity, and due to their cost-effectiveness and ability to quickly evaluate the toxicity of different substances (Kimmel et al., 1995, Chahardehi et al., 2020).

In previous chapters, the effect of the PLCγ2 inhibitor U73122 was investigated and characterised using human platelets and DT40 cells. However, there is a lack of evidence in the literature on the effect of U73122 on zebrafish embryos. Therefore, to be able to test the effect of PLCγ2 inhibition on zebrafish development and thrombus formation, it was firstly important to characterise its effect and toxicity on zebrafish embryos and their development. Due to the fact that U73343 has no effect on PLC's but, also like U73122 it inhibits cPLA2 activation, it was used a negative control (Heemskerk et al., 1997). Also, since the effect of ibrutinib on vascular development has been established in zebrafish, it was used as a positive control.

Zebrafish embryos were either incubated with DMSO (0.1%(v/v) (vehicle control), U73122 (figure 5.4 A), U73343 (figure 5.4 B), or ibrutinib (figure 5.4 C) at 6 hpf for 72 hours. Media containing the compounds was changed and survival was observed every 24 hours. In vehicle control fish, it was observed that 90% of fish survived up to 72 hours post-treatment, where only 10% died during the 24 hours-post treatment period. This is normal as the 10% mortality threshold is accepted in zebrafish toxicology assays according to OECD Guidelines for the Testing of Chemicals. Similar results were observed when treating the fish with 0.01μM of U73122. When treated with 0.1μM U73122, 75% of fish survived up to 72 hours post treatment.

Surprisingly, figure 5.4 A shows that treating the embryos with 1μM and over of U73122, resulted in 100% lethality at 24 hours post treatment.

On the other hand, when fish were treated with U73343 (U73122 analogue), most fish survived up to 72 hours post treatment. Even when treated with high concentrations (10μM and 20μM), the survival rate was around 90%.
In zebrafish embryos treated with 1μM and 3μM ibrutinib, 90%-95% of fish survived up to 72 hours post treatment, respectively. This is consistent previous data in the literature where fish treated with 1μM survived up to 144 hpf 6 dpf (Wang et al., 2020). When the survival rate was observed in zebrafish treated with 10μM ibrutinib however, 95% of fish survived the first 24 hours of treatment (hpt) but 10μM was lethal to all fish between 24 hpt and 48 hpt. Also, 20μM of ibrutinib was lethal to all fish by 24 hpt. These results demonstrate that U73122 can be toxic and lethal to zebrafish embryos even at low concentrations.

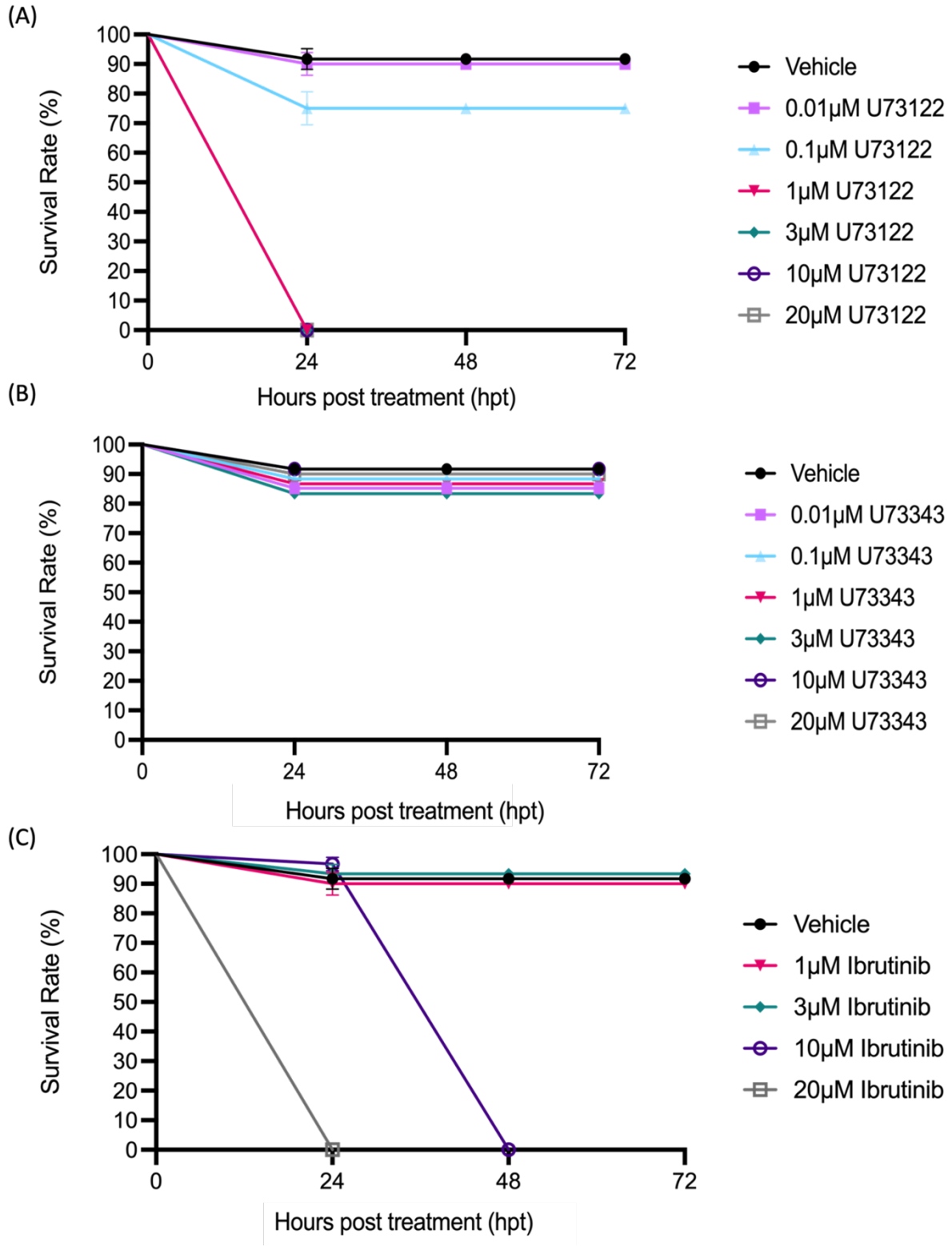

Figure 5.4: U73122 is lethal to zebrafish embryos.

20 zebrafish embryos were treated with (A) U73122, (B) U73343, (C) ibrutinib, or DMSO for vehicle control for 72 hours. Drugs were changed and survival was observed every 24 hours. Survival percentage was generated using Kaplan-Meier plot (n=3).

5.3.3 U73122 has no significant effect on the development of the vascular and lymphatic systems in zebrafish.

Given its possible role in angiogenesis and vascular maintenance, the function of PLCγ2 in the maturation of vasculature has been previously investigated in mice (Ichise et al., 2009b). Using genetic approaches and mouse models, Ichise et al., have demonstrated the critical role PLCγ2 plays in initiating and maintaining the separation of blood and lymphatic vasculature.

In this study, using U73122, the effect of inhibiting PLCγ2 on the development of the vascular and lymphatic system was investigated in zebrafish embryos.

A transgenic zebrafish reporter line, which expresses lyve1: DsRed, a marker for the lymphatic vessels, and kdrl:GFP, a marker for the blood vessels were treated with vehicle control (0.1% DMSO(v/v), U73122 (0.01μM, 0.1μM), U73343 (1μM, 3μM, 10μM),or ibrutinib (1μM, 3μM, 10μM) for 96 hours. Zebrafish embryos were then fixed, mounted, and imaged using confocal microscopy.

Figure 5.5 showed that when treated with 0.01μM or 0.1μM of U73122, there were no visible abnormalities of deformities in the development of the blood vasculature in the zebrafish head and trunk. Additionally, when compared to vehicle control-treated fish, there was no significant effect on the length (figure 5.6 A) or the number of the intersegmental vessels (ISV) (figure 5.6 B). Similar results were also observed when embryos were treated with U73343 and ibrutinib.

The effect of U73122 was also tested on the lymphatic development in zebrafish. However, similar to the development of the blood vasculature, no visible effects were observed (figure 5.5). When quantified, the number and length of the intersegmental lymphatic vessels (ISL) were also similar to vehicle control fish (figure 5.7).

In conclusion, these results demonstrate that the inhibition of PLCγ2 using U73122 has no significant effect on the vascular or lymphatic development in the surviving zebrafish embryos at 96 hpf.

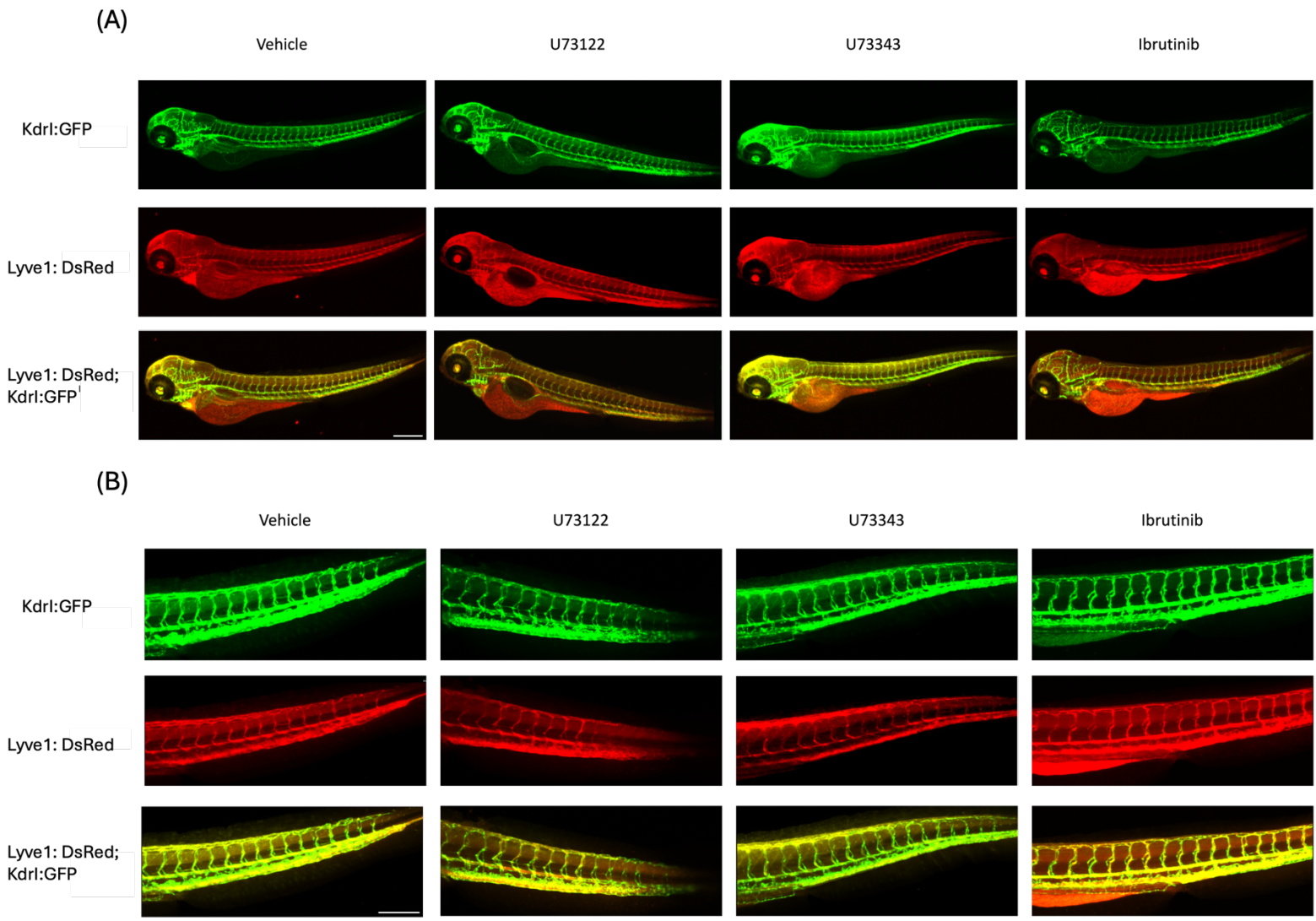

Figure 5.5: Figure: U73122 has no effect on the development of the vascular and lymphatic systems in zebrafish.

Zebrafish embryos were treated with U73122 (0.01μM, 0.1μM), U73343 (1μM, 3μM, 10μM) or ibrutinib (1μM, 3μM, 10μM) or DMSO (0.1(v/v)) for vehicle control at 6 hpf. Embryos were then fixed, mounted in low melting temperature agarose, and imaged using confocal microscopy at 96 hpf. Whole fish (A) were imaged using 4x lens and trunks (B) were imaged using 10x lens. Scale bar:50μm.

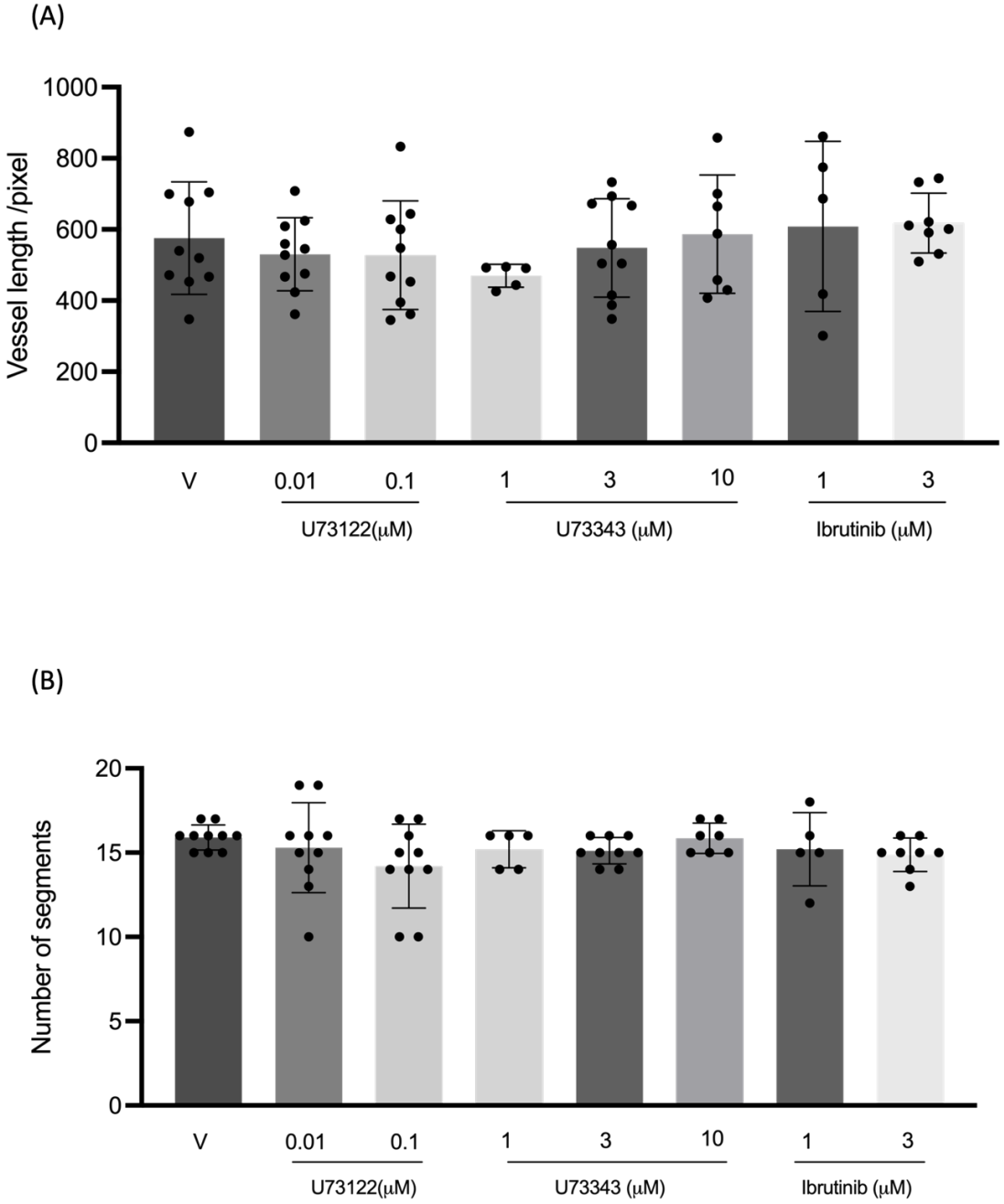

Figure 5.6: U73122 has no significant effect on the length or number of intersegmental vessels in zebrafish embryos.

Zebrafish embryos were treated with DMSO (V) (0.1%(v/v)), U73122 (0.01μM, 0.1μM), U73343 (1μM, 3μM, 10μM), or ibrutinib (1μM, 3μM) 6 hours post fertilization. Embryos were then fixed, mounted, and imaged using confocal microscopy 96 hours post fertilization. Each point represents an individual fish over multiple experiment. (A) The intersegmental vessel length was measure and analyzed using Image J.(B) The number of intersegmental vessels was counted manually. Statistical significance was determined using one-way ANOVA with Dunnett's post-test. Graph shows mean ± SD. n values range from 5 to10.

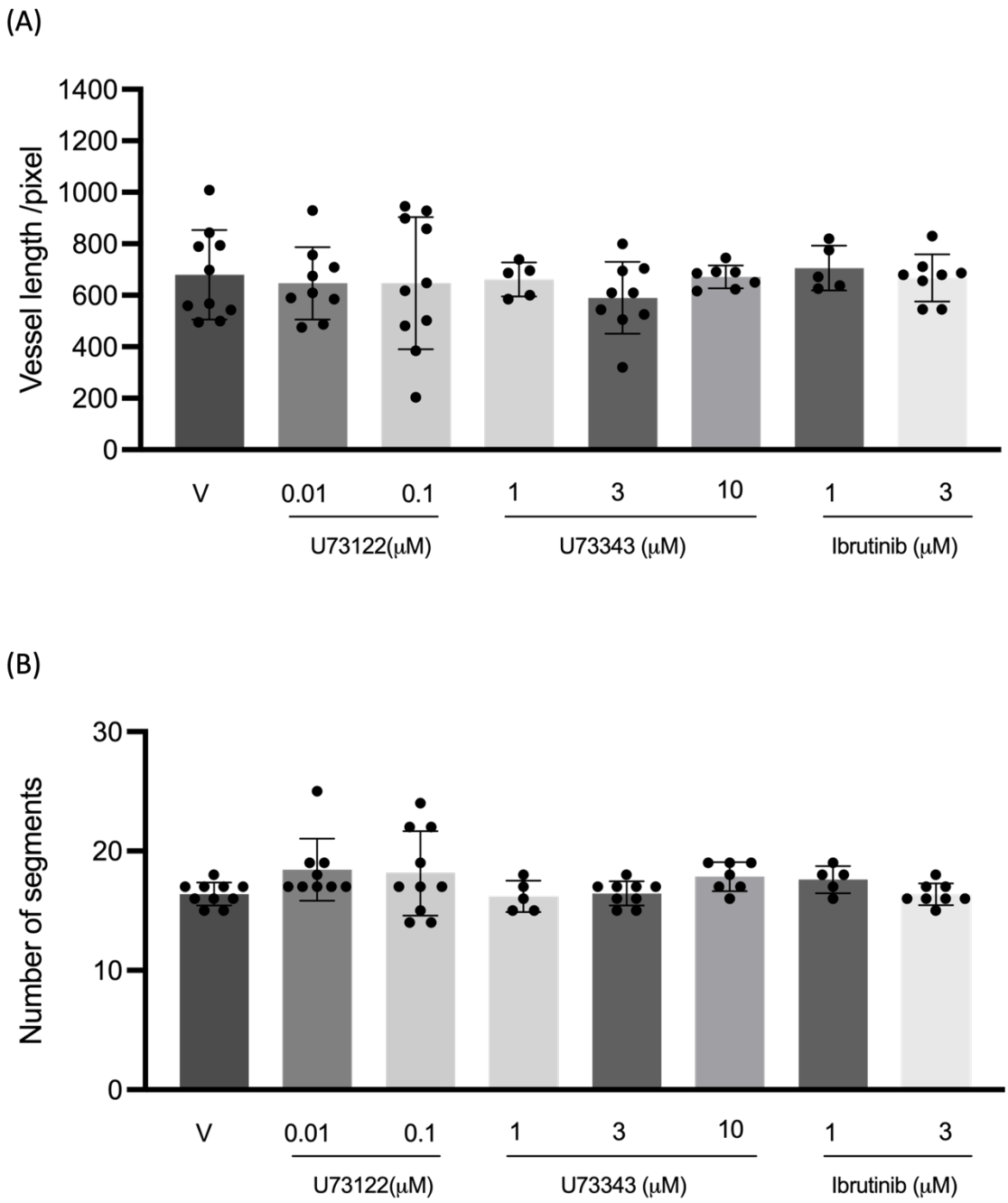

Figure 5.7: U73122 has no significant effect on the length or number of intersegmental lymphatic vessels in zebrafish embryos.

Zebrafish embryos were treated with DMSO (V) (0.1%(v/v)), U73122 (0.01μM, 0.1μM), U73343 (1μM, 3μM, 10μM), or ibrutinib (1μM, 3μM) 6 hours post fertilization. Embryos were then fixed, mounted, and imaged using confocal microscopy 96hours post fertilization. Each point represents an individual fish over multiple experiment. (A) The intersegmental vessel length was measure and analyzed using Image J. (B) The number of intersegmental lymphatic vessels was counted manually. Statistical significance was determined using one-way ANOVA with Dunnett's post-test. Graph shows mean ± SD. n values range from 5 to10.

5.3.4 The inhibition of PLCγ2 leads to extended time to occlusion and lack of thrombus formation.

The role of PLCγ2 in platelet activation and thrombus formation has been investigated in previous studies using mouse models. Using PLCγ2 deficient mice, Mangin et al., have demonstrated that the absence of PLCγ2 leads to a prolonged bleeding time (Mangin et al., 2003). When using laser injury in PLCγ2 deficient mice, Nonne et al., demonstrated lack of thrombus formation in mesenteric arterioles *in vivo* (Nonne et al., 2005). Although zebrafish has been previously used as a model for laser injury, there was no evidence in the literature exploring the role PLCγ2 plays in thrombus formation in zebrafish.

At 4 days post fertilisation, zebrafish embryos were incubated with DMSO vehicle control (0.1% (v/v)), U73122 (0.01μM, 0.1μM), U73343 (1μM, 3μM, 10μM), or ibrutinib (1μM, 3μM, 10μM) for 2 hours. Zebrafish larvae were anesthetized in MS-222 and mounted on glass bottom dish in low melting temperature agarose. Laser ablation was induced by 4 pulses to the caudal artery directly above the cloaca and time to occlusion was observed for 5 minutes.

The average time to occlusion observed in control fish was 134 seconds. When compared to vehicle control larvae, treating the fish with 0.01μM and 0.1μM of U73122 led to a significantly extended time to occlusion. In the majority of the fish treated with 0.01μM and 0.1μM U73122, there was no occlusion observed at the 5 minutes cut-off. However, occlusion was observed in some of the U73122 treated fish. The average time to occlusion in fish treated with 0.01μM and 0.1μM U73122 was 216 seconds and 266 seconds respectively, a significant increase of 61.19 % and 98.51% respectively. When fish were treated with 10μM of the analogue

(U73343), occlusion time was similar to that in control fish (160 seconds) at the 5 minutes cut-off (figure 5.8A).

When treated with 1μM ibrutinib, time to occlusion was similar to that in control fish, however there was no occlusion observed in fish treated with 3μM and 10μM ibrutinib at the 5-minute cut-off. On another note, it should be noted that in some fish multiple thrombocytes adhere to injury site. However, the thrombus formed is not stable enough and ends up embolised hence no occlusion (figure 5.7 C, ibrutinib). The thrombus size was also quantified using ImageJ (figure 5.7B). Surprisingly, fish treated with 0.01μM of U73122 had a significantly larger thrombus in comparison to control fish.

All together, these results demonstrate that the inhibition of PLCγ2 results in inhibition of thrombus formation in zebrafish.

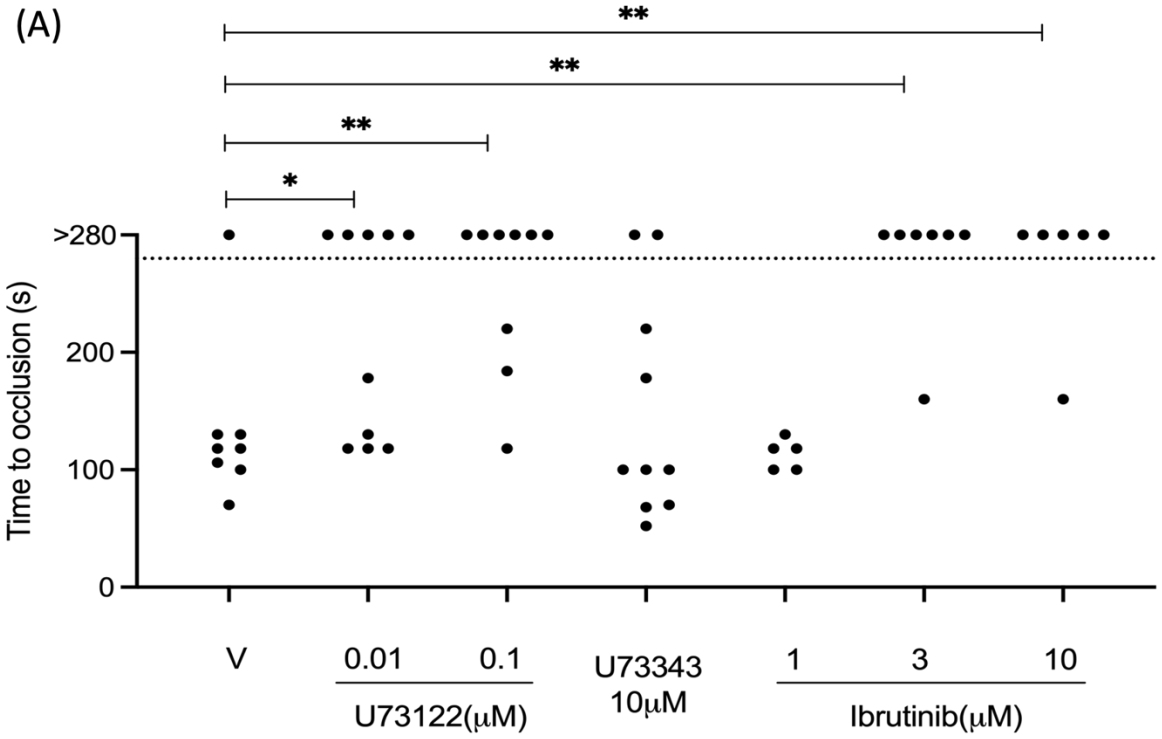
(A)
**
**
**
*
>280
200
100
0
Time to occlusion (s)
V
0.01
0.1
U73122(μM)
U73343
10μM
1
3
10
Ibrutinib(μM)

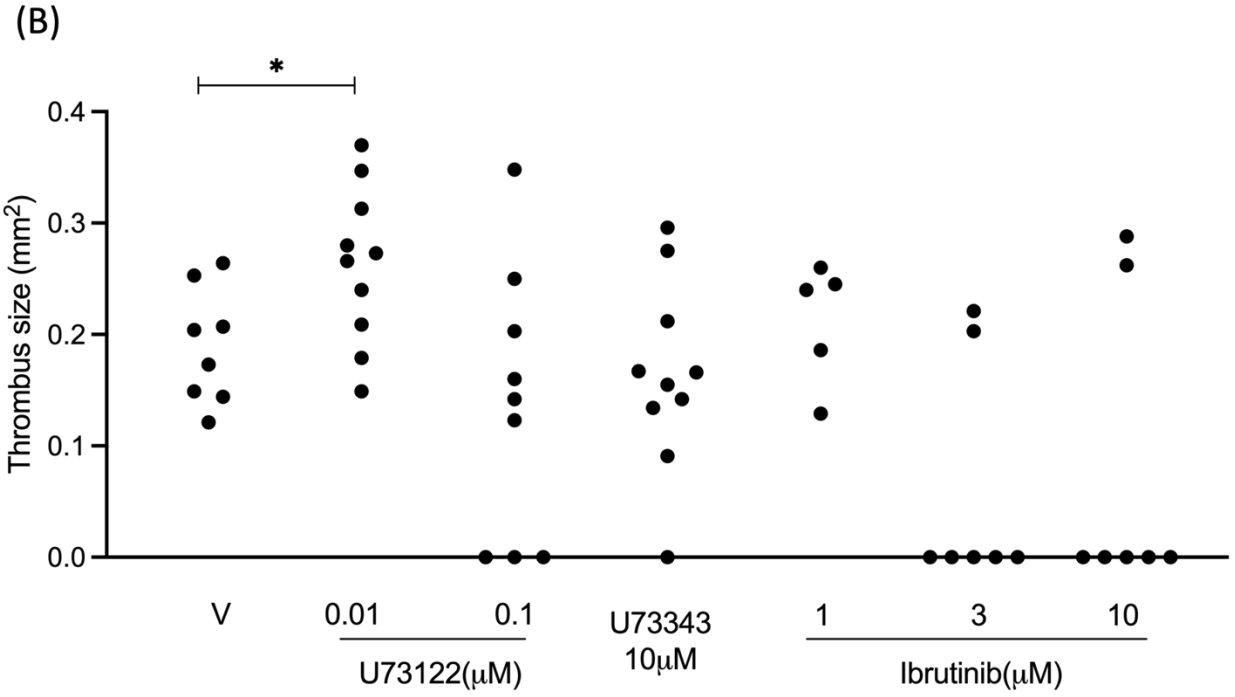
(B)
*
0.4
0.3
0.2
0.1
0.0
Thrombus size (mm2)
V
0.01
0.1
U73122(μM)
U73343
10μM
1
3
10
Ibrutinib(μM)

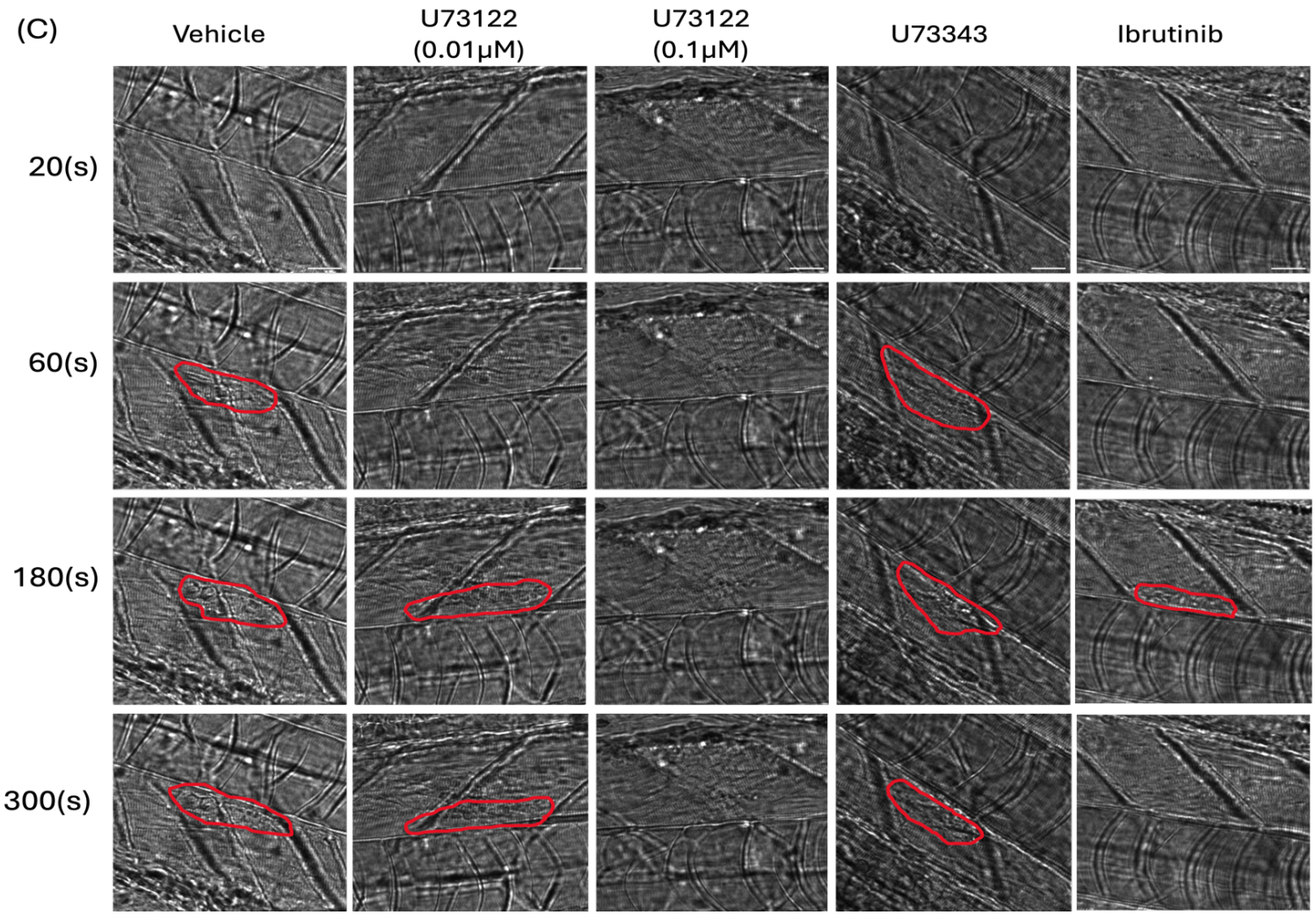

Figure 5.8: U73122 significantly reduces the time to occlusion upon laser injury in zebrafish.

At 96 hpf, zebrafish embryos were treated with DMSO (0.1%(v/v)), U73122 (0.01μM, 0.1μM), U73343 (1μM, 3μM, 10μM), or ibrutinib (1μM, 3μM, 10μM) for 2 hours prior to laser-induced injury and time to occlusion was observed. (A) Time to occlusion was observed upon laser injury in the dorsal aorta. A 300 second cut off is used to determine no occlusion. (B) Size of occlusion as measure using ImageJ. (C) Time lapse images of larvae before and after laser induced injury. n values range from 5 to 10.

5.4 Discussion

The genetic and functional similarities between zebrafish and humans in relation to haemostatic factors and platelet function have made zebrafish a good model for studying thrombosis. Zebrafish thrombosis models have also been successfully developed by researchers to evaluate antithrombotic medications and explore the impact of different substances on thrombosis (Zhu et al., 2016). In addition, zebrafish have become an important model for investigating vascular and lymphatic development. The presence of a lymphatic vascular system and their transparency enables easy visualisation (Jung et al., 2017, Jung et al., 2016)
In this study, the zebrafish was used as an *in vivo* model to investigate the role of PLCγ2 in thrombus formation and lymphatic vascular development.

Previous studies using mouse models have established that the lack of PLCγ2 leads to lack of separation of blood and lymphatic vessels (Ichise et al., 2009b). And since zebrafish embryos were treated with a variety of drugs before vasculogenesis begins a 12 hpf, it was expected for U73122 to have an effect on the development of the vasculature. However, when zebrafish embryos were treated with 0.01μM and 0.1μM of the U73122, there were no significant malformations observed in the lymphatic or vascular system. It's worth noting however that this was only in the surviving fish as most of fish did not survive. Indeed, when examining the toxicity effect of the drugs, U73122 seemed to be toxic to zebrafish embryos where 1μM, 3μM, and 10μM were lethal to zebrafish embryos just 24 hours post treatment. This could be due to the fact that the inhibition of PLCγ2 perturbs the lymphatic/vascular development of zebrafish and hence lethal to zebrafish embryos (Ichise et al., 2016).

In a study by Manne et al., mice either deficient in Btk or Tec had normal separation in their blood and lymphatic vessels. But when introducing a Btk/Tec double knockout, mice displayed blood-filled lymphatics (Manne et al., 2015). And when the role of ibrutinib was examined on the vascular development, the results have shown a significant decrease on the number of normal ISVs forming. However, when this mechanism was further examined, the authors have found that the malformations caused by ibrutinib is not by the direct inhibition of Btk. But due to its established effect on the lymphatic and vascular development, ibrutinib was used as a positive control in this study (Wang et al., 2020).

Similar results were seen when embryos were treated with ibrutinib. 1μM and 3μM ibrutinib seem to have no significant effect on the development of the vasculature or lymphatic system in zebrafish embryos. However, 10μM of ibrutinib was lethal to zebrafish embryos around 48 hours post treatment. This could indicate that ibrutinib disturbs the vascular and lymphatic development in zebrafish. This is supported by evidence in the literature where 5μM and 10μM ibrutinib led to malformation of the vasculature and a decrease in the number of normal ISVs observed (Wang et al., 2020).

Moreover, U73122 and ibrutinib showed no significant effect on the lymphatic development in zebrafish embryos up to 96 hpf. This could be explained by the fact that the full lymphatic development and establishment in zebrafish takes place at later stages that the vasculature development (Figure 5.1). Therefore, potential future work could either expose the zebrafish to treatments for longer time period of times or treat the fish with the drug at a later stage.

The PLCγ2 inhibitor U73122 was used and characterised in previous chapters. When tested on human platelets, 3μM and 10μM of U73122 led to a significant

decrease in platelet aggregation in comparison to untreated platelets. In addition, previous evidence in the literature has shown that PLCγ2 deficient mice have prolonged bleeding time (Mangin et al., 2003) and impaired thrombus formation upon laser injury (Nonne et al., 2005). Therefore, it was hypothesised that zebrafish embryos treated with U73122 would have prolonged occlusion time and reduced thrombus formation.

Results from this chapter align with previous evidence in the literature where PLCγ2 deficient mice have a defective and delayed thrombus formation (Nonne et al., 2005). In 50% and 77% of embryos treated with as low concentrations as 0.01μM and 0.1μM of U73122 respectively, there was a significant decrease in the time to occlusion at the 5-minute cut off. However, larger thrombi were observed when zebrafish were treated with 0.01μM U73122.

Where several thrombocytes adhered to the site of injury however, the thrombus was not stable enough to lead to occlusion. Although U73122 could impair the ability of thrombocytes to form a stable thrombus, coagulation factors such fibrin or red blood cells can get caught in thrombus. This could lead to the formation of larger but less stable thrombus.

This shows that the inhibition of PLCγ2 even by low concentrations of U73122 has a significant effect on thrombus formation in zebrafish.

In conclusion, results from this chapter demonstrate the central role PLCγ2 plays in thrombus formation in zebrafish. Also, although low concentration of U73122 showed no significant effect on the vasculature lymphatic development in zebrafish, the death of zebrafish embryos when treated with higher U73122 concentrations could be related to disruptions in the development of zebrafish embryos.

Chapter 6: General discussion

6.1 Summary of results

This study investigates the structure/function relationship of PLCγ2 downstream of GPVI and CLEC-2. This was established by using the PLC inhibitor U73122 *in vivo* and *in vitro* along with PLCγ2 ibrutinib-resistant mutations in cell line models.

Firstly, the role PLCγ2 plays downstream of hem(ITAM) receptors was studied using U73122 in several platelet function assays. This allowed the characterisation of U73122 downstream of CLEC-2 for the first time. The effect of U73122 was initially screened using PBA as it allows the use of several agonist and inhibitor concentrations. Using PBA also allows the selection of appropriate agonist concentration to use in other platelet function assays. The effect of U73122 on inhibiting platelet aggregation and platelet adhesion was more significant downstream of GPVI. Whereas U73122 significantly decreased the calcium flux and platelet spreading in a similar manner downstream both GPVI and CLEC-2

Secondly, this study further investigates the structure/function relationship of PLCγ2 using the ibrutinib-resistant gain of function PLCγ2 mutations and U73122. This was achieved by using an overexpression system and an NFAT-luciferase assay. PLCγ2 knockout cells were transiently transfected with plasmids containing the PLCγ2 mutations and the luciferase activity was examined. The results showed that in comparison to cells transfected with WT hPLCγ2, cells with the mutations showed a significant increase in the GPVI and CLEC-2 mediated signalling. However, U73122 significantly decreases the signalling downstream of both GPVI and CLEC-

2. In collagen stimulated cells bearing the R665W and S707Y mutation, U73122 significantly decreased the signalling at 3μM and 10μM, whereas in cells bearing L845F and D993G only 10μM of U73122 have a significant effect on decreasing the luciferase activity downstream of GPVI. In contrast, in cells with the S707Y and D993G mutation, U73122 was able to decrease the luciferase activity significantly at 3 and 10μM. Also, U73122 significantly decreased the luciferase activity of cells bearing R665W and L845F and only 10μM downstream of CLEC-2. This highlighted the potential difference in the role of PLCγ2 domains downstream of GPVI and CLEC-2.

The overexpression system is considered to be qualitative due to the expression level of the protein of interest not being similar to the physiological level of protein expression. Therefore, the CRISPR/Cas9 approach was used in parallel with the overexpression system to generate PLCγ2 mutation knock ins in WT DT40. Using this approach, we were able to introduce the R665W mutation in the SH2 domain in WT DT40 cells.

On the other hand, using the CRISPR/Cas9 approach led to the introduction of an intended mutation upstream of R665W. Additionally, attempts to knock-in other mutation such as S707Y, L845F, and D993G were unsuccessful. Consequently, no further work was done using this mutant cell line.

Finally, the role of PLCγ2 plays in thrombus formation and the lymphatic vascular development was examined *in vivo* using zebrafish as a model. U73122's toxicity was firstly assessed in zebrafish embryos, and the results show that concentration including and above 1μM are lethal to zebrafish embryos at 24 hours post treatment.

Consequently, lower concentrations (0.01μM and 0.1μM) were used. The role PLCγ2 plays in blood and lymphatic vasculature development was examined in Tg (lyve1: DsRed; kdrl:GFP) zebrafish using U73122. It was surprising to see that U73122 had no significant effect on the number and length of intersegmental vessels in zebrafish at 96 hours post fertilization. But this could be explained by the fact that the survival rate in treated zebrafish embryos was low, which is possibly a result of defects and malformations in the blood and lymphatic vasculature.

6.2 Future directions for PLCγ2 structure/function: the role of key tyrosines

As previously described, PLCγ2 has 4 key tyrosine phosphorylation sites: Y753, Y759, Y1197, and Y1217 (Watanabe et al., 2001). Y753 and Y759 are located between the SH2 and the SH3 domain, while Y1197 and Y1217 are in the C terminal domain (figure 6.1).

In a study by Kim et al, it was suggested that Y753 and Y759 are the primary locations of phosphorylation in both platelets and T-cells, but in B-cells, Y753, Y759 and Y1217 were all phosphorylated following receptor activation. Furthermore, in stimulated B-cells, Y1217 was phosphorylated at three times higher levels compared to Y753 and Y759. In all three cell types, Y1197 did not appear to be significantly phosphorylated. The authors also linked lipase activity to these phosphorylations, concluding therefore that lipase activity was correlated with pY753 and pY759 (Kim et al., 2004). This suggests that Y1217 does not contribute to the lipase activity of PLCγ2.

This is interesting because a number of studies in platelets have measured pY753, pY759 and pY1217 in both GPVI and CLEC-2 activated platelets in a somewhat routine manner, although direct measures of lipase activity are not routine. In a pair of studies by Nicholson et al., pY1217 is shown following either GPVI or CLEC-2 activation, which disagrees with May et al., (Nicolson et al., 2018, Nicolson et al., 2021). They do however, show residual phosphorylation of Y1217 following ibrutinib treatment downstream of GPVI, which suggests that this residue is indeed dispensable for lipase activity, somewhat agreeing with May et al.,.

In a different study by Watanabe et al., the authors suggested, using *in vitro* kinase assays that all four tyrosine residues in rat PLCγ2 (which are also conserved in humans) are phosphorylation sites that are phosphorylated by Btk and are critical for BCR signalling. A number of mutant PLCγ2 constructs were used to measure signalling in PLCγ2 deficient DT40 cells, with tyrosine replaced with phenylalanine (Y753F, Y759F, Y1197F, and Y1217F) (Watanabe et al., 2001). Although the exact mechanism underlying the function of these tyrosine residues remains unclear, this study showed the role of Btk in phosphorylating the four residues.
When assessing how the activation of PLCγ2 was influenced by mutating each tyrosine residue individually, the maximal calcium mobilisation levels were 55%, 66%, 32%, or 30% for the single mutants Y753F, Y759F, Y1197F, and Y1217F, respectively when compared to the cells expressing the WT PLCγ2. Moreover, 45 % of the calcium mobilisation was observed when mutating two tyrosine residues at the same time (Y753F/Y759F). On the other hand, the substitution mutations in all the tyrosine residues led to a decrease in IP_3 production and calcium mobilization downstream of BCR where mutations in all four sites together had only 16% of the

calcium mobilization. This emphasises that all four of tyrosine residues are essential to mediate PLCγ2 activation and function in B cells. The tyrosine residues might also impact several aspects of PLCγ2's activation and function including conformational changes, improved recognition of the PIP2 substrate, and change of protein-protein interactions. Consequently, the relative orientation of domains, such as the SH2 or PH domains, may impact PLCγ2's interaction with membrane lipids or other signalling proteins.

Interestingly in platelets, Nicolson et al., found that Btk kinase function is required for CLEC-2 signalling, agreeing with Watanabe et al., but for GPVI signalling, Btk kinase function was not required. This suggests heterogeneity in how PLCγ2 lipase function is regulated, and that this is not only cell-type dependent, but receptor-dependent.

Mutating the PLCγ2 tyrosine residues could also be as used to examine the exact mechanism and significance of these tyrosine residues on the structure and function of PLCγ2 downstream of GPVI and CLEC-2. The overexpression system or the CRISPR/Cas9 approach could be used to mutate these key residues, while the NFAT luciferase assay could be used to measure the signalling when stimulated by collagen or rhodocytin. There are two known phosphorylation sites near one of the gains of function mutation S707Y, Y753 and Y759. Zhou et al., assumed that the substitution of serine to tyrosine at 707 may potentially generate a new PLCγ2 phosphorylation site (Zhou et al., 2012b). Hence, it would be interesting to see the effect of the ibrutinib-resistant PLCγ2 mutations on these tyrosine residues and consequently PLCγ2 activation and phosphorylation (Zhou et al., 2012b).

An additional option would be to investigate the real-time phosphorylation kinetics at each tyrosine residue by other methods like surface plasmon resonance (SPR) or Förster Resonance Energy Transfer (FRET).

Studies investigating these tyrosine residues have mainly used cell models and mouse models. Moreover, since these tyrosine residues are conserved in human and zebrafish, zebrafish could be used as a model where knock in mutations in the tyrosine residues could be introduced using CRISPR/Cas9.

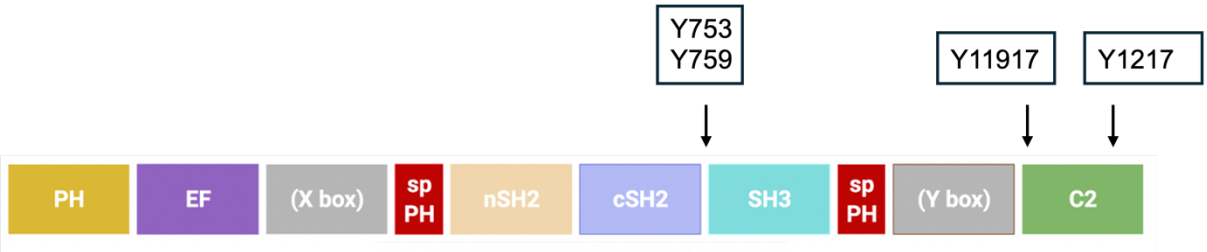

Figure 6.1: PLCγ2 domains and tyrosine residues.

PLCγ2 tyrosine residues, Y753 and Y759, are located between the SH2 and the SH3 domain. Y1197 and Y1217 are located in the C terminal domain

Due to the multiplicity of functional domains, the structure of PLCγ2 allows it to play a key role in signal transduction pathways induced by GPVI and CLEC-2, among others. Upon stimulation, PLCγ2's SH2 domains bind to adaptor proteins phosphorylated on tyrosine residues, while its PH domain binds to PIP2, which is playing a critical role in its recruitment, activation and function. This structure/function relationship enables PLCγ2 to play an important role in platelet activation, thrombus formation, and immune responses, consequently contributing to both hemostasis and pathologies so as rheumatoid arthritis and B-cell malignancies. This study focused on understanding these mechanisms which may help developing potential therapeutic targets of platelet function and immune regulation in diseases.

Although the effect of the gain-of function mutations was examined using an overexpression system, using CRISPR-Cas9 gene editing approach provides an advantage overexpression system because the expression level of the protein of interest may not be similar to the physiological level of protein expression (Ran et al., 2013). In comparison to the protein levels produced in the cells naturally, the levels of the protein produced in an overexpression are higher. Consequently, previous studies have shown that the overexpression might disrupt cellular pathways and interactions resulting in interactions that might not be representative of the typical processes in the natural cell. It is also possible to misinterpret the results if phenotypic changes caused by overexpressing a protein do not correspond to the protein's typical function (Prelich, 2012).

Therefore, the CRISPR/Cas9 approach can be used to further study the role of the PLCγ2 domains by introducing the domain-altering PLCγ2 mutations in other cell lines. Although DT40 cells have the essential signalling components necessary for platelet (hem)ITAM receptor signalling, they do not express GPVI and CLEC-2 endogenously. In contrast to LAT, which is involved in the GPVI signalling pathway, the adaptor protein B cell-linker molecule (BLNK) mediates the development of a signalosome, and Syk and Lyn can phosphorylate Btk (Rawlings et al., 1996, Park et al., 1996).

As an alternative, induced pluripotent stem (IPS) cells could be chosen using this approach. Fend et al., have previously established that IPS cells have the potential to differentiate into platelets,(Feng et al., 2014) . In addition, CRISPR/Cas9 could be

employed to introduce the PLCγ2 knock-ins to further study the PLCγ2 domains needed for signalling.

The CRISPR/Cas9 approach could also be used in zebrafish to either generate PLCγ2 knockouts, or to try and knock in the gain of function PLCγ2 mutations to further investigate the effect of disrupting the PLCγ2 domain on thrombus formation or zebrafish vascular and lymphatic development. Moreover, mRNA for wild type human PLCγ2 may be introduced into zebrafish at the one-cell stage. This technique allows for the expression of human proteins in zebrafish to assess their functionality. This technique was used by Lim et al., where they established and validated a zebrafish model for Bernard-Soulier syndrome (BSS), a rare inherited bleeding disorder, using a specific GP9 mutations (gp9SMU15) created by the CRISPR/Cas9 approach (Lin et al., 2022).

6.3 Conclusion

In conclusion, this thesis identifies the key role PLCγ2 plays in platelet function downstream of both GPVI and CLEC-2. The inhibition of PLCγ2 using the PLC inhibitor, U73122, significantly decreases platelet function. This highlights the potential of PLCγ2 as a therapeutic target for drug development and could be a promising strategy for regulating platelet activity in cardiovascular diseases.

Using an overexpression to investigate the effect of PLCγ2 mutations associated with ibrutinib resistance, the results show that all the mutations tested (R665W, S707Y, L834F, and D993G) led to a gain of function which is however susceptible to

U73122.This gain of function suggests that these mutations may increase platelet activity, potentially increasing cardiovascular risk. However, the fact that these mutations are susceptible to U73122 inhibition provides a potential therapeutic approach, even in the presence of gain of function mutations.

Finally, using Zebrafish as an *in vivo* model, the inhibition of PLCγ2 using U73122 led to a significant decrease in thrombus formation. This demonstrates the potential of utilising zebrafish as a model to investigate thrombosis and evaluate the efficacy of novel treatments. Due to their genetic and physiological similarities to humans, zebrafish might be a valuable model for understanding cardiovascular disease and developing new therapies.

References:

ABTAHIAN, F., GUERRIERO, A., SEBZDA, E., LU, M. M., ZHOU, R., MOCSAI, A., MYERS, E. E., HUANG, B., JACKSON, D. G., FERRARI, V. A., TYBULEWICZ, V., LOWELL, C. A., LEPORE, J. J., KORETZKY, G. A. & KAHN, M. L. 2003. Regulation of blood and lymphatic vascular separation by signaling proteins SLP-76 and Syk. *Science,* 299**,** 247-51.

ALEXANDROPOULOS, K., CHENG, G. & BALTIMORE, D. 1995. Proline-rich sequences that bind to Src homology 3 domains with individual specificities. *Proc Natl Acad Sci U S A,* 92**,** 3110-4.

ALSHEHRI, O. M., HUGHES, C. E., MONTAGUE, S., WATSON, S. K., FRAMPTON, J., BENDER, M. & WATSON, S. P. 2015a. Fibrin activates GPVI in human and mouse platelets. *Blood,* 126**,** 1601-8.

ALSHEHRI, O. M., MONTAGUE, S., WATSON, S., CARTER, P., SARKER, N., MANNE, B. K., MILLER, J. L., HERR, A. B., POLLITT, A. Y., O'CALLAGHAN, C. A., KUNAPULI, S., ARMAN, M., HUGHES, C. E. & WATSON, S. P. 2015b. Activation of glycoprotein VI (GPVI) and C-type lectin-like receptor-2 (CLEC-2) underlies platelet activation by diesel exhaust particles and other charged/hydrophobic ligands. *Biochem J,* 468**,** 459-73.

ANDERSON, B. L., BOLDOGH, I., EVANGELISTA, M., BOONE, C., GREENE, L. A. & PON, L. A. 1998. The Src homology domain 3 (SH3) of a yeast type I myosin, Myo5p, binds to verprolin and is required for targeting to sites of actin polarization. *J Cell Biol,* 141**,** 1357-70.

ANGOM, R. S. & NAKKA, N. M. R. 2024. Zebrafish as a Model for Cardiovascular and Metabolic Disease: The Future of Precision Medicine. *Biomedicines,* 12.

ARTHUR, J. F., DUNKLEY, S. & ANDREWS, R. K. 2007. Platelet glycoprotein VI-related clinical defects. *Br J Haematol,* 139**,** 363-72.

ASAZUMA, N., WILDE, J. I., BERLANGA, O., LEDUC, M., LEO, A., SCHWEIGHOFFER, E., TYBULEWICZ, V., BON, C., LIU, S. K., MCGLADE, C. J., SCHRAVEN, B. & WATSON, S. P. 2000. Interaction of linker for activation of T cells with multiple adapter proteins in platelets activated by the glycoprotein VI-selective ligand, convulxin. *J Biol Chem,* 275**,** 33427-34.

ASSELIN, J., GIBBINS, J. M., ACHISON, M., LEE, Y. H., MORTON, L. F., FARNDALE, R. W., BARNES, M. J. & WATSON, S. P. 1997. A collagen-like peptide stimulates tyrosine phosphorylation of syk and phospholipase C gamma2 in platelets independent of the integrin alpha2beta1. *Blood,* 89**,** 1235-42.

AURSNES, I. & PEDERSEN, O. O. 1979. Petechial hemorrhage in the ciliary processes of thrombocytopenic rabbits. An electron microscopic study. *Microvasc Res,* 17**,** 12-21.

BABA, T. W., GIROIR, B. P. & HUMPHRIES, E. H. 1985. Cell lines derived from avian lymphomas exhibit two distinct phenotypes. *Virology,* 144**,** 139-51.

BADIMON, L., PADRÓ, T. & VILAHUR, G. 2012. Atherosclerosis, platelets and thrombosis in acute ischaemic heart disease. *Eur Heart J Acute Cardiovasc Care,* 1**,** 60-74.

BADOLIA, R., INAMDAR, V., MANNE, B. K., DANGELMAIER, C., EBLE, J. A. & KUNAPULI, S. P. 2017. G(q) pathway regulates proximal C-type lectin-like receptor-2 (CLEC-2) signaling in platelets. *J Biol Chem,* 292**,** 14516-14531.

BALUK, P., FUXE, J., HASHIZUME, H., ROMANO, T., LASHNITS, E., BUTZ, S., VESTWEBER, D., CORADA, M., MOLENDINI, C., DEJANA, E. & MCDONALD, D. M. 2007. Functionally specialized junctions between endothelial cells of lymphatic vessels. *J Exp Med,* 204**,** 2349-62.

BAR-SAGI, D., ROTIN, D., BATZER, A., MANDIYAN, V. & SCHLESSINGER, J. 1993. SH3 domains direct cellular localization of signaling molecules. *Cell,* 74**,** 83-91.

BEARER, E. L. 1995. Cytoskeletal domains in the activated platelet. *Cell Motil Cytoskeleton,* 30**,** 50-66.

BECK, F., GEIGER, J., GAMBARYAN, S., VEIT, J., VAUDEL, M., NOLLAU, P., KOHLBACHER, O., MARTENS, L., WALTER, U., SICKMANN, A. & ZAHEDI, R. P. 2014. Time-resolved characterization of cAMP/PKA-dependent signaling reveals that platelet inhibition is a concerted process involving multiple signaling pathways. *Blood,* 123**,** e1-e10.

BENSCHOP, R. J., BRANDL, E., CHAN, A. C. & CAMBIER, J. C. 2001. Unique Signaling Properties of B Cell Antigen Receptor in Mature and Immature B Cells: Implications for Tolerance and Activation1. *The Journal of Immunology,* 167**,** 4172-4179.

BERGER, G., MASSÉ, J. M. & CRAMER, E. M. 1996. Alpha-granule membrane mirrors the platelet plasma membrane and contains the glycoproteins Ib, IX, and V. *Blood,* 87**,** 1385-95.

BERGMEIER, W., BOUVARD, D., EBLE, J. A., MOKHTARI-NEJAD, R., SCHULTE, V., ZIRNGIBL, H., BRAKEBUSCH, C., FÄSSLER, R. & NIESWANDT, B. 2001. Rhodocytin (aggretin) activates platelets lacking alpha(2)beta(1) integrin, glycoprotein VI, and the ligand-binding domain of glycoprotein Ibalpha. *J Biol Chem,* 276**,** 25121-6.

BERLANGA, O., TULASNE, D., BORI, T., SNELL, D. C., MIURA, Y., JUNG, S., MOROI, M., FRAMPTON, J. & WATSON, S. P. 2002. The Fc receptor gamma-chain is necessary and sufficient to initiate signalling through glycoprotein VI in transfected cells by the snake C-type lectin, convulxin. *Eur J Biochem,* 269**,** 2951-60.

BERNAL-QUIRÓS, M., WU, Y. Y., ALARCÓN-RIQUELME, M. E. & CASTILLEJO-LÓPEZ, C. 2013. BANK1 and BLK act through phospholipase C gamma 2 in B-cell signaling. *PLoS One,* 8**,** e59842.

BERRIDGE, M. J., BOOTMAN, M. D. & RODERICK, H. L. 2003. Calcium signalling: dynamics, homeostasis and remodelling. *Nat Rev Mol Cell Biol,* 4**,** 517-29.

BERTOZZI, C. C., SCHMAIER, A. A., MERICKO, P., HESS, P. R., ZOU, Z., CHEN, M., CHEN, C. Y., XU, B., LU, M. M., ZHOU, D., SEBZDA, E., SANTORE, M. T., MERIANOS, D. J., STADTFELD, M., FLAKE, A. W., GRAF, T., SKODA, R., MALTZMAN, J. S., KORETZKY, G. A. & KAHN, M. L. 2010. Platelets regulate lymphatic vascular development through CLEC-2-SLP-76 signaling. *Blood,* 116**,** 661-70.

BEST, D., SENIS, Y. A., JARVIS, G. E., EAGLETON, H. J., ROBERTS, D. J., SAITO, T., JUNG, S. M., MOROI, M., HARRISON, P., GREEN, F. R. & WATSON, S. P. 2003. GPVI levels in platelets: relationship to platelet function at high shear. *Blood,* 102**,** 2811-8.

BIRD, G. S., AZIZ, O., LIEVREMONT, J. P., WEDEL, B. J., TREBAK, M., VAZQUEZ, G. & PUTNEY, J. W., JR. 2004. Mechanisms of phospholipase C-regulated calcium entry. *Curr Mol Med,* 4**,** 291-301.

BLAIR, P. & FLAUMENHAFT, R. 2009. Platelet alpha-granules: basic biology and clinical correlates. *Blood reviews,* 23**,** 177-189.

BLEASDALE, J. E., BUNDY, G. L., BUNTING, S., FITZPATRICK, F. A., HUFF, R. M., SUN, F. F. & PIKE, J. E. 1989. Inhibition of phospholipase C dependent processes by U-73, 122. *Adv Prostaglandin Thromboxane Leukot Res,* 19**,** 590-3.

BLEASDALE, J. E., THAKUR, N. R., GREMBAN, R. S., BUNDY, G. L., FITZPATRICK, F. A., SMITH, R. J. & BUNTING, S. 1990. Selective inhibition of receptor-coupled phospholipase C-dependent processes in human platelets and polymorphonuclear neutrophils. *J Pharmacol Exp Ther,* 255**,** 756-68.

BOGAERT, D. J., DULLAERS, M., LAMBRECHT, B. N., VERMAELEN, K. Y., DE BAERE, E. & HAERYNCK, F. 2016. Genes associated with common variable immunodeficiency: one diagnosis to rule them all? *J Med Genet,* 53**,** 575-90.

BORI-SANZ, T., INOUE, K. S., BERNDT, M. C., WATSON, S. P. & TULASNE, D. 2003. Delineation of the region in the glycoprotein VI tail required for association with the Fc receptor gamma-chain. *J Biol Chem,* 278**,** 35914-22.

BORN, G. V. R. 1962. Aggregation of Blood Platelets by Adenosine Diphosphate and its Reversal. *Nature,* 194**,** 927-929.

BOULAFTALI, Y., HESS, P. R., GETZ, T. M., CHOLKA, A., STOLLA, M., MACKMAN, N., OWENS, A. P., 3RD, WARE, J., KAHN, M. L. & BERGMEIER, W. 2013. Platelet ITAM signaling is critical for vascular integrity in inflammation. *J Clin Invest,* 123**,** 908-16.

BOURNE, J. H., COLICCHIA, M., DI, Y., MARTIN, E., SLATER, A., ROUMENINA, L. T., DIMITROV, J. D., WATSON, S. P. & RAYES, J. 2021. Heme induces human and mouse platelet activation through C-type-lectin-like receptor-2. *Haematologica,* 106**,** 626-629.

BRASS, L. F. & JOSEPH, S. K. 1985. A role for inositol triphosphate in intracellular Ca2+ mobilization and granule secretion in platelets. *J Biol Chem,* 260**,** 15172-9.

BREITENEDER-GELEFF, S., SOLEIMAN, A., KOWALSKI, H., HORVAT, R., AMANN, G., KRIEHUBER, E., DIEM, K., WENINGER, W., TSCHACHLER, E., ALITALO, K. & KERJASCHKI, D. 1999. Angiosarcomas express mixed endothelial phenotypes of blood and lymphatic capillaries: podoplanin as a specific marker for lymphatic endothelium. *Am J Pathol,* 154**,** 385-94.

BROOKS, S. R., LI, X., VOLANAKIS, E. J. & CARTER, R. H. 2000. Systematic Analysis of the Role of CD19 Cytoplasmic Tyrosines in Enhancement of Activation in Daudi Human B Cells: Clustering of Phospholipase C and Vav and of Grb2 and Sos with Different CD19 Tyrosines1. *The Journal of Immunology,* 164**,** 3123-3131.

BROOS, K., FEYS, H. B., DE MEYER, S. F., VANHOORELBEKE, K. & DECKMYN, H. 2011. Platelets at work in primary hemostasis. *Blood Rev,* 25**,** 155-67.

BUERSTEDDE, J. M. & TAKEDA, S. 1991. Increased Ratio of Targeted to Random Integration after Transfection of Chicken B-Cell Lines. *Cell,* 67**,** 179-188.

BURGDORF, C., SCHÄFER, U., RICHARDT, G. & KURZ, T. 2010. U73122, an aminosteroid phospholipase C inhibitor, is a potent inhibitor of cardiac phospholipase D by a PIP2-dependent mechanism. *J Cardiovasc Pharmacol,* 55**,** 555-9.

BURGER, J. A., LANDAU, D. A., TAYLOR-WEINER, A., BOZIC, I., ZHANG, H., SAROSIEK, K., WANG, L., STEWART, C., FAN, J. & HOELLENRIEGEL, J. 2016. Clonal evolution in patients with chronic lymphocytic leukaemia developing resistance to BTK inhibition. *Nature communications,* 7**,** 11589.

BURKHART, J. M., VAUDEL, M., GAMBARYAN, S., RADAU, S., WALTER, U., MARTENS, L., GEIGER, J., SICKMANN, A. & ZAHEDI, R. P. 2012. The first comprehensive and quantitative analysis of human platelet protein composition allows the comparative analysis of structural and functional pathways. *Blood,* 120**,** e73-e82.

BYE, A. P., UNSWORTH, A. J., VAIYAPURI, S., STAINER, A. R., FRY, M. J. & GIBBINS, J. M. 2015. Ibrutinib Inhibits Platelet Integrin αIIbβ3 Outside-In Signaling and Thrombus Stability But Not Adhesion to Collagen. *Arterioscler Thromb Vasc Biol,* 35**,** 2326-35.

CARMELIET, P., FERREIRA, V., BREIER, G., POLLEFEYT, S., KIECKENS, L., GERTSENSTEIN, M., FAHRIG, M., VANDENHOECK, A., HARPAL, K., EBERHARDT, C., DECLERCQ, C., PAWLING, J., MOONS, L., COLLEN, D., RISAU, W. & NAGY, A. 1996. Abnormal blood vessel development and lethality in embryos lacking a single VEGF allele. *Nature,* 380**,** 435-9.

CARRAMOLINO, L., FUENTES, J., GARCIA-ANDRES, C., AZCOITIA, V., RIETHMACHER, D. & TORRES, M. 2010. Platelets play an essential role in separating the blood and lymphatic vasculatures during embryonic angiogenesis. *Circ Res,* 106**,** 1197-201.

CHAHARDEHI, A. M., ARSAD, H. & LIM, V. 2020. Zebrafish as a Successful Animal Model for Screening Toxicity of Medicinal Plants. *Plants (Basel),* 9.

CHAN, M. V., LEADBEATER, P. D., WATSON, S. P. & WARNER, T. D. 2018. Not all light transmission aggregation assays are created equal: qualitative differences between light transmission and 96-well plate aggregometry. *Platelets,* 29**,** 686-689.

CHANG, Y. W., HSIEH, P. W., CHANG, Y. T., LU, M. H., HUANG, T. F., CHONG, K. Y., LIAO, H. R., CHENG, J. C. & TSENG, C. P. 2015. Identification of a novel platelet antagonist that binds to CLEC-2 and suppresses podoplanin-induced platelet aggregation and cancer metastasis. *Oncotarget,* 6**,** 42733-48.

CHEN, T., REPETTO, B., CHIZZONITE, R., PULLAR, C., BURGHARDT, C., DHARM, E., ZHAO, Z., CARROLL, R., NUNES, P., BASU, M., DANHO, W., VISNICK, M., KOCHAN, J., WAUGH, D. & GILFILLAN, A. M. 1996. Interaction of phosphorylated FcepsilonRIgamma immunoglobulin receptor tyrosine activation motif-based peptides with dual and single SH2 domains of p72syk. Assessment of binding parameters and real time binding kinetics. *J Biol Chem,* 271**,** 25308-15.

CHILDS, S., CHEN, J. N., GARRITY, D. M. & FISHMAN, M. C. 2002. Patterning of angiogenesis in the zebrafish embryo. *Development,* 129**,** 973-82.

CHOI, T. Y., CHOI, T. I., LEE, Y. R., CHOE, S. K. & KIM, C. H. 2021. Zebrafish as an animal model for biomedical research. *Exp Mol Med,* 53**,** 310-317.

CHRISTOU, C. M., PEARCE, A. C., WATSON, A. A., MISTRY, A. R., POLLITT, A. Y., FENTON-MAY, A. E., JOHNSON, L. A., JACKSON, D. G., WATSON, S. P. & O'CALLAGHAN, C. A. 2008. Renal cells activate the platelet receptor CLEC-2 through podoplanin. *Biochem J,* 411**,** 133-40.

CLEMETSON, J. M., POLGAR, J., MAGNENAT, E., WELLS, T. N. & CLEMETSON, K. J. 1999. The platelet collagen receptor glycoprotein VI is a member of the immunoglobulin superfamily closely related to FcalphaR and the natural killer receptors. *J Biol Chem,* 274**,** 29019-24.

CLEMETSON, K. J., MCGREGOR, J. L., JAMES, E., DECHAVANNE, M. & LÜSCHER, E. F. 1982. Characterization of the platelet membrane glycoprotein abnormalities in Bernard-Soulier syndrome and comparison with normal by surface-labeling techniques and high-resolution two-dimensional gel electrophoresis. *J Clin Invest,* 70**,** 304-11.

CLIPSTONE, N. A. & CRABTREE, G. R. 1992. Identification of calcineurin as a key signalling enzyme in T-lymphocyte activation. *Nature,* 357**,** 695-7.

COLONNA, M., SAMARIDIS, J. & ANGMAN, L. 2000. Molecular characterization of two novel C-type lectin-like receptors, one of which is selectively expressed in human dendritic cells. *Eur J Immunol,* 30**,** 697-704.

COX, A. C., CARROLL, R. C., WHITE, J. G. & RAO, G. H. 1984. Recycling of platelet phosphorylation and cytoskeletal assembly. *J Cell Biol,* 98**,** 8-15.

DANIEL, J. L., MOLISH, I. R., RIGMAIDEN, M. & STEWART, G. 1984. Evidence for a role of myosin phosphorylation in the initiation of the platelet shape change response. *J Biol Chem,* 259**,** 9826-31.

DERANLEAU, D. A., DUBLER, D., ROTHEN, C. & LÜSCHER, E. F. 1982. Transient kinetics of the rapid shape change of unstirred human blood platelets stimulated with ADP. *Proc Natl Acad Sci U S A,* 79**,** 7297-301.

DETRICH, H. W., 3RD, KIERAN, M. W., CHAN, F. Y., BARONE, L. M., YEE, K., RUNDSTADLER, J. A., PRATT, S., RANSOM, D. & ZON, L. I. 1995. Intraembryonic hematopoietic cell migration during vertebrate development. *Proc Natl Acad Sci U S A,* 92**,** 10713-7.

DIOP, A., SANTORELLI, D., MALAGRINÒ, F., NARDELLA, C., PENNACCHIETTI, V., PAGANO, L., MARCOCCI, L., PIETRANGELI, P., GIANNI, S. & TOTO, A. 2022. SH2 Domains: Folding, Binding and Therapeutical Approaches. *Int J Mol Sci,* 23.

DOLMETSCH, R. E., LEWIS, R. S., GOODNOW, C. C. & HEALY, J. I. 1997. Differential activation of transcription factors induced by Ca2+ response amplitude and duration. *Nature,* 386**,** 855-8.

DOVIZIO, M., MAIER, T. J., ALBERTI, S., DI FRANCESCO, L., MARCANTONI, E., MÜNCH, G., JOHN, C. M., SUESS, B., SGAMBATO, A., STEINHILBER, D. & PATRIGNANI, P. 2013. Pharmacological inhibition of platelet-tumor cell cross-talk prevents platelet-induced overexpression of cyclooxygenase-2 in HT29 human colon carcinoma cells. *Mol Pharmacol,* 84**,** 25-40.

DUNSTER, J. L., MAZET, F., FRY, M. J., GIBBINS, J. M. & TINDALL, M. J. 2015. Regulation of Early Steps of GPVI Signal Transduction by Phosphatases: A Systems Biology Approach. *PLoS computational biology,* 11**,** e1004589-e1004589.

EBLE, J. A., BEERMANN, B., HINZ, H. J. & SCHMIDT-HEDERICH, A. 2001. alpha 2beta 1 integrin is not recognized by rhodocytin but is the specific, high affinity target of rhodocetin, an RGD-independent disintegrin and potent inhibitor of cell adhesion to collagen. *J Biol Chem,* 276**,** 12274-84.

EILKEN, H. M., NISHIKAWA, S. & SCHROEDER, T. 2009. Continuous single-cell imaging of blood generation from haemogenic endothelium. *Nature,* 457**,** 896-900.

EVERETT, K. L., BUNNEY, T. D., YOON, Y., RODRIGUES-LIMA, F., HARRIS, R., DRISCOLL, P. C., ABE, K., FUCHS, H., DE ANGELIS, M. H., YU, P., CHO, W. & KATAN, M. 2009. Characterization of phospholipase C gamma enzymes with gain-of-function mutations. *The Journal of biological chemistry,* 284**,** 23083-23093.

EZUMI, Y., SHINDOH, K., TSUJI, M. & TAKAYAMA, H. 1998. Physical and functional association of the Src family kinases Fyn and Lyn with the collagen receptor glycoprotein VI-Fc receptor gamma chain complex on human platelets. *J Exp Med,* 188**,** 267-76.

FABRE, J.-E., NGUYEN, M., LATOUR, A., KEIFER, J. A., AUDOLY, L. P., COFFMAN, T. M. & KOLLER, B. H. 1999. Decreased platelet aggregation, increased bleeding time and resistance to thromboembolism in P2Y1-deficient mice. *Nature Medicine,* 5**,** 1199-1202.

FALASCA, M., LOGAN, S. K., LEHTO, V. P., BACCANTE, G., LEMMON, M. A. & SCHLESSINGER, J. 1998. Activation of phospholipase Cγ by PI 3-kinase-induced PH domain-mediated membrane targeting. *The EMBO Journal,* 17**,** 414-422.

FAN, Y., JIANG, M., GONG, D. & ZOU, C. 2016. Efficacy and safety of low-molecular-weight heparin in patients with sepsis: a meta-analysis of randomized controlled trials. *Sci Rep,* 6**,** 25984.

FENG, Q., SHABRANI, N., THON, J. N., HUO, H., THIEL, A., MACHLUS, K. R., KIM, K., BROOKS, J., LI, F., LUO, C., KIMBREL, E. A., WANG, J., KIM, K.-S., ITALIANO, J., CHO, J., LU, S.-J. & LANZA, R. 2014. Scalable generation of universal platelets from human induced pluripotent stem cells. *Stem cell reports,* 3**,** 817-831.

FENG, X., TRAVISANO, S., PEARSON, C. A., LIEN, C. L. & HARRISON, M. R. M. 2021. The Lymphatic System in Zebrafish Heart Development, Regeneration and Disease Modeling. *J Cardiovasc Dev Dis,* 8.

FERRARA, N., GERBER, H. P. & LECOUTER, J. 2003. The biology of VEGF and its receptors. *Nat Med,* 9**,** 669-76.

FERSHT, A. R., MATOUSCHEK, A. & SERRANO, L. 1992. The folding of an enzyme. I. Theory of protein engineering analysis of stability and pathway of protein folding. *J Mol Biol,* 224**,** 771-82.

FLAUMENHAFT, R. 2003. Molecular basis of platelet granule secretion. *Arterioscler Thromb Vasc Biol,* 23**,** 1152-60.

FLUCKIGER, A. C., LI, Z., KATO, R. M., WAHL, M. I., OCHS, H. D., LONGNECKER, R., KINET, J. P., WITTE, O. N., SCHARENBERG, A. M. & RAWLINGS, D. J. 1998. Btk/Tec kinases regulate sustained increases in intracellular Ca2+ following B-cell receptor activation. *Embo j,* 17**,** 1973-85.

FREIRE, C., FISH, R. J., VILAR, R., DI SANZA, C., GRZEGORSKI, S. J., RICHTER, C. E., SHAVIT, J. A. & NEERMAN-ARBEZ, M. 2020. A genetic modifier of venous thrombosis in zebrafish reveals a functional role for fibrinogen AαE in early hemostasis. *Blood Adv,* 4**,** 5480-5491.

FULLER, G. L., WILLIAMS, J. A., TOMLINSON, M. G., EBLE, J. A., HANNA, S. L., POHLMANN, S., SUZUKI-INOUE, K., OZAKI, Y., WATSON, S. P. & PEARCE, A. C. 2007. The C-type lectin receptors CLEC-2 and Dectin-1, but not DC-SIGN, signal via a novel YXXL-dependent signaling cascade. *J Biol Chem,* 282**,** 12397-409.

GACHET, C. 2008. P2 receptors, platelet function and pharmacological implications. *Thromb Haemost,* 99**,** 466-72.

GAIDANO, G., FOÀ, R. & DALLA-FAVERA, R. 2012. Molecular pathogenesis of chronic lymphocytic leukemia. *The Journal of clinical investigation,* 122**,** 3432-3438.

GHIA, P., CHIORAZZI, N. & STAMATOPOULOS, K. 2008. Microenvironmental influences in chronic lymphocytic leukaemia: the role of antigen stimulation. *J Intern Med,* 264**,** 549-62.

GIANNELOU, A., ZHOU, Q. & KASTNER, D. L. 2014. When less is more: primary immunodeficiency with an autoinflammatory kick. *Curr Opin Allergy Clin Immunol,* 14**,** 491-500.

GIBBINS, J. M., OKUMA, M., FARNDALE, R., BARNES, M. & WATSON, S. P. 1997. Glycoprotein VI is the collagen receptor in platelets which underlies tyrosine phosphorylation of the Fc receptor gamma-chain. *FEBS Lett,* 413**,** 255-9.

GITZ, E., POLLITT, A. Y., GITZ-FRANCOIS, J. J., ALSHEHRI, O., MORI, J., MONTAGUE, S., NASH, G. B., DOUGLAS, M. R., GARDINER, E. E., ANDREWS, R. K., BUCKLEY, C. D., HARRISON, P. & WATSON, S. P. 2014. CLEC-2 expression is maintained on activated platelets and on platelet microparticles. *Blood,* 124**,** 2262-70.

GOLEBIEWSKA, E. M. & POOLE, A. W. 2015. Platelet secretion: From haemostasis to wound healing and beyond. *Blood Reviews,* 29**,** 153-162.

GONCALVES, I., HUGHAN, S. C., SCHOENWAELDER, S. M., YAP, C. L., YUAN, Y. & JACKSON, S. P. 2003. Integrin alpha IIb beta 3-dependent calcium signals regulate

platelet-fibrinogen interactions under flow. Involvement of phospholipase C gamma 2. *J Biol Chem,* 278**,** 34812-22.
GREGORY, M., HANUMANTHAIAH, R. & JAGADEESWARAN, P. 2002. Genetic Analysis of Hemostasis and Thrombosis Using Vascular Occlusion. *Blood Cells, Molecules, and Diseases,* 29**,** 286-295.
GRESSET, A., HICKS, S. N., HARDEN, T. K. & SONDEK, J. 2010. Mechanism of phosphorylation-induced activation of phospholipase C-gamma isozymes. *The Journal of biological chemistry,* 285**,** 35836-35847.
GROBLER, J. A. & HURLEY, J. H. 1998. Catalysis by phospholipase C delta1 requires that Ca2+ bind to the catalytic domain, but not the C2 domain. *Biochemistry,* 37**,** 5020-8.
GROSS, B. S., LEE, J. R., CLEMENTS, J. L., TURNER, M., TYBULEWICZ, V. L., FINDELL, P. R., KORETZKY, G. A. & WATSON, S. P. 1999. Tyrosine phosphorylation of SLP-76 is downstream of Syk following stimulation of the collagen receptor in platelets. *J Biol Chem,* 274**,** 5963-71.
HAAS, E. & STANLEY, D. W. 2007. Phospholipase C. *In:* ENNA, S. J. & BYLUND, D. B. (eds.) *xPharm: The Comprehensive Pharmacology Reference.* New York: Elsevier.
HANTGAN, R. R. 1984. A study of the kinetics of ADP-triggered platelet shape change. *Blood,* 64**,** 896-906.
HARRISON, P. & CRAMER, E. M. 1993. Platelet alpha-granules. *Blood Rev,* 7**,** 52-62.
HASHIMOTO, A., TAKEDA, K., INABA, M., SEKIMATA, M., KAISHO, T., IKEHARA, S., HOMMA, Y., AKIRA, S. & KUROSAKI, T. 2000. Cutting Edge: Essential Role of Phospholipase C-γ2 in B Cell Development and Function1. *The Journal of Immunology,* 165**,** 1738-1742.
HASHIMOTO, S., IWAMATSU, A., ISHIAI, M., OKAWA, K., YAMADORI, T., MATSUSHITA, M., BABA, Y., KISHIMOTO, T., KUROSAKI, T. & TSUKADA, S. 1999. Identification of the SH2 domain binding protein of Bruton's tyrosine kinase as BLNK--functional significance of Btk-SH2 domain in B-cell antigen receptor-coupled calcium signaling. *Blood,* 94**,** 2357-64.
HAWIGER, J. 1987. Formation and regulation of platelet and fibrin hemostatic plug. *Hum Pathol,* 18**,** 111-22.
HEEMSKERK, J. W., FARNDALE, R. W. & SAGE, S. O. 1997a. Effects of U73122 and U73343 on human platelet calcium signalling and protein tyrosine phosphorylation. *Biochim Biophys Acta,* 1355**,** 81-8.
HEEMSKERK, J. W. M., FARNDALE, R. W. & SAGE, S. O. 1997b. Effects of U73122 and U73343 on human platelet calcium signalling and protein tyrosine phosphorylation. *Biochimica et Biophysica Acta (BBA) - Molecular Cell Research,* 1355**,** 81-88.
HERISHANU, Y., PÉREZ-GALÁN, P., LIU, D., BIANCOTTO, A., PITTALUGA, S., VIRE, B., GIBELLINI, F., NJUGUNA, N., LEE, E., STENNETT, L., RAGHAVACHARI, N., LIU, P., MCCOY, J. P., RAFFELD, M., STETLER-STEVENSON, M., YUAN, C., SHERRY, R., ARTHUR, D. C., MARIC, I., WHITE, T., MARTI, G. E., MUNSON, P., WILSON, W. H. & WIESTNER, A. 2011. The lymph node microenvironment promotes B-cell receptor signaling, NF-kappaB activation, and tumor proliferation in chronic lymphocytic leukemia. *Blood,* 117**,** 563-74.
HOGAN, B. M. & SCHULTE-MERKER, S. 2017. How to Plumb a Pisces: Understanding Vascular Development and Disease Using Zebrafish Embryos. *Dev Cell,* 42**,** 567-583.
HOWE, K., CLARK, M. D., TORROJA, C. F., TORRANCE, J., BERTHELOT, C., MUFFATO, M., COLLINS, J. E., HUMPHRAY, S., MCLAREN, K., MATTHEWS, L., MCLAREN, S., SEALY, I., CACCAMO, M., CHURCHER, C., SCOTT, C., BARRETT, J. C., KOCH, R., RAUCH, G. J., WHITE, S., CHOW, W., KILIAN, B.,

QUINTAIS, L. T., GUERRA-ASSUNÇÃO, J. A., ZHOU, Y., GU, Y., YEN, J., VOGEL, J. H., EYRE, T., REDMOND, S., BANERJEE, R., CHI, J., FU, B., LANGLEY, E., MAGUIRE, S. F., LAIRD, G. K., LLOYD, D., KENYON, E., DONALDSON, S., SEHRA, H., ALMEIDA-KING, J., LOVELAND, J., TREVANION, S., JONES, M., QUAIL, M., WILLEY, D., HUNT, A., BURTON, J., SIMS, S., MCLAY, K., PLUMB, B., DAVIS, J., CLEE, C., OLIVER, K., CLARK, R., RIDDLE, C., ELLIOT, D., THREADGOLD, G., HARDEN, G., WARE, D., BEGUM, S., MORTIMORE, B., KERRY, G., HEATH, P., PHILLIMORE, B., TRACEY, A., CORBY, N., DUNN, M., JOHNSON, C., WOOD, J., CLARK, S., PELAN, S., GRIFFITHS, G., SMITH, M., GLITHERO, R., HOWDEN, P., BARKER, N., LLOYD, C., STEVENS, C., HARLEY, J., HOLT, K., PANAGIOTIDIS, G., LOVELL, J., BEASLEY, H., HENDERSON, C., GORDON, D., AUGER, K., WRIGHT, D., COLLINS, J., RAISEN, C., DYER, L., LEUNG, K., ROBERTSON, L., AMBRIDGE, K., LEONGAMORNLERT, D., MCGUIRE, S., GILDERTHORP, R., GRIFFITHS, C., MANTHRAVADI, D., NICHOL, S., BARKER, G., et al. 2013. The zebrafish reference genome sequence and its relationship to the human genome. *Nature,* 496**,** 498-503.

HUANG, H., LI, L., WU, C., SCHIBLI, D., COLWILL, K., MA, S., LI, C., ROY, P., HO, K., SONGYANG, Z., PAWSON, T., GAO, Y. & LI, S. S. 2008. Defining the specificity space of the human SRC homology 2 domain. *Mol Cell Proteomics,* 7**,** 768-84.

HUANG, T. F., LIU, C. Z. & YANG, S. H. 1995. Aggretin, a novel platelet-aggregation inducer from snake (Calloselasma rhodostoma) venom, activates phospholipase C by acting as a glycoprotein Ia/IIa agonist. *Biochem J,* 309 (Pt 3)**,** 1021-7.

HUGHES, C. E., AUGER, J. M., MCGLADE, J., EBLE, J. A., PEARCE, A. C. & WATSON, S. P. 2008. Differential roles for the adapters Gads and LAT in platelet activation by GPVI and CLEC-2. *J Thromb Haemost,* 6**,** 2152-9.

HUGHES, C. E., FINNEY, B. A., KOENTGEN, F., LOWE, K. L. & WATSON, S. P. 2015. The N-terminal SH2 domain of Syk is required for (hem)ITAM, but not integrin, signaling in mouse platelets. *Blood,* 125**,** 144-154.

HUGHES, C. E., NAVARRO-NÚÑEZ, L., FINNEY, B. A., MOURÃO-SÁ, D., POLLITT, A. Y. & WATSON, S. P. 2010a. CLEC-2 is not required for platelet aggregation at arteriolar shear. *J Thromb Haemost,* 8**,** 2328-2332.

HUGHES, C. E., POLLITT, A. Y., MORI, J., EBLE, J. A., TOMLINSON, M. G., HARTWIG, J. H., O'CALLAGHAN, C. A., FÜTTERER, K. & WATSON, S. P. 2010b. CLEC-2 activates Syk through dimerization. *Blood,* 115**,** 2947-2955.

HUGHES, C. E., RADHAKRISHNAN, U. P., LORDKIPANIDZÉ, M., EGGINTON, S., DIJKSTRA, J. M., JAGADEESWARAN, P. & WATSON, S. P. 2012. G6f-like is an ITAM-containing collagen receptor in thrombocytes. *PLoS One,* 7**,** e52622.

HUGHES, C. E., SINHA, U., PANDEY, A., EBLE, J. A., O'CALLAGHAN, C. A. & WATSON, S. P. 2013. Critical Role for an acidic amino acid region in platelet signaling by the HemITAM (hemi-immunoreceptor tyrosine-based activation motif) containing receptor CLEC-2 (C-type lectin receptor-2). *J Biol Chem,* 288**,** 5127-35.

HUYNH, M. Q., GOSSMAN, J., GATTENLÖEHNER, S., KLAPPER, W., WACKER, H.-H., RAMASWAMY, A., BITTNER, A., KAISER, U. & NEUBAUER, A. 2015. Expression and pro-survival function of phospholipase Cγ2 in diffuse large B-cell lymphoma. *Leukemia & lymphoma,* 56**,** 1088-1095.

HYVÖNEN, M. & SARASTE, M. 1997. Structure of the PH domain and Btk motif from Bruton's tyrosine kinase: molecular explanations for X‐linked agammaglobulinaemia. *The EMBO Journal,* 16**,** 3396-3404.

ICHISE, H., ICHISE, T., OHTANI, O. & YOSHIDA, N. 2009a. Phospholipase Cgamma2 is necessary for separation of blood and lymphatic vasculature in mice. *Development,* 136**,** 191-5.

ICHISE, H., ICHISE, T., OHTANI, O. & YOSHIDA, N. 2009b. Phospholipase Cγ2 is necessary for separation of blood and lymphatic vasculature in mice. *Development,* 136**,** 191-195.

ICHISE, H., ICHISE, T. & YOSHIDA, N. 2016. Phospholipase Cγ2 Is Required for Luminal Expansion of the Epididymal Duct during Postnatal Development in Mice. *PLoS One,* 11**,** e0150521.

INOUE, O., SUZUKI-INOUE, K., DEAN, W. L., FRAMPTON, J. & WATSON, S. P. 2003. Integrin alpha2beta1 mediates outside-in regulation of platelet spreading on collagen through activation of Src kinases and PLCgamma2. *J Cell Biol,* 160**,** 769-80.

ISOGAI, S., HORIGUCHI, M. & WEINSTEIN, B. M. 2001. The vascular anatomy of the developing zebrafish: an atlas of embryonic and early larval development. *Dev Biol,* 230**,** 278-301.

JACKSON, J. T., MULAZZANI, E., NUTT, S. L. & MASTERS, S. L. 2021. The role of PLCγ2 in immunological disorders, cancer, and neurodegeneration. *Journal of Biological Chemistry,* 297**,** 100905.

JACKSON, S. P., DARBOUSSET, R. & SCHOENWAELDER, S. M. 2019. Thromboinflammation: challenges of therapeutically targeting coagulation and other host defense mechanisms. *Blood,* 133**,** 906-918.

JAGADEESWARAN, P., CARRILLO, M., RADHAKRISHNAN, U. P., RAJPUROHIT, S. K. & KIM, S. 2011. Laser-induced thrombosis in zebrafish. *Methods Cell Biol,* 101**,** 197-203.

JAGADEESWARAN, P., CYKOWSKI, M. & THATTALIYATH, B. 2004. Vascular occlusion and thrombosis in zebrafish. *Methods Cell Biol,* 76**,** 489-500.

JAGADEESWARAN, P., GREGORY, M., DAY, K., CYKOWSKI, M. & THATTALIYATH, B. 2005. Zebrafish: a genetic model for hemostasis and thrombosis. *J Thromb Haemost,* 3**,** 46-53.

JAGADEESWARAN, P. & SHEEHAN, J. P. 1999. Analysis of Blood Coagulation in the Zebrafish. *Blood Cells, Molecules, and Diseases,* 25**,** 239-249.

JAGADEESWARAN, P., SHEEHAN, J. P., CRAIG, F. E. & TROYER, D. 1999. Identification and characterization of zebrafish thrombocytes. *Br J Haematol,* 107**,** 731-8.

JAMASBI, J., MEGENS, R. T., BIANCHINI, M., MÜNCH, G., UNGERER, M., FAUSSNER, A., SHERMAN, S., WALKER, A., GOYAL, P., JUNG, S., BRANDL, R., WEBER, C., LORENZ, R., FARNDALE, R., ELIA, N. & SIESS, W. 2015. Differential Inhibition of Human Atherosclerotic Plaque-Induced Platelet Activation by Dimeric GPVI-Fc and Anti-GPVI Antibodies: Functional and Imaging Studies. *J Am Coll Cardiol,* 65**,** 2404-15.

JANDROT-PERRUS, M., BUSFIELD, S., LAGRUE, A. H., XIONG, X., DEBILI, N., CHICKERING, T., LE COUEDIC, J. P., GOODEARL, A., DUSSAULT, B., FRASER, C., VAINCHENKER, W. & VILLEVAL, J. L. 2000. Cloning, characterization, and functional studies of human and mouse glycoprotein VI: a platelet-specific collagen receptor from the immunoglobulin superfamily. *Blood,* 96**,** 1798-807.

JI, K., KOGAME, T., CHOI, K., WANG, X., LEE, J., TANIGUCHI, Y. & TAKEDA, S. 2009. A novel approach using DNA-repair-deficient chicken DT40 cell lines for screening and characterizing the genotoxicity of environmental contaminants. *Environ Health Perspect,* 117**,** 1737-44.

JIN, J. & KUNAPULI, S. P. 1998. Coactivation of two different G protein-coupled receptors is essential for ADP-induced platelet aggregation. *Proc Natl Acad Sci U S A,* 95**,** 8070-4.
JOSEFSSON, E. C., VAINCHENKER, W. & JAMES, C. 2020. Regulation of Platelet Production and Life Span: Role of Bcl-xL and Potential Implications for Human Platelet Diseases. *Int J Mol Sci,* 21.
JOUKOV, V., PAJUSOLA, K., KAIPAINEN, A., CHILOV, D., LAHTINEN, I., KUKK, E., SAKSELA, O., KALKKINEN, N. & ALITALO, K. 1996. A novel vascular endothelial growth factor, VEGF-C, is a ligand for the Flt4 (VEGFR-3) and KDR (VEGFR-2) receptor tyrosine kinases. *Embo j,* 15**,** 290-98.
JUNG, H. M., CASTRANOVA, D., SWIFT, M. R., PHAM, V. N., VENERO GALANTERNIK, M., ISOGAI, S., BUTLER, M. G., MULLIGAN, T. S. & WEINSTEIN, B. M. 2017. Development of the larval lymphatic system in zebrafish. *Development,* 144**,** 2070-2081.
JUNG, H. M., ISOGAI, S., KAMEI, M., CASTRANOVA, D., GORE, A. V. & WEINSTEIN, B. M. 2016. Imaging blood vessels and lymphatic vessels in the zebrafish. *Methods Cell Biol,* 133**,** 69-103.
JUNG, S. M. & MOROI, M. 2008. Platelet glycoprotein VI. *Adv Exp Med Biol,* 640**,** 53-63.
JUNG, S. M., MOROI, M., SOEJIMA, K., NAKAGAKI, T., MIURA, Y., BERNDT, M. C., GARDINER, E. E., HOWES, J. M., PUGH, N., BIHAN, D., WATSON, S. P. & FARNDALE, R. W. 2012. Constitutive dimerization of glycoprotein VI (GPVI) in resting platelets is essential for binding to collagen and activation in flowing blood. *J Biol Chem,* 287**,** 30000-13.
KAIBUCHI, K., TAKAI, Y., SAWAMURA, M., HOSHIJIMA, M., FUJIKURA, T. & NISHIZUKA, Y. 1983. Synergistic functions of protein phosphorylation and calcium mobilization in platelet activation. *J Biol Chem,* 258**,** 6701-4.
KAN, S., KONISHI, E., ARITA, T., IKEMOTO, C., TAKENAKA, H., YANAGISAWA, A., KATOH, N. & ASAI, J. 2014. Podoplanin expression in cancer-associated fibroblasts predicts aggressive behavior in melanoma. *J Cutan Pathol,* 41**,** 561-7.
KARDEBY, C., FÄLKER, K., HAINING, E. J., CRIEL, M., LINDKVIST, M., BARROSO, R., PÅHLSSON, P., LJUNGBERG, L. U., TENGDELIUS, M., RAINGER, G. E., WATSON, S., EBLE, J. A., HOYLAERTS, M. F., EMSLEY, J., KONRADSSON, P., WATSON, S. P., SUN, Y. & GRENEGÅRD, M. 2019. Synthetic glycopolymers and natural fucoidans cause human platelet aggregation via PEAR1 and GPIbα. *Blood Adv,* 3**,** 275-287.
KARKKAINEN, M. J., HAIKO, P., SAINIO, K., PARTANEN, J., TAIPALE, J., PETROVA, T. V., JELTSCH, M., JACKSON, D. G., TALIKKA, M., RAUVALA, H., BETSHOLTZ, C. & ALITALO, K. 2004. Vascular endothelial growth factor C is required for sprouting of the first lymphatic vessels from embryonic veins. *Nat Immunol,* 5**,** 74-80.
KASIRER-FRIEDE, A., KANG, J., KAHNER, B., YE, F., GINSBERG, M. H. & SHATTIL, S. J. 2014. ADAP interactions with talin and kindlin promote platelet integrin αIIbβ3 activation and stable fibrinogen binding. *Blood,* 123**,** 3156-3165.
KATO, K., KANAJI, T., RUSSELL, S., KUNICKI, T. J., FURIHATA, K., KANAJI, S., MARCHESE, P., REININGER, A., RUGGERI, Z. M. & WARE, J. 2003. The contribution of glycoprotein VI to stable platelet adhesion and thrombus formation illustrated by targeted gene deletion. *Blood,* 102**,** 1701-7.
KEMPSTER, C., BUTLER, G., KUZNECOVA, E., TAYLOR, K. A., KRIEK, N., LITTLE, G., SOWA, M. A., SAGE, T., JOHNSON, L. J., GIBBINS, J. M. & POLLITT, A. Y.

2022a. Fully automated platelet differential interference contrast image analysis via deep learning. *Scientific Reports,* 12**,** 4614.
KEMPSTER, C., BUTLER, G., KUZNECOVA, E., TAYLOR, K. A., KRIEK, N., LITTLE, G., SOWA, M. A., SAGE, T., JOHNSON, L. J., GIBBINS, J. M. & POLLITT, A. Y. 2022b. Fully automated platelet differential interference contrast image analysis via deep learning. *Sci Rep,* 12**,** 4614.
KIM, S., CARRILLO, M., KULKARNI, V. & JAGADEESWARAN, P. 2009. Evolution of primary hemostasis in early vertebrates. *PLoS One,* 4**,** e8403.
KIM, Y. J., SEKIYA, F., POULIN, B., BAE, Y. S. & RHEE, S. G. 2004. Mechanism of B-cell receptor-induced phosphorylation and activation of phospholipase C-gamma2. *Mol Cell Biol,* 24**,** 9986-99.
KIMMEL, C. B., BALLARD, W. W., KIMMEL, S. R., ULLMANN, B. & SCHILLING, T. F. 1995. Stages of embryonic development of the zebrafish. *Dev Dyn,* 203**,** 253-310.
KISUCKA, J., BUTTERFIELD, C. E., DUDA, D. G., EICHENBERGER, S. C., SAFFARIPOUR, S., WARE, J., RUGGERI, Z. M., JAIN, R. K., FOLKMAN, J. & WAGNER, D. D. 2006. Platelets and platelet adhesion support angiogenesis while preventing excessive hemorrhage. *Proc Natl Acad Sci U S A,* 103**,** 855-60.
KITCHENS, C. S. & WEISS, L. 1975. Ultrastructural changes of endothelium associated with thrombocytopenia. *Blood,* 46**,** 567-78.
KLEIN, R. R., BOURDON, D. M., COSTALES, C. L., WAGNER, C. D., WHITE, W. L., WILLIAMS, J. D., HICKS, S. N., SONDEK, J. & THAKKER, D. R. 2011. Direct activation of human phospholipase C by its well known inhibitor u73122. *J Biol Chem,* 286**,** 12407-16.
KOBAYASHI, I. 2018. Development of Hematopoietic Stem Cells in Zebrafish. *In:* HIRATA, H. & IIDA, A. (eds.) *Zebrafish, Medaka, and Other Small Fishes: New Model Animals in Biology, Medicine, and Beyond.* Singapore: Springer Singapore.
KONO, H., FUJII, H., SUZUKI-INOUE, K., INOUE, O., FURUYA, S., HIRAYAMA, K., AKAZAWA, Y., NAKATA, Y., SUN, C., TSUKIJI, N., SHIRAI, T. & OZAKI, Y. 2017. The platelet-activating receptor C-type lectin receptor-2 plays an essential role in liver regeneration after partial hepatectomy in mice. *J Thromb Haemost,* 15**,** 998-1008.
KOSS, H., BUNNEY, T. D., BEHJATI, S. & KATAN, M. 2014. Dysfunction of phospholipase Cgamma in immune disorders and cancer. *Trends Biochem Sci,* 39**,** 603-11.
KÜCHLER, A. M., GJINI, E., PETERSON-MADURO, J., CANCILLA, B., WOLBURG, H. & SCHULTE-MERKER, S. 2006. Development of the zebrafish lymphatic system requires VEGFC signaling. *Curr Biol,* 16**,** 1244-8.
KUROSAKI, T. 2011. Regulation of BCR signaling. *Mol Immunol,* 48**,** 1287-91.
KUROSAKI, T., TAKATA, M., YAMANASHI, Y., INAZU, T., TANIGUCHI, T., YAMAMOTO, T. & YAMAMURA, H. 1994. Syk activation by the Src-family tyrosine kinase in the B cell receptor signaling. *J Exp Med,* 179**,** 1725-9.
LANCRIN, C., SROCZYNSKA, P., STEPHENSON, C., ALLEN, T., KOUSKOFF, V. & LACAUD, G. 2009. The haemangioblast generates haematopoietic cells through a haemogenic endothelium stage. *Nature,* 457**,** 892-5.
LANDAU, D. A., SUN, C., ROSEBROCK, D., HERMAN, S. E., FEIN, J., SIVINA, M., UNDERBAYEV, C., LIU, D., HOELLENRIEGEL, J. & RAVICHANDRAN, S. 2017. The evolutionary landscape of chronic lymphocytic leukemia treated with ibrutinib targeted therapy. *Nature communications,* 8**,** 2185.
LANG, M. R., GIHR, G., GAWAZ, M. P. & MULLER, II 2010. Hemostasis in Danio rerio: is the zebrafish a useful model for platelet research? *J Thromb Haemost,* 8**,** 1159-69.

LAPETINA, E. G., REEP, B., GANONG, B. R. & BELL, R. M. 1985. Exogenous sn-1,2-diacylglycerols containing saturated fatty acids function as bioregulators of protein kinase C in human platelets. *Journal of Biological Chemistry,* 260**,** 1358-1361.
LEBOWITZ, E. A. & COOKE, R. 1978. Contractile properties of actomyosin from human blood platelets. *J Biol Chem,* 253**,** 5443-7.
LEE, S. B., RAO, A. K., LEE, K.-H., YANG, X., BAE, Y. S. & RHEE, S. G. 1996a. Decreased Expression of Phospholipase C-β2 Isozyme in Human Platelets With Impaired Function. *Blood,* 88**,** 1684-1691.
LEE, S. B., RAO, A. K., LEE, K. H., YANG, X., BAE, Y. S. & RHEE, S. G. 1996b. Decreased expression of phospholipase C-beta 2 isozyme in human platelets with impaired function. *Blood,* 88**,** 1684-91.
LEFKOVITS, J., PLOW, E. F. & TOPOL, E. J. 1995. Platelet glycoprotein IIb/IIIa receptors in cardiovascular medicine. *N Engl J Med,* 332**,** 1553-9.
LEMMON, M. A., FERGUSON, K. M., O'BRIEN, R., SIGLER, P. B. & SCHLESSINGER, J. 1995. Specific and high-affinity binding of inositol phosphates to an isolated pleckstrin homology domain. *Proc Natl Acad Sci U S A,* 92**,** 10472-6.
LEVADE, M., DAVID, E., GARCIA, C., LAURENT, P. A., CADOT, S., MICHALLET, A. S., BORDET, J. C., TAM, C., SIÉ, P., YSEBAERT, L. & PAYRASTRE, B. 2014. Ibrutinib treatment affects collagen and von Willebrand factor-dependent platelet functions. *Blood,* 124**,** 3991-5.
LIAN, L., WANG, Y., DRAZNIN, J., ESLIN, D., BENNETT, J. S., PONCZ, M., WU, D. & ABRAMS, C. S. 2005. The relative role of PLCβ and PI3Kγ in platelet activation. *Blood,* 106**,** 110-117.
LIAO, F., SHIN, H. S. & RHEE, S. G. 1993. In vitro tyrosine phosphorylation of PLC-gamma 1 and PLC-gamma 2 by src-family protein tyrosine kinases. *Biochem Biophys Res Commun,* 191**,** 1028-33.
LIN, Q., ZHOU, R., MENG, P., WU, L., YANG, L., LIU, W., WU, J., CHENG, Y., SHI, L. & ZHANG, Y. 2022. Establishment of a Bernard-Soulier syndrome model in zebrafish. *Haematologica,* 107**,** 1655-1668.
LIPSKY, A. H., FAROOQUI, M. Z., TIAN, X., MARTYR, S., CULLINANE, A. M., NGHIEM, K., SUN, C., VALDEZ, J., NIEMANN, C. U., HERMAN, S. E., SABA, N., SOTO, S., MARTI, G., UZEL, G., HOLLAND, S. M., LOZIER, J. N. & WIESTNER, A. 2015. Incidence and risk factors of bleeding-related adverse events in patients with chronic lymphocytic leukemia treated with ibrutinib. *Haematologica,* 100**,** 1571-8.
LIU, J., LU, F., ITHYCHANDA, S. S., APOSTOL, M., DAS, M., DESHPANDE, G., PLOW, E. F. & QIN, J. 2023. A mechanism of platelet integrin αIIbβ3 outside-in signaling through a novel integrin αIIb subunit–filamin–actin linkage. *Blood,* 141**,** 2629-2641.
LIU, T. M., WOYACH, J. A., ZHONG, Y., LOZANSKI, A., LOZANSKI, G., DONG, S., STRATTAN, E., LEHMAN, A., ZHANG, X., JONES, J. A., FLYNN, J., ANDRITSOS, L. A., MADDOCKS, K., JAGLOWSKI, S. M., BLUM, K. A., BYRD, J. C., DUBOVSKY, J. A. & JOHNSON, A. J. 2015. Hypermorphic mutation of phospholipase C, γ2 acquired in ibrutinib-resistant CLL confers BTK independency upon B-cell receptor activation. *Blood,* 126**,** 61-8.
LIU, Y., BUNNEY, T. D., KHOSA, S., MACÉ, K., BECKENBAUER, K., ASKWITH, T., MASLEN, S., STUBBS, C., DE OLIVEIRA, T. M., SADER, K., SKEHEL, M., GAVIN, A. C., PHILLIPS, C. & KATAN, M. 2020. Structural insights and activating mutations in diverse pathologies define mechanisms of deregulation for phospholipase C gamma enzymes. *EBioMedicine,* 51**,** 102607.

LOCKEY, C., YOUNG, H., BROWN, J. & DIXON, A. M. 2022. Characterization of interactions within the Igα/Igβ transmembrane domains of the human B-cell receptor provides insights into receptor assembly. *J Biol Chem,* 298**,** 101843.
MA, Y. Q., QIN, J. & PLOW, E. F. 2007. Platelet integrin alpha(IIb)beta(3): activation mechanisms. *J Thromb Haemost,* 5**,** 1345-52.
MACIAN, F. 2005. NFAT proteins: key regulators of T-cell development and function. *Nat Rev Immunol,* 5**,** 472-84.
MAGNO, L., LESSARD, C. B., MARTINS, M., LANG, V., CRUZ, P., ASI, Y., KATAN, M., BILSLAND, J., LASHLEY, T., CHAKRABARTY, P., GOLDE, T. E. & WHITING, P. J. 2019. Alzheimer's disease phospholipase C-gamma-2 (PLCG2) protective variant is a functional hypermorph. *Alzheimers Res Ther,* 11**,** 16.
MAMMADOVA-BACH, E., OLLIVIER, V., LOYAU, S., SCHAFF, M., DUMONT, B., FAVIER, R., FREYBURGER, G., LATGER-CANNARD, V., NIESWANDT, B., GACHET, C., MANGIN, P. H. & JANDROT-PERRUS, M. 2015. Platelet glycoprotein VI binds to polymerized fibrin and promotes thrombin generation. *Blood,* 126**,** 683-691.
MANGIN, P., NONNE, C., ECKLY, A., OHLMANN, P., FREUND, M., NIESWANDT, B., CAZENAVE, J. P., GACHET, C. & LANZA, F. 2003. A PLC gamma 2-independent platelet collagen aggregation requiring functional association of GPVI and integrin alpha2beta1. *FEBS Lett,* 542**,** 53-9.
MANGIN, P. H., ONSELAER, M. B., RECEVEUR, N., LE LAY, N., HARDY, A. T., WILSON, C., SANCHEZ, X., LOYAU, S., DUPUIS, A., BABAR, A. K., MILLER, J. L., PHILIPPOU, H., HUGHES, C. E., HERR, A. B., ARIËNS, R. A., MEZZANO, D., JANDROT-PERRUS, M., GACHET, C. & WATSON, S. P. 2018. Immobilized fibrinogen activates human platelets through glycoprotein VI. *Haematologica,* 103**,** 898-907.
MANGIN, P. H., TANG, C., BOURDON, C., LOYAU, S., FREUND, M., HECHLER, B., GACHET, C. & JANDROT-PERRUS, M. 2012. A humanized glycoprotein VI (GPVI) mouse model to assess the antithrombotic efficacies of anti-GPVI agents. *J Pharmacol Exp Ther,* 341**,** 156-63.
MANNE, B. K., BADOLIA, R., DANGELMAIER, C., EBLE, J. A., ELLMEIER, W., KAHN, M. & KUNAPULI, S. P. 2015. Distinct pathways regulate Syk protein activation downstream of immune tyrosine activation motif (ITAM) and hemITAM receptors in platelets. *J Biol Chem,* 290**,** 11557-68.
MANNE, B. K., GETZ, T. M., HUGHES, C. E., ALSHEHRI, O., DANGELMAIER, C., NAIK, U. P., WATSON, S. P. & KUNAPULI, S. P. 2013. Fucoidan is a novel platelet agonist for the C-type lectin-like receptor 2 (CLEC-2). *J Biol Chem,* 288**,** 7717-7726.
MARTÍN-NALDA, A., FORTUNY, C., REY, L., BUNNEY, T. D., ALSINA, L., ESTEVE-SOLÉ, A., BULL, D., ANTON, M. C., BASAGAÑA, M., CASALS, F., DEYÁ, A., GARCÍA-PRAT, M., GIMENO, R., JUAN, M., MARTINEZ-BANACLOCHA, H., MARTINEZ-GARCIA, J. J., MENSA-VILARÓ, A., RABIONET, R., MARTIN-BEGUE, N., RUDILLA, F., YAGÜE, J., ESTIVILL, X., GARCÍA-PATOS, V., PUJOL, R. M., SOLER-PALACÍN, P., KATAN, M., PELEGRÍN, P., COLOBRAN, R., VICENTE, A. & AROSTEGUI, J. I. 2020. Severe Autoinflammatory Manifestations and Antibody Deficiency Due to Novel Hypermorphic PLCG2 Mutations. *J Clin Immunol,* 40**,** 987-1000.
MARUYAMA, S., KONO, H., FURUYA, S., SHIMIZU, H., SAITO, R., SHODA, K., AKAIKE, H., HOSOMURA, N., KAWAGUCHI, Y., AMEMIYA, H., KAWAIDA, H., SUDO, M., INOUE, S., SHIRAI, T., SUZUKI-INOUE, K. & ICHIKAWA, D.

2020. Platelet C-Type Lectin-Like Receptor 2 Reduces Cholestatic Liver Injury in Mice. *Am J Pathol,* 190**,** 1833-1842.
MASSBERG, S., GAWAZ, M., GRÜNER, S., SCHULTE, V., KONRAD, I., ZOHLNHÖFER, D., HEINZMANN, U. & NIESWANDT, B. 2003. A crucial role of glycoprotein VI for platelet recruitment to the injured arterial wall in vivo. *J Exp Med,* 197**,** 41-9.
MAY, F., HAGEDORN, I., PLEINES, I., BENDER, M., VOGTLE, T., EBLE, J., ELVERS, M. & NIESWANDT, B. 2009. CLEC-2 is an essential platelet-activating receptor in hemostasis and thrombosis. *Blood,* 114**,** 3464-72.
MAZHARIAN, A., THOMAS, S. G., DHANJAL, T. S., BUCKLEY, C. D. & WATSON, S. P. 2010. Critical role of Src-Syk-PLCγ2 signaling in megakaryocyte migration and thrombopoiesis. *Blood,* 116**,** 793-800.
MCKINNEY, M. C. & WEINSTEIN, B. M. 2008. Chapter 4. Using the zebrafish to study vessel formation. *Methods Enzymol,* 444**,** 65-97.
MENG, D., MA, X., LI, H., WU, X., CAO, Y., MIAO, Z. & ZHANG, X. 2021. A Role of the Podoplanin-CLEC-2 Axis in Promoting Inflammatory Response After Ischemic Stroke in Mice. *Neurotox Res,* 39**,** 477-488.
MEYERS, K. M., HOLMSEN, H. & SEACHORD, C. L. 1982. Comparative study of platelet dense granule constituents. *Am J Physiol,* 243**,** R454-61.
MICHELSON, A. D., CATTANEO, M., FRELINGER, A. & NEWMAN, P. 2019. *Platelets*, Elsevier Science.
MISHRA, V. K., PALGUNACHARI, M. N., KRISHNA, R., GLUSHKA, J., SEGREST, J. P. & ANANTHARAMAIAH, G. M. 2008. Effect of leucine to phenylalanine substitution on the nonpolar face of a class A amphipathic helical peptide on its interaction with lipid: high resolution solution NMR studies of 4F-dimyristoylphosphatidylcholine discoidal complex. *J Biol Chem,* 283**,** 34393-402.
MIURA, Y., OHNUMA, M., JUNG, S. M. & MOROI, M. 2000. Cloning and expression of the platelet-specific collagen receptor glycoprotein VI. *Thromb Res,* 98**,** 301-9.
MIURA, Y., TAKAHASHI, T., JUNG, S. M. & MOROI, M. 2002. Analysis of the interaction of platelet collagen receptor glycoprotein VI (GPVI) with collagen. A dimeric form of GPVI, but not the monomeric form, shows affinity to fibrous collagen. *J Biol Chem,* 277**,** 46197-204.
MOROI, A. J. & WATSON, S. P. 2015. Impact of the PI3-kinase/Akt pathway on ITAM and hemITAM receptors: haemostasis, platelet activation and antithrombotic therapy. *Biochem Pharmacol,* 94**,** 186-94.
MOROI, M. & JUNG, S. M. 2004. Platelet glycoprotein VI: its structure and function. *Thromb Res,* 114**,** 221-33.
MOROI, M., JUNG, S. M., SHINMYOZU, K., TOMIYAMA, Y., ORDINAS, A. & DIAZ-RICART, M. 1996. Analysis of platelet adhesion to a collagen-coated surface under flow conditions: the involvement of glycoprotein VI in the platelet adhesion. *Blood,* 88**,** 2081-92.
MORRELL, C. N., AGGREY, A. A., CHAPMAN, L. M. & MODJESKI, K. L. 2014. Emerging roles for platelets as immune and inflammatory cells. *Blood,* 123**,** 2759-2767.
MORTON, L. F., HARGREAVES, P. G., FARNDALE, R. W., YOUNG, R. D. & BARNES, M. J. 1995. Integrin alpha 2 beta 1-independent activation of platelets by simple collagen-like peptides: collagen tertiary (triple-helical) and quaternary (polymeric) structures are sufficient alone for alpha 2 beta 1-independent platelet reactivity. *Biochem J,* 306 (Pt 2)**,** 337-44.

MOURÃO-SÁ, D., ROBINSON, M. J., ZELENAY, S., SANCHO, D., CHAKRAVARTY, P., LARSEN, R., PLANTINGA, M., VAN ROOIJEN, N., SOARES, M. P., LAMBRECHT, B. & REIS E SOUSA, C. 2011. CLEC-2 signaling via Syk in myeloid cells can regulate inflammatory responses. *Eur J Immunol,* 41**,** 3040-53.

NAKAMURA, Y. & FUKAMI, K. 2017. Regulation and physiological functions of mammalian phospholipase C. *The Journal of Biochemistry,* 161**,** 315-321.

NAVARRO-NÚÑEZ, L., POLLITT, A. Y., LOWE, K., LATIF, A., NASH, G. B. & WATSON, S. P. 2015. Platelet adhesion to podoplanin under flow is mediated by the receptor CLEC-2 and stabilised by Src/Syk-dependent platelet signalling. *Thromb Haemost,* 113**,** 1109-20.

NEVES, J. F., DOFFINGER, R., BARCENA-MORALES, G., MARTINS, C., PAPAPIETRO, O., PLAGNOL, V., CURTIS, J., MARTINS, M., KUMARARATNE, D., CORDEIRO, A. I., NEVES, C., BORREGO, L. M., KATAN, M. & NEJENTSEV, S. 2018. Novel PLCG2 Mutation in a Patient With APLAID and Cutis Laxa. *Front Immunol,* 9**,** 2863.

NICOLSON, P. L. R., HUGHES, C. E., WATSON, S., NOCK, S. H., HARDY, A. T., WATSON, C. N., MONTAGUE, S. J., CLIFFORD, H., HUISSOON, A. P., MALCOR, J. D., THOMAS, M. R., POLLITT, A. Y., TOMLINSON, M. G., PRATT, G. & WATSON, S. P. 2018. Inhibition of Btk by Btk-specific concentrations of ibrutinib and acalabrutinib delays but does not block platelet aggregation mediated by glycoprotein VI. *Haematologica,* 103**,** 2097-2108.

NICOLSON, P. L. R., NOCK, S. H., HINDS, J., GARCIA-QUINTANILLA, L., SMITH, C. W., CAMPOS, J., BRILL, A., PIKE, J. A., KHAN, A. O., POULTER, N. S., KAVANAGH, D. M., WATSON, S., WATSON, C. N., CLIFFORD, H., HUISSOON, A. P., POLLITT, A. Y., EBLE, J. A., PRATT, G., WATSON, S. P. & HUGHES, C. E. 2021. Low-dose Btk inhibitors selectively block platelet activation by CLEC-2. *Haematologica,* 106**,** 208-219.

NIESWANDT, B., BRAKEBUSCH, C., BERGMEIER, W., SCHULTE, V., BOUVARD, D., MOKHTARI-NEJAD, R., LINDHOUT, T., HEEMSKERK, J. W., ZIRNGIBL, H. & FÄSSLER, R. 2001a. Glycoprotein VI but not alpha2beta1 integrin is essential for platelet interaction with collagen. *Embo j,* 20**,** 2120-30.

NIESWANDT, B., SCHULTE, V., BERGMEIER, W., MOKHTARI-NEJAD, R., RACKEBRANDT, K., CAZENAVE, J. P., OHLMANN, P., GACHET, C. & ZIRNGIBL, H. 2001b. Long-term antithrombotic protection by in vivo depletion of platelet glycoprotein VI in mice. *J Exp Med,* 193**,** 459-69.

NIESWANDT, B. & WATSON, S. P. 2003. Platelet-collagen interaction: is GPVI the central receptor? *Blood,* 102**,** 449-61.

NIGAM, A., MANJUPRASANNA, V. N., NAIK, M. U. & NAIK, U. P. 2024. Platelet Spreading and Clot Retraction are Regulated by two Distinct α(IIb)β(3) Outside-in Signaling Pathways. *J Pharmacol Exp Ther*.

NINOMOTO, J., MOKATRIN, A., KINOSHITA, T., MARIMPIETRI, C., BARRETT, T. D., CHANG, B. Y., SUKBUNTHERNG, J., JAMES, D. F. & CROWTHER, M. 2020. Effects of ibrutinib on in vitro platelet aggregation in blood samples from healthy donors and donors with platelet dysfunction. *Hematology,* 25**,** 112-117.

NISHIDA, M., SUGIMOTO, K., HARA, Y., MORI, E., MORII, T., KUROSAKI, T. & MORI, Y. 2003. Amplification of receptor signalling by Ca²⁺ entry‐mediated translocation and activation of PLCγ2 in B lymphocytes. *The EMBO Journal,* 22**,** 4677-4688.

NONNE, C., LENAIN, N., HECHLER, B., MANGIN, P., CAZENAVE, J. P., GACHET, C. & LANZA, F. 2005. Importance of platelet phospholipase Cgamma2 signaling in

arterial thrombosis as a function of lesion severity. *Arterioscler Thromb Vasc Biol,* 25**,** 1293-8.
NOVICE, T., KARIMINIA, A., DEL BEL, K. L., LU, H., SHARMA, M., LIM, C. J., READ, J., LUGT, M. V., HANNIBAL, M. C., O'DWYER, D., HOSLER, M., SCHARNITZ, T., RIZZO, J. M., ZACUR, J., PRIATEL, J., ABDOSSAMADI, S., BOHM, A., JUNKER, A., TURVEY, S. E., SCHULTZ, K. R. & ROZMUS, J. 2020. A Germline Mutation in the C2 Domain of PLCγ2 Associated with Gain-of-Function Expands the Phenotype for PLCG2-Related Diseases. *J Clin Immunol,* 40**,** 267-276.
OKUDA, K. S., ASTIN, J. W., MISA, J. P., FLORES, M. V., CROSIER, K. E. & CROSIER, P. S. 2012. lyve1 expression reveals novel lymphatic vessels and new mechanisms for lymphatic vessel development in zebrafish. *Development,* 139**,** 2381-91.
OMBRELLO, M. J., REMMERS, E. F., SUN, G., FREEMAN, A. F., DATTA, S., TORABI-PARIZI, P., SUBRAMANIAN, N., BUNNEY, T. D., BAXENDALE, R. W., MARTINS, M. S., ROMBERG, N., KOMAROW, H., AKSENTIJEVICH, I., KIM, H. S., HO, J., CRUSE, G., JUNG, M. Y., GILFILLAN, A. M., METCALFE, D. D., NELSON, C., O'BRIEN, M., WISCH, L., STONE, K., DOUEK, D. C., GANDHI, C., WANDERER, A. A., LEE, H., NELSON, S. F., SHIANNA, K. V., CIRULLI, E. T., GOLDSTEIN, D. B., LONG, E. O., MOIR, S., MEFFRE, E., HOLLAND, S. M., KASTNER, D. L., KATAN, M., HOFFMAN, H. M. & MILNER, J. D. 2012. Cold urticaria, immunodeficiency, and autoimmunity related to PLCG2 deletions. *N Engl J Med,* 366**,** 330-8.
PAN, Z., SCHEERENS, H., LI, S. J., SCHULTZ, B. E., SPRENGELER, P. A., BURRILL, L. C., MENDONCA, R. V., SWEENEY, M. D., SCOTT, K. C., GROTHAUS, P. G., JEFFERY, D. A., SPOERKE, J. M., HONIGBERG, L. A., YOUNG, P. R., DALRYMPLE, S. A. & PALMER, J. T. 2007. Discovery of selective irreversible inhibitors for Bruton's tyrosine kinase. *ChemMedChem,* 2**,** 58-61.
PARGUIÑA, A. F., ALONSO, J., ROSA, I., VÉLEZ, P., GONZÁLEZ-LÓPEZ, M. J., GUITIÁN, E., EBLE, J. A., LOZA, M. I. & GARCÍA, Á. 2012. A detailed proteomic analysis of rhodocytin-activated platelets reveals novel clues on the CLEC-2 signalosome: implications for CLEC-2 signaling regulation. *Blood,* 120**,** e117-e126.
PARK, H., WAHL, M. I., AFAR, D. E., TURCK, C. W., RAWLINGS, D. J., TAM, C., SCHARENBERG, A. M., KINET, J. P. & WITTE, O. N. 1996. Regulation of Btk function by a major autophosphorylation site within the SH3 domain. *Immunity,* 4**,** 515-25.
PAYNE, H., PONOMARYOV, T., WATSON, S. P. & BRILL, A. 2017. Mice with a deficiency in CLEC-2 are protected against deep vein thrombosis. *Blood,* 129**,** 2013-2020.
PAYRASTRE, B., MISSY, K., TRUMEL, C., BODIN, S., PLANTAVID, M. & CHAP, H. 2000. The integrin αIIb/β3 in human platelet signal transduction. *Biochemical Pharmacology,* 60**,** 1069-1074.
PEREZ-MORENO, M., AVILA, A., ISLAS, S., SANCHEZ, S. & GONZÁLEZ-MARISCAL, L. 1998. Vinculin but not α-actinin is a target of PKC phosphorylation during junctional assembly induced by calcium. *Journal of Cell Science,* 111**,** 3563-3571.
POLLITT, A. Y., GRYGIELSKA, B., LEBLOND, B., DESIRE, L., EBLE, J. A. & WATSON, S. P. 2010. Phosphorylation of CLEC-2 is dependent on lipid rafts, actin polymerization, secondary mediators, and Rac. *Blood,* 115**,** 2938-46.
POULTER, N. S., POLLITT, A. Y., OWEN, D. M., GARDINER, E. E., ANDREWS, R. K., SHIMIZU, H., ISHIKAWA, D., BIHAN, D., FARNDALE, R. W., MOROI, M., WATSON, S. P. & JUNG, S. M. 2017. Clustering of glycoprotein VI (GPVI) dimers

upon adhesion to collagen as a mechanism to regulate GPVI signaling in platelets. *J Thromb Haemost,* 15**,** 549-564.
PRELICH, G. 2012. Gene overexpression: uses, mechanisms, and interpretation. *Genetics,* 190**,** 841-854.
PREVO, R., BANERJI, S., FERGUSON, D. J., CLASPER, S. & JACKSON, D. G. 2001. Mouse LYVE-1 is an endocytic receptor for hyaluronan in lymphatic endothelium. *J Biol Chem,* 276**,** 19420-30.
PULCINELLI, F. M., GRESELE, P., BONUGLIA, M. & GAZZANIGA, P. P. 1998. Evidence for separate effects of U73122 on phospholipase C and calcium channels in human platelets. *Biochem Pharmacol,* 56**,** 1481-4.
QUEK, L. S., BOLEN, J. & WATSON, S. P. 1998. A role for Bruton's tyrosine kinase (Btk) in platelet activation by collagen. *Curr Biol,* 8**,** 1137-40.
QUEK, L. S., PASQUET, J. M., HERS, I., CORNALL, R., KNIGHT, G., BARNES, M., HIBBS, M. L., DUNN, A. R., LOWELL, C. A. & WATSON, S. P. 2000. Fyn and Lyn phosphorylate the Fc receptor gamma chain downstream of glycoprotein VI in murine platelets, and Lyn regulates a novel feedback pathway. *Blood,* 96**,** 4246-53.
RAICA, M., CIMPEAN, A. M. & RIBATTI, D. 2008. The role of podoplanin in tumor progression and metastasis. *Anticancer Res,* 28**,** 2997-3006.
RAN, F. A., HSU, P. D., WRIGHT, J., AGARWALA, V., SCOTT, D. A. & ZHANG, F. 2013. Genome engineering using the CRISPR-Cas9 system. *Nature Protocols,* 8**,** 2281-2308.
RAWLINGS, D. J., SCHARENBERG, A. M., PARK, H., WAHL, M. I., LIN, S., KATO, R. M., FLUCKIGER, A. C., WITTE, O. N. & KINET, J. P. 1996. Activation of BTK by a phosphorylation mechanism initiated by SRC family kinases. *Science,* 271**,** 822-5.
RHEE, S. G. & BAE, Y. S. 1997. Regulation of phosphoinositide-specific phospholipase C isozymes. *J Biol Chem,* 272**,** 15045-8.
RHEE, S. G. & CHOI, K. D. 1992. Regulation of inositol phospholipid-specific phospholipase C isozymes. *J Biol Chem,* 267**,** 12393-6.
RIGG, R. A., ASLAN, J. E., HEALY, L. D., WALLISCH, M., THIERHEIMER, M. L., LOREN, C. P., PANG, J., HINDS, M. T., GRUBER, A. & MCCARTY, O. J. 2016. Oral administration of Bruton's tyrosine kinase inhibitors impairs GPVI-mediated platelet function. *Am J Physiol Cell Physiol,* 310**,** C373-80.
RINE, J. 1991. Gene overexpression in studies of Saccharomyces cerevisiae. *Methods Enzymol,* 194**,** 239-51.
RISAU, W., SARIOLA, H., ZERWES, H. G., SASSE, J., EKBLOM, P., KEMLER, R. & DOETSCHMAN, T. 1988. Vasculogenesis and angiogenesis in embryonic-stem-cell-derived embryoid bodies. *Development,* 102**,** 471-8.
RISMAN, R. A., BELCHER, H. A., RAMANUJAM, R. K., WEISEL, J. W., HUDSON, N. E. & TUTWILER, V. 2024. Comprehensive Analysis of the Role of Fibrinogen and Thrombin in Clot Formation and Structure for Plasma and Purified Fibrinogen. *Biomolecules,* 14.
RITTENHOUSE, S. E. 1996. Phosphoinositide 3-Kinase Activation and Platelet Function. *Blood,* 88**,** 4401-4414.
RIVERA, J., LOZANO, M. L., NAVARRO-NÚÑEZ, L. & VICENTE, V. 2009. Platelet receptors and signaling in the dynamics of thrombus formation. *Haematologica,* 94**,** 700-11.
RODRIGUEZ, R., MATSUDA, M., PERISIC, O., BRAVO, J., PAUL, A., JONES, N. P., LIGHT, Y., SWANN, K., WILLIAMS, R. L. & KATAN, M. 2001. Tyrosine residues in phospholipase Cgamma 2 essential for the enzyme function in B-cell signaling. *J Biol Chem,* 276**,** 47982-92.

RODVIEN, R. & MIELKE, C. H., JR. 1976. Role of platelets in hemostasis and thrombosis. *West J Med,* 125**,** 181-6.

ROGERS, K. A., THOMPSON, P. A., ALLAN, J. N., COLEMAN, M., SHARMAN, J. P., CHESON, B. D., JONES, D., IZUMI, R., FRIGAULT, M. M., QUAH, C., RAMAN, R. K., PATEL, P., WANG, M. H. & KIPPS, T. J. 2021. Phase II study of acalabrutinib in ibrutinib-intolerant patients with relapsed/refractory chronic lymphocytic leukemia. *Haematologica,* 106**,** 2364-2373.

ROWLEY, R. B., BURKHARDT, A. L., CHAO, H. G., MATSUEDA, G. R. & BOLEN, J. B. 1995. Syk protein-tyrosine kinase is regulated by tyrosine-phosphorylated Ig alpha/Ig beta immunoreceptor tyrosine activation motif binding and autophosphorylation. *J Biol Chem,* 270**,** 11590-4.

SALEH-GOHARI, N. & HELLEDAY, T. 2004. Conservative homologous recombination preferentially repairs DNA double-strand breaks in the S phase of the cell cycle in human cells. *Nucleic Acids Res,* 32**,** 3683-8.

SCHAMEL, W. W. & RETH, M. 2000. Monomeric and oligomeric complexes of the B cell antigen receptor. *Immunity,* 13**,** 5-14.

SCHARENBERG, A. M., EL-HILLAL, O., FRUMAN, D. A., BEITZ, L. O., LI, Z., LIN, S., GOUT, I., CANTLEY, L. C., RAWLINGS, D. J. & KINET, J. P. 1998. Phosphatidylinositol-3,4,5-trisphosphate (PtdIns-3,4,5-P3)/Tec kinase-dependent calcium signaling pathway: a target for SHIP-mediated inhibitory signals. *Embo j,* 17**,** 1961-72.

SCHOLEY, J. M., TAYLOR, K. A. & KENDRICK-JONES, J. 1980. Regulation of non-muscle myosin assembly by calmodulin-dependent light chain kinase. *Nature,* 287**,** 233-5.

SCHURGERS, E., MOORLAG, M., HEMKER, C., LINDHOUT, T., KELCHTERMANS, H. & DE LAAT, B. 2016. Thrombin Generation in Zebrafish Blood. *PLoS One,* 11**,** e0149135.

SCHWER, H. D., LECINE, P., TIWARI, S., ITALIANO, J. E., JR., HARTWIG, J. H. & SHIVDASANI, R. A. 2001. A lineage-restricted and divergent beta-tubulin isoform is essential for the biogenesis, structure and function of blood platelets. *Curr Biol,* 11**,** 579-86.

SCOTT, S. P., TEH, A., PENG, C. & LAVIN, M. F. 2002. One-step site-directed mutagenesis of ATM cDNA in large (20kb) plasmid constructs. *Hum Mutat,* 20**,** 323.

SEBZDA, E., HIBBARD, C., SWEENEY, S., ABTAHIAN, F., BEZMAN, N., CLEMENS, G., MALTZMAN, J. S., CHENG, L., LIU, F., TURNER, M., TYBULEWICZ, V., KORETZKY, G. A. & KAHN, M. L. 2006. Syk and Slp-76 mutant mice reveal a cell-autonomous hematopoietic cell contribution to vascular development. *Developmental cell,* 11**,** 349-361.

SEO, H.-H., LEE, C. Y., LEE, J., LIM, S., CHOI, E., PARK, J.-C., LEE, S. & HWANG, K.-C. 2016. The role of nuclear factor of activated T cells during phorbol myristate acetate-induced cardiac differentiation of mesenchymal stem cells. *Stem Cell Research & Therapy,* 7**,** 90.

SÉVERIN, S., POLLITT, A. Y., NAVARRO-NUÑEZ, L., NASH, C. A., MOURÃO-SÁ, D., EBLE, J. A., SENIS, Y. A. & WATSON, S. P. 2011. Syk-dependent phosphorylation of CLEC-2: a novel mechanism of hem-immunoreceptor tyrosine-based activation motif signaling. *The Journal of biological chemistry,* 286**,** 4107-4116.

SEYOUM, M., ENAWGAW, B. & MELKU, M. 2018. Human blood platelets and viruses: defense mechanism and role in the removal of viral pathogens. *Thromb J,* 16**,** 16.

SHAPIRO, V. S., MOLLENAUER, M. N., GREENE, W. C. & WEISS, A. 1996. c-rel regulation of IL-2 gene expression may be mediated through activation of AP-1. *J Exp Med,* 184**,** 1663-9.
SHATTIL, S. J. & NEWMAN, P. J. 2004. Integrins: dynamic scaffolds for adhesion and signaling in platelets. *Blood,* 104**,** 1606-15.
SHIN, Y. & MORITA, T. 1998. Rhodocytin, a functional novel platelet agonist belonging to the heterodimeric C-type lectin family, induces platelet aggregation independently of glycoprotein Ib. *Biochem Biophys Res Commun,* 245**,** 741-5.
SHIRAI, T., INOUE, O., TAMURA, S., TSUKIJI, N., SASAKI, T., ENDO, H., SATOH, K., OSADA, M., SATO-UCHIDA, H., FUJII, H., OZAKI, Y. & SUZUKI-INOUE, K. 2017. C-type lectin-like receptor 2 promotes hematogenous tumor metastasis and prothrombotic state in tumor-bearing mice. *J Thromb Haemost,* 15**,** 513-525.
SHONNARD, G. C., HUD, N. V. & MOHRENWEISER, H. W. 1996. Arginine to tryptophan substitution in the active site of a human lactate dehydrogenase variant--LDHB GUA1: postulated effects on subunit structure and catalysis. *Biochim Biophys Acta,* 1315**,** 9-14.
SMITH, R. J., SAM, L. M., JUSTEN, J. M., BUNDY, G. L., BALA, G. A. & BLEASDALE, J. E. 1990. Receptor-coupled signal transduction in human polymorphonuclear neutrophils: effects of a novel inhibitor of phospholipase C-dependent processes on cell responsiveness. *J Pharmacol Exp Ther,* 253**,** 688-97.
SOBANOV, Y., BERNREITER, A., DERDAK, S., MECHTCHERIAKOVA, D., SCHWEIGHOFER, B., DUCHLER, M., KALTHOFF, F. & HOFER, E. 2001. A novel cluster of lectin-like receptor genes expressed in monocytic, dendritic and endothelial cells maps close to the NK receptor genes in the human NK gene complex. *Eur J Immunol,* 31**,** 3493-503.
SPALTON, J. C., MORI, J., POLLITT, A. Y., HUGHES, C. E., EBLE, J. A. & WATSON, S. P. 2009. The novel Syk inhibitor R406 reveals mechanistic differences in the initiation of GPVI and CLEC-2 signaling in platelets. *J Thromb Haemost,* 7**,** 1192-9.
STEFANINI, L., RODEN, R. C. & BERGMEIER, W. 2009. CalDAG-GEFI is at the nexus of calcium-dependent platelet activation. *Blood,* 114**,** 2506-2514.
STEVENSON, F. K., KRYSOV, S., DAVIES, A. J., STEELE, A. J. & PACKHAM, G. 2011. B-cell receptor signaling in chronic lymphocytic leukemia. *Blood,* 118**,** 4313-20.
SUGIYAMA, T., OKUMA, M., USHIKUBI, F., SENSAKI, S., KANAJI, K. & UCHINO, H. 1987. A novel platelet aggregating factor found in a patient with defective collagen-induced platelet aggregation and autoimmune thrombocytopenia. *Blood,* 69**,** 1712-20.
SUN, L., MAO, G. & RAO, A. K. 2004. Association of CBFA2 mutation with decreased platelet PKC-θ and impaired receptor-mediated activation of GPIIb-IIIa and pleckstrin phosphorylation: proteins regulated by CBFA2 play a role in GPIIb-IIIa activation. *Blood,* 103**,** 948-954.
SUZUKI-INOUE, K., FULLER, G. L., GARCIA, A., EBLE, J. A., POHLMANN, S., INOUE, O., GARTNER, T. K., HUGHAN, S. C., PEARCE, A. C., LAING, G. D., THEAKSTON, R. D., SCHWEIGHOFFER, E., ZITZMANN, N., MORITA, T., TYBULEWICZ, V. L., OZAKI, Y. & WATSON, S. P. 2006. A novel Syk-dependent mechanism of platelet activation by the C-type lectin receptor CLEC-2. *Blood,* 107**,** 542-9.
SUZUKI-INOUE, K., INOUE, O., DING, G., NISHIMURA, S., HOKAMURA, K., ETO, K., KASHIWAGI, H., TOMIYAMA, Y., YATOMI, Y., UMEMURA, K., SHIN, Y., HIRASHIMA, M. & OZAKI, Y. 2010. Essential in vivo roles of the C-type lectin receptor CLEC-2: embryonic/neonatal lethality of CLEC-2-deficient mice by

blood/lymphatic misconnections and impaired thrombus formation of CLEC-2-deficient platelets. *J Biol Chem,* 285**,** 24494-507.
SUZUKI-INOUE, K., INOUE, O., FRAMPTON, J. & WATSON, S. P. 2003a. Murine GPVI stimulates weak integrin activation in PLCgamma2-/- platelets: involvement of PLCgamma1 and PI3-kinase. *Blood,* 102**,** 1367-73.
SUZUKI-INOUE, K., INOUE, O., FRAMPTON, J. & WATSON, S. P. 2003b. Murine GPVI stimulates weak integrin activation in PLCγ2–/– platelets: involvement of PLCγ1 and PI3-kinase. *Blood,* 102**,** 1367-1373.
SUZUKI-INOUE, K., INOUE, O. & OZAKI, Y. 2011. Novel platelet activation receptor CLEC-2: from discovery to prospects. *J Thromb Haemost,* 9 Suppl 1**,** 44-55.
SUZUKI-INOUE, K., KATO, Y., INOUE, O., KANEKO, M. K., MISHIMA, K., YATOMI, Y., YAMAZAKI, Y., NARIMATSU, H. & OZAKI, Y. 2007. Involvement of the snake toxin receptor CLEC-2, in podoplanin-mediated platelet activation, by cancer cells. *J Biol Chem,* 282**,** 25993-6001.
SUZUKI-INOUE, K., OZAKI, Y., KAINOH, M., SHIN, Y., WU, Y., YATOMI, Y., OHMORI, T., TANAKA, T., SATOH, K. & MORITA, T. 2001. Rhodocytin induces platelet aggregation by interacting with glycoprotein Ia/IIa (GPIa/IIa, Integrin alpha 2beta 1). Involvement of GPIa/IIa-associated src and protein tyrosine phosphorylation. *J Biol Chem,* 276**,** 1643-52.
SUZUKI-INOUE, K., TSUKIJI, N., SHIRAI, T., OSADA, M., INOUE, O. & OZAKI, Y. 2018. Platelet CLEC-2: Roles Beyond Hemostasis. *Semin Thromb Hemost,* 44**,** 126-134.
SUZUKI-INOUE, K., TULASNE, D., SHEN, Y., BORI-SANZ, T., INOUE, O., JUNG, S. M., MOROI, M., ANDREWS, R. K., BERNDT, M. C. & WATSON, S. P. 2002. Association of Fyn and Lyn with the proline-rich domain of glycoprotein VI regulates intracellular signaling. *J Biol Chem,* 277**,** 21561-6.
TAKATA, M. & KUROSAKI, T. 1996. A role for Bruton's tyrosine kinase in B cell antigen receptor-mediated activation of phospholipase C-gamma 2. *J Exp Med,* 184**,** 31-40.
TAKATA, M., SABE, H., HATA, A., INAZU, T., HOMMA, Y., NUKADA, T., YAMAMURA, H. & KUROSAKI, T. 1994. Tyrosine kinases Lyn and Syk regulate B cell receptor-coupled Ca2+ mobilization through distinct pathways. *Embo j,* 13**,** 1341-9.
THOMAS, S. G. 2019. The structure of resting and activated platelets. *Platelets***,** 47-77.
THON, J. N. & ITALIANO, J. E. 2012. Platelets: Production, Morphology and Ultrastructure. *In:* GRESELE, P., BORN, G. V. R., PATRONO, C. & PAGE, C. P. (eds.) *Antiplatelet Agents.* Berlin, Heidelberg: Springer Berlin Heidelberg.
TOMLINSON, M. G., CALAMINUS, S. D., BERLANGA, O., AUGER, J. M., BORI-SANZ, T., MEYAARD, L. & WATSON, S. P. 2007. Collagen promotes sustained glycoprotein VI signaling in platelets and cell lines. *J Thromb Haemost,* 5**,** 2274-83.
TSAI, A. P., DONG, C., LIN, P. B., OBLAK, A. L., VIANA DI PRISCO, G., WANG, N., HAJICEK, N., CARR, A. J., LENDY, E. K., HAHN, O., ATKINS, M., FOLTZ, A. G., PATEL, J., XU, G., MOUTINHO, M., SONDEK, J., ZHANG, Q., MESECAR, A. D., LIU, Y., ATWOOD, B. K., WYSS-CORAY, T., NHO, K., BISSEL, S. J., LAMB, B. T. & LANDRETH, G. E. 2023. Genetic variants of phospholipase C-γ2 alter the phenotype and function of microglia and confer differential risk for Alzheimer's disease. *Immunity,* 56**,** 2121-2136.e6.
TSUJI, M., EZUMI, Y., ARAI, M. & TAKAYAMA, H. 1997. A novel association of Fc receptor gamma-chain with glycoprotein VI and their co-expression as a collagen receptor in human platelets. *J Biol Chem,* 272**,** 23528-31.

VAN KOLEN, K. & SLEGERS, H. 2006. Integration of P2Y receptor-activated signal transduction pathways in G protein-dependent signalling networks. *Purinergic Signal,* 2**,** 451-69.
VARGA-SZABO, D., BRAUN, A. & NIESWANDT, B. 2009. Calcium signaling in platelets. *J Thromb Haemost,* 7**,** 1057-66.
VOGELI, K. M., JIN, S. W., MARTIN, G. R. & STAINIER, D. Y. 2006. A common progenitor for haematopoietic and endothelial lineages in the zebrafish gastrula. *Nature,* 443**,** 337-9.
WALLISER, C., HERMKES, E., SCHADE, A., WIESE, S., DEINZER, J., ZAPATKA, M., DÉSIRÉ, L., MERTENS, D., STILGENBAUER, S. & GIERSCHIK, P. 2016. The Phospholipase Cγ2 Mutants R665W and L845F Identified in Ibrutinib-resistant Chronic Lymphocytic Leukemia Patients Are Hypersensitive to the Rho GTPase Rac2 Protein. *J Biol Chem,* 291**,** 22136-22148.
WALLISER, C., WIST, M., HERMKES, E., ZHOU, Y., SCHADE, A., HAAS, J., DEINZER, J., DÉSIRÉ, L., LI, S. S. C., STILGENBAUER, S., MILNER, J. D. & GIERSCHIK, P. 2018. Functional characterization of phospholipase C-γ(2) mutant protein causing both somatic ibrutinib resistance and a germline monogenic autoinflammatory disorder. *Oncotarget,* 9**,** 34357-34378.
WANG, D., FENG, J., WEN, R., MARINE, J. C., SANGSTER, M. Y., PARGANAS, E., HOFFMEYER, A., JACKSON, C. W., CLEVELAND, J. L., MURRAY, P. J. & IHLE, J. N. 2000. Phospholipase Cgamma2 is essential in the functions of B cell and several Fc receptors. *Immunity,* 13**,** 25-35.
WANG, D. S., SHAW, R., WINKELMANN, J. C. & SHAW, G. 1994. Binding of PH domains of beta-adrenergic receptor kinase and beta-spectrin to WD40/beta-transducin repeat containing regions of the beta-subunit of trimeric G-proteins. *Biochem Biophys Res Commun,* 203**,** 29-35.
WANG, J., SOHN, H., SUN, G., MILNER, J. D. & PIERCE, S. K. 2014. The autoinhibitory C-terminal SH2 domain of phospholipase C-γ2 stabilizes B cell receptor signalosome assembly. *Sci Signal,* 7**,** ra89.
WANG, K., XU, Q. & ZHONG, H. 2020. The Bruton's Tyrosine Kinase Inhibitor Ibrutinib Impairs the Vascular Development of Zebrafish Larvae. *Front Pharmacol,* 11**,** 625498.
WATANABE, D., HASHIMOTO, S., ISHIAI, M., MATSUSHITA, M., BABA, Y., KISHIMOTO, T., KUROSAKI, T. & TSUKADA, S. 2001. Four tyrosine residues in phospholipase C-gamma 2, identified as Btk-dependent phosphorylation sites, are required for B cell antigen receptor-coupled calcium signaling. *J Biol Chem,* 276**,** 38595-601.
WATSON, S., BERLANGA, O., BEST, D. & FRAMPTON, J. 2000. Update on collagen receptor interactions in platelets: is the two-state model still valid? *Platelets,* 11**,** 252-8.
WATSON, S. P., HERBERT, J. M. & POLLITT, A. Y. 2010. GPVI and CLEC-2 in hemostasis and vascular integrity. *J Thromb Haemost,* 8**,** 1456-67.
WELSH, J. D., KAHN, M. L. & SWEET, D. T. 2016. Lymphovenous hemostasis and the role of platelets in regulating lymphatic flow and lymphatic vessel maturation. *Blood,* 128**,** 1169-73.
WENG, Z., THOMAS, S. M., RICKLES, R. J., TAYLOR, J. A., BRAUER, A. W., SEIDEL-DUGAN, C., MICHAEL, W. M., DREYFUSS, G. & BRUGGE, J. S. 1994. Identification of Src, Fyn, and Lyn SH3-binding proteins: implications for a function of SH3 domains. *Mol Cell Biol,* 14**,** 4509-21.

WERNER, M. H., BIELAWSKA, A. E. & HANNUN, Y. A. 1992. Quantitative analysis of diacylglycerol second messengers in human platelets: correlation with aggregation and secretion. *Mol Pharmacol,* 41**,** 382-6.

WEYAND, A. C. & SHAVIT, J. A. 2014. Zebrafish as a model system for the study of hemostasis and thrombosis. *Curr Opin Hematol,* 21**,** 418-22.

WHITE, J. G. 2013. Chapter 7 - Platelet Structure. *In:* MICHELSON, A. D. (ed.) *Platelets (Third Edition).* Academic Press.

WIESTNER, A. 2015. The role of B-cell receptor inhibitors in the treatment of patients with chronic lymphocytic leukemia. *Haematologica,* 100**,** 1495-1507.

WIGLE, J. T. & OLIVER, G. 1999. Prox1 function is required for the development of the murine lymphatic system. *Cell,* 98**,** 769-78.

WILLOUGHBY, S., HOLMES, A. & LOSCALZO, J. 2002. Platelets and Cardiovascular Disease. *European Journal of Cardiovascular Nursing,* 1**,** 273-288.

WONEROW, P., PEARCE, A. C., VAUX, D. J. & WATSON, S. P. 2003. A critical role for phospholipase Cgamma2 in alphaIIbbeta3-mediated platelet spreading. *J Biol Chem,* 278**,** 37520-9.

WOYACH, J. A., FURMAN, R. R., LIU, T.-M., OZER, H. G., ZAPATKA, M., RUPPERT, A. S., XUE, L., LI, D. H.-H., STEGGERDA, S. M., VERSELE, M., DAVE, S. S., ZHANG, J., YILMAZ, A. S., JAGLOWSKI, S. M., BLUM, K. A., LOZANSKI, A., LOZANSKI, G., JAMES, D. F., BARRIENTOS, J. C., LICHTER, P., STILGENBAUER, S., BUGGY, J. J., CHANG, B. Y., JOHNSON, A. J. & BYRD, J. C. 2014a. Resistance Mechanisms for the Bruton's Tyrosine Kinase Inhibitor Ibrutinib. *New England Journal of Medicine,* 370**,** 2286-2294.

WOYACH, J. A., FURMAN, R. R., LIU, T. M., OZER, H. G., ZAPATKA, M., RUPPERT, A. S., XUE, L., LI, D. H., STEGGERDA, S. M., VERSELE, M., DAVE, S. S., ZHANG, J., YILMAZ, A. S., JAGLOWSKI, S. M., BLUM, K. A., LOZANSKI, A., LOZANSKI, G., JAMES, D. F., BARRIENTOS, J. C., LICHTER, P., STILGENBAUER, S., BUGGY, J. J., CHANG, B. Y., JOHNSON, A. J. & BYRD, J. C. 2014b. Resistance mechanisms for the Bruton's tyrosine kinase inhibitor ibrutinib. *N Engl J Med,* 370**,** 2286-94.

WOYACH, J. A., JOHNSON, A. J. & BYRD, J. C. 2012. The B-cell receptor signaling pathway as a therapeutic target in CLL. *Blood,* 120**,** 1175-1184.

XIE, Z., SHAO, B., HOOVER, C., MCDANIEL, M., SONG, J., JIANG, M., MA, Z., YANG, F., HAN, J., BAI, X., RUAN, C. & XIA, L. 2020. Monocyte upregulation of podoplanin during early sepsis induces complement inhibitor release to protect liver function. *JCI Insight,* 5.

XU, S., HUO, J., CHEW, W.-K., HIKIDA, M., KUROSAKI, T. & LAM, K.-P. 2006. Phospholipase Cγ2 Dosage Is Critical for B Cell Development in the Absence of Adaptor Protein BLNK1. *The Journal of Immunology,* 176**,** 4690-4698.

YAMAMOTO, T., YAMANASHI, Y. & TOYOSHIMA, K. 1993. Association of Src-family kinase Lyn with B-cell antigen receptor. *Immunol Rev,* 132**,** 187-206.

YASEEN, N. R., PARK, J., KERPPOLA, T., CURRAN, T. & SHARMA, S. 1994. A central role for Fos in human B- and T-cell NFAT (nuclear factor of activated T cells): an acidic region is required for in vitro assembly. *Mol Cell Biol,* 14**,** 6886-95.

YU, P., CONSTIEN, R., DEAR, N., KATAN, M., HANKE, P., BUNNEY, T. D., KUNDER, S., QUINTANILLA-MARTINEZ, L., HUFFSTADT, U., SCHRÖDER, A., JONES, N. P., PETERS, T., FUCHS, H., DE ANGELIS, M. H., NEHLS, M., GROSSE, J., WABNITZ, P., MEYER, T. P., YASUDA, K., SCHIEMANN, M., SCHNEIDER-FRESENIUS, C., JAGLA, W., RUSS, A., POPP, A., JOSEPHS, M., MARQUARDT, A., LAUFS, J., SCHMITTWOLF, C., WAGNER, H., PFEFFER, K. & MUDDE, G.

C. 2005. Autoimmunity and inflammation due to a gain-of-function mutation in phospholipase C gamma 2 that specifically increases external Ca2+ entry. *Immunity,* 22**,** 451-65.

YUN, S.-H., SIM, E.-H., GOH, R.-Y., PARK, J.-I. & HAN, J.-Y. 2016. Platelet Activation: The Mechanisms and Potential Biomarkers. *BioMed research international,* 2016**,** 9060143-9060143.

YURCHENCO, P. D. 2011. Basement membranes: cell scaffoldings and signaling platforms. *Cold Spring Harbor perspectives in biology,* 3**,** a004911.

ZEILER, M., MOSER, M. & MANN, M. 2014. Copy number analysis of the murine platelet proteome spanning the complete abundance range. *Mol Cell Proteomics,* 13**,** 3435-45.

ZHANG, Y., GUO, S.-Y., ZHU, X., ZHOU, J., LIAO, W. H., ZHENG, G.-L., ZUGUANG, Y., QI, C. & LI. Arachidonic Acid Induced Thrombosis in Zebrafish Larvae for Assessing Human Anti-Thrombotic Drugs. 2017.

ZHENG, Y., ADAMS, T., ZHI, H., YU, M., WEN, R., NEWMAN, P. J., WANG, D. & NEWMAN, D. K. 2015. Restoration of responsiveness of phospholipase Cgamma2-deficient platelets by enforced expression of phospholipase Cgamma1. *PLoS One,* 10**,** e0119739.

ZHOU, Q., LEE, G. S., BRADY, J., DATTA, S., KATAN, M., SHEIKH, A., MARTINS, M. S., BUNNEY, T. D., SANTICH, B. H., MOIR, S., KUHNS, D. B., LONG PRIEL, D. A., OMBRELLO, A., STONE, D., OMBRELLO, M. J., KHAN, J., MILNER, J. D., KASTNER, D. L. & AKSENTIJEVICH, I. 2012a. A hypermorphic missense mutation in PLCG2, encoding phospholipase Cgamma2, causes a dominantly inherited autoinflammatory disease with immunodeficiency. *Am J Hum Genet,* 91**,** 713-20.

ZHOU, Q., LEE, G. S., BRADY, J., DATTA, S., KATAN, M., SHEIKH, A., MARTINS, M. S., BUNNEY, T. D., SANTICH, B. H., MOIR, S., KUHNS, D. B., LONG PRIEL, D. A., OMBRELLO, A., STONE, D., OMBRELLO, M. J., KHAN, J., MILNER, J. D., KASTNER, D. L. & AKSENTIJEVICH, I. 2012b. A hypermorphic missense mutation in PLCG2, encoding phospholipase Cγ2, causes a dominantly inherited autoinflammatory disease with immunodeficiency. *Am J Hum Genet,* 91**,** 713-20.

ZHU, X. Y., LIU, H. C., GUO, S. Y., XIA, B., SONG, R. S., LAO, Q. C., XUAN, Y. X. & LI, C. Q. 2016. A Zebrafish Thrombosis Model for Assessing Antithrombotic Drugs. *Zebrafish,* 13**,** 335-44.